

**Dysregulation of the complement
alternative pathway during
dengue virus infection: *in vitro*
and *in vivo* evidence**

by

Sheila Cabezas Falcon

*Thesis
Submitted to Flinders University
for the degree of*

Doctor of Philosophy

College of Medicine and Public Health

13-12-2018

TABLE OF CONTENTS

TABLE OF CONTENTS.....	I
TABLES AND FIGURES.....	VI
SUMMARY	VIII
DECLARATION.....	X
ACKNOWLEDGEMENTS	XI
LIST OF ABBREVIATIONS	XII
PUBLICATIONS AND PRESENTATIONS	XVIII
CHAPTER I REVIEW OF THE LITERATURE	1
I.1 DENGUE VIRUS	1
I.1.1 <i>General aspects and transmission</i>	1
I.1.2 <i>Epidemiology</i>	1
I.1.3 <i>Clinical manifestations</i>	4
I.1.4 <i>Vaccine and treatment</i>	6
I.1.5 <i>Structural overview of dengue virion, proteins and replication strategy</i>	7
I.1.6 <i>Receptors and routes of dengue virus entry into the host cells</i>	12
I.1.7 <i>Immune responses triggered during DENV infection</i>	14
I.1.7.1 Innate immune response	14
I.1.7.2 Adaptive immune response against DENV	18
I.1.7.2.a The humoral response	18
I.1.7.2.b The cellular immune response to DENV	18
I.1.8 <i>Dengue virus pathogenesis</i>	20
I.1.8.1 Host risk factors.....	20
I.1.8.1.a The humoral response and antibody-dependent enhancement	20
I.1.8.1.b T-cell response.....	21
I.1.8.1.c Cytokine storm	22
I.1.8.1.d Other host factors.....	23
I.1.8.2 Viral factors.....	24
I.1.8.2.a NS1	24
I.1.9 <i>Animal models to study dengue virus pathogenesis</i>	24
I.1.9.1 Human and non-human primate models.....	25
I.1.9.2 Mouse models	26
I.1.9.2.a Wild-type mice.....	26
I.1.9.2.b Humanised mice	27
I.1.9.2.c Immunocompromised mice	28
I.2 THE COMPLEMENT SYSTEM.....	30
I.2.1 <i>The three pathways</i>	30
I.2.1.1 Complement Classical Pathway	30

1.2.1.2	Complement Lectin Pathway	30
1.2.1.3	Complement Alternative Pathway	31
1.2.1.4	Terminal Pathway	31
1.2.2	<i>Effector functions of the complement proteins</i>	34
1.2.3	<i>Regulation of the complement response</i>	35
1.2.3.1	Regulation of the AP. Features and specific roles of its components	36
1.2.3.1.a	C3	36
1.2.3.1.b	FB	36
1.2.3.1.c	FD	37
1.2.3.1.d	Properdin	37
1.2.3.1.e	FI	37
1.2.3.1.f	FH	38
1.2.3.2	Regulation of the AP: mechanisms	41
1.3	THE COMPLEMENT SYSTEM AND VIRAL INFECTIONS	42
1.3.1	<i>Protective role of complement during viral infections</i>	42
1.3.1.1	Protective role of complement during DENV infection	44
1.3.2	<i>Viral evasion of the complement system</i>	45
1.3.3	<i>Pathogenic role of complement during viral infections</i>	46
1.3.3.1	Pathogenic role of complement during DENV infection	47
1.4	HYPOTHESIS AND AIMS	49
1.4.1	<i>Hypothesis</i>	49
1.4.2	<i>Aims</i>	49
CHAPTER II	MATERIALS AND METHODS	50
II.1	MATERIALS	50
II.1.1	<i>Cells and cell lines</i>	50
II.1.2	<i>Cell culture media and reagents</i>	51
II.1.2.1	Media for maintaining and culturing cells	51
II.1.2.2	Cell culture buffers and reagents	51
II.1.2.3	Plaque assay: media and reagents	51
II.1.3	<i>Virus strains</i>	52
II.1.4	<i>TLR ligands</i>	52
II.1.5	<i>Primers</i>	52
II.1.6	<i>Molecular biology reagents and buffers</i>	54
II.1.6.1	RNA extraction	54
II.1.6.2	DNase treatment	54
II.1.6.3	Reverse transcription	54
II.1.6.4	Real time PCR	54
II.1.6.5	Agarose gel electrophoresis	54
II.1.7	<i>Antibodies</i>	55
II.1.8	<i>ELISA: materials, buffers and reagents</i>	58
II.1.9	<i>Sodium dodecyl sulphate (SDS) PAGE and Western blot: buffers and reagents</i>	58
II.1.10	<i>Immunofluorescence: buffers and reagents</i>	59

II.1.11	<i>Flow cytometry: buffers and reagents</i>	59
II.1.12	<i>Alternative pathway assay: buffers and reagents</i>	59
II.2	METHODS.....	60
II.2.1	<i>Cell maintenance</i>	60
II.2.1.1	HUVEC	60
II.2.1.2	MDM	60
II.2.2	<i>Viral stocks and infection</i>	61
II.2.2.1	Virus production.....	61
II.2.2.2	Viral infection	61
II.2.3	<i>TLR treatment of cells</i>	61
II.2.4	<i>Viral quantitation by plaque assay</i>	62
II.2.5	<i>RNA extraction</i>	62
II.2.6	<i>DNase I treatment</i>	63
II.2.7	<i>Reverse transcription</i>	63
II.2.8	<i>Real-time quantitative polymerase chain reaction (RT-qPCR)</i>	63
II.2.9	<i>SDS PAGE and Western Blot</i>	63
II.2.10	<i>Human complement FH purification</i>	64
II.2.11	<i>Quantitation of protein concentration</i>	64
II.2.12	<i>Development of an in-house ELISA to detect human and mouse FH</i>	64
II.2.12.1	Quantitation of human and mouse FH proteins by ELISA.....	65
II.2.13	<i>Quantitation of human and mouse FB proteins by ELISA</i>	66
II.2.14	<i>Treatment of supernatant samples with Triton X-100 or heat</i>	66
II.2.15	<i>AP in vitro activity assay</i>	66
II.2.16	<i>Flow cytometry</i>	67
II.2.17	<i>Immunostaining and high-throughput image analysis</i>	67
II.2.18	<i>Promoter analysis</i>	68
II.2.19	<i>DENV- seropositive and seronegative human serum samples used for quantitation of circulating FH and FB</i>	69
II.2.20	<i>Mice</i>	69
II.2.20.1	C57BL/6 mice	69
II.2.20.2	C57BL/6 mouse model of intracranial DENV infection.....	69
II.2.20.3	AG129 mouse model of DENV infection	69
II.2.20.4	AG129 mouse model of ADE of DENV infection.....	70
II.2.21	<i>Ethics statement</i>	70
II.2.22	<i>Statistical analysis</i>	71

CHAPTER III ESTABLISHMENT AND TECHNICAL VALIDATION OF DIFFERENT METHODS TO DETECT RNA AND PROTEIN OF COMPLEMENT FH AND FB IN A VARIETY OF HUMAN AND MOUSE SAMPLES 72

III.1	INTRODUCTION	72
III.2	RESULTS.....	73
III.2.1	<i>Validation of RT-PCR for human and mouse FH and FB</i>	73

III.2.1.1	Validation of human FH and FB RT-PCR	73
III.2.1.2	Validation of mouse FH and FB RT-PCR.....	77
III.2.2	<i>Establishment of a method to detect FH and FB proteins</i>	80
III.2.2.1	Validation of Western Blot to detect FH and FB proteins in serum and DENV-infected supernatants 80	
III.2.2.2	Purifying FH protein from human sera	82
III.2.2.3	ELISA to detect human and mouse FH proteins	84
III.2.2.4	ELISA to detect human and mouse FB proteins	88
III.2.3	<i>Validation of identification of nuclei and DENV-infected cells by high-content imaging system</i>	88
III.3	DISCUSSION	92
CHAPTER IV DENGUE VIRUS INDUCES INCREASED ACTIVITY OF THE COMPLEMENT		
ALTERNATIVE PATHWAY IN INFECTED CELLS..... 95		
IV.1	INTRODUCTION	95
IV.2	DISCUSSION	116
CHAPTER V THE ROLE OF INTERFERON IN DRIVING CHANGES IN FH AND FB EXPRESSION		
DURING DENV INFECTION 118		
V.1	INTRODUCTION	118
V.2	RESULTS.....	119
V.2.1	<i>MatInspector computational prediction of transcription factor binding sites in the human FB and FH promoters</i>	119
V.2.2	<i>IFN-β regulates FB and FH expression in HUVEC but not in MDM</i>	127
V.3	DISCUSSION	135
CHAPTER VI EVALUATION OF FB AND FH DURING DENGUE VIRUS INFECTION IN <i>IN VIVO</i> MODELS		
141		
VI.1	INTRODUCTION	141
VI.2	RESULTS.....	143
VI.2.1	<i>FH is unchanged but FB is reduced in dengue seropositive compared with seronegative patient samples</i>	143
VI.2.2	<i>Protein levels of FB are unchanged but FH is decreased during severe disease in DENV-infected AG129 mice, although mRNA for both proteins is induced in the liver</i>	145
VI.2.3	<i>Protein levels of FH are decreased but FB are increased during acute, more severe secondary dengue infection in AG129 mice</i>	148
VI.2.4	<i>FB and FH are unchanged at moribund stage during DENV infection but deranged in the model of severe secondary DENV infection in AG129 mice</i>	150
VI.2.5	<i>FH and FB promoters contain potentially important IFN-driven elements</i>	154
VI.2.6	<i>FB mRNA but not FH is increased in the brain of immunocompetent mouse model at end-stage disease</i>	158
VI.3	DISCUSSION	160
CHAPTER VII GENERAL DISCUSSION AND FUTURE DIRECTIONS..... 168		

VII.1 CONCLUSIONS.....	172
APPENDICES	173
BIBLIOGRAPHY	176

TABLES AND FIGURES

FIGURE I-1. AVERAGE NUMBER OF SUSPECTED OR CONFIRMED DENGUE CASES REPORTED TO WHO, 2010-2016....	3
TABLE I-1. CRITERIA FOR DENGUE WARNING SIGNS AND SEVERE DENGUE (WHO, 2009).....	5
FIGURE I-2. SCHEMATIC REPRESENTATION OF THE STRUCTURE OF DENV GENOME WITH STRUCTURAL AND NON- STRUCTURAL PROTEINS	9
FIGURE I-3. SCHEMATIC REPRESENTATION OF A DENV PARTICLE	10
FIGURE I-4. SCHEMATIC REPRESENTATION OF DENV REPLICATION CYCLE.....	11
FIGURE I-5. HOST INNATE IMMUNE RESPONSE TO DENV INFECTION	15
FIGURE I-6. TYPE I IFN RESPONSE IS TRIGGERED UPON DENV INFECTION	17
FIGURE I-7. SCHEMATIC REPRESENTATION OF THE THREE PATHWAYS OF THE COMPLEMENT SYSTEM	33
FIGURE I-8. REGULATORY ROLE OF FH	39
TABLE II-1. CELL LINES EMPLOYED IN THIS STUDY	50
TABLE II-2. OLIGONUCLEOTIDE SEQUENCES UTILISED FOR AMPLIFICATION OF MRNA.....	53
TABLE II-3. PRIMARY ANTIBODIES	56
TABLE II-4. SECONDARY ANTIBODIES	57
FIGURE III-1. VALIDATION OF A RT-PCR FOR HUMAN FH	74
FIGURE III-2. VALIDATION OF A RT-PCR FOR HUMAN FB	76
FIGURE III-3. VALIDATION OF A RT-PCR FOR MOUSE FH	78
FIGURE III-4. VALIDATION OF A RT-PCR FOR MOUSE FB	79
FIGURE III-5. VALIDATION OF WESTERN BLOT TO DETECT HUMAN AND MOUSE FH AND FB PROTEINS	81
FIGURE III-6. EVALUATION OF THE PURIFIED FH PROTEIN.....	83
FIGURE III-7. VALIDATION OF HUMAN FH ELISA	85
FIGURE III-8. VALIDATION OF MOUSE FH ELISA	87
FIGURE III-9. IMAGE ANALYSIS TO IDENTIFY THE NUCLEUS AND CYTOPLASM USING THE HARMONY SOFTWARE.....	90
FIGURE III-10. VALIDATION OF DENV INTRACELLULAR STAINING USING THE OPERETTA.....	91
TABLE V-1. PUTATIVE TRANSCRIPTION BINDING SITES IN THE HUMAN FB PROMOTER REGION.....	120
TABLE V-2. PUTATIVE TRANSCRIPTION BINDING SITES IN THE HUMAN FH PROMOTER REGION.....	121
FIGURE V-1. IDENTIFICATION OF PUTATIVE TRANSCRIPTION FACTOR BINDING SITES IN THE HUMAN FB PROMOTER REGION USING MATINSPECTOR SOFTWARE	122
FIGURE V-2. IDENTIFICATION OF PUTATIVE TRANSCRIPTION FACTOR BINDING SITES IN THE HUMAN FH PROMOTER REGION USING MATINSPECTOR SOFTWARE	123
TABLE V-3. SUMMARY OF KEY PREDICTED TF ELEMENTS IN THE HUMAN FB AND FH PROMOTER REGIONS.....	126
FIGURE V-3. BLOCKING OF IFN- β ACTIONS INCREASES DENV MRNA IN HUVEC	128
FIGURE V-4. BLOCKING OF IFN- β ACTIONS REDUCES MRNA FOR DENV-INDUCED ISGs IN HUVEC	129
FIGURE V-5. BLOCKING OF IFN- β ACTIONS REDUCES MRNA FOR DENV-INDUCED FH AND FB MRNA AND PROTEIN IN HUVEC	130
FIGURE V-6. BLOCKING OF IFN- β ACTIONS INDUCES DENV MRNA IN MDM.....	132
FIGURE V-7. BLOCKING OF IFN- β ACTIONS HAS NO EFFECT ON MRNA FOR DENV-INDUCED ISGs IN MDM	133
FIGURE V-8. BLOCKING OF IFN- β ACTIONS HAS NO EFFECT DENV-INDUCED FH AND FB IN MDM	134

FIGURE VI-1. FH IS UNCHANGED BUT FB IS REDUCED DURING PRIMARY DENGUE INFECTION IN HUMANS.....	144
FIGURE VI-2. CIRCULATING FH IS DECREASED BUT FB IS UNCHANGED DURING ACUTE PRIMARY DENGUE INFECTION IN AG129 MICE	146
FIGURE VI-3. CIRCULATING CHANGES OF FB AND FH ARE NOT REFLECTED BY MRNA IN THE LIVER OR KIDNEY OF DENV-INFECTED AG129 MICE	147
FIGURE VI-4. CIRCULATING FH IS DECREASED AND FB INCREASED DURING ACUTE, SEVERE SECONDARY DENGUE INFECTION IN AG129 MICE.....	149
FIGURE VI-5. AT MORIBUND STAGE, COMPLEMENT IS UNCHANGED DURING DENV INFECTION OF AG129 MICE	151
FIGURE VI-6. COMPLEMENT IS DERANGED DURING LATE STAGES OF SEVERE SECONDARY DENV INFECTION IN AG129 MICE	152
FIGURE VI-7. FB AND FH MRNA LEVELS ARE UNCHANGED IN THE LIVER OR KIDNEY DURING SEVERE SECONDARY DENV INFECTION IN AG129 MICE	153
FIGURE VI-8. COMPARISON BETWEEN MOUSE AND HUMAN FB PROMOTERS	155
FIGURE VI-9. COMPARISON BETWEEN MOUSE AND HUMAN FH PROMOTERS	156
TABLE VI-1. COMPARISON BETWEEN HUMAN AND MOUSE FB AND FH PROMOTERS	157
FIGURE VI-10. FB MRNA BUT NOT FH IS INCREASED IN BRAIN FOLLOWING INTRACRANIAL DENV INFECTION	159
APPENDIX 1. ANALYSIS SEQUENCE OF BUILDING BLOCKS USED IN THE HIGH-THROUGHPUT IMAGING SYSTEM (OPERETTA).....	173
APPENDIX 2. SCHEMATIC REPRESENTATION OF THE SANDWICH ELISA DEVELOPED TO DETECT HUMAN AND MOUSE FH PROTEINS.....	174
APPENDIX 3. COURSE OF VIREMIA IN AG129 MICE INFECTED WITH 10 ⁴ PFU OF D2Y98P STRAIN.....	175

SUMMARY

Dengue virus (DENV) is responsible for one of the most important human viral diseases in terms of geographical distribution and morbidity. The pathogenesis of severe DENV results from a combination of multiple factors that act in concert to promote a dysregulated immune response. Hyperactivity of the complement alternative pathway (AP) is associated with severe forms of DENV disease, dengue haemorrhagic fever (DHF) and dengue shock syndrome (DSS). The AP is constitutively active at basal levels and thus is highly regulated by soluble and membrane-associated proteins, keeping the activity of the AP tightly controlled. Factor B (FB) and factor H (FH) are considered two main regulators of the AP. While FB promotes activation of the AP, FH is the major negative regulator responsible for keeping a fine control of this pathway. The overall goal of this thesis is to gain insights into complement dysregulation by investigation of the induction of FH and FB during DENV infection.

Firstly, different methods were established to detect, identify and quantitate FH and FB mRNAs and proteins that were further applied to study changes in *in vitro* and *in vivo* models of DENV infection. *In vitro* DENV infection showed that FH mRNA was significantly increased in DENV-infected endothelial cells (EC) and macrophages but surprisingly, production of extracellular FH was not. This phenomenon was not seen for FB, with DENV induction of both FB mRNA and protein, or with Toll-like receptor 3 or 4 stimulation of EC and macrophages, which induced both FH mRNA and protein. Further, an imbalance in AP components in the local microenvironment of EC and macrophages was detected, with lower FH relative to FB protein along with increased deposition of the complement component C3b on the surface of DENV-infected cells. These changes are predicted to result in higher complement activity locally on the endothelium, with the potential to induce functional changes that may result in increased vascular permeability, a hallmark of DENV disease. Further using MatInspector software, several IFN-responsive elements along with NF κ B and STAT binding elements were identified within the human FB and FH promoter regions, suggesting that both factors are stimulated by similar transcription factors. Experimentally it was demonstrated that IFN- β mediates induction of FB and FH mRNA and FB protein in EC in a co-ordinated manner consistent with other interferon-stimulated genes. Finally, this study was extended to investigate the roles of FB and FH in DENV-infected AG129 mice, deficient in type I and type II IFN receptors. An early increase in FB

followed by a decrease at moribund stage was detected in mice with severe DENV. In contrast, FH was decreased during the acute phase of infection and increased at end-stage of severe disease. These DENV-induced FB and FH responses in AG129 mice suggest an initial acute-phase response to activate the AP, followed by excessive complement consumption and hyper-activation of the AP. This latter response is consistent with changes in FB and FH described in DHF and DSS patients. Surprisingly, circulating FB and FH protein levels did not correlate with changes in liver mRNA. Similar MatInspector computational analysis of the mouse FB and FH promoters again showed predicted dependence on IFN responsive elements, NF κ B and STAT transcription factors, with clearly the IFN-independent elements such as NF κ B likely to play a major regulatory role in the responses to DENV described in the AG129 IFN-receptor deficient mouse model. DENV-infection in the brain of immunocompetent mice induced FB but not FH mRNA, demonstrating discordant regulation of these genes in this setting that could be mediated via transcription factors such as NF κ B.

Altogether this study suggests potential roles of the AP complement cascade in DENV disease and has provided *in vitro* and *in vivo* evidence of a dysregulation of the AP during DENV infection that can be mediated by changes in FB and FH. This in turn could expand strategies for developing therapeutics to prevent or control the increased vascular permeability and treating the severe forms of DENV disease.

DECLARATION

I certify that this thesis does not incorporate without acknowledgment any material previously submitted for a degree or diploma in any university; and that to the best of my knowledge and belief it does not contain any material previously published or written by another person except where due reference is made in the text.

Signed Sheila Cabezas Falcon

Date 29/08/2018

ACKNOWLEDGEMENTS

Firstly, I would like to express my gratitude to my supervisor Associate Professor Jill Carr for her continuous professional and personal support during this long journey. I really appreciate her guidance, expertise and the time she has spent on me all these years.

I would like to thank my co-supervisor Prof. David Gordon for his help, support and advice during the course of my thesis.

I would like to especially thank Dr. Gustavo Bracho for his collaboration, helpful scientific discussions and for his contribution to this thesis.

I am very grateful to Dr. Amanda Aloia, Dr. Penny Adamson, Ms Julie Calvert and Dr Jen Clarke for their professional and technical laboratory support, for the useful scientific discussions and for their friendship.

A special thank you to present and former students of my lab, especially to Alexander Mathews, Jarrod Hulme-Jones and Josh Dubowsky for their help and support.

I would also like to thank our collaborators Prof. Justine Smith from Flinders University for providing ARPE-19 and HRECT cells; Dr. Penny Rudd and Prof. Suresh Mahalingam from Griffith University, Australia, and Dr. Lee Ching and Prof. Sylvie Alonso from the University of Singapore, Singapore, for providing serum and tissue samples from AG129 DENV-infection model.

Thank you to the International Student Service, Flinders University, especially to Mr Klaus Koefer for his help, support and guidance from the very first day I arrived at Flinders University.

I would like to thank and acknowledge the Government of Australia and Flinders University for awarding me the International Postgraduate Research Scholarship that gave me the opportunity to do my PhD in Australia.

Finally, I would like to thank my family, especially my husband Gustavo Bracho and my son Lucas Bracho for their constant and unconditional support, for their understanding, patience and encouragement throughout my studies.

LIST OF ABBREVIATIONS

ADE	Antibody-dependent enhancement
a-HUS	Atypical haemolytic-uremic syndrome
AP	Alternative pathway
ARPE-19	Human retinal pigment epithelial cells
ATCC	American type culture collection
BHK-21	Baby hamster kidney clone 21
BSA	Bovine serum albumin
C	Capsid protein
C1qR	C1q receptor
C4bp	Complement 4b binding protein
cDNA	Complementary DNA
CP	Classical pathway
CR	Complement receptor
CREB	cAMP responsive elements
CRP	C-reactive protein
DAF	Decay accelerating factor
DC-SIGN	Adhesion molecule 3-grabbing non-integrin
DENV	Dengue virus
DF	Dengue fever
DHF	Dengue haemorrhagic fever

DHIM	Dengue human infection model
DMEM	Dulbecco's Modified Eagle's Medium
DNA	Deoxyribonucleic acid
dNTPs	Deoxyribonucleotide triphosphates
dpi	days post-infection
DSS	Dengue shock syndrome
dsRNA	Double-stranded RNA
E	Envelope protein
EC	Endothelial cells
EDTA	Ethylenediaminetetraacetic acid
EGR	Early growth response proteins
EGRF	EGR/nerve growth factor induced protein C & related factors
ELISA	Enzyme linked immunosorbent assay
ER	Endoplasmic reticulum
ETSF	E26 transformation-specific family
FB	Factor B
FBS	Foetal bovine serum
FD	Factor D
FH	Factor H
FHL-1	Factor H-like protein 1
FI	Factor I

FKHD	Fork head domain factors
GAG	Glycosaminoglycans
GAPDH	glyceraldehyde-3-phosphate dehydrogenase
HBSS	Hank's balanced salt solution
HCV	Hepatitis C virus
HepG2	Human hepatocellular carcinoma cells
HIV-1	Human immunodeficiency virus-1
HLA	Human leukocyte antigen
hpi	Hours post-infection
HREC	HPV E6/E7 transduced human retinal endothelial cells
HSP	Heat shock protein
HUVEC	Human umbilical endothelial cells
IBC	Institutional Biosafety Committee
IFN	Interferon
IFNAR ^{-/-}	Mice deficient in interferon receptors α and β
IL	Interleukin
IRFF	Interferon regulatory factors
ISGs	Interferon stimulated genes
ISRE	Interferon-stimulated response elements
LP	Lectin pathway
LPS	Lipopolysaccharide

L-SIGN	Liver-specific adhesion molecule 3-grabbing non-integrin
MAC	Membrane attack complex
MASPs	Mannose binding lectins-associated serine proteases
MBL	Mannose binding lectins
MCP	Membrane cofactor protein
MDM	Monocyte derived macrophages
MEF	Mouse embryonic fibroblast
MOI	Multiplicity of infection
mRNA	Messenger ribonucleic acid
MTF1	Metal induced transcription factors
NF κ β	Nuclear factor kappa β
NHS	Normal human serum
NOD	Nonobese diabetic mice
NS	Non-structural proteins
ORF	Open reading frame
PAGE	Polyacrylamide gel electrophoresis
PBS	Phosphate buffered saline
PFA	Paraformaldehyde
PFU	Plaque forming unit
pi	Post-infection
Poly (I:C)	polyinosinic:polycytidylic acid poly (I:C)

prM	Precursor membrane protein
PRRs	Pattern recognition receptors
PRRSV	Porcine reproductive and respiratory syndrome virus
RT-qPCR	Real-time quantitative polymerase chain reaction
RIG-I	Retinoic acid-inducible gene I
RNA	Ribonucleic acid
RRV	Ross river virus
RT	Room temperature
SAC/HREC	Southern Adelaide Clinical Human Research Ethics Committee
SCID	Severe combined immunodeficiency
SCR	Short consensus repeat
SDS	Sodium dodecyl sulphate
SRFF	Serum response element binding factors
STAT	Signal transducer and activation of transcription
TAM	Family of receptor tyrosine kinases including Tyro-3 , Axl , and Mer receptors
TF	Transcription factor
TIM	T-cell immunoglobulin and mucin domain
TLR	Toll-like receptor
TNF	Tumour necrosis factor
TRAF	TNF receptor associated factors

UI	Uninfected
v/v	Volume per volume
w/v	Weight per volume
WHO	World Health Organisation
WNV	West Nile virus
ZIKV	Zika virus

PUBLICATIONS AND PRESENTATIONS

Accepted peer reviewed Journal Publications

Cabezas S, Bracho G, Aloia AL, Adamson PJ, Bonder CS, Smith JR, Gordon DL, Carr JM. Dengue Virus Induces Increased Activity of the Complement Alternative Pathway in Infected Cells. *J Virol.* 2018 Jun 29;92(14). pii: e00633-18. doi: 10.1128/JVI.00633-18. Print 2018 Jul 15. PMID: 29743365

Manuscripts in progress

Cabezas S., Gordon DL. and Carr JM. Alternative pathway *in vitro* activity assay in dengue virus infected supernatants.

Cabezas S, Rudd P., Mahalingam S., Ong L-C., Alonso, SL, Gordon DL. and Carr JM. Evaluation of FB and FH complement factors during severe DENV infection in AG129 mice.

Presentations

Cabezas S, Rudd P., Mahalingam S., Gordon DL. and Carr JM. Factor B and factor H dysregulation during dengue virus infection: *in vitro* and *in vivo* evidence. Australian Society for Microbiology (SA Branch), BD-Student Award Night, Adelaide, Australia, March 2016 (Oral presentation).

Cabezas S, Rudd P., Mahalingam S., Gordon DL. and Carr JM. Factor B and factor H dysregulation during dengue virus infection: *in vitro* and *in vivo* evidence. International Congress of Immunology (ICI) 2016, Melbourne, Australia, August 2016 (Poster presentation).

Cabezas S, Adamson PJ, Bonder CS, Smith JR, Gordon DL, Carr JM. Is the imbalance between factor B and factor H a major contributor to vascular dysfunction seen during severe dengue? Australian Society for Immunology (SA Branch), Immunology Retreat, Adelaide, Australia, May 2017 (Oral Presentation).

Cabezas S, Bracho G, Aloia AL, Adamson PJ, Gordon DL, Carr JM. Dengue virus induces dysregulation of the alternative complement pathway in human endothelial cells and macrophages by induction of factor B but defective production of extracellular factor H.

Australian Virology Society Scientific Meeting, AVS, Adelaide, Australia, December 5th-8th, 2017 (Oral Presentation).

Cabezas S, Bracho G, Aloia AL, Adamson PJ, Bonder CS, Smith JR, Gordon DL, Carr JM. Dengue virus induced alternative complement pathway dysregulation: contrasting effects on factor B and extracellular factor H production. 10th Global summit on Immunology and Cell biology, Osaka, Japan, May 11-12, 2018 (Oral Presentation).

CHAPTER I REVIEW OF THE LITERATURE

I.1 Dengue virus

I.1.1 General aspects and transmission

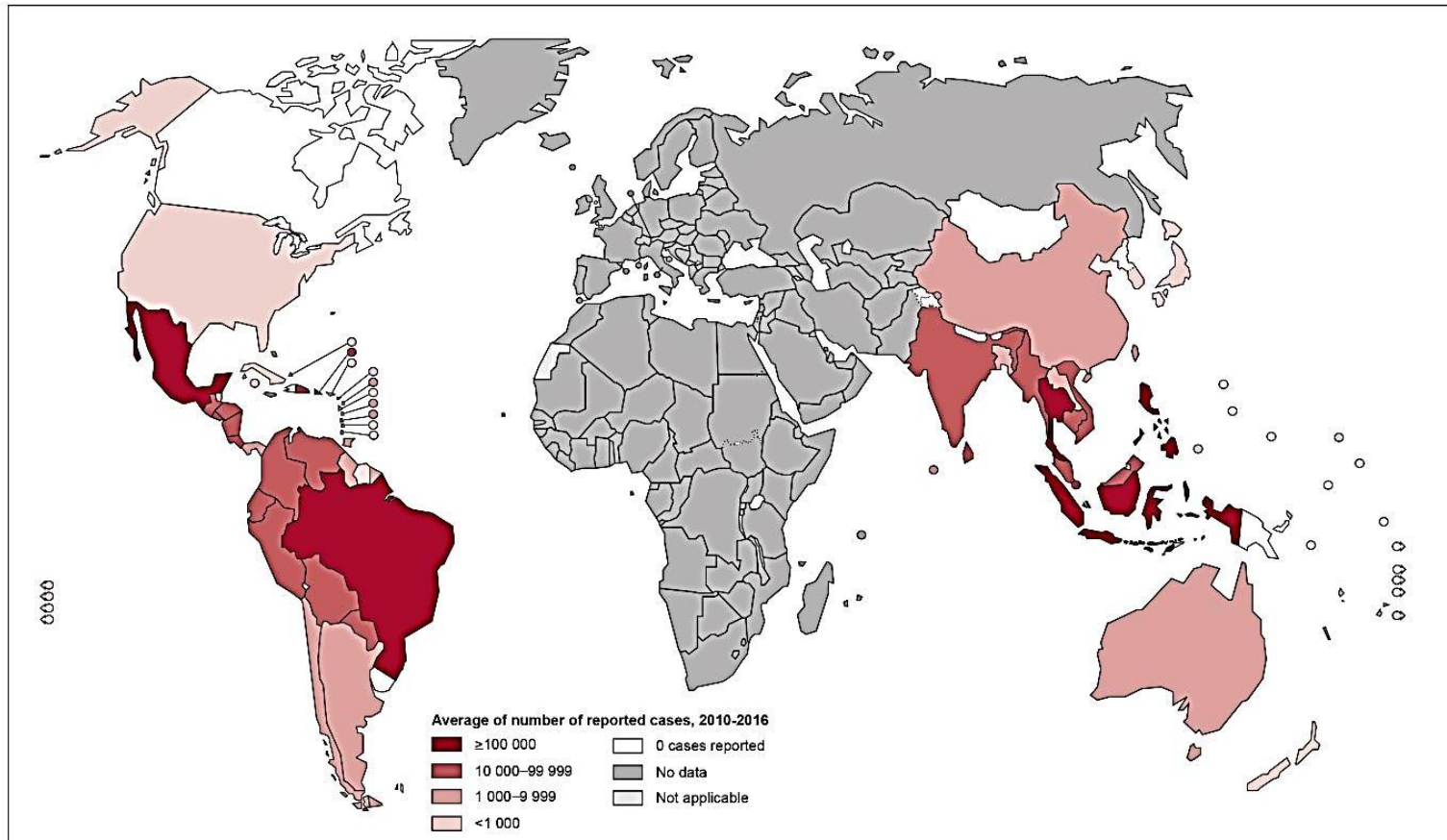
Dengue virus (DENV) has emerged as the most prevalent arthropod-borne virus affecting humans worldwide (Bhatt et al., 2013). DENV is an enveloped virus that belongs to the family *Flaviviridae*, genus *Flavivirus* and comprises four serotypes, DENV 1-4, which are clinically indistinguishable but genetically and antigenically distinct (Gubler, 1998). Serotypes 1 and 4 have a sequence homology of 73%, serotypes 3 and 4 have 54% homology while serotype 2 is considerably distinct from the other serotypes (Blok, 1985). The primary vector for DENV transmission is the mosquito *Aedes aegypti*, although *Aedes albopictus* is also responsible for the virus spread but to a lesser extent (Paupy et al., 2009). DENV is transmitted via the bite of infected mosquitoes and is mainly maintained in an urban cycle i.e. human-mosquito-human transmission cycle (Henchal and Putnak, 1990). Other modes of transmission have been described such as transplantation, transfusion of blood components, needle-stick injury and vertical transmission, but these are not responsible for the global spread and threat posed by DENV (Chye et al., 1997, Boussemart et al., 2001, Langgartner et al., 2002, Tan et al., 2005, Lanteri and Busch, 2012).

I.1.2 Epidemiology

The numbers of DENV infections have intensified in the past decades. This viral infection was first reported in 1954 (Quintos FN, 1954) and today around half of the world's population is estimated to be at risk of infection, especially in areas with cocirculation of multiple virus serotypes (Guzman et al., 2010, Bhatt et al., 2013). The World Health Organization (WHO) has estimated that 50 to 100 million dengue cases occur each year across the world, particularly in hyper-endemic regions in South America, Africa, Southeast Asia and Pacific (Figure I-1). Around 67 to 136 million cases manifest clinical symptoms at any level of severity and approximately 20 000 deaths occur annually. DENV is currently endemic in more than 100 countries (<http://www.who.int/denguecontrol/epidemiology/en/>, accessed 25 June 2018). Over 70% of the global burden of disease lies in South and South-East Asia, although an increase in the number of DENV cases has been reported in other parts of Asia, Latin America and the Caribbean (Nimmannitya et al., 1969, Guzman et al., 2010). DENV transmission also occurs on the African continent, but the number of cases has been difficult to quantify due

to poor public health monitoring (Sessions et al., 2013). Interestingly, in recent years, developed countries have experienced small outbreaks, with reports from Southern Europe, and the United States (Tomasello and Schlagenhauf, 2013). DengueNet represents a database supported by the WHO, to provide surveillance for global dengue epidemiology (<http://apps.who.int/globalatlas/default.asp>).

In Australia, DENV is not considered endemic since in most areas of the country *A. aegypti* or *A. albopictus* mosquitoes do not circulate. Particularly in North Queensland dengue is considered episodic. The incidence of the vector in this region has increased in the last decade, and dengue outbreaks are experienced every year, with all 4 serotypes reported to be present (Russell et al., 2009, Williams et al., 2014). In South Australia, dengue cases have been increasing in the last five years mainly due to travellers returning to the state from tropical holiday destinations such as Indonesia and Thailand (Knape et al., 2014, Quinn et al., 2018).



The boundaries and names shown and the designations used on this map do not imply the expression of any opinion whatsoever on the part of the World Health Organization concerning the legal status of any country, territory, city or area or of its authorities, or concerning the delimitation of its frontiers or boundaries. Dotted lines on maps represent approximate border lines for which there may not yet be full agreement. © WHO 2016. All rights reserved

Data Source: World Health Organization
 Map Production: Control of Neglected
 Tropical Diseases (NTD)
 World Health Organization



Figure I-1. Average number of suspected or confirmed dengue cases reported to WHO, 2010-2016

(<http://www.who.int/denguecontrol/epidemiology/en/>)

I.1.3 Clinical manifestations

Infection caused by any of the four serotypes of DENV are capable of producing dengue disease which is characterised by a spectrum of clinical manifestations ranging from a non-specific febrile illness, through to severe dengue (WHO, 2009). Symptoms may include severe headache, severe joint and muscle pain, retro-orbital pain, nausea and vomiting. The transition from a mild to a severe disease may be very rapid. The platelet count in a dengue patient drops drastically over a couple of days. During defervescence, patients may go into a critical phase characterised by increased capillary permeability, leading to a decrease in plasma volume (Halstead, 2007). Without adequate care or hospital attention, the patient may enter into a toxic stage of severe dengue that can be accompanied by bleeding and plasma leakage (dengue haemorrhagic fever, DHF) or hypovolemic shock (dengue shock syndrome, DSS) and disseminated intravascular coagulation, leading to potentially fatal multi-organ system failure (Halstead, 2007). The most recent WHO description of dengue classifies the disease as dengue with or without warning signs, in order to predict which patients will progress to severe infection (WHO, 2009). The dengue warning signs and the defining features of disease severity are summarised in Table I-1 (WHO, 2009).

Table I-1. Criteria for dengue warning signs and severe dengue (WHO, 2009).

Criteria for dengue warning signs	Criteria for severe dengue
<ul style="list-style-type: none"> -Abdominal pain or tenderness -Persistent vomiting -Clinical fluid accumulation -Mucosal bleed -Lethargy/restlessness -Liver enlargement >2 cm -Laboratory increase in haematocrit concurrent with rapid decrease in platelet count 	<ul style="list-style-type: none"> -Severe plasma leakage leading to <ol style="list-style-type: none"> 1) Shock and/or 2) Fluid accumulation with respiratory distress -Severe bleeding -Severe organ involvement <ul style="list-style-type: none"> • Liver: alanine transaminase or aspartate aminotransferase ≥ 1000 • Central nervous system: impaired consciousness • Heart and other organs

I.1.4 Vaccine and treatment

Effective vaccination is by far the best preventive strategy to reduce the global burden of DENV. Since the earliest efforts of Sabine in the 1940's, the scientific community have tried to develop a safe and effective vaccine; however many factors have hampered our ability to reach this goal. The main challenges to vaccine development include achieving neutralising protection against all four serotypes, the lack of specific animal models for testing vaccine candidates, the poor understanding of the pathogenesis of infection and the risk of dengue-primed individuals developing severe disease on exposure to a different serotype (see section I.1.8.1.a). Many DENV vaccine strategies have been investigated, and some of them are currently in preclinical or clinical stages of development (reviewed in (Ramakrishnan et al., 2015)). The approaches carried out so far include live attenuated, chimeric, DNA, subunit and inactivated vaccines (<http://www.denguevaccine.org>). Currently, the first and only vaccine approved for use in endemic populations is the recombinant tetravalent, live-attenuated, yellow-fever-dengue virus vaccine: CYD-TDV or Dengvaxia® (Guy et al., 2009, Guy et al., 2010), developed and produced by Sanofi Pasteur. Dengvaxia® consists of four recombinant live attenuated vaccines, expressing the structural genes encoding the pre-membrane (prM) and envelope (E) proteins of each of the four serotypes on the attenuated yellow fever 17D virus strain genetic backbone (Guy et al., 2010, Guy and Jackson, 2016). So far, this vaccine has been licensed in 19 dengue endemic countries for individuals 9 years of age and older (Guy and Jackson, 2016, Henein et al., 2017, Rabaa et al., 2017). In November 2017, Sanofi Pasteur released an update on the long-term safety of Dengvaxia®. Vaccine recipients with evidence of prior DENV infection continued to benefit from vaccination, since a decrease in hospitalized and severe dengue cases has been observed. Vaccine recipients without prior DENV infection, however, had an increased risk of hospitalized and severe dengue, including those 9 years of age and older (Wichmann et al., 2017). It has been recommended by WHO to determine pre- vaccination dengue infection status before vaccination (<http://www.who.int/wer/2016/wer9130.pdf>), which is challenging and inconvenient especially in endemic and third world countries due to the absence of the appropriate assays to determine DENV immune status, in addition to the lack of funding and established health surveillance systems.

There is no specific treatment for dengue patients. Generally, medical support is in the form of managing symptoms by administration of antipyretics and fluids and is dependent on symptoms. Severe dengue, DHF or DSS cases often require seven to ten days of

hospitalisation and additional treatments including blood and/or platelet transfusions, blood pressure monitoring and other intensive laboratory and clinical measures (Chuansumrit et al., 2000, Chuansumrit and Chaiyaratana, 2014). This is particularly problematic for healthcare systems during DENV outbreaks, in resource poor settings.

1.1.5 Structural overview of dengue virion, proteins and replication strategy

DENV is a single-stranded, positive-sense enveloped RNA virus of approximately 50 nm in diameter that adopts an icosahedral symmetry (Kuhn et al., 2002, Rey, 2003). The genome is approximately 11 kb that contains a 5' cap, 5' and 3' untranslated regions (UTR) and a single open reading frame (ORF) (Kuhn et al., 2002). The ORF encodes for a large polyprotein that is co- and post-translationally cleaved into three structural proteins: capsid (C), precursor membrane (prM) and envelope (E) and seven non-structural proteins: NS1, NS2A, NS2B, NS3, NS4A, NS4B and NS5 (Figure I-2). E and prM structural proteins are viral surface glycoproteins attached to the lipid bilayer of the virion (Figure I-3), and have roles in host cell entry and virus maturation, respectively (Huang et al., 1997, Lindenbach and Rice, 1999, Lindenbach, 2011). The C protein binds the genomic RNA to form the nucleocapsid core (Figure I-3). The non-structural proteins have a variety of different functions including formation of the viral replication complex inside the host cells (Lindenbach, 2011). NS3 and NS5 possess enzymatic activities of the helicase/protease and methylase/RNA-dependent RNA polymerase, respectively while NS2A, NS2B, NS4A and NS4B are transmembrane proteins located within the membrane of the endoplasmic reticulum (ER) that interacts with NS3 and anchors the replication complex to the ER membrane (Umareddy et al., 2006, Lindenbach, 2011, Zou et al., 2015). NS1 has been suggested to participate in genome replication by associating with the luminal side of the replication compartment. NS1 is also transported to the cell surface, where it either remains associated with the cell membrane or is secreted as a soluble, hexameric molecule (Mackenzie et al., 1996, Muller and Young, 2013). Secreted NS1 is found at high levels in the circulation of dengue patients (Alcon et al., 2002, Muller and Young, 2013), is used as a diagnostic antigen (Muller et al., 2017) and recently has been proposed as an important part of the pathogenic effects of DENV on the vascular endothelium (Beatty et al., 2015, Glasner et al., 2017, Glasner et al., 2018) (see section 1.1.8.2.a).

After virus entry, the viral genome is first transcribed into a negative-sense RNA, thus forming a double strand replication intermediate which then serves as a template for the

synthesis of a number of capped positive single strand RNA viral genomes (reviewed in (Saeedi and Geiss, 2013)). The newly generated positive-strand viral genome is immediately translated into the viral polyprotein and replicated in the ER, which undergoes hypertrophy after flavivirus infection (Stohlman et al., 1975, Mackenzie et al., 1998). All proteins, except for C, NS3 and NS5 that remain in the cytoplasm, are translated into the lumen or membrane of the ER (Perera and Kuhn, 2008, Lindenbach, 2011). The polyprotein is cleaved into individual viral proteins by host signals inside the lumen of the ER and by the viral protease NS2B-NS3 in the cytoplasm (Perera and Kuhn, 2008, Lindenbach, 2011). The assembly of the viral particles (association of the viral genome with the structural proteins), occurs in the ER and the new virions are then transported through the *trans*-Golgi network and finally released from the host cell by exocytosis (Figure I-4) (Mukhopadhyay et al., 2005, Lindenbach, 2011).

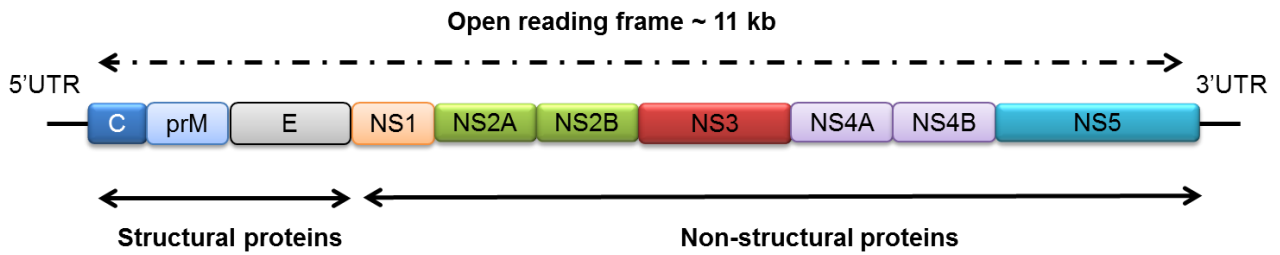


Figure I-2. Schematic representation of the structure of DENV genome with structural and non-structural proteins

The single open reading frame encodes a polyprotein containing three structural proteins and seven non-structural proteins: capsid (C), precursor membrane (prM) and envelope (E) and seven non-structural proteins: NS1, NS2A, NS2B, NS3 (helicase/protease), NS4A, NS4B and NS5 (methylase/RNA-dependent RNA polymerase). 5'UTR and 3'UTR are the non-coding regions.

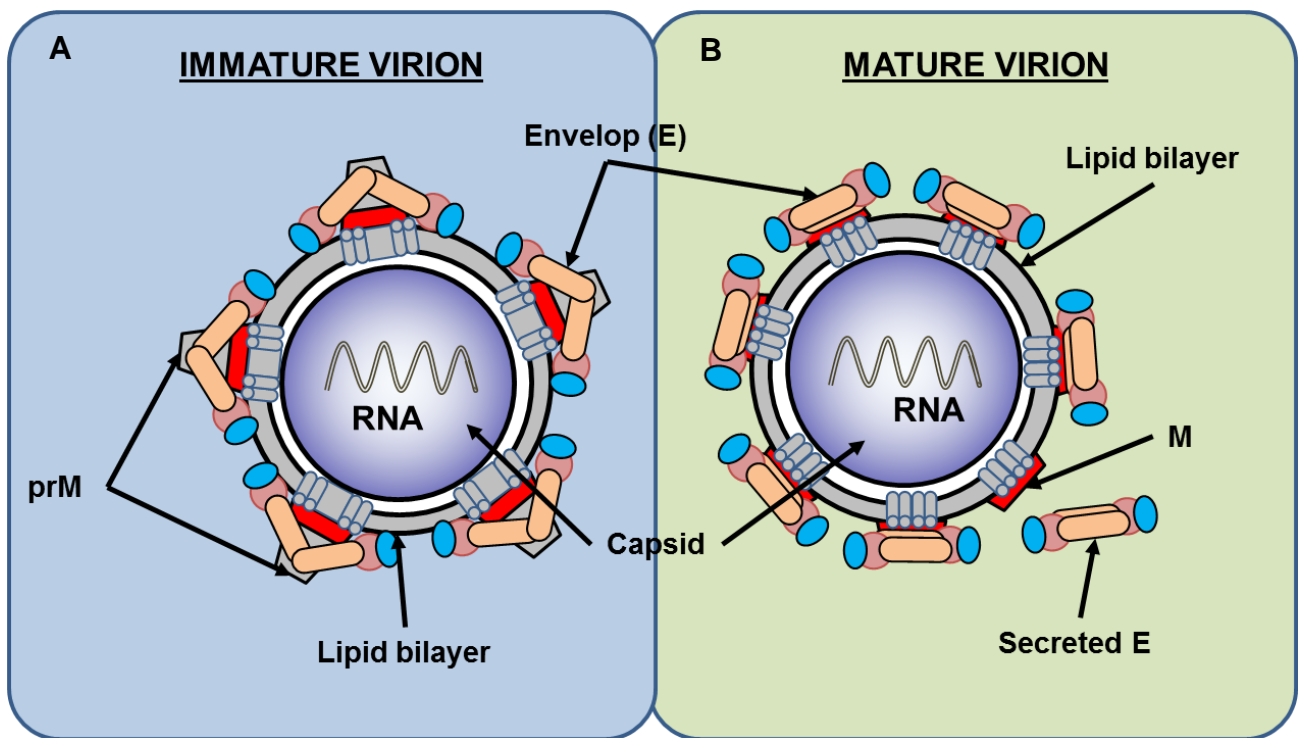


Figure I-3. Schematic representation of a DENV particle

A: immature virion. **B:** mature virion. The structural proteins are designated E, prM/M, and C. The virus particle consists of an RNA-capsid protein complex, surrounded by a lipid bilayer. The proteins present on the surface of the dengue immature virus (**A**) are the E and prM. The maturation process occurs both intra and extracellularly, cleaving prM to yield the mature virus surface containing E and M proteins (**B**).

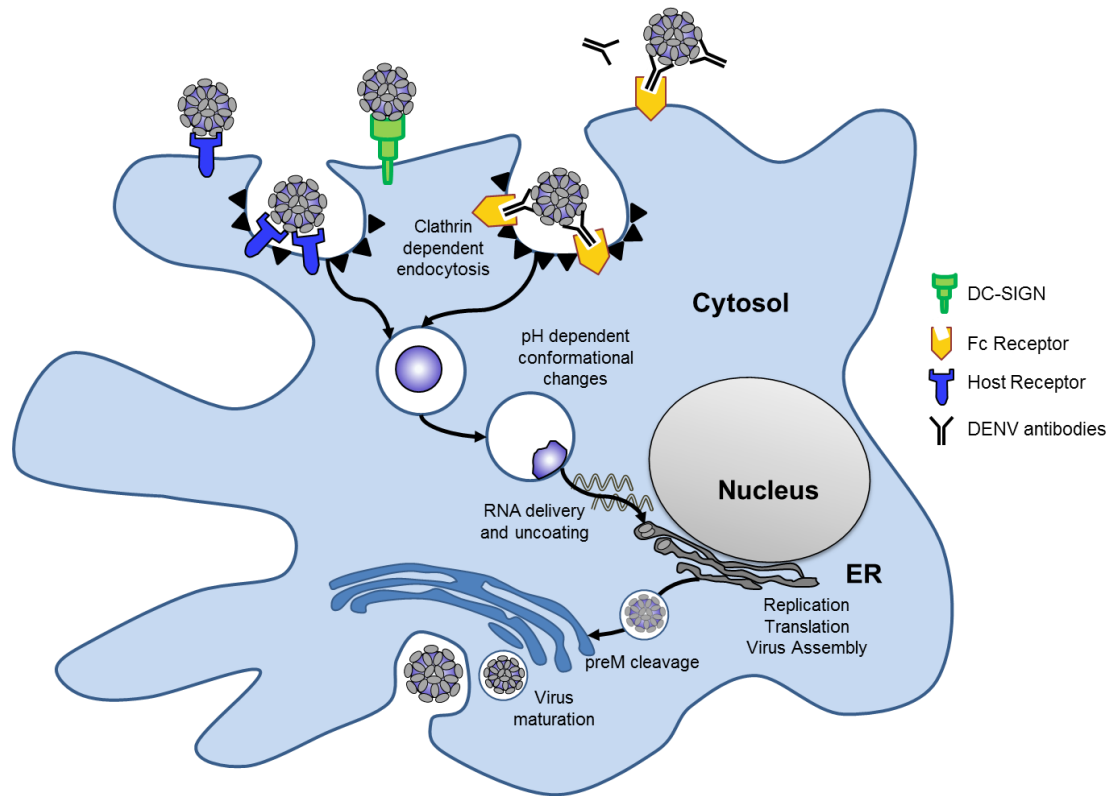


Figure I-4. Schematic representation of DENV replication cycle

DENV binds to target cells via diverse group of receptors: DC-SIGN, Fc receptor, GAG molecules, anti-DENV antibodies. DENV enters host cells via receptor-mediated endocytosis, and following endosomal acidification and conformational changes in the viral prM/M and E proteins, the viral RNA is uncoated and released into the cytosol. The viral RNA migrates to the endoplasmic reticulum (ER) where its translation, replication and assembly occur. Packaged virions are transported to the Golgi, where they undergo proteolytic cleavage that results in virus maturation. Mature DENV virions are then exported from the cell using the host secretory system.

I.1.6 Receptors and routes of dengue virus entry into the host cells

DENV infection starts with virus attachment to the target cell through the interaction between viral surface proteins and receptor molecules on the cell surface. E protein is the main molecule mediating DENV attachment to the cell surface and the domain III of this protein harbors the receptor binding site(s) although the specific-binding motif(s) are yet to be determined (Hung et al., 2004, Gromowski and Barrett, 2007).

A number of cell types are susceptible to DENV infection and the receptors that facilitate this are diverse. Both vertebrate and mosquito hosts harbour different receptors and viral receptors also differ from one cell type to another within the same host (Okamoto et al., 2012, Wan et al., 2013, Cruz-Oliveira et al., 2015). For vertebrate cells, glycosaminoglycans (GAGs) such as heparan sulfate and lectins are responsible for the first contact with the virus and therefore mediate and facilitate concentration and attachment of the virus particles at the cell surface (Chen et al., 1997, Aoki et al., 2006, Wichit et al., 2011). Various cell-type specific receptors that have been suggested for DENV entry are described below.

In dendritic cells, one of the main targets of DENV replication *in vivo* (Wu et al., 2000, Marovich et al., 2001) the adhesion molecule 3-grabbing non-integrin, DC-SIGN has been identified as the main receptor for virus entry (Navarro-Sanchez et al., 2003); while in monocytes and macrophages, another key target of virus replication, the mannose receptor (Miller et al., 2008), the lipopolysaccharide (LPS) receptor CD14 (Chen et al., 1999) and to a lesser extent the stress-induced heat-shock proteins HSP70 and HSP90 (Chen et al., 1999, Reyes-Del Valle et al., 2005) have suggested roles in DENV entry.

In endothelial cells (EC), a major site for DENV disease pathogenesis, the heparan sulfate glycochain and the protein disulfide isomerase have been suggested to mediate virus-specific binding and virus entry, respectively (Okamoto et al., 2012, Wan et al., 2012). Specifically, in liver EC the L-SIGN molecule (a homologue of DC-SIGN) has also been identified as a virus-receptor (Navarro-Sanchez et al., 2003, Tassaneetrithep et al., 2003).

In hepatocytes, a potential target cell for DENV, the ER-resident chaperonin GRP78 has been proposed as a candidate DENV receptor (Jindadamrongwech et al., 2004, Upanan et al., 2008). The role of the T-cell immunoglobulin and mucin domain (TIM) and TAM (TYRO3/AXL/MER) families of transmembrane receptors in DENV infection has also been described, with interaction of these proteins dependent on DENV E protein

phosphatidylserine that potentiates virus endocytosis (Meertens et al., 2012). TIM binds DENV directly, whereas TAM interacts indirectly with DENV via two bridge proteins, Gas6 and ProS (Meertens et al., 2012).

In mosquitoes, the best characterised DENV receptor is prohibitin, a 35KDa protein identified by interaction-studies of DENV-2 with C6/36 cells (a cell lineage derived from the larval stage of *A. albopictus*), CCL-125 cells (an *A. aegypti* derived cell line) and *A. aegypti* adult mosquitoes (Kuadkitkan et al., 2010). Using C6/36 cells and different mosquito tissues such as the midgut and salivary glands, other putative receptors have been identified, such as two glycoproteins of 40 and 45 KDa (Salas-Benito and del Angel, 1997, Yazı Mendoza et al., 2002, Reyes-del Valle and del Angel, 2004).

After DENV recognition by cellular receptors, the viral particle is internalised via clathrin-mediated endocytosis or non-classical clathrin-independent endocytic pathways, depending on the host cell and virus serotype (Krishnan et al., 2007, Acosta et al., 2008, Mosso et al., 2008, Acosta et al., 2009, Acosta et al., 2012, Alhoot et al., 2012, Acosta et al., 2014a, Acosta et al., 2014b). The clathrin-dependent endocytosis is the most common pathway and has been shown in DENV (1 to 4)-infected C6/36, cervical cancer derived cells (HeLa), adenocarcinoma human alveolar basal epithelial cells (A546) and hepatocyte-derived carcinoma cell lines, Huh7 and HepG2 cells (Krishnan et al., 2007, van der Schaar et al., 2007, Acosta et al., 2008, Mosso et al., 2008, Acosta et al., 2009). The non-classical clathrin-independent endocytic pathway has been specifically described in Vero cells infected with DENV-2 (Acosta et al., 2009). Regardless of which pathway the virus uses for cell entry, after endocytosis a pH-dependent conformational change allows the viral RNA to be released from the endosome into the cytoplasm, followed by translation in the ER and replication proceeds as described in section 1.1.5.

It is evident that DENV does not use a unique, specific receptor to enter the host cells, but recognises and binds to a plethora of cell membrane proteins, possibly in a serotype-specific manner. The molecular flexibility that the E-protein must accommodate to achieve this, is remarkable. One hypothesised rationale for this phenomenon is evolutionary i.e.; the virus uses a diversity of receptor molecules as a strategy to increase its infection capacity and pathogenesis (Cruz-Oliveira et al., 2015).

I.1.7 Immune responses triggered during DENV infection

I.1.7.1 Innate immune response

Pattern recognition receptors such as Toll-like receptors (TLRs), particularly TLR3, TLR7 and TLR8, and intracellular sensors such as the helicases melanoma differentiation-associated protein 5 (MDA5) and the retinoic acid-inducible gene I (RIG-I) are some of the first lines of defence in the innate immune recognition of double-stranded RNA (dsRNA), single-stranded RNA or modified RNA. An overview of the general intracellular response to TLRs and RIG-I/MDA-5 recognition of viral RNA, including key signalling intermediates, is shown in Figure I-5. Recognition of viral dsRNA by TLR3 leads to the phosphorylation of Toll/IL-1 receptor (TIR) domain-containing-adaptor-inducing-interferon β (TRIF). TRIF interacts with tumour necrosis factor (TNF) receptor associated factors (TRAF) 3 and 6 which promote the activation and nuclear translocation of the nuclear factor kappa B ($\text{NF}\kappa\beta$). TRAF3 stimulates interferon regulatory factor (IRF) 3 phosphorylation and nuclear translocation of IRF3. Activation and nuclear translocation of IRF3 and $\text{NF}\kappa\beta$ induce transcription and production of type I interferon such as $\text{IFN-}\alpha/\beta$, interferon stimulated genes (ISGs) and chemokines (Figure I-5) (Tsai et al., 2009, Sariol et al., 2011, Lee et al., 2012). Recognition of single-stranded RNA by TLR7 and 8 activates TRAF6 which promotes IRF7 phosphorylation to finally induce transcription of $\text{IFN-}\alpha$ (Sariol et al., 2011) (Figure I-5). MDA5 and RIG-I are pre-existing cellular RNA sensors and are further induced during DENV infection and synergise with TLR3 to limit DENV replication (Nasirudeen et al., 2011). As described above, both molecules are sensors of dsRNA and are able to distinguish host RNA from viral RNA (Zinzula and Tramontano, 2013). Following dsRNA activation of MDA-5/RIG-I, signalling is induced through the mitochondrial antiviral signalling (MAVS) protein on mitochondria, which oligomerises and attracts TRAF3 and 6 to further activate the signalling cascade, as described above (Figure I-5) (Liu et al., 2013).

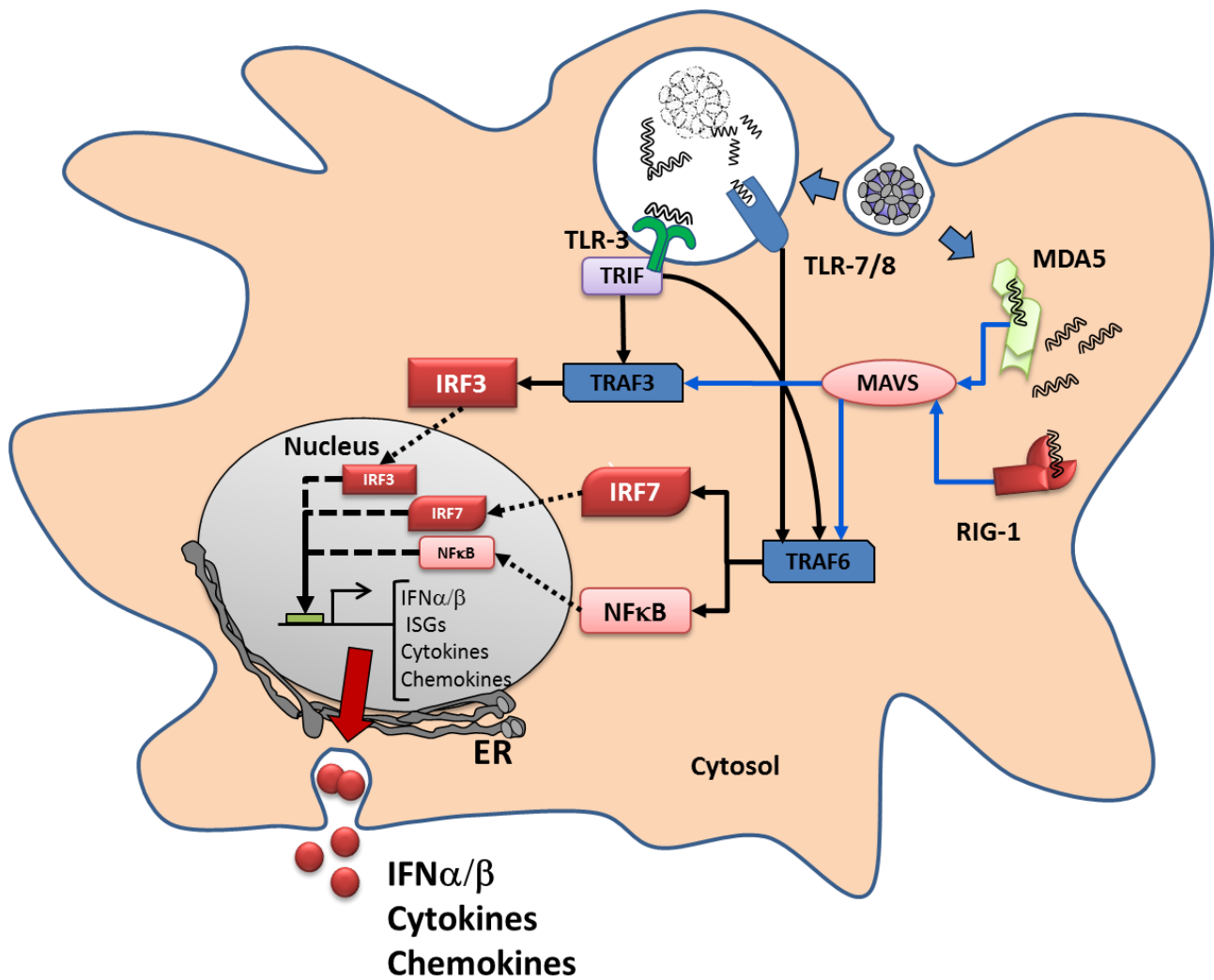


Figure I-5. Host innate immune response to DENV infection

DENV RNA is recognized by pattern recognition receptors TLR3, 7 and 8, MDA5 and RIG-I, resulting in activation of TRAF molecules that will promote the activation of the nuclear factor NFκβ and the production of IFN-α/β, ISGs, cytokines and chemokines.

IFN- α/β induction is a powerful anti-viral response against DENV infection. Virus-infected cells secreting IFN- α/β trigger autocrine and paracrine signals to induce cellular antiviral effector responses that inhibit viral infection. These signals occur through the IFN- α/β receptor (IFNAR) and activates the Janus kinase/signal transducers and activators of transcription (JAK/STAT) signalling pathway (Figure I-6) (Velazquez et al., 1992). The activation of this pathway results in the phosphorylation and dimerization of several signal transducer and activator of transcription (STAT) molecules, including STAT1 to 5. The combination of STAT1, STAT2 and IRF9 forms the interferon stimulating gene factor 3 (ISGF3) complex that translocates to the nucleus and binds to IFN-stimulated response elements (ISRE) located in the promoter region of ISGs (Figure I-6). This in turn, results in the production of numerous antiviral proteins and pro-inflammatory cytokines and chemokines (Platanias, 2005).

Thus, key transcription factors are stimulated in response to DENV infection such as NF κ B, STAT family members and IRF. These known transcription factors that induce IFN and cytokines and chemokines have been specifically investigated *in silico* in relation to induction of complement factor H (FH) and factor B (FB), as further described in chapters V and VI.

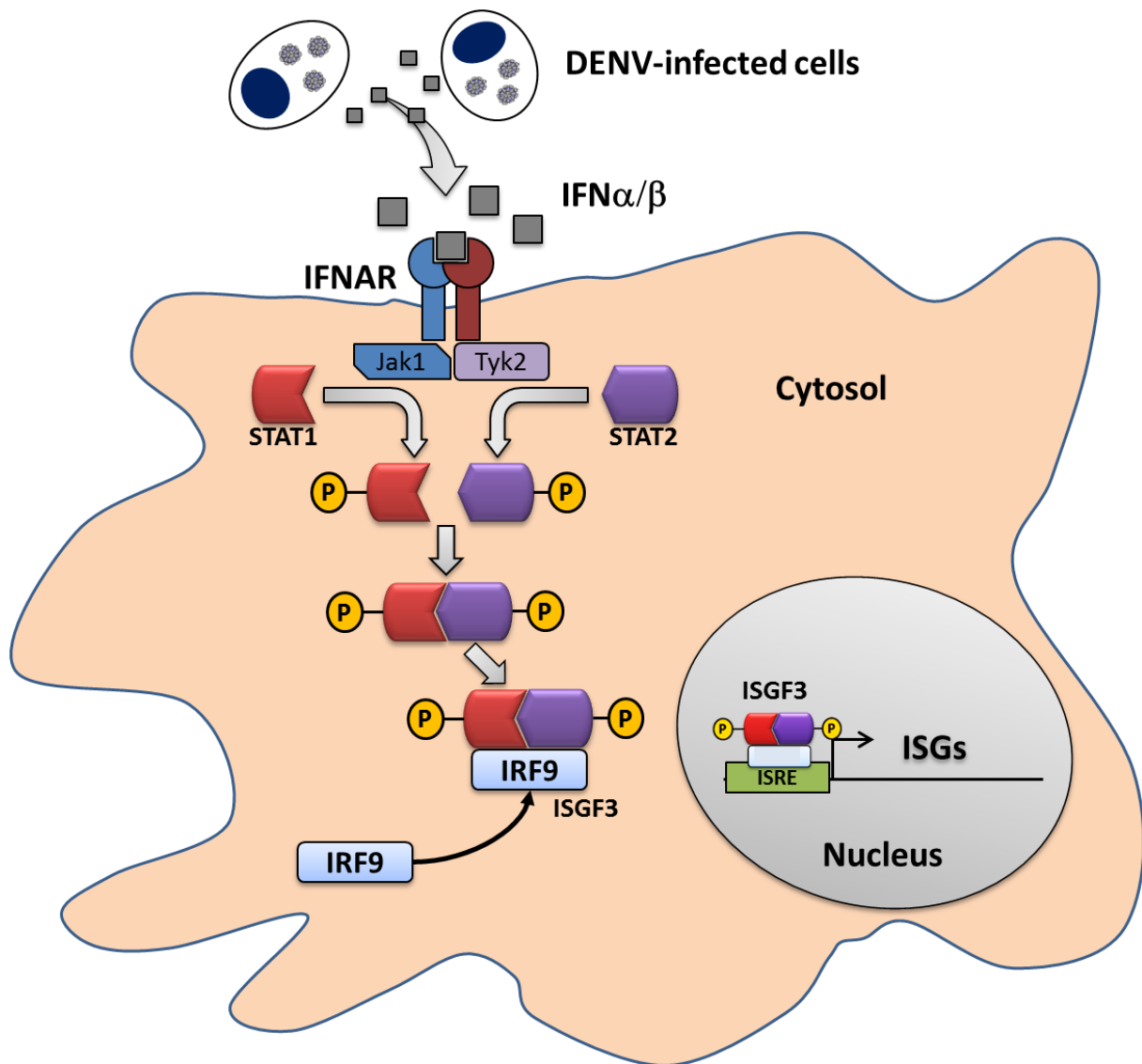


Figure I-6. Type I IFN response is triggered upon DENV infection

Binding of IFN- α/β to its receptor IFNAR leads to the activation of tyrosine kinases, phosphorylation of STAT1 and STAT2 that form a heterodimer that associates with IRF9 to finally form ISGF3 complex, which translocates to the nucleus and binds to ISRE to induce ISGs.

1.1.7.2 Adaptive immune response against DENV

1.1.7.2.a The humoral response

Anti-DENV antibodies are known to be crucial in the protection against DENV infection. Primary DENV infections induce a relatively conventional immune response characterised by an early IgM response and followed by an IgG response (Vaughn et al., 1997, Koraka et al., 2001). In a secondary infection a rapid IgG response is produced with a reduced IgM response (Vaughn et al., 1997). The predominant antibody response is directed against E protein, although an expanded response against C, prM, NS1, NS3 and NS5 is also detected (Churdboonchart et al., 1991, Valdes et al., 2000). Neutralising antibodies are crucial for protection against DENV infection. Neutralisation is achieved when sufficient antibody molecules bind to specific epitopes on the E protein and prevent binding to the target cell (Halstead, 2002). Specifically, it has been shown that effective virion neutralisation is achieved when at least 180 copies of the E protein are targeted by specific antibody molecules (Pierson, 2010). The number of neutralising molecules is not the sole determinant for neutralisation, with antibody affinity and accessibility of the epitope on the virion surface and its interaction with a receptor-binding domain also contributing (Pierson and Diamond, 2008, Rodrigo et al., 2009). Domain III of E protein contains the majority of specific and most potent neutralising epitopes while domain I and II mainly possess cross-reactive and weakly neutralising epitopes (Crill and Roehrig, 2001, Crill and Chang, 2004, Crill et al., 2009, Wahala et al., 2009). The number of specific and neutralising epitopes, however, are very low (Wahala et al., 2009) and these epitopes can differ between serotypes. Thus, long-lasting protective immunity is serotype specific (homotypic immunity) (Sabin, 1952). In contrast, cross-reactive neutralising and non-neutralising antibody responses against heterologous serotype (heterotypic immunity) confer short-term protection only and importantly, these cross-reactive but not cross protective antibodies play a critical role in the enhancement of disease severity, as discussed in section 1.1.8.1.a (Halstead and O'Rourke, 1977a, Halstead and O'Rourke, 1977b, Vaughn et al., 2000, Halstead, 2003).

1.1.7.2.b The cellular immune response to DENV

Dengue-specific CD4⁺ and CD8⁺ T cell responses are needed for protection against the virus and are actually triggered upon infection due to the presence of multiple T cell epitopes mainly in NS3 and NS5 viral proteins (Simmons et al., 2005, Appanna et al., 2007). Interestingly, it has been shown that during the acute phase of a primary infection, the T-cell response is almost undetectable or very low and thus, may play a weak to

moderate role in viral clearance or protection (Gil et al., 2009, Yauch et al., 2009). In contrast, healthy individuals with past dengue infection living in an endemic area, had high levels and polyfunctional T-cell responses to a large number of DENV specific CD8+T-cell epitopes (Weiskopf et al., 2013). Therefore, it seems that elevated levels and polyfunctional CD8 T-cell responses are associated with protection in a particular population (Weiskopf et al., 2013). In fact, several anti-DENV vaccine strategies have sought to induce efficient induction of specific CD8+ and CD4+ T-cell responses (Gil et al., 2016, Marcos et al., 2016, Gil et al., 2017). Conversely, a number of studies have reported that a high but pathogenic cross-reactive T-cell response is triggered in individuals following a secondary natural infection (Mathew et al., 1998, Dong et al., 2007, Imrie et al., 2007). This response is characterised by high level of apoptosis and low avidity for the infecting serotype but higher avidity for the primary virus that caused the first infection. This phenomenon is called 'antigenic sin' and intends to explain the deleterious role of activated T-cell response in the context of secondary infections (Mongkolsapaya et al., 2003, Mongkolsapaya et al., 2006, Sreaton and Mongkolsapaya, 2006).

Cytokines are also part of the cellular immune response that plays a crucial role in protection against DENV infection. The production of proinflammatory cytokines such as IFN- γ , IL-12 and IL-18 is considered essential for protection during infection (Fagundes et al., 2011, Costa et al., 2012). Although the antiviral role of IFN- γ against DENV has been controversial (Shresta et al., 2004, Priyadarshini et al., 2010, Butthep et al., 2012), it has been shown that sustained levels of this cytokine in the sera of DENV-infected individuals correlates with protection and sub-clinical disease, and its secretion correlates with the induction of a cytotoxic T-cell response (Gunther et al., 2011, Weiskopf et al., 2013, Jeewandara et al., 2015). There is evidence, however, that the reactivation of existing memory T-cells by a heterologous serotype in secondary infections results in overly exuberant cytokine responses that lead to increased vascular permeability and severe disease (Rothman, 2010).

The chemokine system also appears to have a protective role during DENV infection. The activation of CXCR3 and the production of CXCL10 have been associated with host resistance. CXCL10 seems to compete with the virus for binding to heparan sulfate on the cell surface and in the presence of high levels of this chemokine there is a reduction of viral replication (Chen et al., 2006). Interestingly, CXCL10 deficient mice had impaired resistance to DENV primary infection, due to a defect in activation of CD8+ T-cells (Hsieh

et al., 2006).

It is worth noting that despite the important role that the humoral and cellular immune responses play in protection against DENV, these responses can also contribute to disease enhancement. This complicates the study and analysis of the immune responses and the understanding of the disease pathogenesis, which as below, is intimately linked to the host immune response.

1.1.8 Dengue virus pathogenesis

The pathogenesis of DENV infection is a multifactorial and a very complex phenomenon. Protective versus pathological outcome depends on several factors including host genetics and the virulence and characteristics of the infective virus/serotype/strain. A major association with severity of disease, however, is the immunological background and prior exposure to DENV (Kouri et al., 1987, Guzman and Kouri, 2008, Rothman, 2011).

1.1.8.1 Host risk factors

1.1.8.1.a The humoral response and antibody-dependent enhancement

As mentioned above, antibody-mediated immune responses are vital for controlling DENV infection and virus-neutralising antibodies have been accepted as a correlate of protection (Monath et al., 2002, Belmusto-Worn et al., 2005, Hombach et al., 2005). As in section 1.1.7.2.a, experimental and epidemiological evidence demonstrate that primary DENV infection provides lifelong immunity and protection against the infecting serotype (homotypic immunity), but secondary infection with a different serotype (heterotypic immunity) confers transient and short-lived cross-protection against heterologous serotypes (Sabin, 1950). These pre-existing heterologous antibodies not only may fail to neutralise a new secondary infecting serotype but can enhance viral uptake through Fcγ receptor-bearing cells, particularly monocytes and macrophages (Halstead and O'Rourke, 1977a, Halstead and O'Rourke, 1977b, Vaughn et al., 2000). This phenomenon, known as antibody dependent-enhancement (ADE), potentially enhances the risks of developing severe disease by increasing the number of virus-infected cells (Halstead, 2003, Mathew and Rothman, 2008) but also may functionally alter the infected cell, for example to increase production of inflammatory cytokines and chemokines (reviewed in (Thomas et al., 2006)). The ADE hypothesis has been supported by epidemiological evidence where the most severe forms of the disease, DHF and DSS, occur mostly in individuals during secondary infection with a different serotype and in infants with a primary infection born to dengue-immune mothers (Chau et al., 2008, Moi et al., 2013, Halstead, 2014).

Additionally, the ADE theory has been supported by experimental models in primates (Moi et al., 2014) and mouse models of secondary DENV infection (Ng et al., 2014, Lee et al., 2016, Martinez Gomez et al., 2016). In particular, a mouse model of maternal enhancement of DENV disease severity in off-spring during a primary infection, is utilised in chapter VI of this thesis, and further described in section I.1.9.2.c.

The role of tertiary and quaternary infections, probably common in endemic countries, in the pathogenesis of the disease is not clear but data from hospitalised patients has suggested that these infections are clinically silent or very mild (Gibbons et al., 2007).

I.1.8.1.b T-cell response

The cellular immune response, although playing a role in clearing DENV infection, is also involved in the development of severe disease. Secondary dengue infections show high expansion of CD8⁺ T-cells with low affinity and avidity for the current infecting serotype and high affinity for the presumed previous infecting serotype (phenomenon of antigenic sin as discussed in section I.1.7.2.b) (Mongkolsapaya et al., 2003, Screaton and Mongkolsapaya, 2006). Due to the low affinity of the memory activated T-cells, mechanisms of viral clearance are less efficient contributing to the pathogenesis of the disease (Rothman, 2011).

In general, high levels of CD8⁺ T-cell activation have been found to correlate with disease severity and capillary leakage (Rothman, 2011). Furthermore, CD8⁺ T-cell responses in severe patients are mostly mono-functional; they only produce IFN- γ and/or TNF α , and rarely CD107a (a marker for cytotoxic degranulation). On the contrary, in patients with mild dengue disease, more CD8⁺ T-cells express CD107a and just a few cells produce only IFN- γ and/or TNF α (Duangchinda et al., 2010).

In contrast to CD8⁺ T-cell responses, DENV-specific CD4⁺ T-cells have been less studied. Within this context, CD4⁺ T-cells stimulated with a peptide from a heterologous serotype resulted in more TNF α -producing cells than IFN- γ producers relative to stimulation with homologous peptides, suggesting that the differential phenotypes amongst these cell populations are dependent on the type of antigenic stimulation (Mangada and Rothman, 2005).

The role of T regulatory cells (Tregs) during DENV infection is not clear. It has been proposed, however, that Tregs are activated and functional in acute infection and probably have a role in suppression of the production of vasoactive cytokines (Luhn et al., 2007). In

addition, the ratio of Treg cells to effector T-cell responses is increased in patients with mild compared to severe disease, suggesting an important role for this cell type in controlling pathogenic effector T-cell responses (Luhn et al., 2007).

1.1.8.1.c Cytokine storm

Increased levels of pro-inflammatory and inflammatory cytokines, secreted from innate and activated cross-reactive T-cells, are observed in patients with DHF/DSS. In particular, higher concentrations of $\text{TNF}\alpha$, IL-10, IL-6, IL-8, macrophage migration inhibitory factor, matrix metalloproteinases among others, have been observed in those patients with severe disease with rapid changes over the course of illness (Perez et al., 2004, Nguyen et al., 2005, Chakravarti and Kumaria, 2006, Basu et al., 2008). This inflammatory environment is thought to mediate permeability in the vascular endothelium, allowing fluid and small molecules to leak from the intravascular space and contributing to the decrease in blood volume and electrolytes, and additionally contribute to thrombocytopenia or reduced platelets, a key haematological measure that is associated with severe dengue (Pang et al., 2007, Appanna et al., 2012). It is hypothesised that secreted cytokines and vasoactive factors play a mutually synergistic role at the endothelial surface to induce vascular changes and dysfunction in the coagulation system. For instance, $\text{TNF}\alpha$ promotes increased endothelial permeability while IL-10 correlates with reduced levels of platelets and reduced platelet function (Anderson et al., 1997, Libraty et al., 2002a). Likewise, elevations of IL-6 and IL-8 have been associated with disordered coagulation and fibrinolysis in dengue (Huang et al., 2001, Martina et al., 2009). This disordered coagulation together with plasma leak and thrombocytopenia is likely to contribute to the haemorrhage and bleeding tendencies, and conversely disseminated intravascular coagulation observed in some cases of severe disease (Martina et al., 2009).

Activated T-cells, monocytes, macrophages and mast cells have been demonstrated to contribute to the increased production of pro- and inflammatory cytokines that converge on the EC and mediate changes in vascular permeability (Luplertlop et al., 2006, Rothman, 2011, Puerta-Guardo et al., 2013). Since EC are not a major site for DENV replication (Calvert et al., 2015), viral infection of these cells is not likely to contribute to circulating viremia but infection or activation of EC may also contribute to the cytokine storm responsible for vascular permeability changes in severe dengue.

1.1.8.1.d Other host factors

Other variables, apart from host-immune factors, such as age, gender, race, genetic susceptibility determinants, and pre-existing medical conditions shape the outcome of DENV infection. Children of 1 to 5 years of age experience more severe symptoms and have higher risks of fatal outcomes than older children and adults (Gamble et al., 2000, Guzman et al., 2002). This has been associated with the fact that young children have intrinsically more permeable vascular endothelium (Gamble et al., 2000).

In relation to gender, women are more likely to develop DSS and have higher mortality rates (Anders et al., 2011). Also, African-American individuals have been reported to experience reduced severity of DENV disease as compared with Caucasians (Sierra et al., 2007).

Pre-existing co-morbidities such as asthma and diabetes increase dengue disease severity (Pang et al., 2017). Additionally, sickle-cell anaemia, perhaps due to changes in red blood cell coagulation, and other host genetic characteristics have been associated with enhanced susceptibility to DSS (Rankine-Mullings et al., 2015). This is the case for human leukocyte antigen (HLA) and non-HLA molecules (e.g., Fc γ receptor IIA and vitamin D receptor) (Sierra et al., 2007). For instance, certain HLA polymorphisms have been associated with either protection from or susceptibility to severe dengue (Stephens et al., 2002, Appanna et al., 2010). Specifically, HLA-A*24 has been found to be a risk factor for developing severe dengue in Vietnam (Loke et al., 2001) and also Malaysia (Appanna et al., 2010). It has been proposed that the association between HLA polymorphisms and dengue severity is probably due to the differential and pathogenic T-cell responses that are generated to specific HLA-restricted viral epitopes (Duan et al., 2012). Specific associations of disease severity with genetic polymorphisms in genes for factors implicated above as part of the 'cytokine storm' have been investigated. TNF- α 308A allele, for instance, is predominant in DF patients with haemorrhagic manifestations (Fernandez-Mestre et al., 2004) In general, these specific risk require more research to understand the underlying rationale and significance of the impact of host factors as determinants of outcome of dengue disease severity. To date, except for children 1-5 years and pre-existing co-morbidities, none of these other host factors have been reliable enough associations to incorporate into clinical algorithms or to use as biomarkers to predict and manage the potential for developing severe dengue.

1.1.8.2 Viral factors

In addition to host immune factors, viral determinants have also been linked epidemiologically to more severe disease. Interestingly, of the four DENV serotypes, DENV-2 and 3 have been associated with more severe outbreaks, while DENV-1 and 4 have been linked to a milder disease phenotype (Fried et al., 2010). Similarly, different genotypes of the same serotype have been related to distinct severity outcomes (Rico-Hesse, 2010). A notable example of this is the Asian/American DENV-2 genotype which is associated with more severe disease and has a replication fitness advantage in infected mosquitoes and macrophages (Pryor et al., 2001) compared to the American DENV-2 genotype (Guzman et al., 1995, Rico-Hesse et al., 1997).

1.1.8.2.a NS1

NS1 of DENV is the only non-structural viral protein considered as a direct toxin due to its association with severe forms of dengue disease (Beatty et al., 2015, Modhiran et al., 2015). High levels of circulating NS1, up to 600 ng/mL in patient sera can be detected from the first day of symptoms and during the course of infection (Libraty et al., 2002b, Avirutnan et al., 2006). High concentration of NS1 in the blood of infected patients correlates with viremia and progression to severe disease; therefore the peak of NS1 levels has been suggested to predict the severity of DENV infections (Libraty et al., 2002b). More recently, it has been demonstrated that NS1 induces, via TLR4, the secretion of pro-inflammatory cytokines such as TNF α , IL-6, IFN- β , IL-1 β and IL-12 from mouse macrophages and human peripheral blood mononuclear cells that can result in increased vascular permeability of the endothelium (Modhiran et al., 2015). In addition, NS1 alone can prompt EC hyper-permeability in *in vitro* and vascular leakage in mice *in vivo* (Beatty et al., 2015, Modhiran et al., 2015). NS1 has also been shown to disrupt the endothelial glycocalyx layer, through induction of changes in gene expression of molecules involved in remodelling of the glycocalyx, which has been proposed as a mechanism by which NS1 induces vascular dysfunction (Puerta-Guardo et al., 2016). Finally, NS1 has been linked with hyper-activation of the complement system with implications for disease severity (Avirutnan et al., 2006), a topic that will be discussed in section 1.3.3.1.

1.1.9 Animal models to study dengue virus pathogenesis

The lack of a suitable animal model is a major drawback that has restricted our understanding of DENV pathogenesis and subsequently hampered the development and evaluation of prophylactic and therapeutic tools against DENV (Plummer and Shresta,

2014a, Plummer and Shresta, 2014b). The development of a relevant animal model has been challenging mainly due to the fact that wildtype mice are naturally resistant to DENV infection. While in humans DENV inhibits IFN signalling pathway to establish infection, in immunocompetent mouse cells the virus is unable to do so (Aguirre et al., 2012). The DENV NS2B/3 protein recognises and cleaves human STING to block induction of IFN but DENV NS2B/3 cannot interact with the murine STING homologue (Aguirre et al., 2012, Zhang et al., 2012). Likewise, DENV NS5 binds and promotes degradation of human but not mouse STAT2 (Ashour et al., 2009). Thus, these DENV non-structural proteins interfere with induction and signalling of IFN- α/β in a species-specific manner and DENV cannot overcome these restrictions to successfully infect mice (Ashour et al., 2010, Aguirre et al., 2012). Several efforts have been made to overcome this difficulty and currently, though not perfect, different animal models are available.

1.1.9.1 Human and non-human primate models

The frequency of DENV epidemics makes the use of data and observations from human infections possible. Pathogenesis studies in humans are descriptive by nature but are of great value to investigate and decipher potential pathogenic mechanisms driving DENV severity (Mammen et al., 2014, Whitehorn et al., 2014). Since the immunological and epidemiological scenarios in humans cannot be manipulated, the use of a dengue human infection model (DHIM) is still limited. Furthermore, in human studies, key parameters such as infecting serotype/genotype/strain, dose, sequence and history of infections, as well as interval between infections are often unclear. It is important to mention, however, that DHIM has been successfully developed to assess the efficacy of live attenuated tetravalent dengue vaccines or therapeutics prior to engaging in efficacy trials (Endy, 2014, Whitehorn et al., 2014, Larsen et al., 2015). Two different DHIM have been developed so far by the National Institutes of Health in the United States. The first model uses a modified DENV-2 strain, DEN2 Δ 30, which induces low levels of viremia and mild clinical signs and symptoms (Blaney et al., 2004, Durbin et al., 2006). The second model is still under investigation and comprises infection with a modified DENV-3 strain, DEN3 Δ 30 (Larsen et al., 2015). Importantly, these models are not characterised by the development of common features of dengue fever or severe disease, and thus they are less useful to study the pathogenesis of DENV disease (Blaney et al., 2004, Durbin et al., 2006). Recently, the Walter Reed Army Institute of Research has identified two additional potential candidates for DHIM studies: DENV-1 45AZ5K and DENV-3 CH53489 as challenge viruses. Both candidates induce dengue fever and thus are being considered for

further studies of pathogenesis of dengue vascular leak syndrome (Larsen et al., 2015).

Given that non-human primates are natural hosts in the sylvatic DENV cycle and are genetically closely related to humans, they have been used in DENV pathogenesis studies (Halstead et al., 1973a, Halstead et al., 1973b, Marchette et al., 1973, Scherer et al., 1978, Onlamoon et al., 2010, Omatsu et al., 2012, Gil et al., 2015). Rhesus monkeys and chimpanzees, subcutaneously infected with DENV, developed a similar course of viremia and viral specific humoral response to that of human infections (Halstead et al., 1973a, Halstead et al., 1973b, Scherer et al., 1978). Although rhesus macaques inoculated intravenously with high dose of virus experienced some degree of haemorrhage (Onlamoon et al., 2010) and infected marmosets were reported to display some symptoms similar to that of dengue in humans such as leukopenia, thrombocytopenia and liver damage (Omatsu et al., 2011, Omatsu et al., 2012), in general primate models of DENV infection do not reproduce the spectrum of dengue and severe dengue as seen in humans. Additionally, the studies in non-human primates are very expensive and difficult to reproduce in a large number of animals.

1.1.9.2 Mouse models

1.1.9.2.a Wild-type mice

As mentioned above, wild-type mice are naturally resistant to DENV infection due to the inability of DENV non-structural proteins to recognise mouse STING and STAT2 (Ashour et al., 2010, Aguirre et al., 2012). Different inoculation routes have been explored for many years in immunocompetent C57BL/6 mice in order to induce typical symptoms of, and immune response against, DENV. Intracranial inoculation is one of the most widely used in the past, (Bray et al., 1989, Falgout et al., 1990, Raut et al., 1996, van Der Most et al., 2000); and while central nervous system involvement is now considered a criteria for severe dengue by WHO (WHO, 2009, Carod-Artal et al., 2013) this route does not mimic a natural DENV infection. Likewise, high dose intravenous or intraperitoneal DENV inoculation can result in neurological abnormalities in C57BL/6 mice (Huang et al., 2000, Paes et al., 2005) and interestingly, a high dose of the 16681 DENV-2 strain following intravenous or intradermal inoculation in C57BL/6 mice, results in abnormal liver function and systemic haemorrhage, respectively; usual signs often observed during human DENV infection (Chen et al., 2004, Chen et al., 2007a). Further, using intravenous infection in C57BL/6 mice, detectable viral load in the serum, spleen, brain and liver were observed, which indicated systemic virus dissemination and replication in those tissues (Chen et al., 2004). Even though these routes seem to be more relevant to replicate some of the clinical

features seen in human, the high prevalence of neurological disease, not widely a feature of DENV infection in humans, and the absence of reproducibility continue to be a major drawback for the use of wild-type mouse models.

1.1.9.2.b Humanised mice

Humanised mice have been exploited in order to study dengue disease pathogenesis. One of the first approaches consisted of grafting human tumour cells into severe combined immunodeficient (SCID) mice lacking T and B cells. Since these mice are unable to reject the graft, the transplanted tumour cells provide a suitable human cell environment for DENV replication (Lin et al., 1998, An et al., 1999). Transplantation of human leukemia K562 and HepG2 cells (K562-SCID and HepG2-SCID models, respectively) prior to DENV infection have been evaluated. Both models were demonstrated to be susceptible to low-passage DENV clinical isolates, showing not only detectable viral load in serum and organs but also signs of thrombocytopenia and elevated haematocrit (Lin et al., 1998, An et al., 1999). Due to the presence of paralysis-associated lethality, suggestive of neurovirulence, and the fact that viral replication is restricted to the transplanted transformed cells, the extrapolation of results to human disease and their utility for understanding DENV disease are limited (Zellweger and Shresta, 2014, Chan et al., 2015).

Another interesting strategy is the use of nonobese diabetic (NOD)/SCID mice, or NOD/SCID/IL-2R γ - null mice, lacking T and B cells and defective in natural killer cells, complement-5 (C5) and macrophage and dendritic cells functions (Bente et al., 2005, Mota and Rico-Hesse, 2009, Mota and Rico-Hesse, 2011). By reconstituting human CD34+ hematopoietic stem cells in these mice the generation of monocytes, dendritic cells, B- and T-cells is induced thus improving their immune system and providing human target cells for DENV infection (Bente et al., 2005). While these mice showed detectable viral load in serum, spleen, liver and skin, and developed human DF-like features such as fever, rash, and thrombocytopenia, they lacked the presence of severe symptoms and signs characteristic of DHF/DSS which limits the application of this model in the study of severe dengue (Bente et al., 2005, Mota and Rico-Hesse, 2009, Mota and Rico-Hesse, 2011, Sridharan et al., 2013).

Similarly, immunodeficient RAG2 $^{-/-}$ / γ C $^{-/-}$ mice, that also fail to generate mature T or B lymphocytes (Shinkai et al., 1992) were reconstituted with human hematopoietic stem cells followed by DENV infection. Detectable viremia, fever and notably, production of human

neutralising IgM and IgG were observed in these mice following DENV infection (Kuruville et al., 2007), indicating that an efficient immune response can be induced in this scenario. However, the magnitude and kinetics of antibody development were not consistent between mice and there was no sign of anti-DENV T-cell responses (Kuruville et al., 2007).

Other strategies have been explored in humanised mice to improve aspects such as symptom profile of severe dengue disease and the magnitude and quality of B and T-cell responses against the virus with no great success (Wege et al., 2008, Frias-Staheli et al., 2014). Altogether, although humanised mouse models may be useful studying several features of DENV disease pathogenesis, the reconstitution with human hematopoietic stem cells is labour-intensive and expensive. These drawbacks, along with the absence of severe dengue symptoms and the lack of a functional immune response have limited their application.

1.1.9.2.c Immunocompromised mice

Considering the inability of DENV to efficiently replicate in immunocompetent mice, immunocompromised mouse models have been developed to achieve a better model that mimics the clinical symptoms and immune pathogenesis observed in humans (reviewed in (Zellweger and Shresta, 2014, Chan et al., 2015)). The majority of immunocompromised mouse models that successfully demonstrate DENV infection have been defective in innate responses and the IFN system since in mice, DENV is not able to suppress IFN signalling pathways to establish infection (Ashour et al., 2010, Green et al., 2014). The natural established C5-deficient mouse (A/J strain) and STAT1^{-/-} mice are sensitive to DENV-2 infection with detectable viral load in the serum, spleen, liver, lymph node and central nervous system. These mice also show signs of paralysis, thrombocytopenia and some DHF-like hallmarks such as haemorrhage and vascular leakage (Huang et al., 2000, Shresta et al., 2005, Chen et al., 2008).

Mice deficient in IFN receptors were further considered as a powerful alternative platform. Mice lacking IFN- α/β receptor (IFNAR^{-/-}) 129/Sv genetic background (A129), or on a C57BL/6 background, develop a sustained DENV replication and severe dengue-like disease after infection with high doses of DENV-2 (Prestwood et al., 2012a, Prestwood et al., 2012b). In addition, this mouse model has been very useful to study the role of CD4⁺ and CD8⁺ T-cell responses in the context of DENV-2 infection (Yauch et al., 2009, Yauch et al., 2010).

AG129 mice lacking IFN- α/β and γ receptors infected with high DENV doses also supported high levels of DENV replication and severe dengue-like disease (Johnson and Roehrig, 1999). Interestingly, inoculation of these mice with a mouse-adapted DENV-strain (D2S10) results in early lethal systemic infection regardless of their age (Johnson and Roehrig, 1999, Shresta et al., 2006). In contrast, infection with non-mouse-adapted DENV-2 strain (D2Y98P) induces cytokine storm, liver damage, and vascular leakage, hallmarks of DHF in humans (Tan et al., 2011, Ng et al., 2014). Recently, this model has been extended to reflect infection with other DENV serotype, with DENV-3- and 4- infected AG129 mice showing DHF-like symptoms as well such as thrombocytopenia and vascular leakage (Milligan et al., 2015, Sarathy et al., 2015).

It is evident that the AG129 mouse model has offered a logistically simpler model of infection, with disease that reflects a more relevant platform for the study of DENV. Therefore, this animal model has become the most widely used in the DENV scientific community, being recently employed for investigating the ADE phenomenon (Ng et al., 2014, Lee et al., 2016, Martinez Gomez et al., 2016). The ADE mouse model of DENV disease is a unique model that reflects ADE infection and recapitulates the enhanced severity of DENV disease during secondary infections, as is seen in humans (Ng et al., 2014). In this model AG129 mice borne to DENV-1 immune mothers are infected with DENV-2 and display higher viremia and increased vascular leakage compared to AG129 mice borne to dengue naïve mothers (Ng et al., 2014, Lee et al., 2016). This model is used in the study herein in chapter VI.

Despite the advantages of the AG129 animal model, the absence of IFN signalling pathway is a clear limitation that must be considered when interpreting results. Thus, discoveries made in these mice may not accurately reflect what would happen in a fully immunocompetent environment (Plummer and Shresta, 2014a, Zellweger and Shresta, 2014).

I.2 The complement system

I.2.1 The three pathways

The complement system is considered as one of the first lines of defence of the innate and adaptive immune systems. The complement system is recognised as the major non-cellular component of the innate immune system that efficiently protects the host from pathogenic microorganisms and contributes to the regulation and solubilisation of immune complexes as well as to the clearance of apoptotic cells. The complement cascade also plays a central role in modulating the activity of B- and T-cell responses and establishes a key link between the innate and adaptive immune system (Ferreira et al., 2010). The complement system is a well-regulated cascade composed of approximately 50 plasma and membrane-bound proteins that act in concert to protect the organism against pathogens. Three different but connected biochemical cascades comprise the complement system: the classical pathway (CP), the lectin pathway (LP) and the alternative pathway (AP) (Merle et al., 2015a, Mastellos et al., 2016). The pathways converge at an amplification stage characterised by the formation of C3 and subsequently C5 convertases, and cooperate closely to form opsonins, anaphylatoxins, chemoattractants, and membrane attack complexes (Kemper et al., 2014, Merle et al., 2015a).

I.2.1.1 Complement Classical Pathway

The CP is activated when immune-complexes: foreign antigens recognised by IgM or IgG antibodies, recruit the initiating component C1q. Some structures like LPS (Clas et al., 1985), C-reactive protein (CRP) (Richards et al., 1977), and degranulation products of cells (Rossen et al., 1988) can bind C1q independently of antibodies and activate CP. Once C1q is activated, it associates with the serine proteases C1r and C1s to form C1, a large enzymatic complex of the CP cascade (Figure I-7). Binding of C1 complex to target surfaces leads to the sequential activation of the serine proteases C1r/C1s which then cleave the plasma protein C4 and in turn, also cleave C2, producing the opsonins C4b and C2a, respectively. The two fragments, C4b and C2a, non-covalently associate to form the C3 convertase, C4b2a (Figure I-7) (Ricklin et al., 2010) which cleaves C3 to C3b liberating the anaphylatoxin C3a. C3b, like C4b, covalently binds to activating surfaces to signal “danger” and trigger the complement terminal pathway which is responsible for eliminating targeted cells (Ricklin et al., 2010).

I.2.1.2 Complement Lectin Pathway

The LP is triggered by carbohydrates signatures, pathogens and target cell surfaces, that

are recognised by mannose binding lectins (MBL) and ficolins and initiate activation of the LP (Figure I-7) (Garred et al., 2009, Endo et al., 2010, Endo et al., 2015). In the circulation MBL and ficolins form complexes with MBL-associated serine proteases (MASPs) and binding of these complexes to target surfaces leads to activation of the serine proteases which results in the formation of the C3 convertase complex (C4b2a) in the same way described above for the CP (Figure I-7) (Merle et al., 2015a). The activation of the complement terminal pathway by the LP C3 convertase complex will also occur in the same way as describe for the CP in the section above (I.2.1.1).

I.2.1.3 Complement Alternative Pathway

The AP, unlike the CP and LP which are activated by specific signals, is constitutively active. The AP has a basal level of activity in all tissues throughout an organism. The pathway is initiated in the fluid phase by the spontaneous hydrolysis of the thioester bond in C3 that allows the generation of a fluid phase initiating protease C3(H₂O)Bb with the ability to cleave C3, generating C3b fragments (Figure I-7). These C3b fragments possess a labile thioester group, allowing it to bind covalently to any nearby membranes with exposed amino or hydroxyl groups. Surface-bound C3b binds FB, which is subsequently cleaved by factor D (FD) producing the Ba and Bb fragments. Ba dissociates from the complex while Bb remains bound to C3b, forming the active AP membrane-bound C3 convertase, C3bBb, which is stabilised by the association of properdin (Figure I-7). Importantly, this convertase has the ability to greatly amplify the deposition of C3b on the target cell surface by activating additional C3 to form more C3b and produce new C3 convertases (surface-bound or fluid-phase convertase), thereby creating a self-amplification loop that leads to efficient opsonisation of unprotected cells and surfaces, and labelling these are targets for the terminal complement pathway (Muller-Eberhard and Gotze, 1972, Isaac et al., 1998, Nilsson and Nilsson Ekdahl, 2012). Clearly, this basal activity of the AP must be regulated to prevent on-going damaging complement activity. This is the main focus of this thesis and the mechanisms that regulate this process are described in section 0.

I.2.1.4 Terminal Pathway

The activities of the CP, LP and AP all converge on cleavage of C3 and formation of C3b (Figure I-7). Increasing density of C3b on the target cell surfaces results in the formation and activation of C5 convertases (i.e. C4b2b3b and C3bBb3b for the CP/LP and AP, respectively) that preferentially cleave complement component C5 (Figure I-7) (Merle et

al., 2015a). Activation of C5 releases the anaphylotoxin C5a and C5b. The latter associates with complement components C6, C7, C8 and multiple copies of C9 to form the membrane-attack complex (MAC) (Figure I-7). It is important to note that although the generation of C3b results from the action of either the CP, LP or AP C3 convertases, the 'tick-over mechanism' of the AP constitutes the major source of this opsonin (Merle et al., 2015a). Additionally, it is also important to recognise that although formation of the MAC seems the final outcome of the activity of the complement system, cell lysis is not the only effector function of complement, as described below.

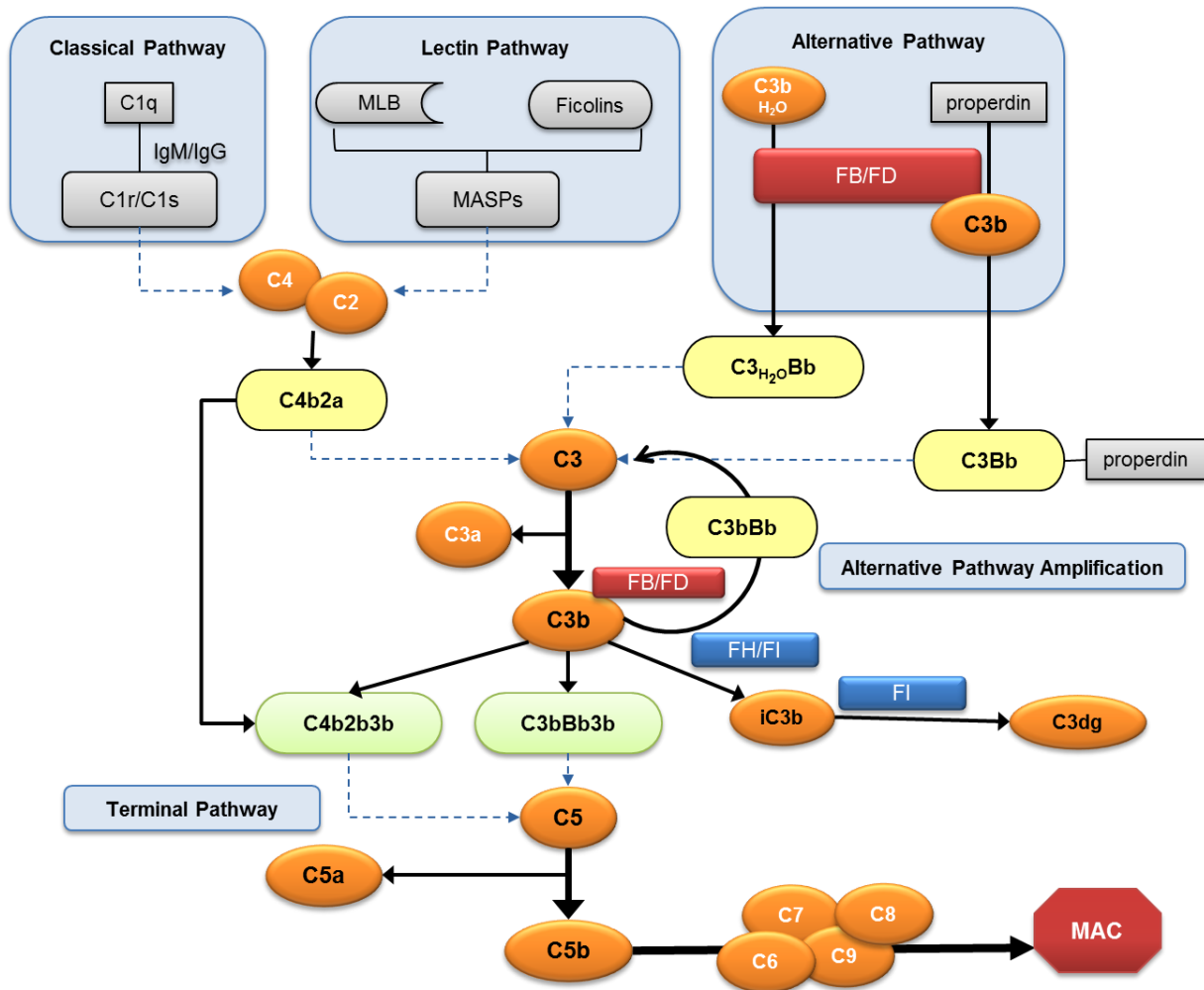


Figure I-7. Schematic representation of the three pathways of the complement system

The classical pathway is activated when C1q interacts with IgM/IgG bound to antigen. C1q associated C1s cleaves C4 and C2 to form the classical pathway C3 convertase (C4b2a). The lectin pathway is initiated by carbohydrate pattern recognition receptors such as mannose-binding lectin (MBL) and the ficolins which are in a complex with MBL-associated serine proteases (MASPs). The alternative pathway is activated by spontaneous hydrolysis of C3. The three pathways converge on the activation of C3 that will result in the formation of C3b, C3 convertase (C3bBb), C5 convertases (C4b2b3b and C3bBb3b) and finally to the formation of C5b-C9 membrane attack complex (MAC) which can directly lyse pathogens or pathogen-infected cells. The alternative pathway also functions as an amplification loop for the cleavage of C3 and is tightly regulated by factors such as FB, FD, FH and FI. C3-H₂O or C3b bound to target surfaces are bound by FB. FD cleaves C3-H₂O or C3b-bound FB, resulting in the generation of Bb and formation of the alternative pathway C3 convertase. The inactivation of C3b to iC3b is mediated by FH and FI, which also mediate degradation of iC3b to C3dg.

1.2.2 Effector functions of the complement proteins

The main effector mechanisms of complement include: i) tagging pathogen and damaged cells to promote their phagocytosis; ii) triggering anaphylatoxic responses that result in local pro-inflammatory and inflammatory reactions; and iii) promoting membrane attack and lysis of pathogenic cells.

(i) tagging pathogen and damaged cells to promote their phagocytosis. C4b and C3b are opsonins that covalently bind to activating surfaces thereby promoting phagocytosis of these surfaces. In other words, deposition of any of these molecules onto a surface has the potential to target that surface for elimination. In fact, surface-bound C3b is considered a key innate immune surveillance mechanism identifying potential pathogenic targets. Since C4b or C3b deposition is not discriminatory between self and non-self, other regulatory proteins are required to differentiate between pathogenic and non-pathogenic targets and convert the C4b or C3b deposition signal into a mechanism for phagocytosis or killing and clearance of targets (Harrison, 2018). This is further described in section 0.

(ii) triggering anaphylatoxic responses that result in local pro-inflammatory and inflammatory reactions. Different potent effectors are generated upon activation and amplification of the complement cascades. C3a and C5a are anaphylotoxins generated as by-products of C3 and C5 convertase, respectively. Both are able to initiate and mediate an inflammatory response by mediating chemotaxis, inflammation and generation of reactive oxygen species (Zhou, 2012, Coulthard and Woodruff, 2015).

(iii) promoting membrane attack and lysis of pathogenic cells. The MAC is probably the best-recognised among effector mechanisms of complement proteins. The main function of this complex is to provoke the lysis of target cells by opening pores in their membranes. Interestingly, when MAC is formed at sublytic levels, it can also act as a proinflammatory mediator by inducing damage or activation of bystander cells (Morgan and Harris, 2015).

Thus, activation of any of the complement pathways results in processes to tag and recognise targets and mechanisms that promote inflammation and directly kill. This effective and damaging potential needs to be tightly regulated.

1.2.3 Regulation of the complement response

Activation of the complement system requires a number of regulatory mechanisms in order to control and confine its activity to appropriate pathogenic organisms and cells; thus preventing collateral damage to healthy host cells and tissues (Ricklin et al., 2016). A complex set of plasma proteins: FH, factor I (FI), C4b binding protein (C4bp) and C1 inhibitor; and cell-associated regulators: decay accelerating factor (DAF or CD55), complement receptors 1 and 2 (CR1 and CR2), CD59, and membrane cofactor protein (MCP or CD46) participate in the fine balance between detection and destruction of 'non-self' and minimisation of damage to 'self' (Seya et al., 1991, Liszewski and Atkinson, 1996, Liszewski et al., 1996, Atkinson and Goodship, 2007, Ricklin et al., 2010). The majority of these proteins (FH, C4bp CR1, MCP, DAF) are encoded by a region of the genome designated as the 'regulators of complement activation' (RCA) gene cluster which is evolutionary well-conserved, thus highlighting the biological importance of these RCA genes (Zipfel and Skerka, 2009). Fluid-phase complement regulators are mostly secreted by the liver, however there are several host cells that secrete and express some of these regulators on their cell surface such as EC, epithelial cells, in particular retinal pigment epithelial cells, and platelets, among others (Brooimans et al., 1990, Licht and Fremeaux-Bacchi, 2009, Sakaue et al., 2010, Tu et al., 2011).

Two general inhibitory mechanisms take place to negatively regulate complement activity, and both act by specifically limiting complement activation at the C3 step (Meri and Pangburn, 1994). One of these is known as 'decay acceleration' and involves the *reversible* dissociation of the C3 convertases: C4b2a of the CP/LP and C3bBb of the AP. Regulatory factors such as FH, C4bp, DAF and CR1 are responsible for this decay acceleration activity and promote the dissociation of C4b from C2a while FH, DAF and CR1 are also involved in the detachment of C3b from Bb (Funahara et al., 1987). The second mechanism involves the irreversible proteolytic cleavage of the C3 convertase components, C3b or C4b, by FI. This inactivation process occurs with the participation of cofactors for FI activity: FH and C4bp are cofactors of FI in plasma and CR1 and MCP, support FI activity at the cell surface (Meri and Pangburn, 1994). These general regulatory mechanisms of reversible dissociation and irreversible cleavage of complement components also apply to the regulation of the C5 convertases, with other specific regulatory factors involved that are not further discussed here but have been reviewed (Merle et al., 2015b).

Furthermore, CD59 or protectin also has a role in regulating complement activation. This cell-membrane associated molecule inhibits formation of MAC by binding to intermediate C5b-8 and C5b-9 terminal complement complexes and preventing incorporation and polymerization of C9 (Meri et al., 1990, Rollins and Sims, 1990).

These examples regulate the convergent sites of CP, LP and AP via C3/C5. The ability of the CP and LP to form C3/C5 is regulated primarily at the point of the initiating stimulus. As indicated above however, the AP is constitutively active and thus requires additional specific regulatory mechanisms to regulate the 'tick-over' basal levels of C3/C5 formation and complement activity.

1.2.3.1 Regulation of the AP. Features and specific roles of its components

The actual activation and regulation of the AP includes six main components: C3, FB, FD, properdin, FI and FH (Pangburn and Muller-Eberhard, 1984, Meri, 2016). While C3 is the starting target for cleavage, the remaining molecules act in concert to maintain a delicate balance of C3 cleavage and AP activity.

1.2.3.1.a C3

C3 is the central molecule in AP activation and is considered critical for the rapid reactivity of the AP. C3 is abundant in plasma with a concentration of approximately 1 mg/ml and is continuously spontaneously hydrolysed at a low rate. In this manner, a C3b-like conformational state is continuously produced which allows the formation, together with FB and FD, of the AP-initiating C3 convertase (Nilsson and Nilsson Ekdhahl, 2012). This is particularly important since the half-life of the C3 convertase (C3bBb) is very short, only 1.5 min (Pangburn and Muller-Eberhard, 1986); thus the continuous generation of C3 convertase keeps the AP in an alert and active state, ready to quickly respond to danger. Clearly, the levels of FB and FD influence the readiness to react of this C3 complex.

1.2.3.1.b FB

FB is a heat-labile serum zymogen that was one of the early defined components that could promote activity of the AP (Alper et al., 1973). In plasma, FB concentrations range from 200-500 µg/ml (Forristal et al., 1977, Silva et al., 2012). FB is a large protein of approximately 95 KDa that consists of two fragments, Ba in its N-terminal region (33 KDa) and Bb in the C-terminal one (60 kDa). Structurally, FB is composed of five domains: three short consensus repeats (SCRs), also known as complement control protein repeats, followed by a von Willebrand type A (vWA) and a serine-protease domain (Milder et al., 2007). The vWA and serine-protease domains comprise the Bb fragment. FB is a

substrate for cleavage by FD with the FD cleavage site located between SCRs and the vWA domain and only accessible when exposed as a consequence of Mg²⁺-dependent binding to C3b (Milder et al., 2007). FB interacts in a Mg²⁺-dependent manner with C3b (the hydrolysed form of C3) to form the pro-convertase C3bB (Pangburn and Muller-Eberhard, 1986). In a presence of FD, FB is cleaved, the Ba fragment is released, leaving the active AP C3-convertase containing the FB Bb fragment and termed C3bBb (Walport, 2001).

1.2.3.1.c FD

As above, FD is critical for cleaving FB to turn the pro-convertase C3bB into the active C3-convertase C3bBb. FD, a glycosylated protein also termed adipsin, is thus similarly considered an activator component of the AP. FD is a serine-protease of 24 kDa produced by several cell types including adipocytes, monocytes, and macrophages (Fantuzzi G 2005). FD is a rate-limiting enzyme of the AP and has the lowest concentration in plasma amongst all the complement proteins, ranging from 500-700 ng/ml (Volanakis et al., 1985). Specifically, FD cleaves FB bound to C3b between Arg233 and Lys234 causing the release of the Ba fragment and leaving the Bb fragment bound to C3b (Mallik et al., 2005). FD is only active and cleaves FB when FB is bound to C3b, generating the membrane-bound C3 convertase. This convertase has the ability to greatly amplify the deposition of C3b on the surface of a cell (Muller-Eberhard and Gotze, 1972, Isaac et al., 1998).

1.2.3.1.d Properdin

Properdin is a glycoprotein composed of multiple identical protein subunits (Smith et al., 1984). It is well-recognised as a positive regulator of the AP that stabilises the AP convertase C3bBb, enhancing the overall complement response (Schwaeble and Reid, 1999). As described above C3bBb is extremely labile, with a half-life of 1.5 min (Pangburn and Muller-Eberhard, 1986) and the binding of properdin increases the stability of the AP convertases 10-fold on target surfaces and immune complexes (Fearon and Austen, 1975). One mechanism that properdin achieves this is by inhibition of the negative regulators of the AP, such as the FH-mediated cleavage of C3b by FI (Medicus et al., 1976). Additionally, properdin has also been demonstrated to promote the association of C3b with FB and promotes C3 convertase assembly on a cell surface (Hourcade, 2006).

1.2.3.1.e FI

FI is a protein present at relatively low concentration in serum and of molecular weight 88 kDa, consisting of two disulphide linked chains of 50 and 38 kDa. FI is a serine protease

responsible for cleaving C3b (and its homolog C4b) to inactivated C3b (iC3b), which thus prevents excessive generation of C3b. The activity of FI depends on cofactors, such as FH, CR1 or MCP (Fearon, 1979, Goldberger et al., 1984, Tsiftoglou et al., 2005).

1.2.3.1.f FH

FH is considered the master regulator of the AP both in the fluid phase and on cellular surfaces (Whaley and Ruddy, 1976, Davis et al., 1984). FH is an abundant serum glycoprotein (~500 ug/ml) expressed constitutively in the liver (Adinolfi and Zenthon, 1982, Estaller et al., 1991). Additionally, FH may be synthesised locally by other cell types including renal, endothelial and epithelial cells, platelets, adipocytes and macrophages (Morris et al., 1982, Schwaeble et al., 1987, Brooimans et al., 1990, Vik et al., 1990, Schwaeble et al., 1991, Chen et al., 2007b, Licht and Fremeaux-Bacchi, 2009, Sakaue et al., 2010, Tu et al., 2010). FH is a single chain polypeptide of approximately 139 kDa when not glycosylated and 155 kDa when is glycosylated (Kristensen and Tack, 1986, Kristensen et al., 1986, Ripoche et al., 1988a) and is structurally comprised of 20 homologous SCR domains of approximately 60 amino acids each (Ripoche et al., 1988a).

The physiological role of the FH protein is to negatively regulate the AP by competing with FB for C3b (Conrad et al., 1978), promoting the decay of the C3 convertase (Weiler et al., 1976) and by acting as a cofactor for FI-mediated proteolytic inactivation of C3b to form iC3b (Weiler et al., 1976) (Figure I-8). Although FH can perform these regulatory functions in both the fluid phase and cell surface, interestingly, the fluid phase convertase, C3(H₂O)Bb, is more resistant to regulation by FH than cell bound convertase, highlighting the importance of actions of FH in the local cellular environment (Bettoni et al., 2016).

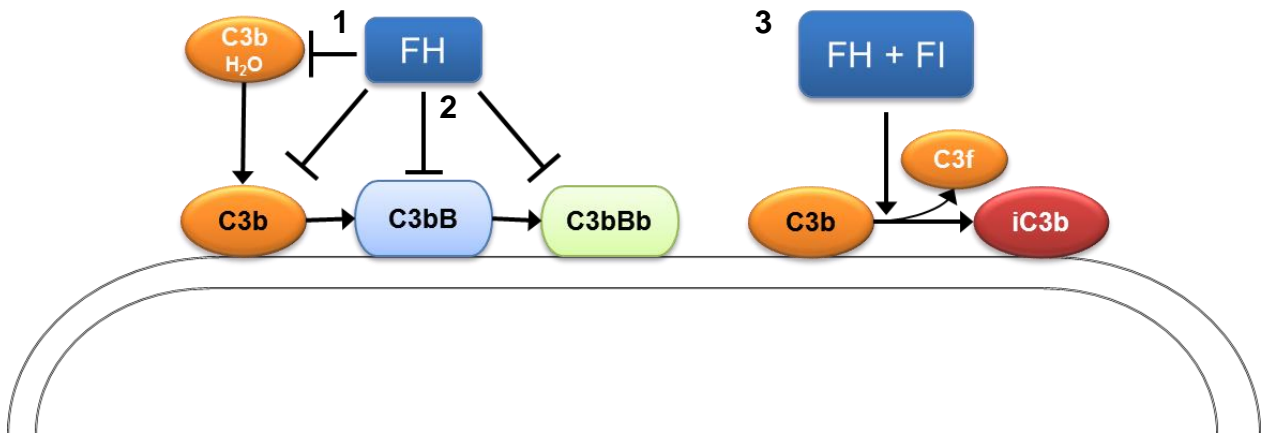


Figure I-8. Regulatory role of FH

FH can inhibit complement activation by three different mechanisms: (1) inhibition of C3b in the fluid phase and bound to cell surfaces, (2) inhibition of the formation of C3bB and decay dissociation of Bb from C3bBb (C3 convertase) and (3) promotion of inactivation of C3b by factor I to form inactivated C3b, iC3b.

Essentially, FH has two main ligands, C3b and GAGs such as heparan sulfate, found on host cells surface. Specifically, the N-terminal SCR 1-4 domains contain the cofactor activity for C3b inactivation and the decay-accelerating activity for the C3bBb convertase (Gordon et al., 1995, Kuhn et al., 1995), while SCR 7 and SCR 19-20 mediate cell surface recognition by binding to sulphated GAGs on host cells (Blackmore et al., 1996, Blackmore et al., 1998, Hellwage et al., 2002, Schmidt et al., 2008a, Schmidt et al., 2008b, Clark et al., 2013). Importantly in relation to DENV, which as described in section 12.1.6, can bind to EC via heparan sulfate, FH and specifically FH SCR 19-20 binds to glomerular EC in a manner that is differentially mediated by heparan sulfate but no other GAGs such as chondroitin sulfate, dermatan sulfate or hyaluronan (Loeven et al., 2016). This cell surface GAG binding is an important determinant of the cell surface regulatory activity of FH.

Another ligand of FH is CRP, which is secreted by the liver in elevated concentrations during an acute phase of infections and inflammation process. In general CRP cooperates with the complement system to remove apoptotic/necrotic cells (Mold et al., 1999) and is able to bind to Fc γ receptors on leukocytes and directly activate phagocytosis (Jarva et al., 1999). Specifically, CRP binds FH via SCR7 and SCR19-20 and can enhance complement inhibition, particularly on apoptotic or damaged cells in an inflammatory scenario (Giannakis et al., 2003, Okemefuna et al., 2010). When FH binds CRP and cell surface glycans, FH downregulates complement and protects the cell from MAC-mediated damage. In fact, the FH Y402H polymorphism that has reduced CRP binding capacity is linked to predisposition to macular degeneration, a progressive cell death in the retina of the eye (Sjoberg et al., 2007, Molins et al., 2016), in which genetic variations in the FH gene are associated with complement dysregulation (McHarg et al., 2015).

Transcription of the FH gene also leads to the production of FH-like 1 (FHL-1), an alternative spliced variant of 43 kDa that similarly has a capacity to regulate the AP, although with much lower affinity/activity (Kuhn et al., 1995). FHL-1 is identical to FH in containing the same first seven SCR domains, but differs in lacking the remaining 13 SCRs and with the addition of four unique amino acids (SFTL) at the C-terminal end (Schwaeble et al., 1987, Kuhn and Zipfel, 1996). Thus, FHL-1 lacks the most critical self-recognition and surface binding domains of the C-terminus of FH (Schwaeble et al., 1987). Hence, it has been proposed that FHL-1 is likely to be more effective as an inhibitor of complement activation within the fluid phase compared to the cell surface (Skerka et al., 2007, Parente et al., 2017).

1.2.3.2 Regulation of the AP: mechanisms

During physiological conditions, the plasma AP is the dominant contributor to overall circulating complement activity by the AP 'tick-over' mechanism. This tick-over mechanism is kept in check by complement regulators and maintains a low and constitutive level of activation of the AP by the spontaneous hydrolysis of C3 and the formation of the bioactive form C3(H₂O) in the fluid phase (Pangburn et al., 1981). Due to the efficient amplification loop of the AP (see Figure I-7), constitutive activation of the AP could result in inflammation and tissue damage in the absence of a pathogen. Thus, the spontaneous and constitutive activity of the AP needs to be strictly regulated so that the downstream final complement products are produced only when needed and targeted only to structures that need to be eliminated. All regulatory factors of the AP contribute, in a robust manner, to discriminate healthy normal human cells from pathogens (bacteria, fungi, and parasites), virus-infected cells and apoptotic cells (Meri, 2016) but FH and FI are particularly important. When the target surface is pathogenic (non-self), such a surface will have little FH bound and thus support AP activation. This means that C3 activation will continuously generate C3b through the positive amplification loop and the target surface will be coated by C3b in minutes. On the contrary, when the target surface is a healthy cell (self or non-activating surface), the C3b molecule will be inactivated by FH and FI, forming iC3b which will be further degraded to C3c and C3dg molecules (see Figure I-7). The latter, remains bound to the cells and are rapidly cleaved to C3d by tissue proteases and thus this process irreversibly removes activated C3b (Meri, 2016).

Thus, the fate of C3b is influenced by the presence of negative regulators such as FH/FI and this is a determinant of whether complement products are further processed towards the terminal pathway or inactivated. In addition to the presence or absence of negative regulators, the fate of C3b is also determined by small differences in the affinity of FH and FB for C3b and this depends on whether C3b is in the fluid phase, bound to pathogenic or non-pathogenic surface (Meri and Pangburn, 1990, Pangburn et al., 2000). FH has higher affinity for soluble C3b as well as self-surface-bound C3b molecules than FB, which results in preferential C3b inactivation (formation of iC3b). Interestingly, soluble C3b seems to accommodate FH binding with synergy via multiple sites that increases the affinity for further FH molecules and at the same time prevent FB binding (Jokiranta et al., 2000). In contrast, the affinity of FH for non-self-surface-bound C3b molecules is relatively low, allowing FB to preferentially binding to C3b and promoting the formation of C3bBb convertase on non-self surfaces (Jokiranta et al., 2000).

Upon the formation of AP C3 convertase on non-self surfaces, more C3 molecules can be activated via the AP amplification loop. This results in continuous generation of new C3b molecules that are deposited on the target surface. Newly formed C3b binds to a target surface via reactivity of its metastable thioester moiety. This reaction takes place within ~60 μ s of cleavage, and during that time C3b can diffuse only up to 30 nm before it becomes covalently bound to a target (Sim et al., 1981). The consequence of this is that newly formed C3b molecules will generate a cluster of C3b molecules around the initial C3b molecule that was initially deposited, generating a localised response to a non-self-target.

In the context of healthy concentrations of FH, a natural mechanism takes place to restrict excessive and pathogenic C3b deposition. It seems that as soon as two C3b molecules are bound to GAG containing target surfaces close enough to each other, a single FH molecule will bind simultaneously to such molecules via SCR 1-4 (N-terminal region) and SCR 19-20 (C-terminal domains) (Morgan et al., 2012). Additionally, it is possible that SCR 19-20 domains bind both C3b and GAG at the same time. Different studies of the C3b binding site on SCR19–20 showed that it may be overlapping, but it is not identical with the GAG-binding site (Bhattacharjee et al., 2010, Morgan et al., 2012, Blaum et al., 2015). It is proposed that when the density of C3b molecules reaches a certain threshold value, the binding of FH is favoured over FB on the targeted surfaces (Koistinen, 1991). In this way, the activity of the AP is controlled and delicately balanced to prevent excessive C3b build-up and activation and switch off the AP activity.

In summary, the AP possesses complex and ingenious mechanisms to block activation of complement on self surfaces, thereby preventing self-tissue damage and excess inflammation during the phase of constitutive 'tick-over', but additional mechanisms to promote complement activation on non-self surfaces when activity to clear a pathogen is needed and finally, strategies to reduce complement activity once pathogen clearance is achieved, to restore balance to the complement system.

1.3 The complement system and viral infections

1.3.1 Protective role of complement during viral infections

The important role of the complement system in protecting and clearing bacterial infections is well established (reviewed in (Merle et al., 2015b)). The actions of complement against viruses are less well described. The complement system, however, plays a key role in

protection against viral pathogens which are attacked by all three complement pathways through several mechanisms. Any of these proteolytic cascades that activate complement or a combination of them, act to eliminate not only viral particles but also virus-infected cells in the host in an effective and specific manner. These mechanisms include: direct inactivation of viral particles by MBL; recruitment and activation by the anaphylotoxins C3a and C5a of monocytes and granulocytes; opsonisation of viral particles mediated by either C3b, iC3b, C3d and C3dg; priming of T and B cell antiviral responses; antigen uptake and presentation mediated by C3 and lysis of enveloped viral particles and infected cells by the MAC (Stoermer and Morrison, 2011, Merle et al., 2015b).

Specific protective roles of the complement system against viral infections include the direct MBL-mediated complement neutralisation of human immunodeficiency virus-1 (HIV-1) (Ezekowitz et al., 1989), severe acute respiratory syndrome coronavirus (Zhang et al., 2005), Ebola virus (Ji et al., 2005) and West Nile virus (WNV) infections (Fuchs et al., 2010). For the CP, immune complexes formed by polyreactive IgM antibody and vesicular stomatitis virus antigens, activate C1 of the CP and initiate complement activity on the viral surface, neutralising the virus by a lytic mechanism (Beebe and Cooper, 1981). Likewise, binding of IgM and influenza virus induce CP activation and virus neutralisation, but in this case by coating and aggregation of viral particles (Jayasekera et al., 2007). In a similar way, complement activation enhances antibody-mediated neutralisation of many viruses: herpes simplex virus (Lerner et al., 1974), varicella zoster virus (Schmidt and Lennette, 1975), Epstein-Barr virus (Sairenji et al., 1984), respiratory syncytial virus (Yoder et al., 2004), and HIV (Aasa-Chapman et al., 2005, Verity et al., 2006) as well as different flaviviruses like WNV, yellow fever virus, and Kunjin virus (Schlesinger et al., 1993, Mehlhop et al., 2005).

The complement system is well known to link the innate and adaptive responses and a different but efficient way that complement can protect against viral infection is by inducing B lymphocyte responses. The CP has been shown to play a key role in regulating the antibody response against herpes simplex virus type 1 infection (Da Costa et al., 1999), and WNV (Mehlhop et al., 2005). In the latter this is via interference with effector functions rather than immunoglobulin production, where components such as C1q restrict ADE by anti-flavivirus antibodies *in vitro* and *in vivo* in an IgG subclass specific manner (Mehlhop et al., 2007). Although the precise mechanism of this phenomenon remains unclear, this study showed that in WNV-infected wild-type mice, ADE is limited and only mediated by IgG1 that binds C1q with very low affinity. In WNV-infected C1q^{-/-} mice, IgG2a but not IgG1

or IgG2b, promote ADE possibly due to the high affinity between IgG2a and C1q (Mehlhop et al., 2007). The authors proposed that C1q restriction of ADE could limit virus attachment to cells by directly blocking Fc γ R binding to the Fc region on the antibody (Mehlhop et al., 2007).

Increasing experimental evidence suggests that complement also enhances T-cell responses to viral infections. C3 for example, is required to induce a normal T-cell response against influenza and lymphocytic choriomeningitis viruses (Kopf et al., 2002, Suresh et al., 2003) while C4 and FB drive the induction of anti-WNV CD8⁺ T-cell response (Mehlhop and Diamond, 2006).

1.3.1.1 Protective role of complement during DENV infection

Several findings support the role of the complement system in the context of protective immunity against DENV. The LP, for example, has been shown to mediate a key role in DENV neutralisation (Fuchs et al., 2010, Avirutnan et al., 2011, Shresta, 2012). This is supported by experiments where the authors pre-treated C6/36 cell- and Vero cell-derived DENV-2 with naïve sera from wild-type C57BL/6 mice and several congenic mouse strains lacking different complement proteins. The authors found that neutralization of both insect cell- and mammalian cell-derived DENV-2 is dependent on MBL and MBL-associated serine protease 2 (MASP-2), but not C1q or C5 (Avirutnan et al., 2011). Additionally, and consistent with the results using wild-type mice serum, the authors demonstrated that both C6/36 cell- and Vero cell-derived DENV-2 are neutralised by human serum. Furthermore, a direct correlation between the concentration of MBL in human serum and the percentage of neutralisation of DENV was found (Avirutnan et al., 2011). Finally, this study showed that in the absence of FB or FD (both positive mediators of the AP), DENV-2 neutralisation was partially inhibited, and increased deposition of C3 on the virion surface was detected; supporting the protective role of the AP (Avirutnan et al., 2011).

Additionally, it has been shown by *in vitro* ADE assays that specific monoclonal antibodies against DENV-2 and 4 as well as IgG from DENV-infected patients that have enhancing activities also have neutralising activities in the presence of fresh human serum with normal levels of complement proteins (Yamanaka et al., 2008). Further studies showed that C1q could be responsible for this effect in an IgG subclass specific-manner, implying that this complement component could limit the severity of DENV disease (Mehlhop et al., 2007). The authors incubated DENV-1 with increasing concentrations of two flavivirus cross-reactive monoclonal antibodies (IgG2a and IgG1 subclasses) in the presence or not

of purified C1q. Results demonstrated that C1q inhibited IgG2a monoclonal antibody-dependent ADE but not ADE induced by IgG1 (Mehlhop et al., 2007). More recently, C1q was demonstrated to bind to DENV E protein and to whole DENV-2 virions. DENV-infected human monocyte leukaemia cell line pre-incubated with C1q-DENV complex, resulted in decreased virus infectivity and modulation of mRNA expression of immunoregulatory molecules (Douradinha et al., 2014).

1.3.2 Viral evasion of the complement system

Probably, the best evidence implying a protective role of complement against viral infection comes from the extensive mechanisms that viruses have developed to subvert complement activity. Several viruses, for example, encode proteins that bind and inhibit or sequester complement components. The coat protein of human astrovirus type 1 binds MBL and C1q to inhibit activation of the LP and CP, respectively (Bonaparte et al., 2008, Hair et al., 2010). Herpes simplex virus 1 encodes the immune modulator glycoprotein C that binds C3 and C3b to inhibit the complement cascade and protect virus-infected cells from complement mediated-lysis (Friedman et al., 1984, Fries et al., 1986, Harris et al., 1990, Kostavasili et al., 1997). As another example, the matrix 1 protein of influenza A binds C1q and blocks the interaction between C1q and IgG to prevent complement-mediated neutralisation (Zhang et al., 2009). More recently, it has been found that zika virus (ZIKV) induces specific antibodies against E protein that also cross-react with C1q, phenomenon that was confirmed by ELISA in sera collected from ZIKV-infected immunocompetent mice and non-human primates (Koma et al., 2018). The authors speculate that E protein from ZIKV could prevent complement CP activation by inhibiting C1q actions (Koma et al., 2018).

In a similar strategy, viruses can encode homologs of complement regulatory proteins. Poxvirus such as variola virus and vaccinia virus encode complement regulatory proteins that have structural and functional homology to the human RCA family. In both cases, the viral regulators bind to and inhibit C3b and C4b and act as cofactors for FI-mediated cleavage of C3b, in some ways presenting as functional viral homologues of FH. The consequences of the actions of these viral complement regulatory proteins is the inhibition of the C3/C5 convertases, which are necessary for complement-mediated viral clearance, thus contributing to viral infection and potentially the pathogenesis of the disease (Rosengard et al., 2002, Bernet et al., 2003, Liszewski et al., 2006).

Another approach some viruses use, similar to that used by bacteria such as

Streptococcus pneumoniae or *Neisseria meningitidis* (Parente et al., 2017), is to recruit host complement regulatory proteins into the surface of the virions. For example, HIV and human cytomegalovirus incorporate DAF/CD55 and CD59 into their viral envelope structure, and thus protect the virions from complement-mediated lytic killing (Sadlon et al., 1994, Saifuddin et al., 1995, Spear et al., 1995). Similarly, mumps virus incorporates CD46, thus affecting the FI-mediated cleavage of C3b and C4b and increasing viral resistance to complement-dependent neutralisation (Johnson et al., 2009).

While poxviruses and herpes viruses are large and as discussed above can contain the sequence capacity to encode viral homologs of a number of cellular factors (Friedman et al., 1984, Harris et al., 1990, Bernet et al., 2003, Liszewski et al., 2006), smaller viruses such as flaviviruses do not encode proteins with any sequence homology to host regulators. Yet, these viruses can still antagonise the complement system. The flavivirus NS1 protein has been suggested to prevent complement activation in different ways. NS1 from DENV, WNV and yellow fever virus, promotes cleavage of C4 and C4b by forming a complex with C1s and C4 or by direct association with the regulatory protein C4bp, leading to attenuation of the CP and LP (Avirutnan et al., 2010). In addition, soluble and cell-surface associated WNV NS1 is able to bind and recruit FH to enhance the cofactor activity of this protein for FI-mediated cleavage of C3b to iC3b. This results in decreased complement activation in solution and attenuated deposition of C3b and C5b-9 membrane attack complexes on cell surfaces and thus increased survival of virions and virus-infected cells (Chung et al., 2006). Interestingly, this property of NS1 is not conserved across the flavivirus family, with NS1 of DENV unable to bind FH (Chung et al., 2006). A recent study, however has demonstrated another alternative that NS1 uses to evade the complement system. NS1 from DENV, ZIKV and WNV can inhibit the terminal complement pathway by binding to vitronectin, a terminal complement regulator, and inhibiting C9 polymerisation and the formation of MAC (Conde et al., 2016). Thus, complement must have an important anti-viral role and aligning with this, viruses, including DENV, have evolved varied strategies to overcome this.

1.3.3 Pathogenic role of complement during viral infections

While the protective role of the complement system during viral infections is clear, the pathogenic effects of complement have also been documented. There are many examples that support the harmful actions of complement during viral infections, as discussed below.

Complement activation via C1q as a result of hepatitis C virus (HCV) infection has been associated with altered T-cell responses and hepatic inflammation. The complex formed by C1q receptor (C1qR) and the core protein of this virus is able to inhibit the proliferation of human peripheral blood T-cells in a mouse model (Kittlesen et al., 2000). Furthermore, binding of HCV core protein via C1qR on activated T-cells decreased the production of IL-2 and IFN- γ as well as the expression of IL-2 receptor and CD69 (Kittlesen et al., 2000). In addition, binding of HCV core protein with C1qR on dendritic cells isolated from chronic patients, limited the induction of Th1 response (Cummings et al., 2007). In a similar context of chronic HCV infections, continuous complement activation has been associated with liver fibrosis, while high levels of C5 and C5a in the serum of a mouse model of fibrosis induced-disease, have led to severe hepatic damage (Hillebrandt et al., 2005). Thus, during HCV infection complement leads to dysregulation of T-cell responses that may influence the establishment of persistence, while chronic elevated complement activity may itself be associated with HCV-associated liver damage.

Another interesting example is the role of complement in Ross River virus (RRV) infections. Evidence of elevated levels of the anaphylotoxin C3a, an indicator of complement activation, has been detected in synovial fluid from RRV-infected patients (Morrison et al., 2007). Consistent with these findings, RRV-infected C3 and CR3-deficient mice exhibit less severe tissue damage and signs of disease than wild wild-typetype mice (Morrison et al., 2007, Morrison et al., 2008). Further, high levels of MBL in the serum and synovial fluid have been correlated with severity of disease in naturally RRV-infected patients, while RRV-infection of MBL-deficient mice results in enhanced severity of disease (Gunn et al., 2012).

1.3.3.1 Pathogenic role of complement during DENV infection

Differences in DENV disease severity are associated with complement activity, and this constitutes a very good example of the pathogenic consequences of inappropriate activity of complement system. Several lines of evidence suggest that excessive complement activation is associated with the most severe forms of the disease, DHF and DSS. Early studies demonstrated the presence of lower levels of C3, C4 and FB (which indicates excessive consumption of these molecules) and higher levels of the anaphylotoxins C3a and C5a (i.e. complement split products) in the circulation of severe DHF patients compare to DF patients (Bokisch et al., 1973, Churdboonchart et al., 1983). Consistent with these findings, Nascimento and collaborators in 2009 also found low levels of C3 and increased levels of C3 cleavage products in DHF cases compare to DF cases. Interestingly, these

authors detected higher levels of FD (which promotes complement AP activity, see section I.2.3.1.c) and lower levels of FH (a negative regulator of complement AP activity, see section I.2.3.1.f) in patients with DHF/DSS compared to patients with DF suggesting a hyper-activation of the complement AP (Nascimento et al., 2009).

On the other hand, soluble and cell-associated NS1 as well as anti-NS1 antibodies have been shown to enhance complement activation, leading to an increase of local and systemic generation of anaphylotoxins like C5a and the terminal complement complex C5b-9 in pleural fluids from patients with DHF, which interestingly accumulate before the onset of plasma leakage (Avirutnan et al., 2006).

In conclusion, the complement system is crucial for protection against DENV infection but hyper-activation of the complement system is clearly a potential factor that contributes to the pathogenesis of DENV disease. The ways that complement may become dysregulated and the subsequent mechanisms by which this cascade influences DENV pathogenesis are, as yet, not well understood.

I.4 Hypothesis and Aims

I.4.1 Hypothesis

The complement alternative pathway is activated during DENV infection by IFN-driven responses resulting in reduced production of FH and increased production of FB, that are associated with increased disease severity.

I.4.2 Aims

The overall goal is to evaluate the production of FH and FB during DENV infection. Specifically, this thesis aimed to:

- 1) Develop techniques to specifically measure FH and FB mRNA and protein in human and mouse experimental systems:
 - a) RT-PCR
 - b) ELISA
 - c) High content imaging of intracellular protein (Operetta)
- 2) Quantitate DENV-induced FH and FB mRNA and protein changes in primary human DENV-infected cells, macrophages and EC, the main targets for DENV replication and pathogenesis, respectively, *in vivo*, and the consequences of this for:
 - a) C3b deposition on infected cells and
 - b) AP activity *in vitro*
- 3) To define human FH and FB transcriptional regulation by:
 - a) Matinspector computational prediction of promoter elements; and
 - b) Evaluating the role of IFN- β in driving FH and FB mRNA production from DENV-infected macrophages and EC.
- 4) Quantitate DENV-induced FH and FB mRNA and protein changes in sera and tissues from DENV-infected mice and link this to:
 - a) DENV disease severity *in vivo*
 - b) Potential influences of FB and FH induction during DENV infection such as IFN-signalling

CHAPTER II MATERIALS AND METHODS

II.1 Materials

II.1.1 Cells and cell lines

The primary cell types and cell lines employed in this study are listed in Table II-1.

Table II-1. Cell lines employed in this study

Cells	Description	Cell types	Use	Source
HUVEC	Human umbilical endothelial cells	Primary endothelial cells	DENV infection; Immunofluorescence, ELISA, PCR, Flow cytometry	Provided by A/Prof Claudine Bonder, Centre for Cancer Biology, UniSA.
MDM	Human monocyte derived macrophages	Primary macrophages	DENV infection; Immunofluorescence, ELISA, PCR, Flow cytometry	Isolated from healthy blood donors at the Australian Red Cross Blood Service
HepG2	Human hepatocellular carcinoma	Liver hepatocytes	DENV infection, PCR	Gift from Dr. Dong Gui Hu, Flinders University
MEF	Mouse embryonic fibroblast	Primary fibroblast	DENV infection, PCR, ELISA	Generated by Dr. Briony Gliddon, UniSA.
ARPE-19	Human retinal pigment epithelial cells	Retinal epithelium	DENV infection; Immunofluorescence, ELISA, PCR	Provided by Prof Justine Smith, Flinders University
HREC	HPV E6/E7-transduced human retinal endothelial cells	Primary retinal endothelium	DENV infection, Immunofluorescence, ELISA, PCR	Generated and provided by Prof Justine Smith, Flinders University
Vero	African green monkey	Kidney epithelial	Plaque assay	ATCC® CCL-81™
BHK-21	Baby hamster kidney clone 21	Kidney fibroblast	Virus production	ATCC® CCL-10™
C6/36	Aedes albopictus	Larva tissue	Virus production	ATCC® CRL-1660™

II.1.2 Cell culture media and reagents

II.1.2.1 Media for maintaining and culturing cells

HUVEC were cultured in M199 medium (Hyclone) supplemented with 20% (v/v) foetal bovine serum (FBS), 100 U/mL penicillin and 0.1 mg/mL streptomycin, 2 mM L-glutamine (all from Gibco, Life Technologies) and 0.3% (w/v) endothelial cell growth supplement (BD Bioscience). MDM were cultured in Dulbecco's Modified Eagle's Medium (DMEM) (HyClone, Thermo Scientific) supplemented with 10% (v/v) FBS, 10% (v/v) human heat-inactivated serum, 100 U/mL penicillin and 0.1 mg/mL streptomycin, 2 mM L-glutamine. HepG2, MEF and Vero cells were cultured in DMEM supplemented with 10% (v/v) FBS, 100 U/mL penicillin, 0.1 mg/mL streptomycin, and 2 mM L-glutamine. The HREC line was cultured in MCDB-131 medium (Sigma) with 5% (v/v) FBS and endothelial growth factors (EGM-2 SingleQuots supplement, omitting FBS, hydrocortisone and gentamicin; Clonetics-Lonza, Walkersville, MD). The ARPE-19 cell line was cultured in DMEM:F12 supplemented with 5% (v/v) FBS.

II.1.2.2 Cell culture buffers and reagents

- 1X Dulbecco's phosphate buffered saline solution (PBS) without calcium and magnesium (HyClone™, Thermo Scientific), pH 7.4.
- 1X Hank's balanced salt solution (HBSS) with calcium and magnesium (Hyclone™, Thermo Scientific), pH 7.4.
- 0.4% (w/v) Trypan Blue dissolved in PBS and filtered (0.22µM, Millipore) (BDH).
- 0.25% (v/v) Trypsin Protease (HyClone™, Life Sciences).

II.1.2.3 Plaque assay: media and reagents

- 2X DMEM (Millipore) supplemented with 3.5% (w/v) sodium bicarbonate, 100 U/mL penicillin and 0.1 mg/mL streptomycin, 2 mM L-glutamine, and 10 mM HEPES (Sigma).
- 0.7% (w/v) SeaPlaque agarose: 2.8 g of SeaPlaque agarose (Lonza) in 400 mL cell culture grade water (HyClone™). Autoclaved prior to use.
- 0.33% (w/v) Neutral red: 3.3g Neutral red (ICN Biomedicals) in 1L PBS. Filtered, sterilised and stored in the dark at room temperature (RT).

II.1.3 Virus strains

- Mon601, a laboratory clone of the DENV-2 New Guinea C strain (Gulano 1998)
- Cosmopolitan ZIKV strain, PRVABC59, kindly provided by Professor David Smith, University of Western Australia.

II.1.4 TLR ligands

- TLR3: 10 µg/ml polyinosinic:polycytidylic acid poly (I:C) (Sigma)
- TLR4: 1 µg/ml LPS (Sigma)

II.1.5 Primers

All oligonucleotides primers used in this study were purchase from GeneWorks (Thebarton, SA). Each oligonucleotide dried pellet was resuspended in sterile water (Baxter) to obtain a final stock concentration of 100 µM and stored at -20°C until use. Unless specified, all primers were further diluted to a working solution of 20 µM. Human and mouse oligonucleotide sequences utilised in this study are listed in Table II-2.

Table II-2. Oligonucleotide sequences utilised for amplification of mRNA

Primer	Sequence	Accession Number	Amplicon size (bp)
DENV-2	F: GCAGATCTCTGATGAATAACCAAC R: TTGTCAGCTGTTGTACAGTCG	NM_AF038403.1	102
Human Cyclophilin	F: GGCAAATGCTGGACCCAACACAAA R: CTAGGCATGGGAGGGAACAAGGAA	NM_021130.4	355
Human FH	F: AGGCCCTGTGGACATC R: AACTTCACATATAGGAATATC	NM_001014975.2	183
Human FB	F: ACTGAGCCAAGCAGACAAGC R: AGAAGCCAGAAGGACACACG	NM_001710.5	280
Human IFN-β	F: TGTCAACATGACCAACAAGTGTCT R: GCAAGTTGTAGCTCATGGAAAGAG	NM_002176.2	86
Human Viperin	F: GTGAGCAATGGAAGCCTGATC R: GCTGTACAGGAGATAGCGAGAA	NM_080657.4	84
Human OAS-1	F: TCCACCTGCTTCACAGAACTACA R: GGC GGATGAGGCTCTTGAG	NM_001320151.1	73
Human IFIT-1	F: AACTTAATGCAGGAAGAACATGACAA R: CTGCCAGTCTGCCCATGTG	NM_001270930.1	100
Mouse GAPDH	F: GACGGCCGCATCTTCTTGTGC R: TGCCACTGCAAATGGCAGCC	NM_008084.3	120
Mouse FH	F: CGTGAATGTGGTGCAGATGGG R: AGAATTTCCACACATCGTGCC	NM_009888.3	248
Mouse FB	F: CTCCTCTGGAGGTGTGAGCG R: GGTCGTGGGCAGCGTATTG	NM_008198.2	264

II.1.6 Molecular biology reagents and buffers

II.1.6.1 RNA extraction

- TRIzol® Reagent (Ambion™ Life Technologies)
- Isopropyl Alcohol 100% (Ajax Finechem)
- Ethanol Denatured 100% (Chem-Supply), diluted to 70% (v/v) in water
- Chloroform (Chem-Supply)

II.1.6.2 DNase treatment

- 10X DNase I Reaction buffer (New England BioLabs)
- DNase I (RNase-free) 2000 U/mL (New England BioLabs)
- 0.5M ethylenediaminetetraacetic acid (EDTA) (New England BioLabs)

II.1.6.3 Reverse transcription

- 60 µM Random Primer Mix (New England BioLabs)
- 10X Moloney Murine Leukaemia Virus (M-MuLV) Reverse Transcriptase Reaction Buffer (New England BioLabs)
- M-MuLV Reverse Transcriptase 200 000 U/mL (New England BioLabs)
- RNase Inhibitor, Human placenta 40 000 U/mL (New England BioLabs)
- 10 mM Deoxyribonucleotide triphosphates Mix (dNTPs) (Qiagen)
- Nuclease-free water (Promega)

II.1.6.4 Real time PCR

- 2X iTaq™ Universal SYBER® Green Supermix (Bio-Rad)
- 1X Sterile water for irrigation (Baxter)

II.1.6.5 Agarose gel electrophoresis

- 0.5X Tris Borate EDTA (TBE) buffer: 20 mM Tris base, 20 mM boric acid and 0.5 mM EDTA, pH 8.3
- 2% (w/v) DNA grade agarose dissolved in 0.5 X TBE (Progen)
- 6X EZ-Vision® Three Dye, DNA dye as loading buffer (Amresco)

- HpaII cut pUC19 DNA marker (500 ng/ml) (GeneWorks)

II.1.7 Antibodies

Primary and secondary antibodies used in this study are presented in Table II-3 and Table II-4, respectively.

Table II-3. Primary antibodies

Antibody	Use	Source
Mouse monoclonal 4G2 anti DENV-2	Immunofluorescence, Flow Cytometry	Kindly provided by Dr. Nicholas Eyre, University of Adelaide, ATCC® HB-112TM
Goat polyclonal anti-human FH	Immunofluorescence, ELISA, Western blot, Flow Cytometry	Calbiochem (Cat # 341276)
Mouse monoclonal anti-human FH	ELISA	Abcam (Cat # ab17928)
Goat polyclonal anti-mouse FH	Western blot	Santa Cruz (Cat # sc-17951)
Rabbit polyclonal anti-human and anti-mouse FB	Immunofluorescence, Western Blot	Santa Cruz (Cat # sc-67141)
Mouse monoclonal anti-human C3b	Flow cytometry	Biolegend (Cat # 846102)
Sheep polyclonal anti-mouse FH	ELISA	R&D Systems (Cat # AF4999)
Rat monoclonal anti-mouse FH	ELISA	R&D Systems (Cat # MAB 4999)
Rabbit polyclonal anti-human IFN- β	IFN- β blocking studies	Sapphire Bioscience (Cat # 31410-1)

Table II-4. Secondary antibodies

Antibody	Use	Source
Anti-goat conjugated to horseradish peroxidase	ELISA, Western blot	Calbiochem (Cat # AP106P)
Anti-mouse conjugated to horseradish peroxidase	ELISA	Promega (Cat # W4021)
Anti-rabbit conjugated to horseradish peroxidase	ELISA	Promega (Cat # W4011)
Anti-rat conjugated to peroxidase	ELISA	R&D Systems (Cat # AF005)
Anti-goat Alexa Fluor 546	Immunofluorescence, Flow cytometry	Invitrogen (Cat # A11056)
Anti-mouse Alexa Fluor 488	Immunofluorescence, Flow cytometry	Invitrogen (Cat # 11055)
Anti-rabbit Alexa Fluor 647	Immunofluorescence	Invitrogen (Cat # A27040)

II.1.8 ELISA: materials, buffers and reagents

- 96 well-microtitre plates medium-high binding (Greiner)
- Coating buffer: 50 mM Carbonate/Bicarbonate Buffer pH 9.6: 1.59g Na₂CO₃ (BDH), 2.93g NaHCO₃ (BDH), dissolved in 1L of deionized water
- Blocking solution: 2% (w/v) bovine serum albumin (BSA) (Sigma) in PBS
- Sample diluent: 1% (w/v) BSA in PBS
- Wash buffer: 1X PBS, 0.05% (v/v) Tween 20 (Sigma)
- Stop solution: Sulphuric Acid 0.5 M
- Developed solution: 3, 3', 5, 5'-Tetramethylbenzidine (TMB) peroxidase substrate (KPL)
- 0.05% (v/v) Triton X-100 (Sigma)
- Recombinant mouse FH commercial protein (R&D Systems 4999-FH)

II.1.9 Sodium dodecyl sulphate (SDS) PAGE and Western blot: buffers and reagents

- SDS PAGE lower gel buffer: 1.5 M Tris, pH 8.8, 0.4% (w/v) sodium dodecyl sulphate (SDS)
- SDS PAGE upper gel buffer: 0.5 M Tris pH 6.8, 0.4% (w/v) SDS
- 40% (w/v) Acrylamide solution (Biorad)
- 2% (w/v) Bis-Acrylamide (National Diagnostics)
- 10% (w/v) Ammonium persulfate dissolved in water (Biorad)
- Tetramethylethylenediamine (TEMED) (Biorad)
- Loading sample buffer: 0.25 M Tris-HCL, 8% (w/v) SDS, 20% (w/v) glycerol (Ajax Chemicals), 0.05% (w/v) bromophenol blue, 0.05% (v/v) 2-mercaptoethanol
- Running buffer: 25 mM Tris-HCL pH 7.6, 192 mM glycine, 0.1% (w/v) SDS
- Transfer buffer: 20 mM Tris-HCL pH 8.5, 150 mM glycine, 20% (v/v) ethanol
- Washing buffer: 10 mM Tris pH 7.6, 50 mM NaCl, 0.1% (v/v) Tween 20 (TBS-T)
- Blocking buffer: 5% (w/v) skim milk powder diluted in TBS-T

- Membrane: Life Sciences BioTrace™ NT pure nitrocellulose blotting membrane, 0.2 µm pore size (Pall Corporation)
- Marker: P7711S ColorPlus prestained ladder (New England Biolabs)
- Clarity™ Western ECL Substrate (Biorad)

II.1.10 Immunofluorescence: buffers and reagents

- 2% paraformaldehyde (PFA) (Sigma) in PBS
- 1% (w/v) BSA in PBS
- HBSS (Hyclone™, Thermo Scientific), pH 7.4
- 0.05% (w/v) octylphenoxy poly(ethyleneoxy) ethanol (IGEPAL® CA-630, Sigma) in PBS
- Buffered glycerol, 80% (v/v), pH 8.3: 1:2 of 0.5M Sodium carbonate buffer (0.5M Na₂CO₃ (BDH), 0.5M NaHCO₃ (BDH), and glycerol (Ajax Chemicals)

II.1.11 Flow cytometry: buffers and reagents

- 5mM EDTA in PBS
- 2% PFA (Sigma) in PBS
- 1% (w/v) BSA in PBS

II.1.12 Alternative pathway assay: buffers and reagents

- Alternative pathway buffer (AP buffer): Barbitone complement diluent tablets (Oxoid) diluted in 100 mL of warm distilled water, 0.01M ethylene glycol tetraacetic acid (EGTA) and 0.1% gelatin (Sigma), pH 7.5
- 1% (w/v) BSA in PBS
- Saline buffer: 0.15 M NaCl

II.2 Methods

II.2.1 Cell maintenance

Cell lines were maintained using aseptic technique in 25 cm² or 75 cm² surface cell culture flasks (Falcon) in a humidified incubator at 37 °C with 5% CO₂ (Heraeus, Function Line). Cells were passage every 3-4 days. Briefly, existing media was discarded, and cells were washed twice with PBS to remove the remaining FBS. Cells were trypsinised with 1 mL of 0.25% (v/v) trypsin for 2-3 minutes (min) at 37 °C. Rapidly, 3-5 mL of the corresponding complete media (section II.1.2.1) was added to the cells to inhibit the trypsinisation reaction and cells harvested. Cells were enumerated using trypan blue in a Hawksley counting chamber. Cells were re-seeded at 1x10⁵ (25 cm² flask) or 1x10⁶ (75 cm² flask) into 7 mL or 17 mL of their respective media and incubated at 37 °C and 5% CO₂ as above.

II.2.1.1 HUVEC

HUVEC were isolated from human umbilical cords, with approval from the Central Northern Adelaide Health Service human ethics approval and in accordance with the World Medical Association Declaration of Helsinki, by collagenase digestion and kindly provided by Professor Claudine Bonder. Frozen stocks of HUVEC were made at passage 2-3 and HUVEC were utilised in infection studies at passage 1-4.

II.2.1.2 MDM

Human MDM were isolated from healthy blood donors supplied by the Australian Red Cross Blood Service under a materials transfer agreement and used in accordance with approval from the Southern Adelaide Clinical Human Research Ethics Committee (SAC/HREC), approval number 343.16. Monocytes were isolated by adherence and cultured for four-five days in complete DMEM (section II.1.2.1) to differentiate into MDM, as previously described (Pryor et al., 2001, Wati et al., 2007). Briefly, peripheral blood mononuclear cells were prepared by density gradient centrifugation (Lymphoprep; Nycomed Pharma, Oslo, Norway) of buffy coat blood packs. Peripheral blood mononuclear cells were transferred to tissue culture flasks and monocytes were selected by adherence to flask surfaces after 2h. Non-adherent cells were further subjected to a second round of adherence. Adherent cells were washed with HBSS and fresh complete DMEM (section II.1.2.1) was added to the cells. After 48h adherent monocytes from 2–4 different blood donors were detached, pooled, cultured in complete DMEM. Cells were allowed to differentiate in culture for four-five days into macrophages. After this time, MDMs were

detached by gentle scraping in HBSS. The purity of MDM preparations was visually assessed and has been previously validated in our laboratory as MDM by Wright-Giemsa staining and morphological analysis by light microscopy and 85-90% CD14+ by flow cytometry (Wati et al., 2007).

II.2.2 Viral stocks and infection

II.2.2.1 Virus production

Mon601, a laboratory clone of the DENV-2 New Guinea C strain, was used for infections (Gualano et al., 1998) and is hereafter referred to as DENV. DENV-2 is a predominant global DENV serotype and hence used in this study. Virus stocks were produced from *in vitro* transcribed RNA that was transfected into BHK-21 cells and amplified in C6/36 cells. Cell culture supernatants containing virus were harvested, clarified, filtered (0.22µm, Sartorius), and stored at -80°C until use. The titer of infectious virus was determined by plaque assay using Vero cells and quantitated as plaque forming unit (pfu) per mL. ZIKV infections utilised the cosmopolitan ZIKV strain, PRVABC59 that was amplified in C6/36 cells, stocks collected, and titred as described above for DENV. ZIKV was used as a comparative control. Viral stocks were generated and kindly provided by Associate Professor J Carr.

II.2.2.2 Viral infection

For DENV and ZIKV infection cells were seeded in 6-well culture plates (Falcon) at 3×10^5 in the corresponding cell culture media. Plates were incubated overnight to allow cells to attach. The corresponding viral stock was diluted in serum-free media at a multiplicity of infection (MOI) of 1. MDM were infected with a MOI of 3 as previously described (Wati et al., 2007). Cells were left uninfected (UI) or infected by adding 300 µl of serum-free media or the diluted virus, respectively. Plates were incubated for 90 min with gentle rocking every 15 min. After this time, the inoculum was removed, cells washed with PBS, and fresh complete medium was added. Supernatants and cells were harvested after 24 and 48hpi. Supernatants were clarified by centrifugation at $2900 \times g$ (Dynamica velocity 13µ centrifuge). Cells were treated with 500 µl of TRIzol reagent for RNA extraction as described in section II.2.5. Collected supernatant and cells were stored at -80°C until analysis.

II.2.3 TLR treatment of cells

HUVEC or MDM cells were seeded at 3×10^5 in 6-well plate as above and treated with 10 µg/ml poly (I:C) (TLR3) or 1 µg/ml LPS (TLR4) for 24 and 48h. DENV infection was carried

out in parallel and as described above. Supernatants and cells were harvested after 24 and 48hpi and stored at -80°C until analysis.

II.2.4 Viral quantitation by plaque assay

Vero cells were seeded into 6-well plates at 3×10^5 cells per well in 2 mL of DMEM complete media (section II.1.2.1) and incubated at 37°C with 5% CO₂ overnight. Ten-fold serial dilutions from 10^{-1} to 10^{-5} of test supernatants from infected cells or positive control (DENV or ZIKV stocks of known titre) were prepared in serum-free media. 300 µl of the diluted supernatants or positive control were added to each well-containing cells. Plates were incubated at 37°C, 5% CO₂ and rocked every 15 min for a total of 90 min. After this time the inoculum was removed, and the cells were washed once with PBS. Cells were then overlaid with 3 mL of a 1:1 mix of 0.7% (w/v) SeaPlaque Agarose and 2X DMEM containing 10% (v/v) FBS. Plates were incubated for five days at 37°C, 5% CO₂ and overlaid for a second time with 2 mL of 1:1 mix of 0.7% (w/v) SeaPlaque Agarose and 2X DMEM containing 10% (v/v) FBS and 0.03% (w/v) Neutral Red. Plates were incubated for another five days at 37°C, 5% CO₂ and the number of visual plaques were counted from dilutions that yielded countable plaques (10-50). PFU/mL for each sample was calculated following the following equation:

$$PFU/mL = \frac{\text{Number of plaques}}{\text{Volume added for infection}(0.3 \text{ mL})} \times \text{dilution factor}$$

II.2.5 RNA extraction

Total RNA was extracted from cells and mouse tissues using TRIzol. To extract RNA from mouse tissues, samples were first homogenised in TRIzol using a sonicator (Heat System Ultrasonics Inc Sonicator Cell Disruptor). Heart and kidney samples were submitted to 2 x 30 seconds (sec) cycles of sonication while the liver samples were sonicated using 3-4 cycles of 30 sec each. In all cases the sonication was performed on ice and at power 375 Watts, 60/60 Hz. RNA extraction was performed according to the manufacturer's instructions. In brief, 200 µl of chloroform was added per 1 mL TRIzol and incubated for 10 min at RT. After this time, samples were centrifuged at 12 000 x g for 15 min at 4°C (Heraeus Fresco 17 Microcentrifuge, Thermo Scientific). The RNA present in the upper aqueous phase was collected and precipitated with 1.5 mL of 100% isopropanol per 1 mL of TRIzol. Samples were incubated for another 10 min at RT and centrifuged, as above. The RNA pellet was washed with 1 mL of 70% (v/v) ethanol per 1 mL of TRIzol followed by a centrifugation for 5 min at 7 500 x g. The pellet was air-dried and resuspended in 10 µl of

nuclease free water for RNA extracted from cells and 200 μ l for mouse tissues RNA.

II.2.6 DNase I treatment

The extracted RNA was DNase I treated to eliminate any contaminating genomic DNA that may produce false-positive PCR results. Briefly, 20 μ l of RNA was incubated with 10U DNase I enzyme and 1X DNase I reaction buffer for 15 min at 37°C. The reaction was stopped by adding 1 μ l of 125 mM EDTA to yield a final concentration of 5 mM EDTA and incubated for 10 min at 75°C. Total RNA was quantitated by spectrophotometry (NanoDrop elite, Thermo Scientific) at 260nm and stored at -80 °C until use.

II.2.7 Reverse transcription

The DNase-free RNA was reverse transcribed into cDNA in two steps using a thermocycler (Applied Biosystems). In the first step, 0.5 μ g RNA was incubated with 60 μ M random hexamers and RNase free-water at 65 °C for 5 min then rapidly cooled to 4°C (RT-1). In the second step, a mix of 10 U M-MuLV reverse transcriptase, 5 mM dNTPs, 10 U RNase inhibitor and 1X M-MuLV reaction buffer was added to RT-1 (RT-2). The RT-2 was incubated at 37°C for 90 min, 5 min at 95°C (to inactivate the enzyme) and cooled to 4°C. The resulting cDNA was stored at -20°C until used.

II.2.8 Real-time quantitative polymerase chain reaction (RT-qPCR)

cDNA template was subjected to real-time RT-qPCR using iTaq SYBER green in a Rotor-gene 6000 (Corbett Research), using primers listed in Table II-2. All PCRs, except mouse FB PCR, were performed under the following conditions: one cycle of 95°C for 5 min; 40 cycles of 95°C for 15 sec, 59°C for 30 sec, and 72°C for 30 sec; and one cycle of 72°C for 5 min. Mouse FB PCR used the following cycling profile: one cycle of 95°C for 10 min; 40 cycles of 95°C for 15 sec, 60°C for 30 sec, and 72°C for 30 sec; and one cycle of 72°C for 5 min. All PCR reactions were performed in duplicate and included high and low copy number comparative controls. Results were normalized against the reference housekeeping genes: cyclophilin (for human PCR) or glyceraldehyde-3-phosphate dehydrogenase (GAPDH, for mouse PCR). The relative RNA level was determined by Δ Ct method as described (Schmittgen and Livak, 2008).

II.2.9 SDS PAGE and Western Blot

Human and mouse sera (diluted 1:100 in PBS), and supernatants harvested from HUVEC or MEF-infected cells were prepared with 5X SDS loading buffer (section II.1.9) and denatured at 90°C for 10min. The samples were loaded onto an 8% (w/v) polyacrylamide

resolving gel with 4% (w/v) polyacrylamide stacking gel (section II.1.9), an appropriate gel percentage to detect proteins bigger than 100 kDa. The gel was electrophoresed for approximately 2h at 20 mA and then proteins transferred to a nitrocellulose membrane at 100mA for 1h. The membrane was blocked with blocking buffer (section II.1.9) and incubated overnight at 4°C with the desired primary antibody as described in Table II-3. The membrane was then incubated with the corresponding secondary antibody (Table II-4) 1: 30 000 for 2h at RT. Bound complexes were detected by chemiluminescence (Clarity™ Western ECL Substrate), visualised and images captured with a LAS4000 (Fuji Imaging Systems).

II.2.10 Human complement FH purification

FH was purified from human serum by a one-step affinity chromatography using CNBr-activated sepharose 4B coupled to a sheep anti-human FH polyclonal antibody (Ormsby et al., 2006). Briefly, total human serum was diluted 1:2 in PBS and loaded onto the column and the flow-through re-loaded at least four times. After washing with PBS, FH was eluted with 0.1 M glycine (pH 2.3) and immediately neutralised with 1M Tris-HCL (pH 8.8). Eluted fractions were analysed by SDS-PAGE under reducing and non-reducing conditions and Western blot using the primary goat anti-human FH (1:2000) and secondary anti-goat IgG coupled to horseradish peroxidase (1:30 000), as described in section II.1.9. FH containing fractions were pooled and concentrated using Amicon Ultra 0.5 mL centrifugal filter (100 MWCO, Millipore) and purity of FH re-assessed by Western blot, as in section II.1.9. Protein concentration of the purified FH protein was determined by Bio-Rad protein assay as described in the section below II.2.11.

II.2.11 Quantitation of protein concentration

Protein concentration of fractions-containing purified FH protein (section II.2.10) was determined by Bio-Rad protein assay (catalogue # 500-0006) following manufacturer's instructions. Serial dilutions of BSA from 1 mg/mL to 0.00781 mg/mL were used as a standard curve. Purified FH fractions were diluted from 1:10 to 1:10 000 in PBS. Standards and samples were incubated with the commercial Bio-Rad protein assay dye reagent concentrate at RT for 15 min. The absorbance was read at 595 nm in a microplate reader (Beckman Coulter).

II.2.12 Development of an in-house ELISA to detect human and mouse FH

Human and mouse FH ELISAs were standardised using purified human FH (isolated as above section II.2.10) and commercial recombinant mouse FH, respectively. 96 well-

microtitre plates were coated with goat anti-human FH at 2.5, 5 and 10 µg/mL or with sheep polyclonal anti-mouse FH antibody at 2.5 and 5 µg/mL (Table II-3), diluted in coating buffer (section II.1.8) and incubated overnight at 4°C. Plates were blocked with ELISA blocking solution (section II.1.8) for 1h at 37°C. Purified human FH protein, diluted in sample diluent (section II.1.8) from 400 to 10 ng/mL or recombinant mouse FH, diluted from 200 to 20 ng/mL were used to generate a standard curve and incubated on the plates for 2h at 37°C. Plates were washed five times with washing buffer (section II.1.8) and incubated for 1h at 37°C with three two-fold serial dilutions (1:5000, 1:10 000, 1:20 000) of the detection antibody i.e.: a mouse anti-human FH monoclonal antibody for human FH detection or a rat monoclonal anti-mouse FH for mouse FH detection (Table II-3). Plates were washed again and incubated for 1h at 37°C with the corresponding secondary antibody: anti-mouse IgG or anti-rat IgG coupled to horseradish peroxidase (Table II-4), diluted 1:10 000 in sample diluent. Plates were washed seven times, developed with TMB peroxidase substrate, stopped with 1 M sulphuric acid and absorbance quantitated at 450 nm in a microplate reader (Beckman Coulter). Inter- and intra-assay coefficient of variations were calculated from duplicate values of three different standard concentrations run three times in the same assay or in three independent assays, respectively, using the following formula:

$$\text{Coefficient of Variation (\%)} = \frac{\text{Standard Deviation } (\sigma)}{\text{Mean } (\mu)} \times 100$$

II.2.12.1 Quantitation of human and mouse FH proteins by ELISA

Human or mouse FH proteins were quantitated in human or mouse sera and in supernatants collected from uninfected or DENV-infected cells by ELISA as described in section II.2.12 with selected concentrations for coating, detection and secondary antibodies as follows. 96 well-microtitre plates were coated with goat anti-human FH at 10µg/ml (for human FH detection) or with sheep polyclonal anti-mouse FH antibody at 2.5 µg/mL (for mouse FH detection). Human and mouse serum were diluted 1:1000 and 1:500 in sample diluent, respectively. Supernatant samples were always evaluated neat. A mouse anti-human FH or a rat monoclonal anti-mouse FH diluted 1:10 000 were used as detection antibodies in human and mouse FH, respectively. The methodology was performed as described in section II.2.12. Standard curves with purified human FH or commercial recombinant mouse FH were established using eight standard concentrations and producing a linear regression curve ($R^2 > 0.99$). The range of detection was as described above in section II.2.12.

II.2.13 Quantitation of human and mouse FB proteins by ELISA

The levels of human or mouse FB in serum or in the supernatants from either uninfected or DENV-infected cells were measured using the Human FB (ab137973, Abcam) or the mouse FB (SEC011Mu, Cloud-Clone Corp) ELISA kits, respectively, in accordance with the manufacturer's instructions.

II.2.14 Treatment of supernatant samples with Triton X-100 or heat

To disrupt possible interactions between FH and viral or other protein(s), supernatants from DENV-infected cells were treated with 0.05% of Triton X-100, 30 min at RT or incubated 30 min at 56°C and then evaluated by human FH ELISA as described above (section II.2.12.1). Supernatants from uninfected cells were also treated and evaluated as controls.

II.2.15 AP *in vitro* activity assay

Whole blood was collected under aseptic conditions from a healthy rabbit in accordance with Flinders University Animal Welfare Committee approvals for collection of scavenge material. The blood was placed into a conical glass flask containing glass beads and was gently swirled until a clot was formed. The defibrinated blood was decanted and washed three to four times in AP buffer (section II.1.12) until the supernatant was clear. Cell containing supernatant was enumerated and 5×10^7 cells/ml of rabbit erythrocytes were resuspended in AP buffer and used as a master stock for the haemolysis assay.

For the assay, normal human serum (NHS) was incubated with AP buffer for 15 min on ice to inactivate the CP and the LP. Uninfected and DENV-infected cell supernatants were mixed with treated NHS (to support the AP activity) at different percentages (from 5 to 20%). To evaluate the possible effect of FH, DENV-infected cell supernatant was supplemented with exogenous purified FH protein at 500 µg/mL and serially diluted with different concentrations of NHS as above. 50 µl of each NHS/supernatant mix were added in duplicate to a flat bottom 96-well plate (Costar) and 50 µl of the rabbit erythrocyte master stock was overlaid to the wells. The plate was incubated 30 min at 37°C with intermittent agitation. Three controls were included in the assay: NHS serially diluted in AP buffer, 100% haemolysis control consisting of erythrocytes mixed with water 1:1, and an erythrocyte cell blank consisting in erythrocytes mixed with AP buffer 1:1. After incubation, 150 µl ice-cold saline buffer (section II.1.12) were added to the wells, except to the 100% lysis wells. The plate was centrifuged 5 min at 1400 rpm and 150 µl of the supernatant

transferred to a new plate. Haemolysis was assessed by measuring absorbance at 405 nm in a microplate reader (Beckman Coulter) and % haemolysis calculated by:

$$\% \text{ of Lysis} = \frac{(OD_{405} \text{ Sample} - OD_{405} \text{ Blank})}{(OD_{405} \text{ Total lysis} - OD_{405} \text{ Blank})} \times 100$$

II.2.16 Flow cytometry

For FH and DENV staining, HUVEC or MDM were cultured in a 6-well plate and infected as in section II.2.2.2. After 48h cells were washed twice with PBS and detached by gentle scraping in PBS with 5mM EDTA. Cells were washed again with PBS and blocked with 1% (w/v) BSA for 30 min at RT. Cells were rinsed once with PBS and incubated with a goat anti-human FH (1:25) for 1h at RT (Table II-3). After three washes with PBS-BSA 1% (w/v) cells were incubated for 1h at RT with an anti-goat Alexa 546 (1:200) (Table II-4). Subsequently, cells were fixed with 2% (w/v) PFA for 10 min at RT. After three washes with PBS-BSA 1% (w/v) cells were permeabilised with 0.05% (w/v) IGEPAL® CA-630, in PBS for 20 min, washed again with PBS and blocked with 1% (w/v) BSA for 30 min at RT. Cells were rinsed once with PBS and incubated overnight at 4°C with the mouse 4G2 anti-DENV, 1:10 (Table II-3). After three washes with PBS-BSA 1% (w/v) cells were incubated for 1h at RT with a donkey anti-mouse AlexaFluor 488 (1:200) (Table II-4). Following a final set of PBS-BSA washes, cells were analysed by flow cytometry with a CytoFlex S (Beckman Coulter Inc.) and analysed by CytExpert 2.0.0.153 software (Beckman Coulter Inc.).

For the detection of C3b deposition during complement activation, HUVEC or MDM were cultured and infected as above. After 48h the culture media was removed and cells were incubated in M199 medium (section II.1.2.1) containing 10% NHS (as the external complement source) for 30 min at 37°C in a 5% CO₂ incubator. Cells were also incubated with the corresponding media containing 10% heat inactivated NHS as negative control. Cells were washed, detached with PBS/5mM EDTA and immunostained as described above. C3b deposition was detected with a mouse anti-human C3b (1:25) and a donkey anti-mouse AlexaFluor 488 (1:200) (Table II-3 and Table II-4). Cells were fixed and analysed by flow cytometry as above.

II.2.17 Immunostaining and high-throughput image analysis

1x10⁴ HUVEC, MDM, ARPE19 or HREC cells were plated in a 96 well plate (Cell Carrier Ultra, PerkinElmer) and allowed to attach for 24h. Cells were DENV-infected as described

in section II.2.2.2 and at 48h pi cells were fixed with 2% (w/v) PFA for 10 min at RT. After three washes with PBS, cells were permeabilized with 0.05% (v/v) IGEPAL[®] CA-630 in PBS for 20 min. Cells were washed again with PBS and blocked with 1% (w/v) BSA and 2% (v/v) normal goat serum diluted in HBSS solution for 30 min at RT. Cells were rinsed once with PBS and incubated overnight at 4°C with mouse 4G2 anti-DENV, 1:10, goat anti-human FH (1:25) and a rabbit anti-human FB (1:25) (Table II-3). After three washes with PBS cells were incubated for 1h at RT with the corresponding secondary antibodies: donkey anti-mouse AlexaFluor 488 (1:75), donkey anti-sheep-Cy3 (1:75) and goat anti-rabbit AlexaFluor 647 (1:75) (Table II-4). Nuclei were stained with Hoechst 33342 (5 µg/mL). Following a final set of PBS washes, cells were imaged with an Operetta high-content imaging system with Harmony software (PerkinElmer) at 20x magnification. 49 different images were taken for each well, representing approximately 10000 cells. Nuclei and cytoplasm were discriminated using the Hoechst and Cy3 channels, respectively using the sequence of building blocks detailed in Appendix 1. Mean Alexa-488, Cy3 and Alexa-647 intensity in the cell cytoplasm of each individual cell was calculated as described in Appendix 1. Using visual observation and intensity histograms, an Alexa-488 intensity threshold was set to define DENV-infected cells. Imaging was performed at the Flinders University, Cell Screen South Australia (CeSSA) facility.

II.2.18 Promoter analysis

Human and mouse FB and FH promoter analysis was performed using MatInspector software version 8.4.1, in the 'General Core Promoter Elements' and 'Vertebrates' sections of Matrix Library 11.0 (October 2017) from the Genomatix suit v3.10 (Cartharius et al., 2005). The parameters for selecting the binding sites were set at matrix similarity and core similarity 0.85 (maximum 1.00) as described (Cartharius et al., 2005).

II.2.19 DENV- seropositive and seronegative human serum samples used for quantitation of circulating FH and FB

Human serum samples from DENV-seropositive and seronegative patients form part of a retrospective descriptive study (Quinn et al., 2018). These samples were collected over a 13-month period between 1 January 2014 and 31 January 2015. Samples were identified from SA Pathology DENV diagnostic worklists and database records searched to identify test requests and results from the same clinical episode (Quinn et al., 2018). Sera was obtained from archival material remaining after completion of diagnostic testing and stored at -20°C. The current study includes 8 DENV-seronegative and 29 DENV-seropositive patients of the total cohort (Quinn et al., 2018) and were subjected to human FH and human FB ELISA, as described in sections II.2.12.1 and II.2.13, with the assistance of Mr Jarrod Hulme-Jones, MD Advanced Studies student.

II.2.20 Mice

II.2.20.1 C57BL/6 mice

Liver, kidney and heart tissues were collected from healthy C57BL/6 mice in accordance with Flinders University Animal Welfare Committee approvals for collection of scavenge material. Tissue samples were collected directly into TRIzol reagent for RNA extraction (section II.2.5) and used to validate mouse FB and FH PCRs (section II.2.8).

II.2.20.2 C57BL/6 mouse model of intracranial DENV infection

RNA from brain samples used to evaluate FB and FH mRNA induction were kindly provided by Mr. Wisam AlShujairi, PhD student. Brains were collected from three-four-week-old C57BL/6 mice infected by intracranial injection with DENV-2 MON601 or mock infected, and clinical signs of neurovirulence were monitored as previously described (Al-Shujairi et al., 2017).

II.2.20.3 AG129 mouse model of DENV infection

Serum and tissue samples from an AG129 mice model of DENV infection were kindly provided from experiments performed by Dr. Penny Rudd under the guidance of Professor Suresh Mahalingam, Griffith University, Queensland, Australia. In brief, mice were left uninfected or infected subcutaneously with 10^4 of a DENV-2 strain, D2Y98P, isolated from a patient in Singapore during 2005 (GenBank accession # JF327392). The clinical signs were scored as described in (Ng et al., 2014): 1 - ruffled fur, 2 - hunched back, 3 – severe diarrhea, 4 - moribund stage. Serum, liver and kidney samples were harvested at 2 days pi (dpi), 4dpi and at moribund stage (~20 dpi) when the animals were humanely euthanised

in accordance with animal ethics approval (section II.2.21). Each group of animals consisted of six mice except for the 4dpi group that contained seven animals. All tissue samples were collected directly into TRIzol reagent for RNA extraction (section II.2.5) and sera and tissue samples shipped on dry ice to Flinders University and stored at -80°C prior to analysis.

II.2.20.4 AG129 mouse model of ADE of DENV infection

Serum samples as well as liver and kidney tissues from an AG129 mouse model of ADE of DENV infection were kindly provided from experiments performed by Dr Li Ching under the guidance of Prof. Sylvie Alonso, National University of Singapore, Singapore in accordance with animal ethics approval (section II.2.21). Briefly, pups born from previously DENV-1 infected, but convalescent mothers or DENV-naïve mothers were either left uninfected (UI-N; UI-I, n=3 each) or infected subcutaneously with 10³ pfu of D2Y98P DENV-2 (DENV-N; DENV-I, n=5 each), as described previously (Ng et al., 2014). The clinical symptoms were scored as described in (Ng et al., 2014): 1 - ruffled fur, 2 - hunched back, 3 – severe diarrhoea, 4 - moribund stage. Serum samples were collected at 3 and 6dpi. Liver and kidney samples were harvested at 6dpi when the mice were euthanised. For DENV-N the moribund stage was reached at 12-18 dpi while for DENV-I the moribund stage was as early as 6-7dpi (Ng et al., 2014). Tissue samples were collected directly into TRIzol reagent for RNA extraction (section II.2.5) and sera and tissue samples shipped on dry ice to Flinders University and stored at -80°C prior to analysis.

II.2.21 Ethics statement

HUVEC were isolated from human umbilical cords collected with approval from the Central Northern Adelaide Health Service human ethics approval and in accordance with the World Medical Association Declaration of Helsinki and provided by Professor Claudine Bonder. Normal human serum was collected from healthy donors in accordance with the SAC/HREC approval number 343.16. Data collected from seropositive and seronegative DENV patients were de-identified and stored securely to maintain privacy, in accordance with SAC/HREC approval number 200/15. Stored patient sera were obtained under SAC/HREC approval number 134/15, with all undertakings in accordance with the World Medical Association Declaration of Helsinki. C57BL/6 mice experiments were performed in agreement with Flinders University Animal Welfare Committee approval number 870/14 and in accordance with the Animal Welfare Act 1985 and Institutional Biosafety Committee approval NLRD 2011-10. AG129 mice experiments were performed under the guidelines

of the National Advisory Committee for Laboratory Animal Research (NACLAR) under licence to operate in accredited animal facilities with IACUC/NUS protocol approval number 2013-04751 or and in accordance with approval from Griffith University Animal Welfare Committee number GLY/11/14/AEC. The use of infectious risk group 2 microbiological virus (ZIKV) was undertaken in accordance with Flinders University Institutional Biosafety Committee, (IBC) NLRD 2011-13 reference number 2016-07, and of genetically modified risk group 2 microbiological (DENV Mon601) in accordance with OGTR guidelines and IBC approval 2011-10.5 NLRD PC2.

II.2.22 Statistical analysis

Results were expressed as the mean \pm standard deviation, and statistical analyses were performed using a two-tailed unpaired Student *t*-test, one-way or two-way analysis of variance (ANOVA) in GraphPad Prism, version 7 (GraphPad, La Jolla, CA, USA). Differences were considered statistically significant if $p < 0.05$.

CHAPTER III ESTABLISHMENT AND TECHNICAL VALIDATION OF DIFFERENT METHODS TO DETECT RNA AND PROTEIN OF COMPLEMENT FH AND FB IN A VARIETY OF HUMAN AND MOUSE SAMPLES

III.1 Introduction

FH and FB are two important regulators of the complement AP. While FB is considered as a positive mediator that promotes the activity of the AP (Alper et al., 1973), FH is believed to be the master negative regulator of this pathway (Whaley and Ruddy, 1976, Davis et al., 1984). FH and FB, like the rest of the complement proteins, are primarily synthesised by hepatocytes within the liver (Adinolfi et al., 1981, Perlmutter et al., 1989). Additionally, they may be synthesised locally by other cell types including renal, endothelial and epithelial cells, platelets, adipocytes and macrophages (Morris et al., 1982, Schwaeble et al., 1987, Brooimans et al., 1990, Vik et al., 1990, Chen et al., 2007b, Licht et al., 2009, Sakaue et al., 2010, Tu et al., 2010). Circulating FH and FB proteins are abundant in human plasma (~ 500 µg/mL) (Silva et al., 2012) and detectable in mouse sera (>10 µg/mL) (Nichols et al., 2015).

Variations in FH and FB gene expression and protein levels in plasma have been associated with alterations in AP activity and subsequently with the outcome of different diseases (see Chapter I, section I.3.3) (Hyams et al., 2013, van der Maten et al., 2016). There are precedents in the literature indicating that there are higher levels of FD (an activator of the AP activity) and lower levels of FH (a negative regulator of complement AP activity) in patients with DHF/DSS compared to patients with DF suggesting a hyper-activation of the complement AP (Nascimento et al., 2009). The current thesis project aimed to expand this knowledge and specifically to study the induction of FH and FB following DENV infection in two human primary cell types that are relevant to DENV-disease: HUVEC and macrophages, and in the AG129 mouse model. Therefore, reliable methods were needed to evaluate FH and FB mRNA expression and protein production in these two species. Thus, this chapter describes the development and standardisation of different methods to specifically detect FH and FB mRNAs and proteins that will be applied in later chapters.

III.2 Results

III.2.1 Validation of RT-PCR for human and mouse FH and FB

III.2.1.1 Validation of human FH and FB RT-PCR

A DNA construct of the full-length human FH transcript (GenBank accession number NM_000186.3) cloned into the pBlueScript plasmid (H20 pBlueScript) was kindly provided by Prof. David Gordon (Gordon et al., 1995). Serial dilutions of the H20 pBlueScript from 10^{-3} to 10^{-5} pg/ μ l were evaluated using a range of FH primer concentrations targeting the SCR 2 of FH. Optimal amplification was achieved at 10 μ M for both forward and reverse oligonucleotides (data not shown) and thus used for following experiments. The results from RT-PCR show a melt profile with a single symmetrical peak at 80°C (Figure III-1 A) and linear amplification curves, with approximately a 5-Ct change corresponding to a 10-fold dilution and a sensitivity of at least 10^{-5} pg/ μ l (Figure III-1 B). This generated a standard curve with an R^2 value of 0.992 (Figure III-1 C). No melt curve at 80°C or linear amplification was detected for the negative (no template) controls (Figure III-1 A, B). The end products from this PCR were collected and evaluated by agarose gel electrophoresis (Figure III-1 D). Consistent with the florescent amplification and melt profiles, a single band of 183 bp, the expected size for FH PCR product (Table II-2, Chapter II), was observed for each sample evaluated except for the negative control (Figure III-1 D). H20 DNA at 10^{-4} and 10^{-5} pg/ μ l were used in all subsequent human FH RT-PCR as positive controls.

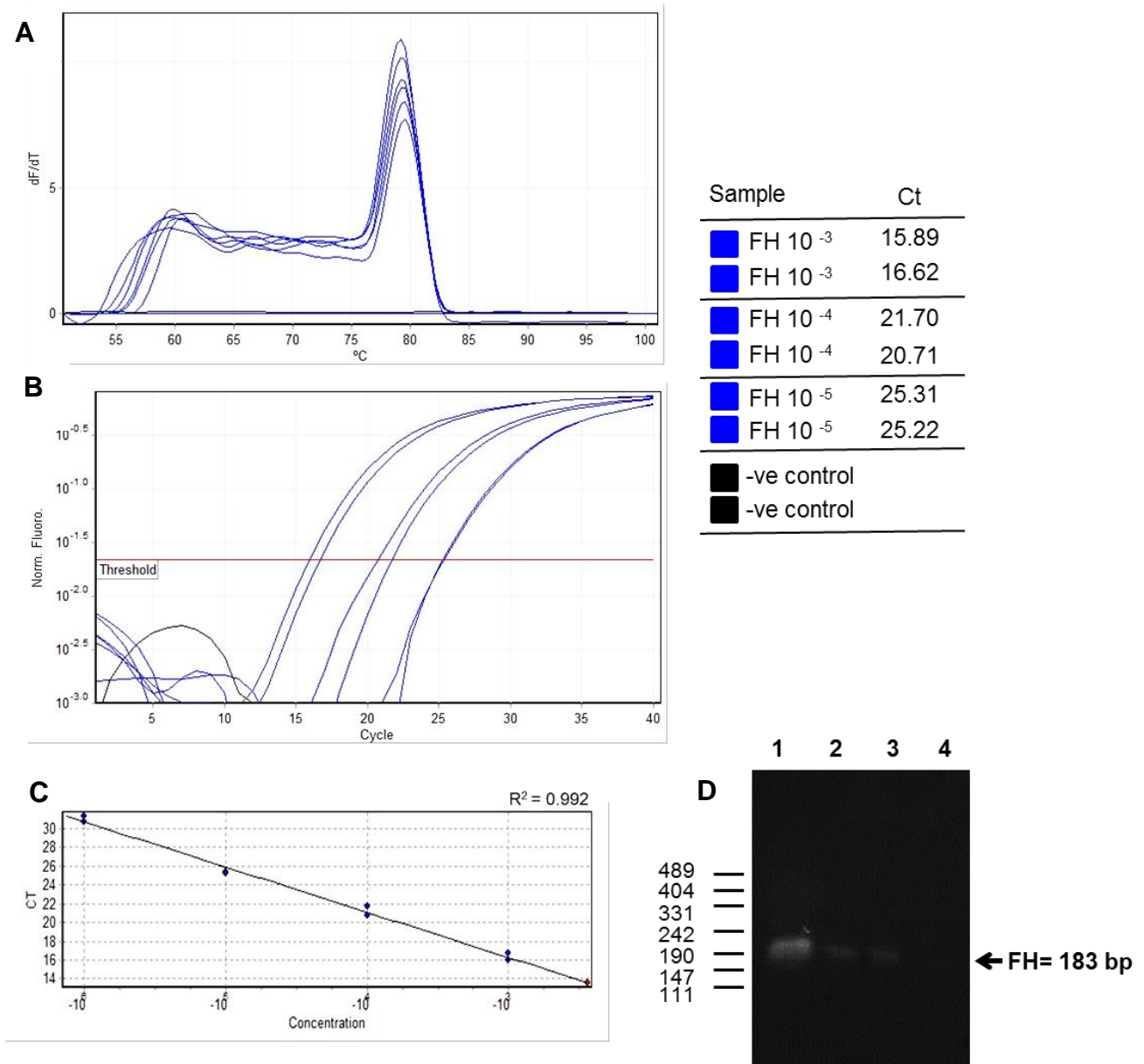


Figure III-1. Validation of a RT-PCR for human FH

H20 pBlueScript containing the full coding sequence of the FH gene was serially diluted from 10^{-3} to 10^{-5} pg/ μ l and subjected to RT-PCR. **(A)** melt curve; **(B)** Amplification curve; **(C)** Standard curve; **(D)** Agarose gel electrophoresis of RT-PCR products. The arrow indicates the expected size of the human FH product of 183 bp. 1: 10^{-3} , 2: 10^{-4} , 3: 10^{-5} , 4: negative control (-ve)

The same set of experiments was performed to validate human FB RT-PCR. In this case plasmid containing the FB coding sequence was not available. As an alternative, cDNA was generated by *in vitro* reverse transcription of RNA isolated from HepG2 cells (a liver cell line) for use as a template known to be positive for FB mRNA, considering that the liver is the primary site of expression and synthesis of complement proteins (Morris et al., 1982). Serial dilutions of the cDNA (neat, 1:10 and 1:100) were evaluated using a range of primer concentrations and the optimal amplification was observed at 10 μ M (data not shown). As observed for FH RT-PCR, the melt curve analysis shows a single, symmetrical peak at 87°C (Figure III-2 A) and amplification with increasing Ct corresponding to increasing cDNA dilution (Figure III-2 B). The negative control also demonstrated a melt peak but at 71°C and thus not at the same melt temperature to that seen for the presumptive human FB product (Figure III-2 A). The presence of a single PCR product was confirmed by agarose gel electrophoresis at the expected size of 280 bp (Figure III-2 C). There were no amplification or reaction products observed in the negative, no template control sample (Figure III-2 B, C). The cDNA from HepG2 neat and 1:10 dilution were used as controls in further human FB PCRs.

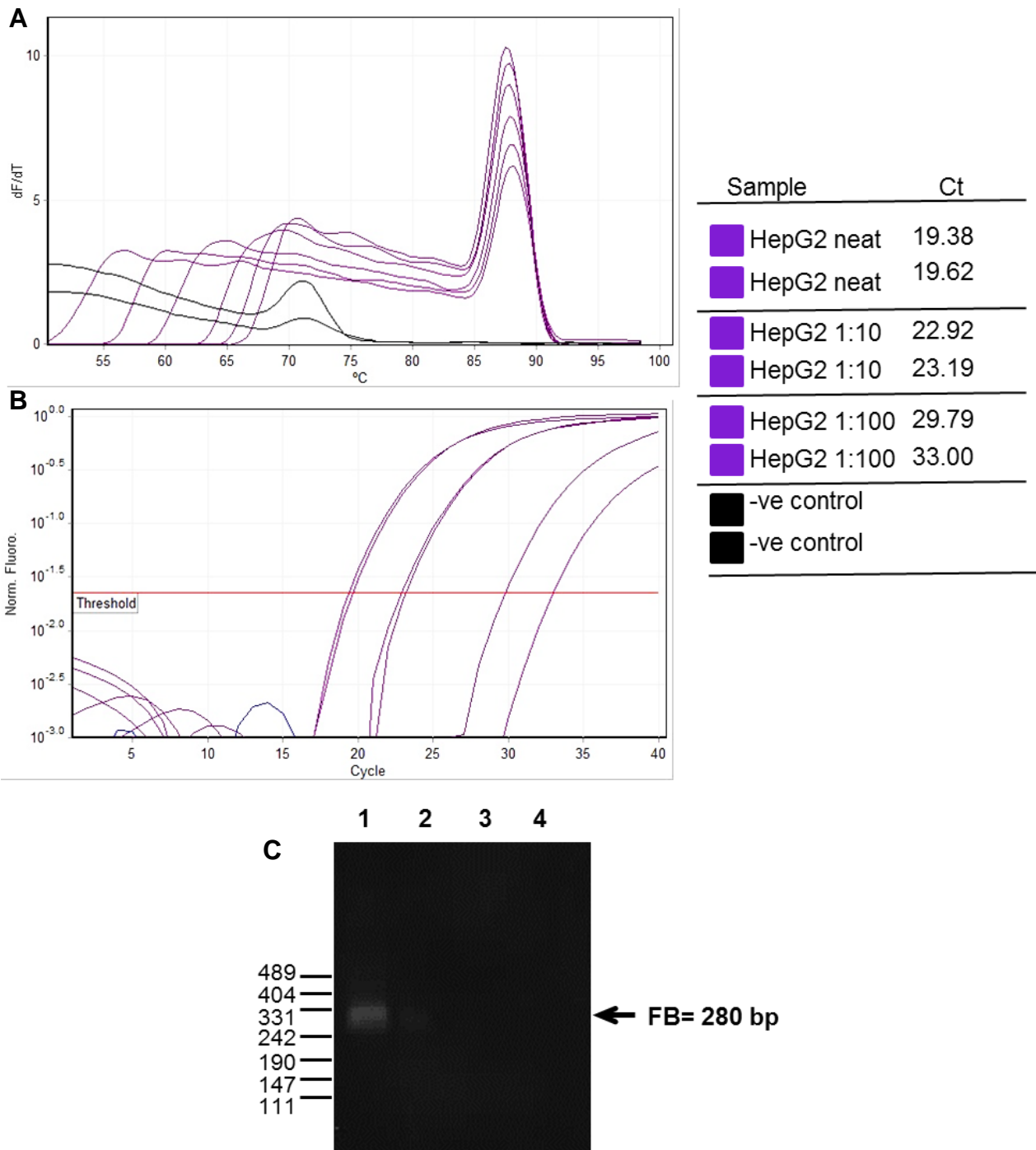


Figure III-2. Validation of a RT-PCR for human FB

cDNA generated from HepG2 RNA was serially diluted 1:10 and 1:100 and subjected to RT-PCR. (A) melt curve; (B) Amplification curve; (C) Agarose gel electrophoresis of RT-PCR products. The arrow indicates the expected size of the human FB product of 280 bp. 1: Neat, 2: 1:10, 3: 1:100, 4: negative control (-ve).

III.2.1.2 Validation of mouse FH and FB RT-PCR

A similar approach to that used above to validate human FB PCR was followed to validate mouse FH and FB RT-PCRs. A cDNA produced from *in vitro* reverse transcribed RNA isolated from a mouse fibroblast cell line, MEF, was used as a positive control. In addition, and to confirm primer's specificity, a cDNA generated from RNA extracted from three different mouse tissues, liver, kidney and heart, that are known to express several genes of the complement system (Fureder et al., 1995, McCurry et al., 1995, Amura et al., 2012) were included in the validation. The optimal concentration achieved for both FH and FB primers was 2 μ M and 10 μ M, respectively (data not shown). For both RT-PCRs, the melt curves show a unique and symmetrical peak resulting from mouse cell lines (MEF) and tissue samples (liver, heart and kidney) (Figure III-3 A and Figure III-4 A). In the case of FH RT-PCR, the negative control also demonstrated a melt peak but not at the same melt temperature to that seen for the mouse FH product (Figure III-3 A). Amplification curves showed increasing Ct with increasing dilution of input cDNA for the MEF positive control (Figure III-3 B and Figure III-4 B). The presence of a single product was again confirmed by agarose gel electrophoresis and bands of the correct sizes of 248 bp and 264 bp (Table II-2, Chapter II) were detected for FH and FB RT-PCR, respectively (Figure III-3 C and Figure III-4 C). The cDNA from MEF neat and 1:10 dilution were used as controls in further mouse FB and FH PCRs.

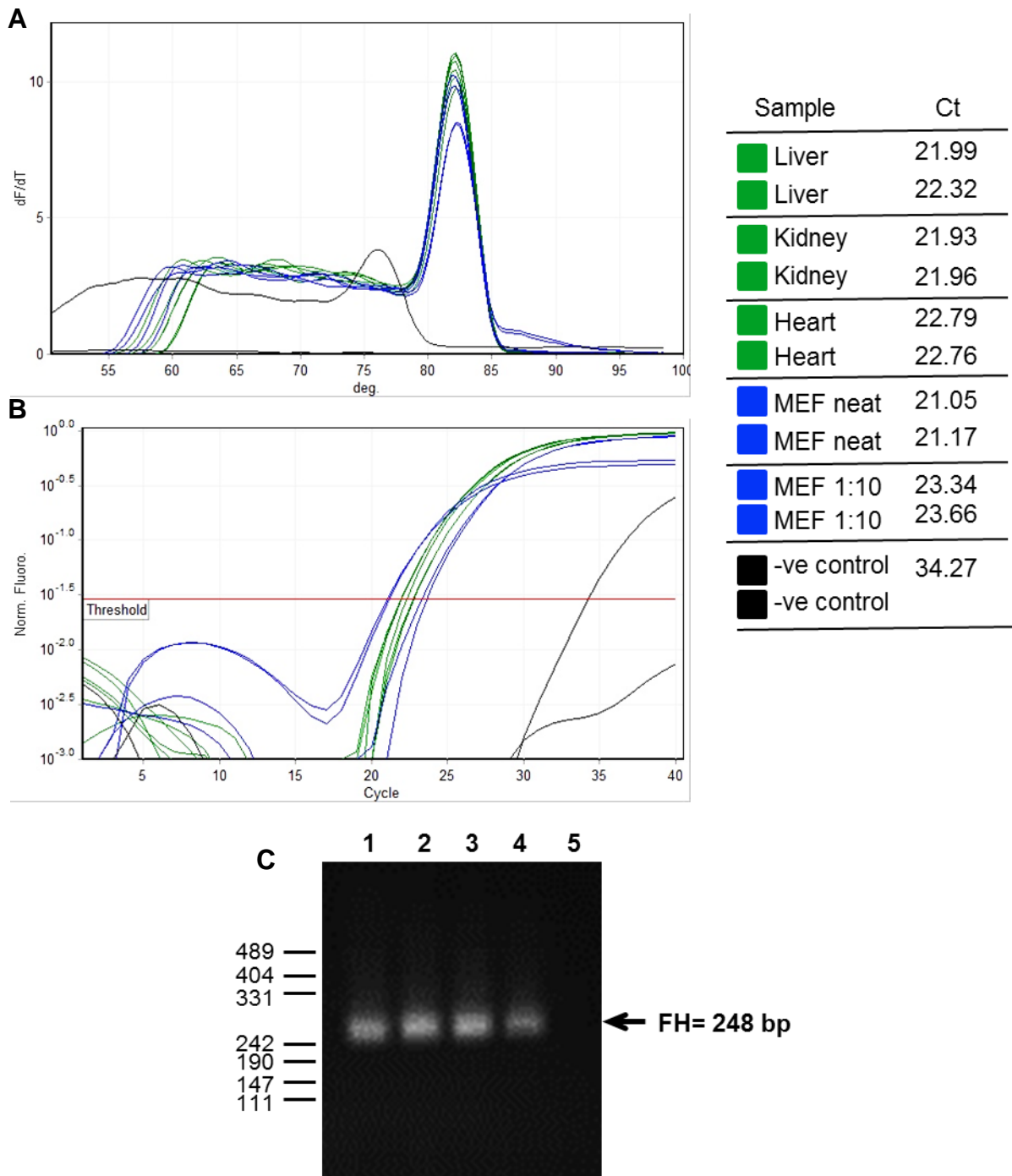


Figure III-3. Validation of a RT-PCR for mouse FH

cDNA generated from RNA extracted from mouse tissues: liver, kidney and heart were diluted 1:20. cDNA generated from MEF RNA was used neat and diluted 1:10. Samples were subjected to RT-PCR. **(A)** melt curve; **(B)** Amplification curve; **(C)** Agarose gel electrophoresis of RT-PCR products. The arrow indicates the expected size of the mouse FH product of 248 bp. 1:liver, 2: kidney, 3: heart, 4: MEF cells, 5: negative control (-ve).

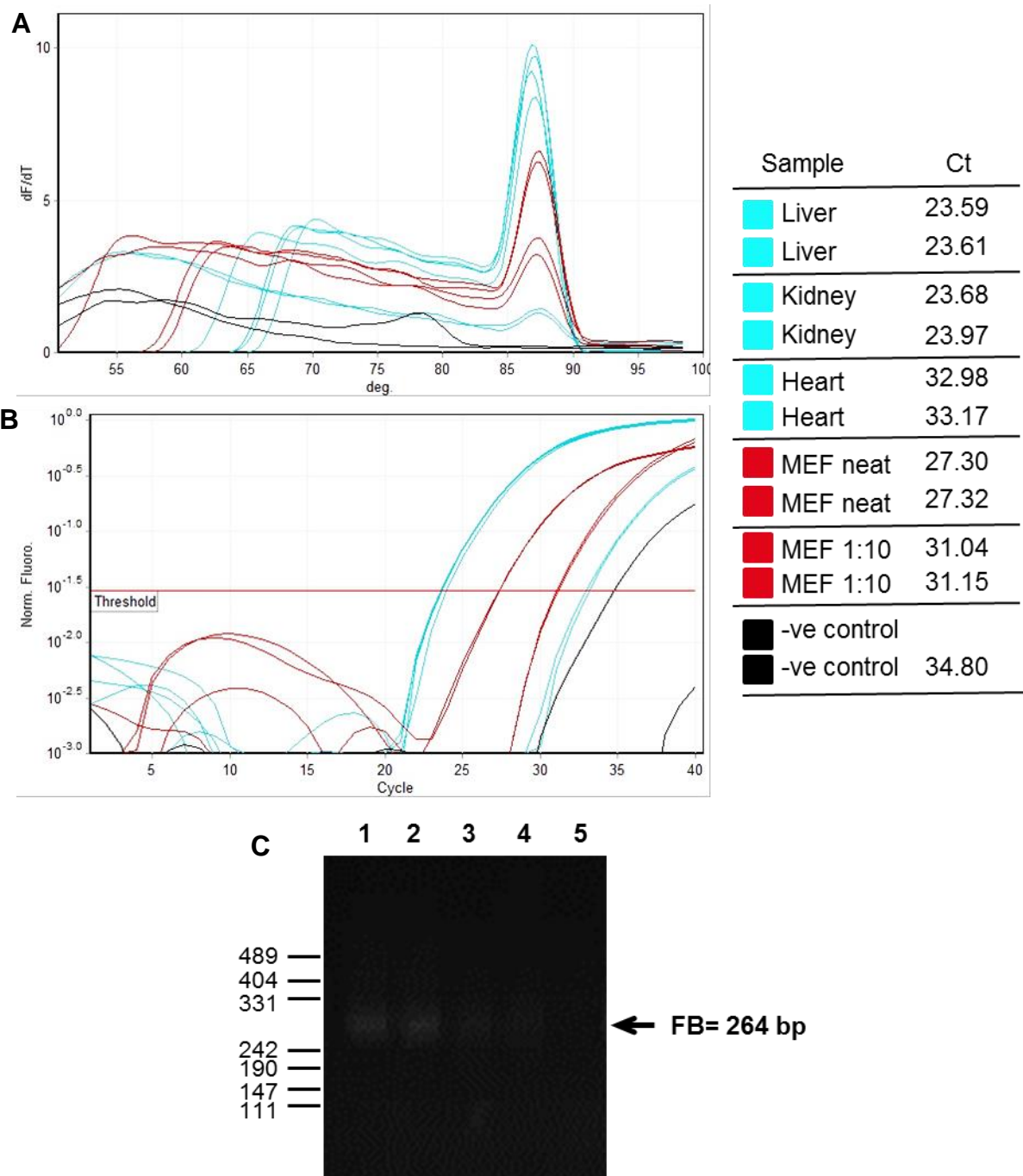


Figure III-4. Validation of a RT-PCR for mouse FB

A cDNA generated from RNA extracted from mouse tissues: liver, kidney and heart, diluted 1:20. cDNA generated from MEF RNA was used neat and diluted 1:10. Samples were subjected to RT-PCR (A) melt curve; (B) Amplification curve; (C) Agarose gel electrophoresis of RT-PCR products. The arrow indicates the expected size of the mouse FB product of 264 bp. 1:liver, 2: kidney, 3: heart, 4: MEF cells, 5: negative control (-ve).

III.2.2 Establishment of a method to detect FH and FB proteins

III.2.2.1 Validation of Western Blot to detect FH and FB proteins in serum and DENV-infected supernatants

The quantitation of either FH or FB proteins in the supernatant of DENV-infected human or mouse cells or in human or mouse DENV-infected sera is part of the aims of this study. The first attempt to quantitate these proteins was focused on human and mouse FH and FB proteins by Western blot. A band at the corresponding size of 150 kDa for FH and around 100 kDa for FB was successfully detected in human (Figure III-5 A, B) and mouse serum samples collected from healthy volunteers and normal mice as in section II.2.21 (Figure III-5 C). This was species-specific with no bands detected in FBS for either human or mouse FH or FB (Figure III-5). Surprisingly, no bands at the corresponding size for FH or FB were detected in cell culture supernatants collected from UI and DENV-infected HUVEC (Figure III-5 A, B) or MEF (Figure III-5 C), even from different batches of supernatants collected from independent experiments (Figure III-5).

Considering these results, the use of an ELISA as a more sensitive method than Western blot for detection of human and mouse FH and FB proteins was next explored.

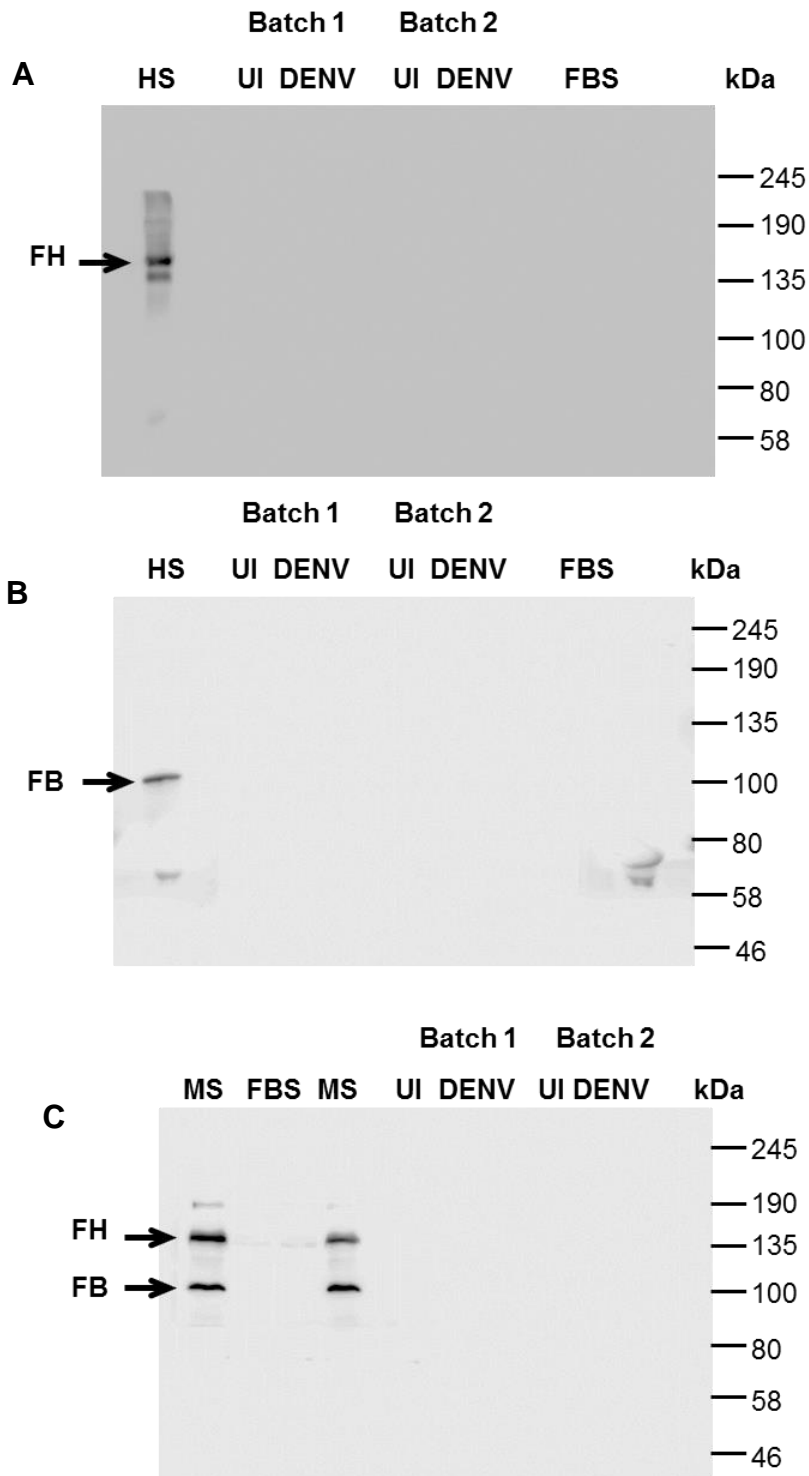


Figure III-5. Validation of Western blot to detect human and mouse FH and FB proteins

Sera or supernatants for uninfected (UI) or DENV-infected cells were subjected to SDS-PAGE and Western blot for (A) human FH, (B) human FB, with human sera (HS) and supernatants collected from HUVEC at 48hpi (C) mouse FH and FB (probed together) with mouse serum (MS) and supernatants from MEF cells (48hpi). Fetal bovine serum (FBS) was used as negative control. Bound complexes were detected with chemiluminescence and images collected using a LAS4000. The arrows indicate the expected size of the human and mouse FH (~150 kDa) and FB (~100 kDa) proteins.

III.2.2.2 Purifying FH protein from human sera

An in-house ELISA for human FH was developed and to achieve a quantitative assay it was necessary to obtain purified FH protein to create a standard curve. Since simple methods were already available to purify FH protein from blood, this protocol was followed. FH protein was isolated from 14 ml of total human serum diluted in PBS by affinity chromatography (Ormsby et al., 2006). After elution with 0.1M glycine, the main peak and two fractions with the highest OD_{280nm} were collected and dialysed against PBS. Dialysed fractions were concentrated using Millipore filter 100 000 MW down to 1.2 mL. The two fractions were pooled (2.4 mL), and a yield of 6.7 ± 0.0274 mg of semi-purified FH was obtained. The purity and identity of the semi-purified protein fractions were evaluated and confirmed by SDS-PAGE and Coomassie staining for total protein (Figure III-6 A) and Western blot, respectively (Figure III-6 B). Results demonstrated a main protein band corresponding to FH protein, but additional proteins of 50-80 kDa by Coomassie staining (Figure III-6 A) and other FH-immunoreactive species of approximately 46-70 kDa (Figure III-6 B). To further purify FH, the protein preparations achieved from the above step were subjected to Amicon Ultra-0.5 centrifugal filtration, a technique cited (<http://www.merckmillipore.com>) to allow fast ultrafiltration to eliminate small proteins of less than 100 kDa. Although Amicon Ultra-0.5 centrifugal filtration of the semi-purified protein sample resulted in a very concentrated protein preparation (11 ± 0.0222 mg/mL), removal of the lower molecular weight proteins and purification of FH protein to homogeneity was not obtained (Figure III-6 C). The lower molecular weight proteins, however, show poor reactivity with FH antibodies (Figure III-6 D). Since it was planned to design a sandwich ELISA to detect FH protein, relying on reactivity of the FH protein standard against two different antibodies, it was decided that the semi-purified FH protein preparation was appropriate for this purpose and further steps to obtain a highly purified FH preparation were not necessary.

To establish an in-house ELISA for mouse FH, a commercial FH protein (R&D Systems) was purchased for use to generate the mouse FH standard curve.

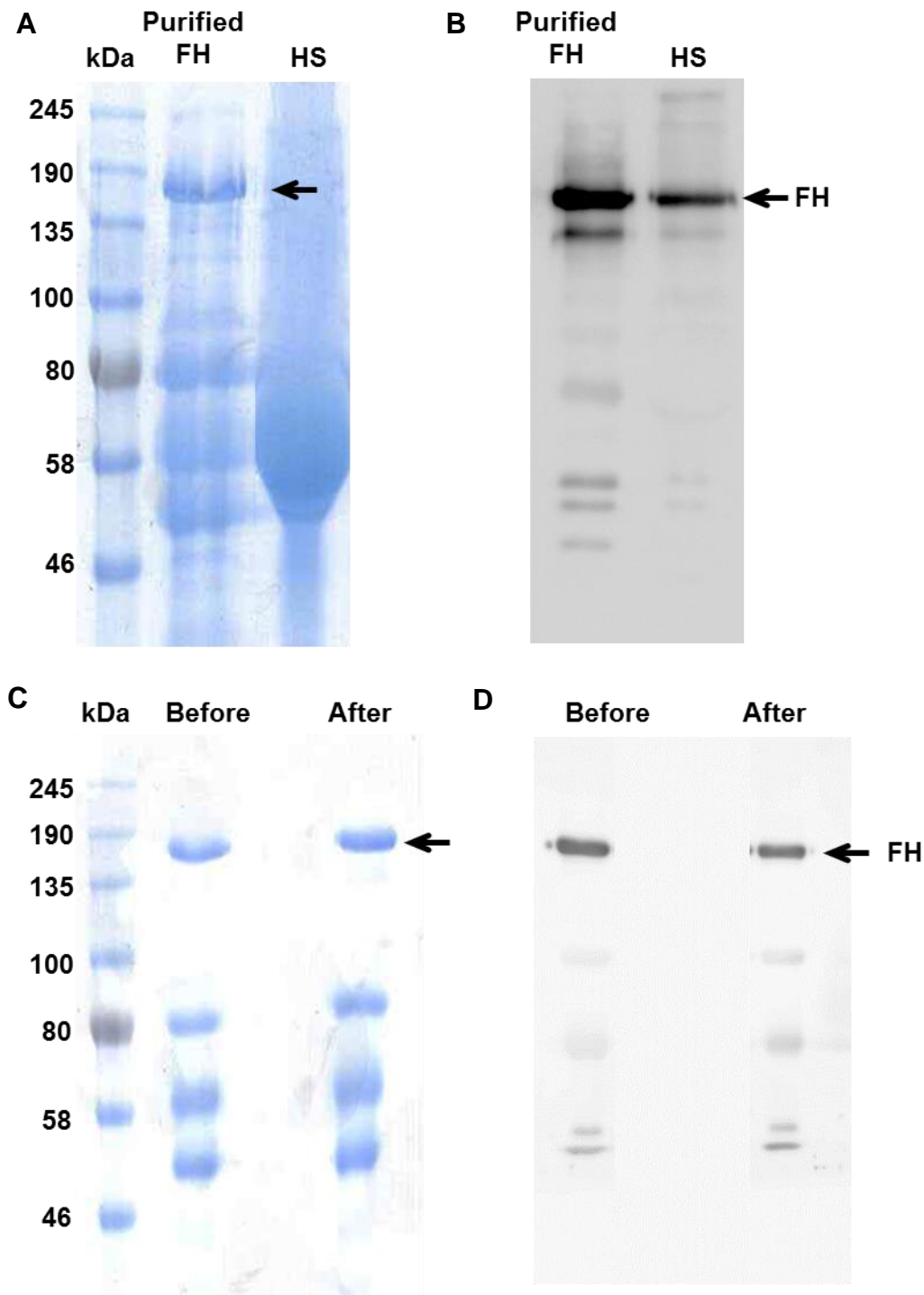


Figure III-6. Evaluation of the purified FH protein

FH was semi-purified from human serum by affinity chromatography and eluted proteins analysed by (A) SDS-PAGE and Coomassie blue staining and (B) Western blot for FH. The human serum (HS) used as starting material was included as control. Affinity chromatography purified FH preparations were further subjected to Amicon Ultra-0.5 centrifugal filtration and samples from before and after filtration were analysed by (C) SDS-PAGE and Coomassie blue staining and (D) Western blot for FH protein. The arrows indicate the expected size of the human FH protein (~150 kDa).

III.2.2.3 ELISA to detect human and mouse FH proteins

A sandwich ELISA approach was developed to quantitate human or mouse FH proteins. This method measures protein between two layers of protein-specific antibodies: capture and detection antibody, thus providing high specificity and amplifying a signal to yield high sensitivity. In the present study, a broadly cross-reactive anti-FH polyclonal antibody was immobilised on a 96-well plate to increase the possibility of capturing any available FH protein in serum samples or cell supernatants, while a monoclonal antibody was used as a detecting molecule to increase the specificity of the assay. A schematic representation of the sandwich ELISA design is shown in Appendix 2.

For the human FH ELISA, three different concentrations of the coating antibody (2.5, 5 and 10 $\mu\text{g/mL}$) were first tested and compared while keeping the remaining ELISA components i.e. FH purified protein, detection antibody, conjugated antibody, at a fixed concentration. From this comparison, 10 $\mu\text{g/mL}$ was determined to be the best coating concentration in this assay (data not shown). The same rationale was followed to determine the best dilution for the secondary detection antibody. Three two-fold serial dilutions (1:5000, 1:10 000, 1:20 000) of the detection antibody were evaluated and 1:10 000 antibody dilution was selected based on the maximum $\text{OD}_{450\text{nm}}$ values that were detected at this concentration (data not shown). At this point, serial dilutions of the purified human FH protein (from 400 to 10 ng/mL) were prepared for generating a standard curve and evaluated by ELISA using the above chosen concentrations for both capture and detection antibody. Figure III-7 A shows a typical linear regression curve and a good correlation ($R^2 > 0.99$), with an intra- and inter-assay coefficient of variation of 6.04% and 11.57%, respectively. To further validate the specificity and reliability of the designed human FH ELISA, the concentration of FH from three different human sera and one FBS sample was evaluated. Around 500 $\mu\text{g/mL}$ of FH protein was detected in each human serum sample, which is consistent with the FH concentration reported in human plasma or serum (Silva et al., 2012), while as expected human FH was not detected in FBS (Figure III-7 B). Similarly, cell culture supernatants were quantitated with detection of FH protein in cultured supernatant, but not in FBS containing starting media, with a sensitivity of 10 ng/mL (Figure III-7 C). Overall, these results demonstrate that the ELISA method developed in-house is specific and appropriate for detecting human FH protein in serum or cell supernatant, the biological samples to be collected and analysed in subsequent experiments.

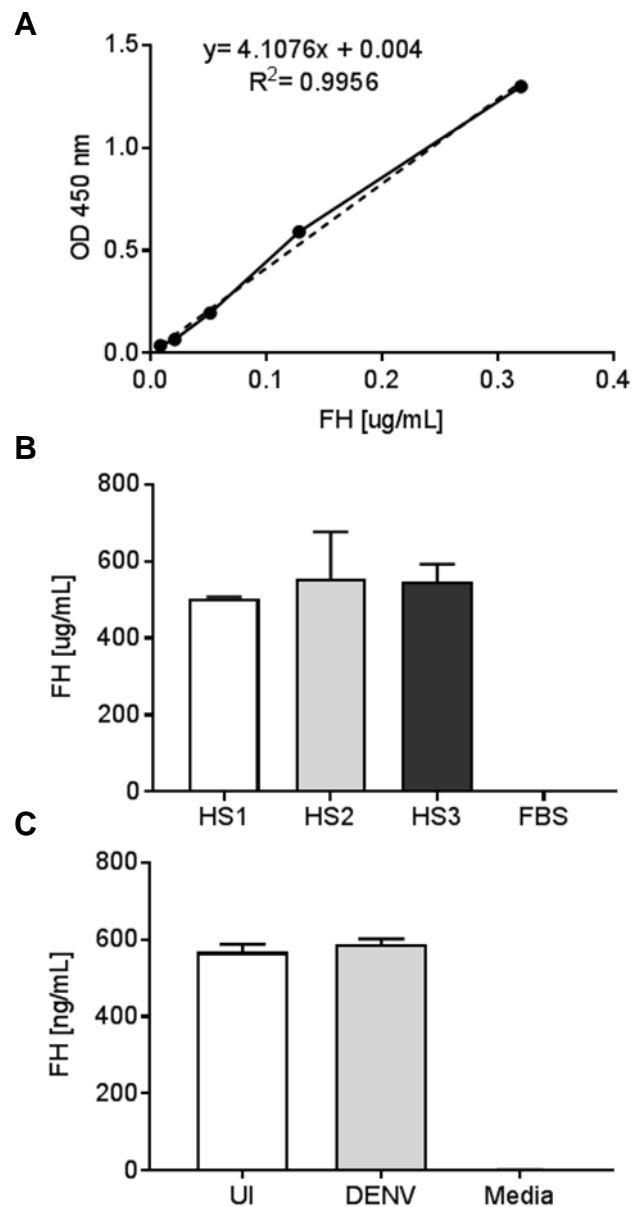


Figure III-7. Validation of human FH ELISA

(A) Purified human FH protein was serially diluted from 400 to 10 ng/mL and evaluated by ELISA to generate the standard curve. R^2 represents the regression coefficient as a measure of the goodness fit of the linear curve. (B) Three human serum (HS) from healthy individuals and foetal bovine serum (FBS) diluted 1:1000; and (C) supernatants collected from UI and DENV- infected HUVEC were assayed by ELISA. FBS and culture media was used as negative control. Results represent mean \pm standard deviation from duplicate samples and are representative of three independent experiments.

To standardise the mouse FH ELISA method, a similar set of experiments were performed to determine ideal concentrations for capture and detection antibodies. The evaluation of two different dilutions of both antibodies showed that 2.5 and 0.5 $\mu\text{g/mL}$ were the optimal working concentrations for capture and detection antibodies, respectively (data not shown). A characteristic linear regression curve and a good correlation ($R^2 > 0.99$) were observed when serial dilutions of mouse FH commercial protein were assessed from 200 to 20 ng/mL (Figure III-8 A), with an intra- and inter-assay coefficients of variation of 4.24% and 10.98%, respectively. Mouse serum samples and cell supernatants from MEF were again assayed using this methodology to evaluate the utility of this ELISA for quantitation from these biological samples. Results reveal that using this ELISA technique it is possible to detect mouse FH protein in mouse serum, with a sensitivity of 20 ng/mL (Figure III-8 B). FH protein was not detected from cultured supernatants from MEF suggesting that this mouse fibroblast cell type does not produce FH (data not shown). Other mouse cell types were not used in this study and thus further validation of detection of mouse FH in cell culture supernatants was not pursued.

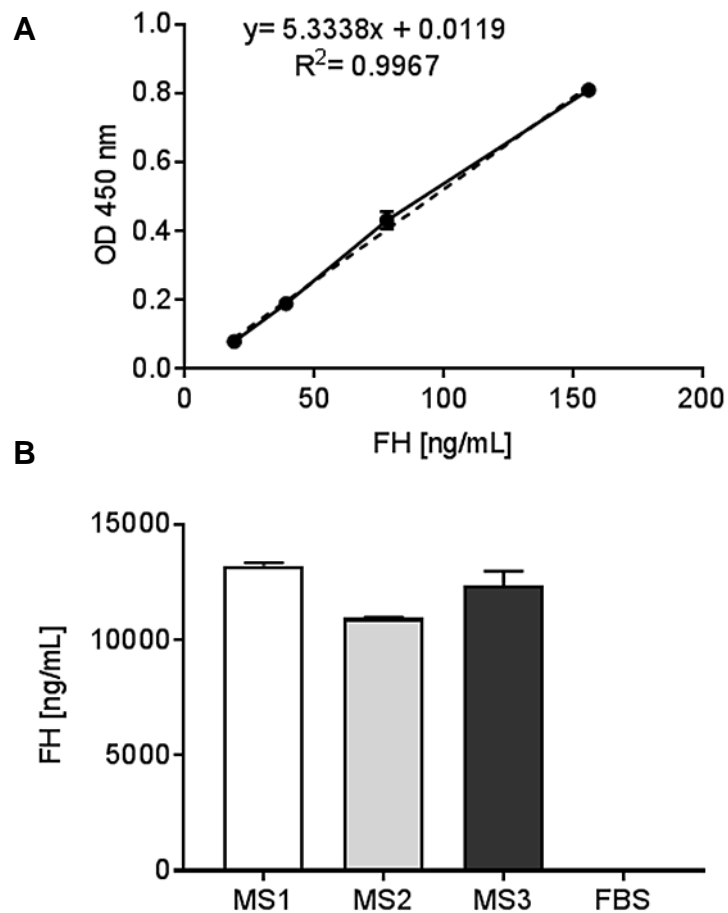


Figure III-8. Validation of mouse FH ELISA

(A) Commercial mouse FH protein was serially diluted from 200 to 20 ng/mL and evaluated by ELISA to generate the standard curve. R^2 represents the regression coefficient as a measure of the goodness fit of the linear curve. (B) Three mouse serum (MS) from naïve mice and foetal bovine serum (FBS) diluted 1:100 were assayed by ELISA. FBS was used as negative control. Results represent mean \pm standard deviation from duplicate samples and are representative of three independent experiments.

III.2.2.4 ELISA to detect human and mouse FB proteins

Although FB protein is a relatively abundant complement component in human or mouse plasma or serum (Li et al., 2011, Silva et al., 2012) its purification process is difficult and laborious. Additionally, polyclonal and monoclonal specific antibody pairs to use as capture and detection antibodies in an in-house designed assay were not commercially available. Therefore, for human and mouse FB protein detection commercial kits were purchased that were successfully employed in accordance with the manufacturer's instructions (see Chapters IV and VI).

III.2.3 Validation of identification of nuclei and DENV-infected cells by high-content imaging system

To quantitate the number of DENV-infected cells, a previously used and common intracellular immunostaining procedure was combined with a novel high-content imaging system (Operetta, PerkinElmer). HUVEC cells were fixed, permeabilised and subsequently immunostained for DENV and nuclei identified by Hoechst staining. Brightfield and fluorescent images were collected using a 20X objective with 49 fields per well captured. The Hoechst staining is an essential control to define the cell nuclei and cytoplasm by the Operetta Harmony Software, by creating a sequence of building blocks as described in Appendix 1.

The first building block generated aimed to create an optimal segmentation of nuclei and separation of single cells which is critical to determine the number of DENV-positive cells. A brightfield image is taken, with an example of a collected image is shown in Figure III-9 A. The Harmony software offers methods for the optimal segmentation of nuclei and cytoplasm based on appropriate nuclei and cytoplasm staining, respectively. Using Hoechst to stain the nucleus along with the brightfield image and the establishment of the appropriate settings on the Operetta (0, Appendix 1) it was possible to observe an adequate separation of nuclei that allowed estimating the number of cells per field of view (Figure III-9 B, C). The next building block was designed to define the bounds of the surrounding cell cytoplasm. Due to the lack of specific cytoplasm staining reagent and considering that FH is produced intracellularly in HUVEC cells at basal levels, along with the need to further evaluate intracellular FH specifically in DENV-positive cells, Cy3 channel (fluorophore used for FH staining) in combination with the brightfield image was employed to delineate the cytoplasmic region (Figure III-9 B, C). Having defined computational bounds to identify both nuclei and cytoplasm, DENV negative and positive

cells were identified by establishing a building block with a cut-off for Alexa 488 intensity (the fluorophore used for DENV-antigen staining). Figure III-10 A shows representative visual results of DENV-staining of HUVEC. As expected, no fluorescent cells are observed in UI cells or in DENV-infected cells with an antibody control (Figure III-10 A). Visual quantitation of the number of DENV-infected cells indicates four DENV-infected out of 55 total cells, and thus 7% DENV-infected cells. Using the Operetta and Harmony software computational definitions of a DENV-positive cell, quantitation of the percentage of infection in 49 different fields calculated $2.92\% \pm .0338$ of the cell population was infected (Figure III-10 B), in broad agreement with visual estimations of 7% in the image shown (Figure III-10) and previous studies (Calvert et al., 2015).

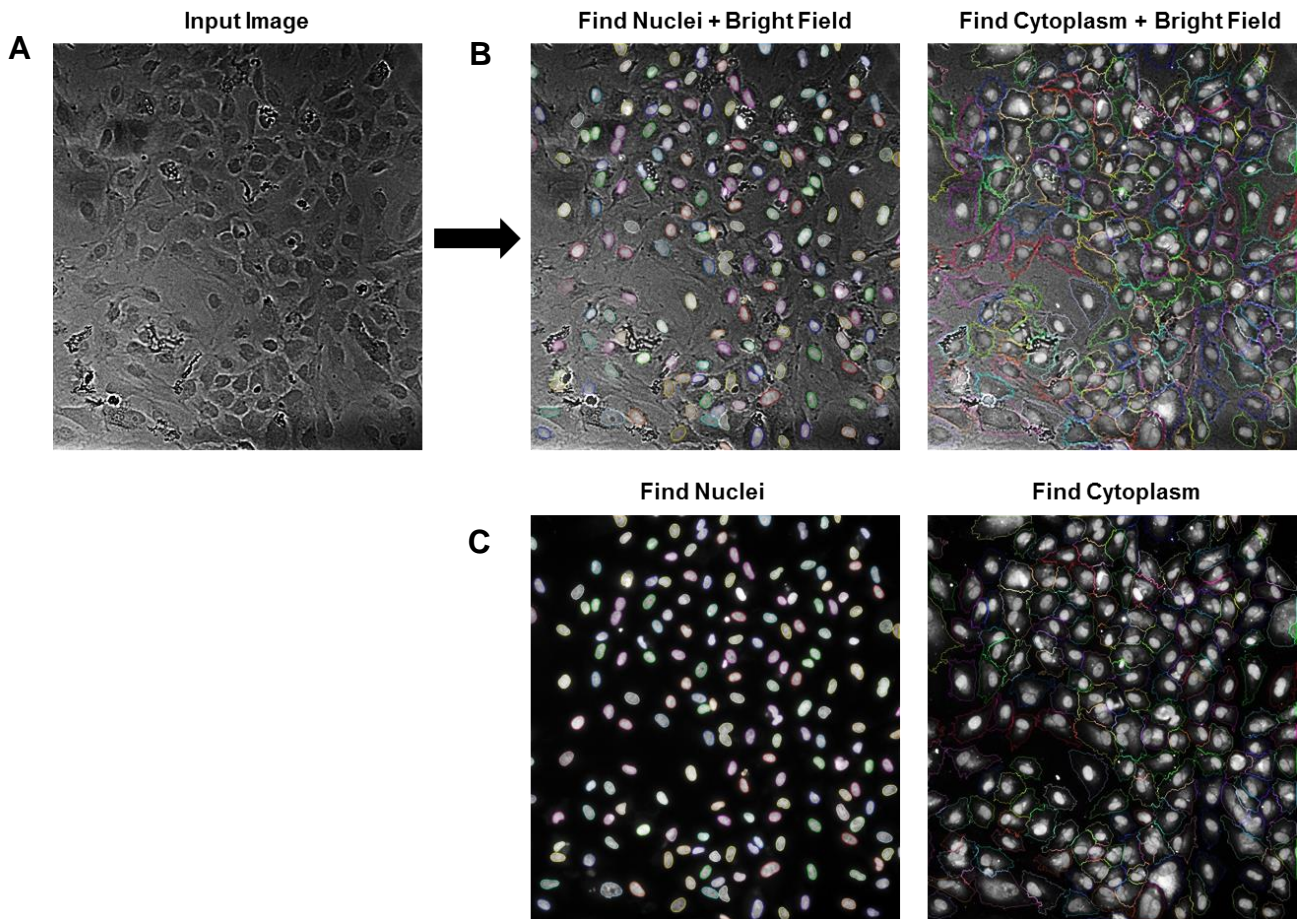


Figure III-9. Image analysis to identify the nucleus and cytoplasm using the Harmony software

HUVEC cells were fixed, permeabilised and subsequently stained with Hoechst to identify the nuclei and immunostained for FH. The Cy3 channel (fluorophore used for FH staining) was used to identify cytoplasm. **(A)** Typical input bright field image showing HUVEC cells. **(B)** Results of the nuclear and cytoplasmic detection with Harmony software using Find Nuclei and Cytoplasm methods. **(C)** Same images taken in **(B)** without the bright field. Lines represent borders of the cytoplasm regions.

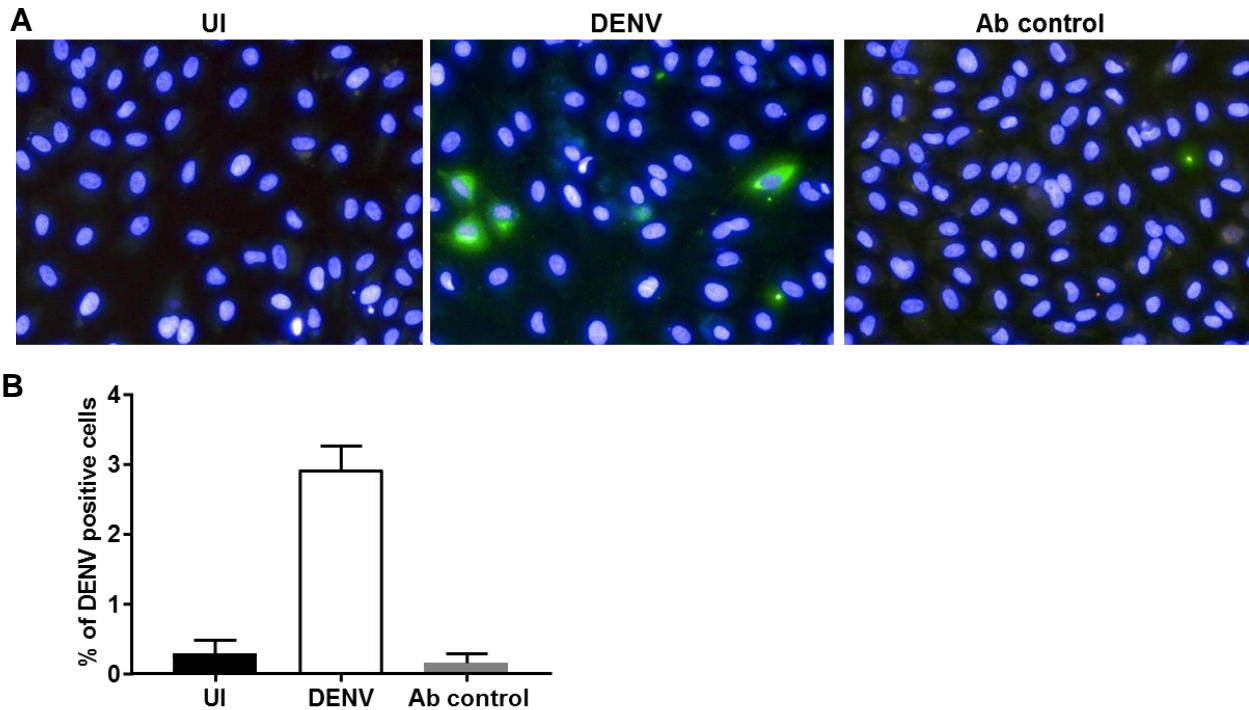


Figure III-10. Validation of DENV intracellular staining using the Operetta.

(A) HUVEC were isolated and left uninfected (UI) or DENV infected. At 48hpi cells were fixed and immunostained for DENV (green) with Alexa 488. Nuclei were stained with Hoechst (blue). Cells were imaged with Operetta High-content Imaging System at 20x magnification. (B) Images of 49 fields of view were analysed using Harmony software and the quantitation of the percentage of infection was calculated. Results represent mean \pm standard deviation of the percentage of infection from triplicate samples and are representative of three independent infection experiments.

III.3 Discussion

The overall objective of this thesis is to define the induction of two opposing regulators of the complement system, FH and FB, during DENV infection in two infection models, human and mouse. Thus, standardisation of different assays to specifically quantitate FH and FB mRNA and proteins in these two species was essential.

Here RT-PCR assays were defined to specifically detect FH and FB mRNA from human and mouse samples. Results for all showed increasing Ct with increasing dilution, a single symmetrical melt curve and a single amplified product of the correct size by gel electrophoresis, demonstrating specificity of these assays. The FH gene can generate a number of different mRNA transcripts (Gordon et al., 1995). The human FH RT-PCR used primers for SCR 2, towards the 5' end of the transcript and thus, should detect all FH and FH-like mRNA transcripts. The H20 FH DNA clone was used in subsequent chapters as a positive control for human FH RT-PCR (see Chapters IV and V). Laboratory DNA clones were not available for mouse FH, or FB from either human or mouse, and thus the RT-PCR assay was validated on RNA from MEF cells and mouse tissues (for mouse FH and FB) and HepG2 cells (for human FB). Previous studies have shown that although several cell lines express FH and FB, such as hepatoma, endothelial and renal cells (Perlmutter et al., 1989, Timmerman et al., 1996, Schlaf et al., 2001), this expression is not always constitutive (Schlaf et al., 2001). Our results support the ability of MEF and HepG2 cells and mouse liver, kidney and heart to express FB and FH genes. The cDNA generated from MEF or HepG2 RNA was used as a positive control in subsequent PCR experiments for mouse (FH and FB) and human (FB) (Chapters IV, V and VI).

Additionally, methods were designed in-house or developed to detect FH and FB proteins in human and mouse cell culture supernatants and sera. The first attempt was focused on validating a Western blot. Although this is not a rigorous quantitative or high-throughput technique, since smaller, immunoreactivity from FH-like proteins have been reported (Hovis et al., 2006, Hannan et al., 2016) and additionally, cleavage of FB can occur during regulation of the complement cascade (Milder et al., 2007) (see section 1.2.1.3), results from this method would provide useful information on the presence of these different molecular weight forms of FH and FB. Although, FH and FB proteins could be identified in the sera from human and mouse, no visible bands representing either protein were detected in any cell culture supernatants. Even though the constitutive expression of FH protein in HUVEC has been described (Ripoche et al., 1988b), the presence of this protein

in cell culture supernatants of HUVEC by Western blot was only demonstrated if the cells were treated with IFN- γ or IFN- γ plus dexamethasone (Dauchel et al., 1990). In addition, FH protein could not be identified in the supernatant of cultured human hepatocytes (Schlaf et al., 2001), while in the supernatant of rat hepatocytes FH is detectable in precipitated cell culture supernatants upon stimulation with IFN- γ for 72h (Schlaf et al., 2001). These data are in accord with further investigations which demonstrated the presence of FH and FB proteins only in lyophilised cell culture supernatants of human neuroblastoma cell lines stimulated with IFN- γ , TNF- α or IL-6 (Thomas et al., 2000). Therefore, it is clear that FH and FB protein concentrations are very low in cell culture supernatants, and unless concentration methods and stimulating agents are employed their detection by Western blot is not possible. Subsequently, concentrations of FH and FB in cell culture supernatants was determined to be in the nanogram range by ELISA (see below), confirming that concentrations of these proteins in cell culture supernatants are below the limit of detection by standard Western blot techniques.

Thus, an ELISA was established to detect FH and FB from mouse and human samples with success. Specifically, an in-house sandwich ELISA was designed and standardised to detect human and mouse FH proteins while two commercial systems based on the same format (sandwich) were used to quantitate human and mouse FB proteins. One of the advantages of the sandwich ELISA is the enhanced sensitivity. Sandwich ELISA is cited to be 5-10 times more sensitive than Western blot and 2-5 times more sensitive than direct or indirect ELISA methods (Crowther, 2009). Our strategy consisted in the use of a broadly cross-reactive anti-FH polyclonal antibody as a capturing molecule while a monoclonal antibody, raised against the full length of human FH native protein or against a highly conserved region of mouse FH protein, was employed as the detecting molecule to increase specificity. Further, the sandwich format removes the necessity for intensive sample purification step before the analysis since two layers of specific antibodies are utilised to detect the target molecule of interest. As a consequence, the ELISA design used herein allowed the use of semi-purified human FH protein as an in-house generated standard and obtained by a very simple and straightforward affinity chromatography method, rather than complicated and time-consuming purification steps. Further, cell culture supernatants and sera samples were assayed straight away without the need of any additional concentration or purification step. All ELISAs utilised demonstrated linear standard curves with R^2 values approaching 1, intra-assay co-efficient of variation less

than 7%, inter-assay coefficient of variation of less than 12% and sensitivities and assay cut-off values between 10-20 ng/ml.

Finally, a high throughput, *in situ* method to detect DENV infected cells was validated. Standard traditional immunofluorescence techniques and flow cytometry are useful tools to detect intracellular proteins; however, these approaches are laborious for data processing and quantitation. The use of high-content imaging in primary screening is becoming more widespread (Martin et al., 2014, Massey, 2015). This study exploited the Operetta high-content/high-throughput imaging system and the Harmony software to quantitate the number of DENV-positive cells. Using HUVEC cells as an infection model and our building block design to identify nuclear and cytoplasmic compartments, it was possible to efficiently discriminate DENV-infected from UI cells. This methodology was further employed to analyse and quantitate FB and FH proteins production specifically in DENV-antigen positive cells (see Chapter IV).

Overall, we have developed and validated useful, powerful and novel methods to detect, identify and quantitate FH and FB mRNAs and proteins that will allow us to assess further the main goal of the current thesis which is to evaluate the induction and production of FH and FB during DENV infection in different human and mouse infection models.

CHAPTER IV DENGUE VIRUS INDUCES INCREASED ACTIVITY OF THE COMPLEMENT ALTERNATIVE PATHWAY IN INFECTED CELLS

This chapter contains the following publication:


Dengue Virus Induces Increased Activity of the Complement Alternative Pathway in Infected Cells. Cabezas S, Bracho G, Aloia AL, Adamson PJ, Bonder CS, Smith JR, Gordon DL, Carr JM. *J Virol.* 2018 Jun 29; 92(14). pii: e00633-18. doi: 10.1128/JVI.00633-18. Print 2018 Jul 15. PMID: 29743365.

IV.1 Introduction

Having established methods in chapter III to evaluate mRNA induction and protein production of two main regulatory factors of the complement AP, FB and FH, the current chapter aims to investigate changes in FB and FH *in vitro*, in the local environment of two important primary cell types relevant to DENV infection *in vivo*, macrophages and EC. The endothelium is an important site where a cascade of pathogenic events converges during DENV infection that contributes to increased vascular permeability, a hallmark of the DENV-disease (Dalrymple and Mackow, 2012b, Dalrymple and Mackow, 2014, Malavige and Ogg, 2017). While there are precedents in the literature suggesting a dysregulation of the AP in the circulation of DHF patients (Nascimento et al., 2009), the cellular mechanisms underlying this increased AP activity specifically at the EC surface during DENV infection, remains to be investigated. The opposing roles of FB and FH are important in keeping the activity of the AP tightly controlled (Horstmann et al., 1985) and thus we have focussed on these complement proteins. This chapter studies FB and FH alterations at the cellular level in macrophages and EC and defines the molecular events that may contribute to a hyper-activation of the AP locally on the endothelium, which in turn could result in increased vascular permeability and severity of DENV disease.



Dengue Virus Induces Increased Activity of the Complement Alternative Pathway in Infected Cells

Sheila Cabezas,^a Gustavo Bracho,^a Amanda L. Aloia,^b Penelope J. Adamson,^a Claudine S. Bonder,^c Justine R. Smith,^a David L. Gordon,^a  Jillian M. Carr^a

^aMicrobiology and Infectious Diseases and Eye & Vision Health, College of Medicine and Public Health, Flinders University, Adelaide, South Australia, Australia

^bCell Screen SA, Flinders Centre for Innovation in Cancer, Flinders University, Adelaide, South Australia, Australia

^cCentre for Cancer Biology, University of South Australia and SA Pathology, Adelaide, South Australia, Australia

ABSTRACT Severe dengue virus (DENV) infection is associated with overactivity of the complement alternative pathway (AP) in patient studies. Here, the molecular changes in components of the AP during DENV infection *in vitro* were investigated. mRNA for factor H (FH), a major negative regulator of the AP, was significantly increased in DENV-infected endothelial cells (EC) and macrophages, but, in contrast, production of extracellular FH protein was not. This discord was not seen for the AP activator factor B (FB), with DENV induction of both FB mRNA and protein, nor was it seen with Toll-like receptor 3 or 4 stimulation of EC and macrophages, which induces both FH and FB mRNA and protein. Surface-bound and intracellular FH protein was, however, induced by DENV, but only in DENV antigen-positive cells, while in two other DENV-susceptible immortalized cell lines (ARPE-19 and human retinal endothelial cells), FH protein was induced both intracellularly and extracellularly by DENV infection. Regardless of the cell type, there was an imbalance in AP components and an increase in markers of complement AP activity associated with DENV-infected cells, with lower FH relative to FB protein, an increased ability to promote AP-mediated lytic activity, and increased deposition of complement component C3b on the surface of DENV-infected cells. For EC in particular, these changes are predicted to result in higher complement activity in the local cellular microenvironment, with the potential to induce functional changes that may result in increased vascular permeability, a hallmark of dengue disease.

IMPORTANCE Dengue virus (DENV) is a significant human viral pathogen with a global medical and economic impact. DENV may cause serious and life-threatening disease, with increased vascular permeability and plasma leakage. The pathogenic mechanisms underlying these features remain unclear; however, overactivity of the complement alternative pathway has been suggested to play a role. In this study, we investigate the molecular events that may be responsible for this observed alternative pathway overactivity and provide novel findings of changes in the complement system in response to DENV infection in primary cell types that are a major target for DENV infection (macrophages) and pathogenesis (endothelial cells) *in vivo*. Our results suggest a new dimension of cellular events that may influence endothelial cell barrier function during DENV infection that could expand strategies for developing therapeutics to prevent or control DENV-mediated vascular disease.

KEYWORDS complement, dengue virus, factor H

Received 14 April 2018 Accepted 4 May 2018
 Accepted manuscript posted online 9 May 2018

Citation Cabezas S, Bracho G, Aloia AL, Adamson PJ, Bonder CS, Smith JR, Gordon DL, Carr JM. 2018. Dengue virus induces increased activity of the complement alternative pathway in infected cells. *J Virol* 92:e00633-18. <https://doi.org/10.1128/JVI.00633-18>.

Editor Michael S. Diamond, Washington University School of Medicine

Copyright © 2018 American Society for Microbiology. All Rights Reserved.

Address correspondence to Jillian M. Carr, jill.carr@flinders.edu.au.

Downloaded from <http://jvi.asm.org/> on July 15, 2018 by FLINDERS UNIVERSITY OF SOUTH AUSTRALIA

Dengue virus (DENV) is currently considered the most important mosquito-borne viral infection of humans worldwide, causing between 50 million and 390 million estimated infections per year in over 100 countries (1, 2). DENV consists of four serotypes (1–4) and belongs to the family *Flaviviridae*, genus *Flavivirus* (3). Disease caused by DENV infection ranges from asymptomatic, undifferentiated fever and classical dengue fever to severe forms of the disease that include dengue hemorrhagic fever (DHF) and dengue shock syndrome (DSS). These clinical descriptions of dengue have been revised as dengue with or without warning signs and severe dengue (4). One life-threatening outcome of DENV infection is increased vascular permeability and plasma leakage, which ultimately can lead to fatal hypovolemic shock (5–8). Although the pathogenic mechanisms underlying the increased vascular permeability remain unclear, a number of studies have demonstrated that DENV infection of macrophages and endothelial cells (EC) plays a critical role in altering cellular responses that control capillary leakage and barrier integrity (9–11). Macrophages are not only the major target for DENV replication *in vivo*, but they also are important sources of cytokines, chemokines, and vasoactive factors that converge on the endothelium to contribute to vascular permeability (12, 13). The role of the endothelium itself has been debated, and while many studies suggest that EC are not a major site for viral replication, the endothelium is undoubtedly a major site for DENV-mediated pathogenesis. DENV is reported to induce effects that alter the barrier function of the endothelium and that increase EC cytokine and chemokine release and EC inflammatory responses (14–18). Multiple immunomodulatory and vasoactive factors, such as tumor necrosis factor alpha (TNF- α), interleukin-1 (IL-1), IL-6, macrophage inhibitory factor, and metalloproteinases, from macrophages or dendritic cells have been implicated in severe dengue or DENV-induced vascular dysfunction (11, 19–21). Recently, the capacity of viral nonstructural protein 1 (NS1) to directly induce vascular leakage and endothelial cell dysfunction has also been shown (22, 23). Thus, the pathogenesis of DENV is clearly multifactorial and overwhelmingly a function of dysregulated immune responses.

The complement system is suggested to be involved in DENV disease and particularly in initiation of vascular leakage (24–27). Complement comprises three pathways, the classical pathway, the lectin pathway, and the alternative pathway (AP), that involve a cascade of proteolytic cleavages forming various vasoactive and immunostimulatory proteins (28, 29). These three pathways converge on C3, which is activated by cleavage to form C3b, with subsequent interactions that lead to the formation of a C3b convertase complex and the terminal membrane attack complex (MAC). The MAC can lyse pathogens and target cells, while other cleavage products of the complement system, such as C3a and C5a, are inflammatory and vasoactive factors (29). While the classical and lectin pathways are stimulated by pathogen recognition, the AP is constitutively active (29, 30) and is tightly controlled to prevent unwanted tissue damage. The AP negative regulatory protein factor H (FH) is considered the master regulator of this pathway that ensures that the AP activity is tightly controlled (30–33). FH can control AP activity by competing with factor B (FB) for C3b binding (30, 31, 34, 35), promoting the decay of the C3 convertase, and stimulating C3b degradation (30, 36). Additionally, FH acts as a cofactor and promotes enzymatic inactivation of C3b by factor I (FI) to form iC3b (37, 38). These actions of FH can occur in the fluid phase but are facilitated at cell surfaces by FH binding to polyanions and glycosaminoglycans (39–41). C3b deposition on surfaces is nondiscriminatory and arises from constitutive AP-driven C3 hydrolysis or “tickover” to form C3b (42). The subsequent binding of FB to C3b forms the C3bB complex, which is cleaved by the serine protease factor D (FD) to produce more AP C3 convertase (C3bBb), which is part of an activation loop that further promotes the complement cascade (29). Alternatively, C3b can be deactivated by the actions of FH, as described above. This balance between the actions of FB and FH can thus determine if a C3b-coated surface is targeted for complement action or not (32, 34, 35).

Overactivity of the AP due to the low activity of FH is associated with human disease, such as atypical hemolytic-uremic syndrome, which shares some common pathogenic

features with dengue disease, such as intravascular hemolysis, thrombocytopenia, damage to the endothelium, and increased vascular leakage (43, 44). We postulated that, similarly, AP overactivity due to the low activity of FH might be involved in DENV pathogenesis. Several reports have supported an association of overactivity of the complement AP with DENV disease severity, with complement protein consumption, low serum levels of FH, and high levels of FD being reported in the circulation of severe DENV patients (8, 25–27, 45, 46).

Herein, the molecular events at the cellular level that align with AP activity are defined and provide evidence of dysregulation of FH production locally within macrophages and EC, the major *in vivo* sites for DENV replication and pathogenesis, respectively. These changes in FH in combination with elevation of other complement components, such as FB and C3b deposition, are associated with increased complement AP activity *in vitro*, which we propose reflects AP activity in the cellular microenvironment *in vivo*. Our results raise the possibility of designing strategies, such as those to promote the levels of FH protein, as therapy to prevent complement-mediated vascular dysfunction during DENV infection.

RESULTS

DENV induces FH mRNA but not protein in primary EC and MDM. The induction of FH, a negative regulator of the complement AP, was evaluated following DENV infection in two cell types that represent major targets for DENV pathogenesis and replication *in vivo*: EC and macrophages, respectively. Active virus replication occurred, with increasing DENV RNA and infectious virus release taking place from 24 to 48 h postinfection (hpi) in primary human umbilical vein EC (HUVEC) (Fig. 1A) and monocyte-derived macrophages (MDM) (Fig. 1B). Quantitation of FH mRNA levels demonstrated a significant induction in both HUVEC (Fig. 1C) and MDM (Fig. 1D) following DENV infection. In contrast, the levels of extracellular FH protein showed no significant change in DENV-infected supernatants from either cell type (Fig. 1E and F). Notably, there were much lower levels of FH mRNA and protein in MDM (Fig. 1D and F) than in HUVEC (Fig. 1C and E). The lack of detectable FH protein in cultured supernatant from DENV-infected cells was not due to blocking of FH antibody binding sites required for enzyme-linked immunosorbent assay (ELISA) detection of FH, for example, by a protein-protein interaction, since supernatants collected from DENV-infected cells and treated with either detergent (Triton X-100) or heat (56°C) prior to ELISA showed no difference in FH quantitation (Fig. 2A and B). Analysis of FH protein by Western blotting was attempted, but consistent with the nanogram levels of protein quantitated by ELISA, FH protein in cultured supernatants was undetectable by this method (data not shown).

The discord between DENV induction of FH mRNA and protein is not observed with FB or following TLR3 or TLR4 stimulation of MDM and EC. To assess if DENV infection specifically prevents induction of FH protein, changes in FB, another AP complement component, were assessed. Quantitation of FB mRNA levels demonstrated a significant induction in both HUVEC (Fig. 3A) and MDM (Fig. 3B) following DENV infection. Similarly, but in contrast to the results for FH, FB protein levels significantly increased in DENV-infected supernatants from both cell types (Fig. 3C and D). FB mRNA and protein levels were comparable between MDM and HUVEC (Fig. 3). To further assess if the induction of FH mRNA but not protein is specific for infection, cells were stimulated with Toll-like receptor 3 (TLR3) and TLR4 ligands: poly(I-C) and lipopolysaccharide (LPS), respectively. Following TLR stimulation, both FH mRNA (Fig. 4A) and protein (Fig. 4B) were significantly increased at 24 and 48 hpi in MDM. In contrast, DENV infection again induced FH mRNA, but not protein, in the supernatant (Fig. 4A and B). Notably, induction of FH mRNA by DENV was comparable to that by poly(I-C) or LPS, but the increased FH mRNA in DENV-infected cells did not translate into an increase in secreted FH protein (Fig. 4A and B). As expected and consistent with the results presented in Fig. 3, both FB mRNA and protein increased in response to TLR stimulation and DENV infection (Fig. 4C and D). Zika virus (ZIKV) infection induced FH mRNA to a level much higher than that seen with DENV at 48 hpi (Fig. 4A) but still failed to increase

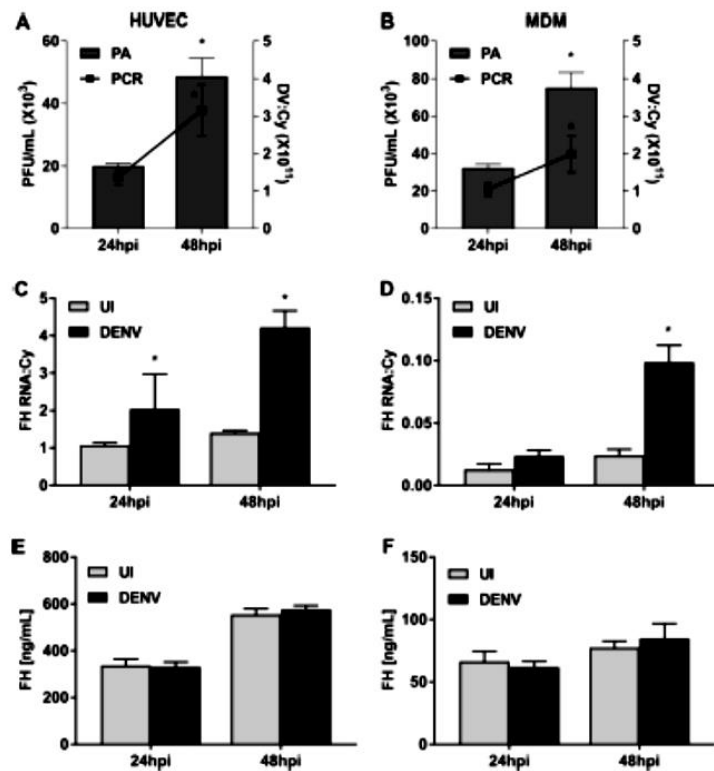


FIG 1 DENV infection of HUVEC and MDM induces FH mRNA but not protein. HUVEC and MDM were isolated and were left uninfected or DENV infected at MOI of 1 and 3, respectively. (A, B) At 24 and 48 hpi, supernatants and total cellular RNA were collected from HUVEC (A) and MDM (B) and analyzed by plaque assay (PA; bars) and RT-PCR (lines), with the values being normalized against those for cyclophilin. (C, D) Cell lysates of HUVEC (C) or MDM (D) were analyzed for FH mRNA by RT-PCR, with the values being normalized against those for cyclophilin. (E, F) Supernatants of HUVEC (E) or MDM (F) were analyzed by ELISA for FH protein. Results represent the mean \pm standard deviation for duplicate samples and are representative of those from three independent infection experiments. *, $P < 0.05$, Student's unpaired *t* test. UI, uninfected; DV, dengue virus.

FH protein (Fig. 4B). ZIKV infection also induced FB mRNA at 48 hpi (Fig. 4C) but, interestingly, and in contrast to DENV infection, not FB protein (Fig. 4D).

Similarly, in HUVEC, poly(I:C) and LPS stimulated both FH mRNA and protein, while DENV induced FH mRNA but not protein (data not shown). ZIKV responses in HUVEC were not reliably defined since ZIKV infection of HUVEC induced a substantial visual cytopathic effect.

Cell surface and intracellular FH is induced in DENV antigen-positive cells. FH also has a cell surface binding capacity (39, 40). To investigate if the lack of an increase in extracellular FH protein is due to FH rebinding to DENV-infected cells, cell surface-bound FH was analyzed by flow cytometry. Surface-bound endogenous FH was lower in DENV-infected HUVEC than in uninfected HUVEC, as determined by the percentage of FH-positive cells when analyzed as combined data from 3 independent experiments (Fig. 5A), although this was significant in only one of three experiments when analyzed individually. Further, as shown in the histogram plot, this finding represents a very minor shift in the FH-positive cell population (Fig. 5A). DENV infection had no significant effect on the mean fluorescent intensity (MFI) of FH binding to cells (Fig. 5A). An increase in FH binding, however, was seen specifically in the DENV antigen-positive but

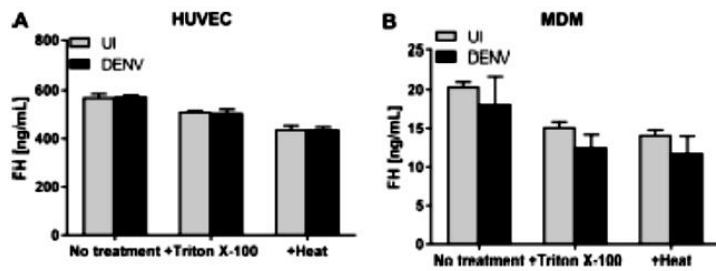


FIG 2 Treatment with detergent or heat does not increase FH protein detection in DENV-infected samples. HUVEC and MDM were isolated and were left uninfected or DENV infected at MOI of 1 and 3, respectively. At 48 hpi, supernatants of HUVEC (A) and MDM (B) were collected, treated with or without 0.05% Triton X-100 or heat (56°C), and analyzed by ELISA for FH protein. Results represent the mean \pm standard deviation for duplicate samples and are representative of those from three independent infection experiments.

not antigen-negative cells of the DENV-infected HUVEC population (Fig. 5B). In contrast to HUVEC, surface-bound endogenous FH was significantly higher in DENV-infected MDM than in uninfected MDM in terms of the percentage of FH-positive cells but not in terms of the intensity and, thus, the amount of FH bound per cell (Fig. 6A). Again, in contrast to HUVEC, this increase in FH binding was seen in both the DENV antigen-positive and the DENV antigen-negative cells of the DENV-infected MDM population (Fig. 6B). Together, these results confirm that the DENV induction of FH mRNA can result in production of FH protein but that at least some of this protein rebinds back to the infected cell or, in the case of MDM, infected and uninfected cell surfaces.

To further confirm the ability of DENV-infected cells to produce FH protein, quantitative immunostaining for intracellular FH and, for comparison, FB was performed.

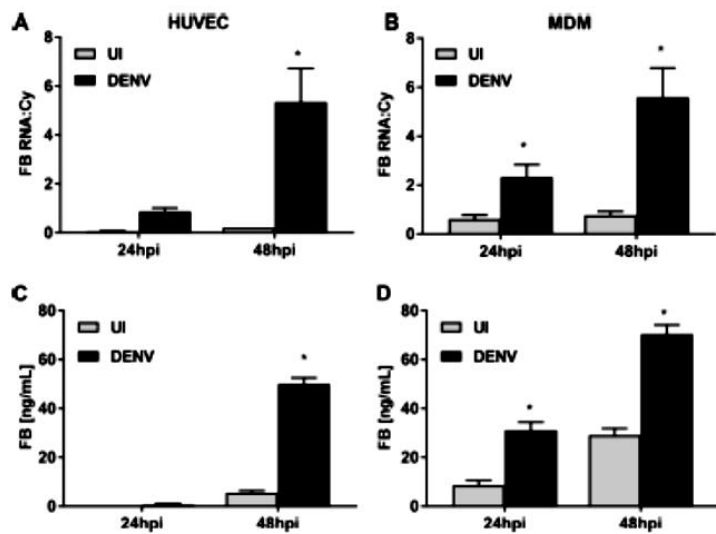


FIG 3 DENV infection of HUVEC and MDM induces FB mRNA and protein. HUVEC and MDM were isolated and were left uninfected or DENV infected at MOI of 1 and 3, respectively. Infection was verified as described in the legend to Fig. 1A and B. (A, B) At 24 and 48 hpi, total HUVEC (A) and MDM (B) RNA was collected and analyzed for FB mRNA by RT-PCR, and the values were normalized against those for cyclophilin. (C, D) HUVEC (C) and MDM (D) supernatants were collected and analyzed by ELISA for FB protein. Results represent the mean \pm standard deviation for duplicate samples and are representative of those from three independent infection experiments. *, $P < 0.05$, Student's unpaired *t* test.

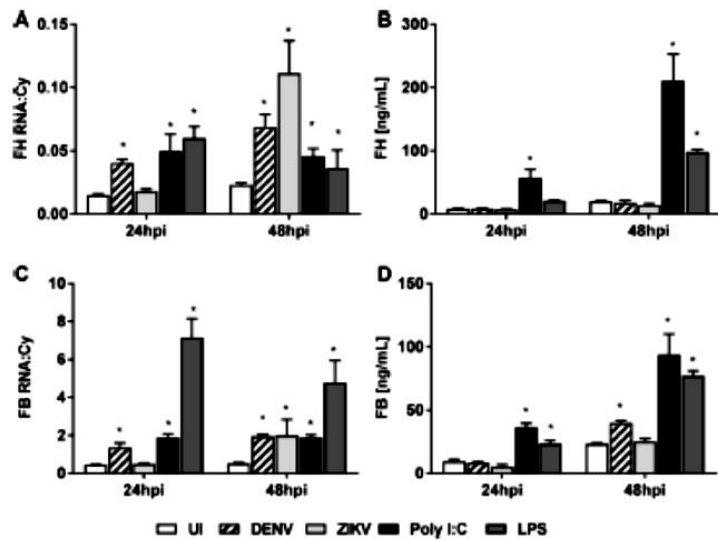


FIG 4 Stimulation with TLR ligands but not DENV or ZIKV induces FH and FB mRNA and protein. MDM were isolated and were left uninfected, DENV or ZIKV infected, or stimulated with poly(I:C) or LPS. (A, C) At 24 and 48 hpi, supernatants were collected, the cells were lysed, and total RNA was extracted and analyzed for FH (A) and FB (C) mRNA by RT-PCR. PCR results were normalized against those for cyclophilin. (B, D) Supernatant was collected and analyzed by ELISA for FH (B) and FB (D) proteins. Results represent the mean \pm standard deviation for duplicate samples at each time point and are representative of those from three independent infection experiments. Significance was calculated in relation to the results for the uninfected control group. *, $P < 0.05$, one-way ANOVA/Tukey's test.

DENV infection of HUVEC (Fig. 7A) or MDM (Fig. 7B) resulted in only a small percentage (3 to 15% of the total cell population) of cells staining DENV antigen positive, as expected from previous studies (11, 18, 47, 48) and evident from the results shown in Fig. 5 and 6. Basal staining for both the FB and FH proteins was detected in uninfected cells. Visually, there was no major change in the overall DENV-infected cell population, but those cells staining for DENV antigen appeared to be more strongly positive for both FH and FB than uninfected cells (Fig. 7A and B). The staining intensity for FB and FH was quantified using an Operetta high-content imaging system. The results showed no increase in the overall FB and FH staining intensity in DENV-infected wells compared to uninfected wells for either cell type (Fig. 7C and D). The FH and FB staining intensities in individual DENV antigen-negative or -positive cells from within the same DENV-infected well were then compared. A significant induction of both the FH and FB proteins in DENV antigen-positive HUVEC compared to antigen-negative cells was apparent (Fig. 7C). In contrast, induction in DENV antigen-negative cells was not significantly different from that in cells in uninfected wells. Similarly, in DENV-infected MDM, FB protein was induced in DENV antigen-positive cells, and although the results were not statistically significant, a similar trend toward increased FH protein was observed (Fig. 7D).

DENV infection can induce FH protein in some immortalized cell lines. The low susceptibility of HUVEC (18) and MDM (47, 48) to DENV infection *in vitro* might account for the observed lack of detectable induction of extracellular FH in these cells. To analyze this, responses were evaluated in another EC transformed cell line (HPV E6/E7-transduced human retinal endothelial cells [HREC]), which have low susceptibility to DENV infection, and ARPE-19 retinal pigment epithelial cells, which have high susceptibility to DENV infection (49). Consistent with the results in HUVEC and MDM, the levels of FB and FH mRNA were significantly increased in DENV-infected HREC and ARPE-19 cells at 48 hpi (Fig. 8A). Both FB and, in contrast to HUVEC and MDM, also FH

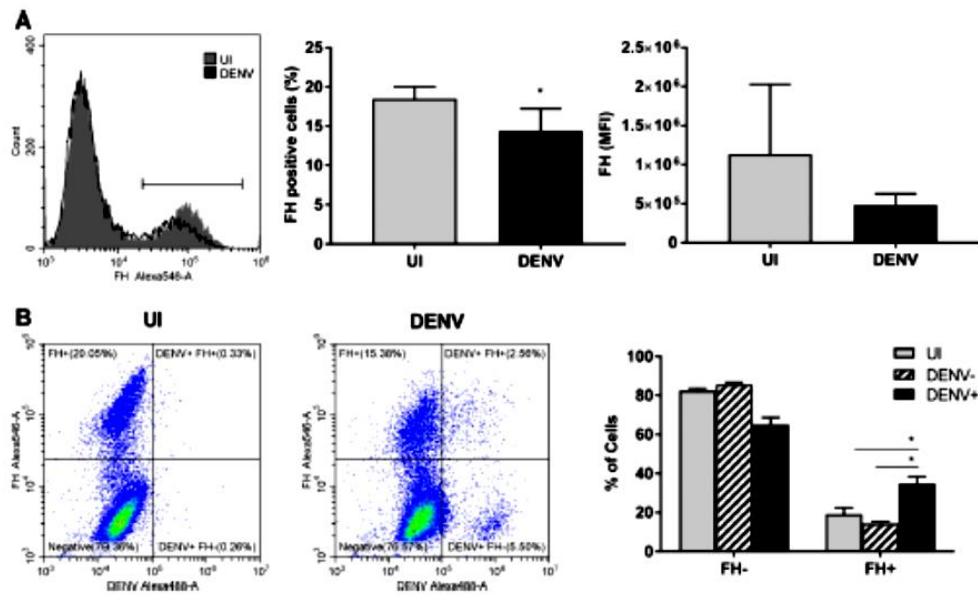


FIG 5 Cell surface FH binding is induced in DENV antigen-positive HUVEC. HUVEC were isolated and were left uninfected or DENV infected at an MOI of 1. (A) HUVEC were detached with 5 mM EDTA, stained for FH on cell surfaces and intracellularly for DENV, and analyzed by flow cytometry. Gray and black plots represent FH staining on uninfected (UI) and DENV-infected cells, respectively. The percentage of FH-positive cells was calculated from the gate indicated on the histogram, and the mean fluorescent intensity (MFI) of the population was determined. *, $P < 0.05$, Student's unpaired *t* test. (B) Representative quad plots of FH-Alexa Fluor 546 versus DENV-Alexa Fluor 488 for uninfected and DENV-infected populations. The percentage of FH-positive and -negative cells from uninfected, DENV antigen-negative, and DENV antigen-positive populations was calculated using gates, as shown. Results represent the mean \pm standard deviation for triplicate samples, and data from three independent infection experiments were combined. *, $P < 0.05$, two-way ANOVA/Tukey's test.

protein were significantly elevated at 48 hpi in HREC and ARPE-19 cells (Fig. 8B). Immunostaining and quantitative analysis for intracellular FH and FB were also performed in HREC and ARPE-19 cells, as shown in Fig. 7 for primary MDM and HUVEC. As expected, DENV infected only a small percentage of HREC but the majority of ARPE-19 cells (Fig. 9A and B). Visually, DENV antigen-positive cells appeared to be more strongly positive for both FH and FB than uninfected cells for both cell types (Fig. 9A and B), and this was confirmed by quantitative imaging, which showed an increase in staining intensity when considered over the entire well or specifically in DENV antigen-positive cells (Fig. 9C and D).

DENV infection is associated with indicators of active complement. Given that the actions of FH as a negative regulator of the AP oppose complement components, such as FB, that promote AP activity, the ratio of FH/FB protein was calculated. The results demonstrated a significantly lower proportion of FH relative to FB in the supernatant from DENV-infected cells than in that from uninfected cells (Fig. 10). Interestingly, there was a decrease in FH/FB of greater than 90% in HUVEC (Fig. 10A) but only approximately 50% in MDM (Fig. 10B). Additionally, although FH was induced in the supernatant of DENV-infected HREC and ARPE-19 cells, analysis of the FH/FB ratio revealed that, consistent with the results from MDM and HUVEC, FB was induced at higher levels relative to FH protein, resulting in a significant decrease in the FH/FB ratio (Fig. 10C and D).

To test the ability of cultured supernatant to promote the complement AP, supernatants were incubated with normal human serum (NHS) under buffer conditions specific for the AP, and lysis of rabbit erythrocytes was quantitated. Supernatant from DENV-infected HUVEC showed a significantly greater ability to promote AP-mediated hemolysis than that from uninfected cells (Fig. 11A). Similar results were obtained with

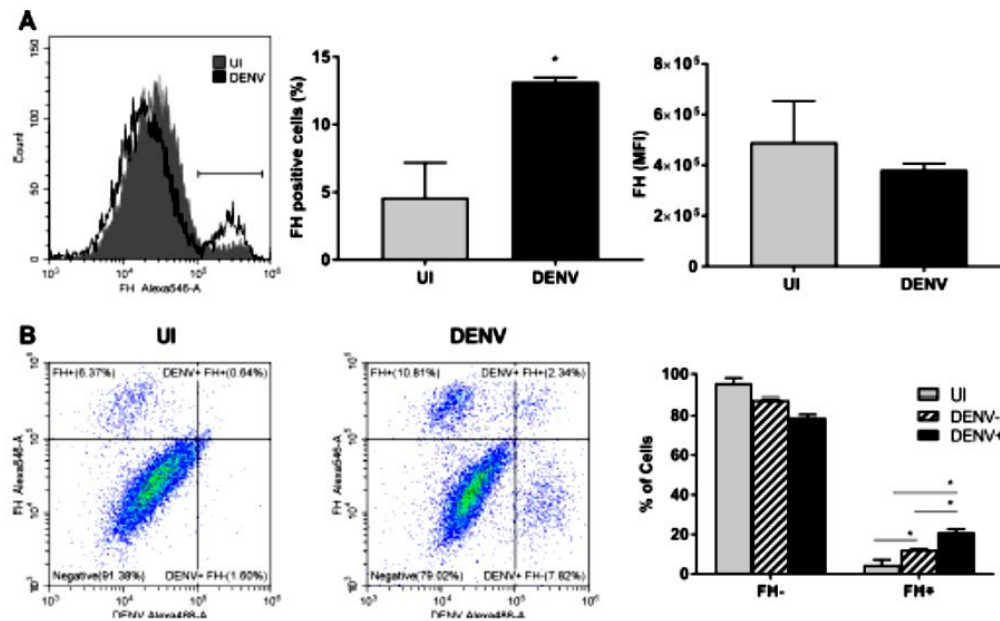


FIG 6 Cell surface FH binding is induced in DENV antigen-positive MDM. MDM were isolated and were left uninfected or DENV infected at an MOI of 3. (A) MDM were detached with 5 mM EDTA, stained for FH on cell surfaces and intracellularly for DENV, and analyzed by flow cytometry. Gray and black plots represent FH staining on uninfected (UI) and DENV-infected cells, respectively. The percentage of FH-positive cells was calculated from the gate indicated on the histogram, and the mean fluorescent intensity (MFI) of the population was determined. *, $P < 0.05$, Student's unpaired *t* test. (B) Representative quad plot graphs of FH-Alexa Fluor 546 versus DENV-Alexa Fluor 488 for uninfected and DENV-infected populations. The percentage of FH-positive and -negative cells from uninfected, DENV antigen-negative, and DENV antigen-positive populations was calculated using gates, as shown. Results represent the mean \pm standard deviation for triplicate samples, and data from three independent infection experiments were combined. *, $P < 0.05$, two-way ANOVA/Tukey's test.

supernatant from DENV-infected MDM (Fig. 11B), suggesting in both cases that DENV-infected cells produce secreted factors that promote AP activity. Importantly, the addition of purified exogenous FH protein to supernatants from DENV-infected HUVEC or MDM significantly impaired the ability of these supernatants to promote the activity of the AP (Fig. 11), supporting a role for FH in controlling complement AP activity in this assay system.

Additionally, during a viral infection and in the presence of the full spectrum of complement proteins, C3b should be deposited onto the surface of infected cells that can be regulated by the opposing roles of FH and FB (30–32). While FB interacts with C3b to promote C3 convertase, FH, acting with FI, cleaved surface-bound C3b to form inactivated C3b (iC3b), avoiding pathogenic C3b deposition (30, 31, 50). Thus, C3b binding to DENV-infected cells was quantitated by flow cytometry, with NHS being used as a source of complement. The results showed a significant increase in C3b binding to DENV-infected EC compared to uninfected cells in terms of the amount of C3b bound and the number of C3b-positive cells seen (Fig. 12A). Consistent with the results in HUVEC, C3b showed a similarly increased binding to DENV-infected MDM (Fig. 12B).

DISCUSSION

The complement system is a vital part of the body's response to pathogens and is an important player in host defenses against DENV (51–53). In contrast, overactivity of complement, in particular, the AP, is associated with increased DENV disease severity (8, 26, 45); thus, fine control of specific aspects of the complement pathways is needed to trigger a protective but nondetrimental immune response. It is well-known that FH is

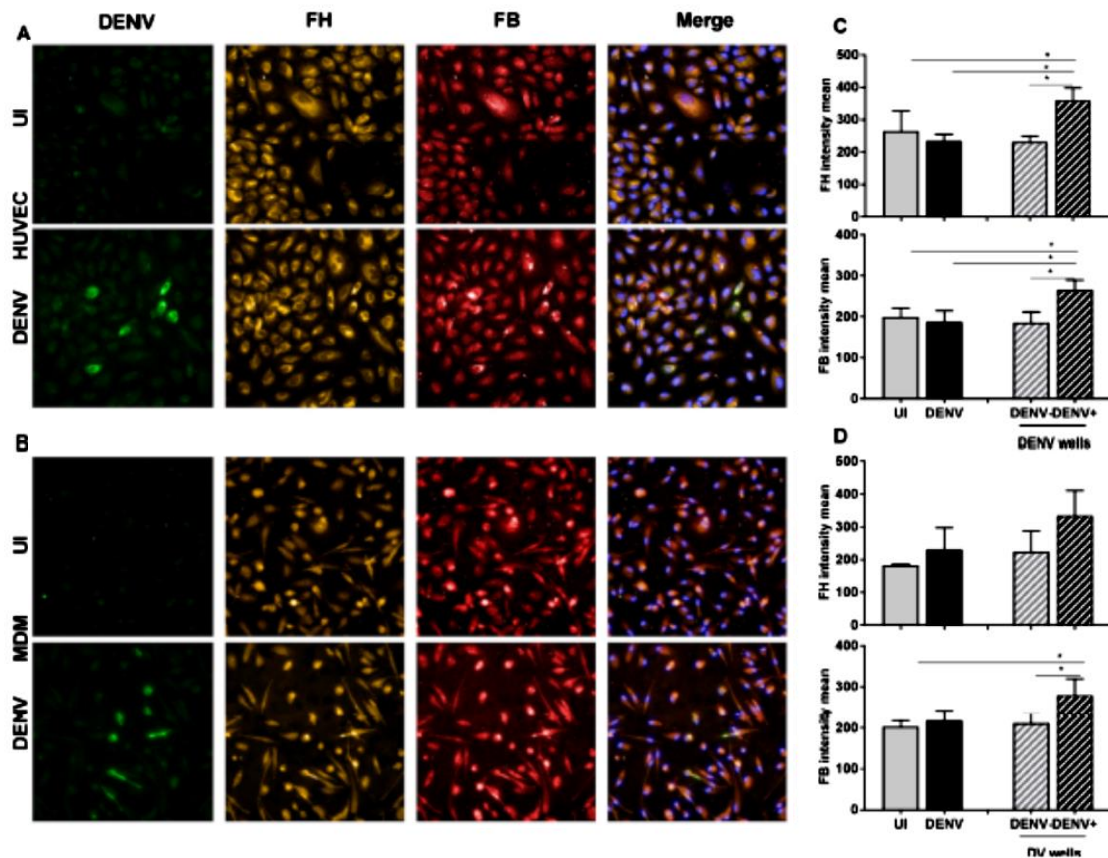


FIG 7 FH and FB are increased specifically in DENV antigen-positive HUVEC and MDM. (A, B) HUVEC (A) and MDM (B) were isolated and were left uninfected (UI) or DENV infected. At 48 hpi, cells were fixed and immunostained for DENV (green), FH (orange), and FB (red). Nuclei were stained with Hoechst (blue). Cells were imaged with an Operetta high-content imaging system at a $\times 20$ magnification. (C, D) Images of 49 fields of view were analyzed, and the intensity means were calculated using Harmony software. The intensity means for FH and FB were compared in uninfected (gray bars) versus DENV-infected (black bars) wells and in DENV-negative cells (gray bars with a hatching pattern) versus DENV-positive cells (black bars with a hatching pattern) within a well. HUVEC (C) and MDM (D) were analyzed. Results represent the mean \pm standard deviation for triplicate samples and are representative of those from three independent infection experiments. $^* P < 0.05$, one-way ANOVA/Tukey's test.

one of the main negative regulators of AP activity (30, 33, 37). Additionally, macrophages and EC are recognized as major targets for DENV replication and pathogenesis *in vivo*, and both these cell types may contribute to FH production, antiviral immune responses, and induction of vascular permeability, a hallmark of DENV disease (11–13, 54). Thus, this work focused on defining the DENV-induced changes in FH in macrophages and EC and linking these with changes in other complement components, FB and C3b, to understand the cellular and molecular responses that contribute to the complement AP overactivity reportedly associated with DENV disease.

First, the results showed that DENV infection of HUVEC and MDM effectively induces both FB and FH mRNA. Surprisingly, however, this translates to a significant increase only in FB protein, while the levels of secreted FH protein remain unchanged from those in uninfected cells for both cell types. Induction of FB mRNA has previously been reported in DENV-infected HUVEC, although with a higher 34-fold induction of mRNA (16). Results presented here confirm induction of FB mRNA and extend this to demonstrate an increase in FB protein. This report is the first to describe the DENV induction of FH mRNA and additionally presents several lines of evidence suggesting that the

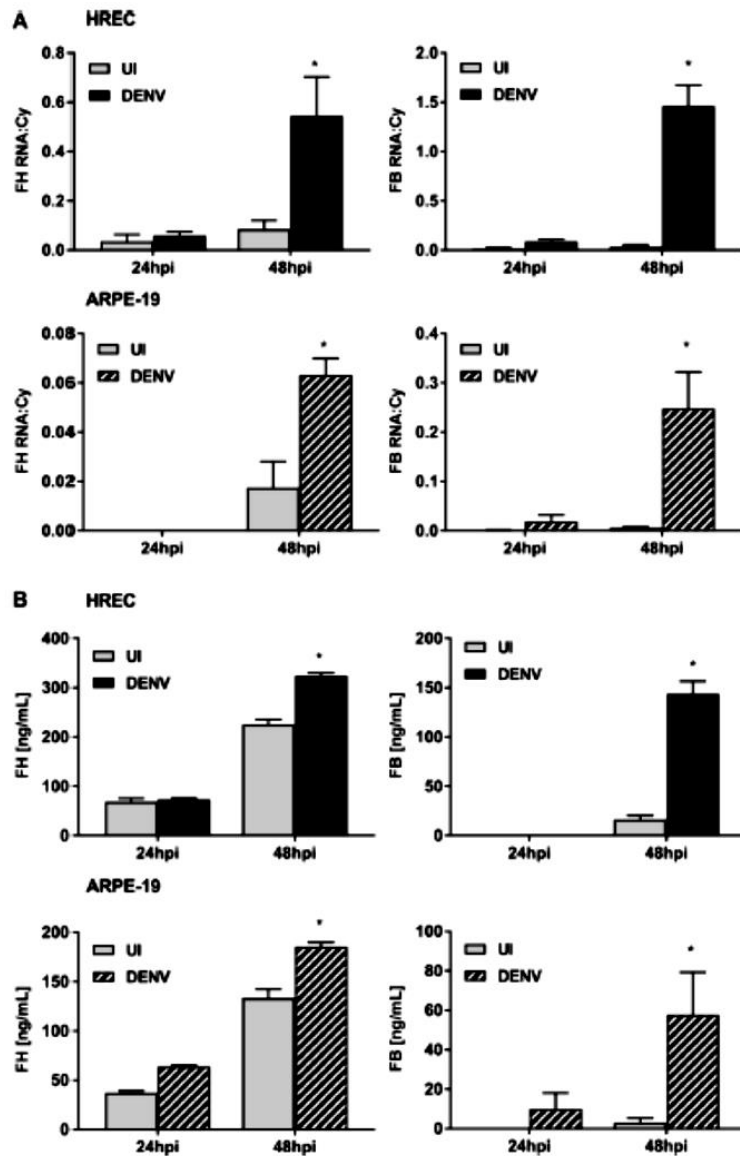


FIG 8 DENV infection of HREC and ARPE-19 cells induces FH and FB mRNA and protein. HREC and ARPE-19 cells were isolated and were left uninfected (UI) or DENV infected at an MOI of 1. (A) At 24 and 48 hpi, supernatants and total cellular RNA were collected and analyzed for FH and FB mRNA by RT-PCR, and the results were normalized against those for cyclophilin. (B) Supernatants were analyzed by ELISA for FH and FB proteins. Results represent the mean \pm standard deviation for duplicate samples and are representative of those from three independent infection experiments. *, $P < 0.05$, Student's unpaired *t* test.

resultant production and/or release of FH protein from the infected cell is compromised. This inability to detect an increase in secreted FH from DENV-infected cells is not due to FH being complexed in the supernatant to other proteins, as validated by detergent (Triton X-100) or heat (56°C) treatment of samples prior to ELISA. Additionally, since FH also exerts its regulatory function on the cell surface via binding to cell

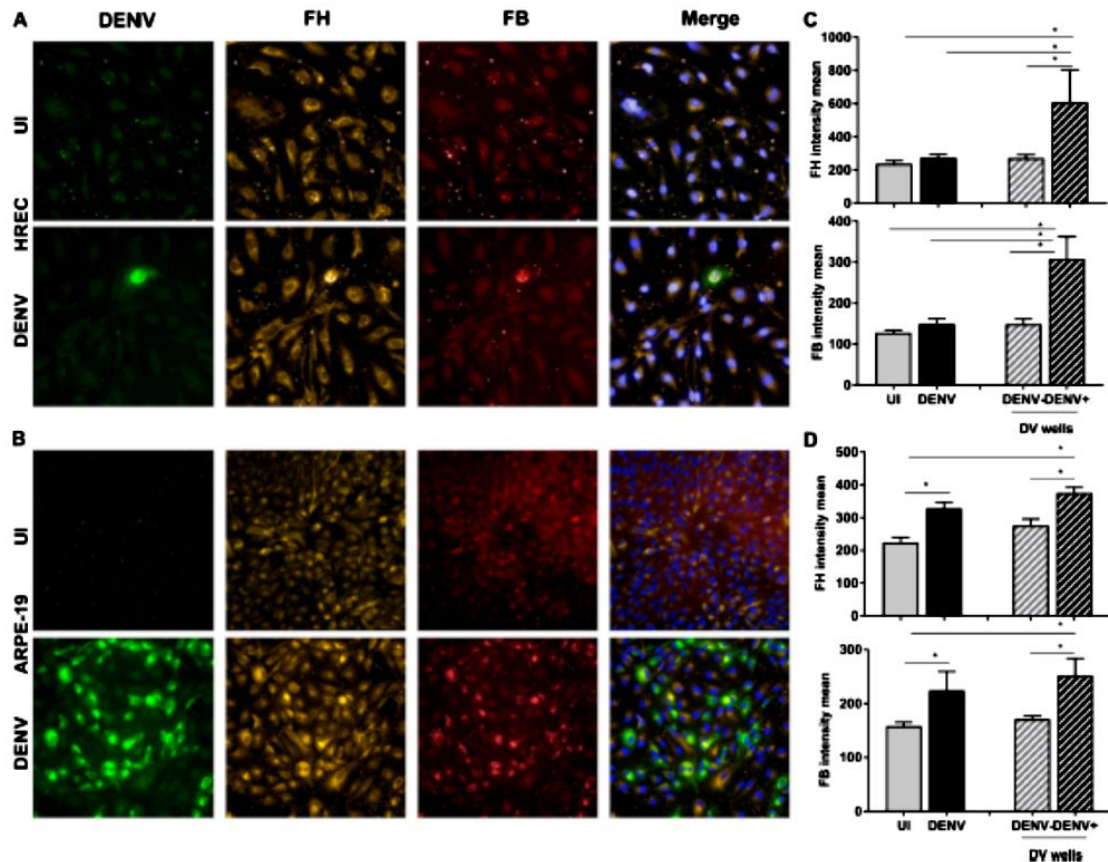


FIG 9 DENV infection of HREC and ARPE-19 cells induces intracellular FH and FB proteins. (A, B) HREC (A) and ARPE-19 cells (B) were isolated and were left uninfected (UI) or DENV infected. At 48 hpi, cells were fixed and immunostained for DENV (green), FH (orange), and FB (red). Nuclei were stained with Hoechst (blue). Cells were imaged with an Operetta high-content imaging system at a $\times 20$ magnification. (C and D) Images of 49 fields of view were analyzed, and the intensity means were calculated using Harmony software. The intensity means of FH and FB were compared in uninfected (gray bars) versus DENV-infected (black bars) wells and in DENV-negative cells (gray bars with a hatching pattern) versus DENV-positive cells (black bars with a hatching pattern) within a well. HUVEC (C) and MDM (D) were analyzed. Results represent the mean \pm standard deviation for triplicate samples and are representative of those from three independent infection experiments. *, $P < 0.05$, one-way ANOVA/Tukey's test.

surface glycosaminoglycans (39–41), DENV could influence the rebinding of FH to infected cells to reduce apparent levels in the supernatant. Indeed, the results showed increased levels of endogenous FH binding at the surface of DENV antigen-positive cells within a DENV-infected population of either HUVEC or MDM. In the DENV-infected population, endogenous surface-bound FH was also increased in the DENV antigen-negative population of DENV-infected MDM but not HUVEC, suggesting cell type differences in the ability of FH to bind and protect the surfaces of uninfected bystander cells. Additionally, the lack of an increase in FH in supernatants from DENV-infected MDM and EC was not due to an inability *per se* of our cell system to induce both FH mRNA and secreted protein, with both being induced following stimulation of HUVEC or MDM with TLR3 or -4 agonists. This is consistent with the findings of other studies demonstrating an upregulation of FB mRNA and protein by LPS and poly(I:C) in macrophages (55, 56), increased production of FH protein in U937 cells upon LPS stimulation (57), and emerging evidence indicating extensive cross talk between complement and TLR signaling (58). Since DENV stimulates TLR3 (59) and TLR4 (22, 23) and

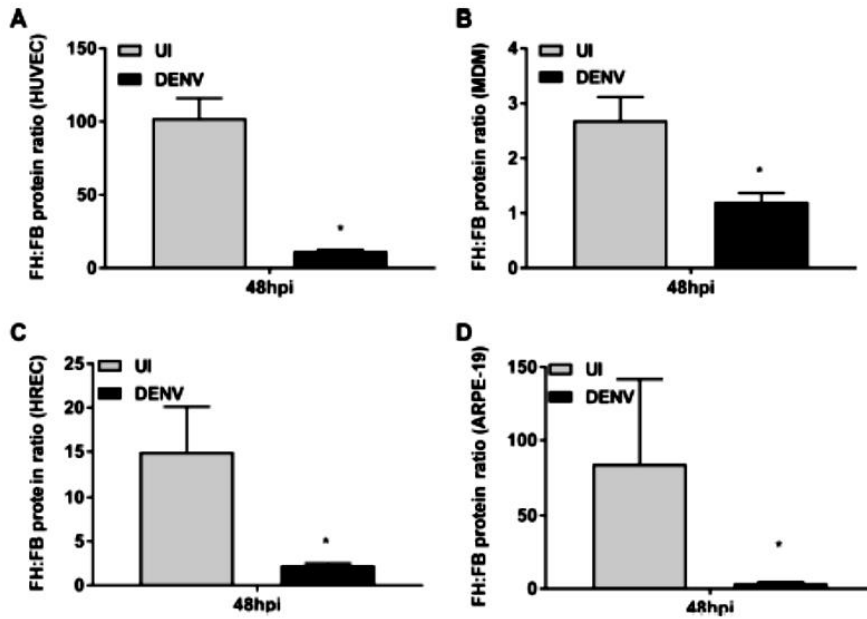


FIG 10 DENV induces lower levels of FH than FB. HUVEC (A), MDM (B), HREC (C), and (D) ARPE-19 cells were isolated and were left uninfected (UI) or DENV infected. At 48 hpi, supernatants were analyzed by ELISA for FH and FB proteins, and the ratio between the two was calculated. A lower ratio implies lower levels of FH than FB. Results represent the mean \pm standard deviation for duplicate samples and are representative of those from three independent infection experiments. *, $P < 0.05$, Student's unpaired t test.

given that the DENV-induced FH mRNA levels are comparable to or greater than those induced by TLR3/4, our results imply that the induction of FH mRNA but not FH protein in the supernatant of DENV-infected cells is due to a virus-induced defect in the ability to produce more FH protein extracellularly in these primary cell types. This discordance between FH mRNA and extracellular levels of FH was also observed following infection with the related flavivirus ZIKV. Additionally, DENV induced both FH mRNA and secreted protein in the cell lines ARPE-19 and HREC.

To investigate FH protein production further, intracellular FH was quantitated.

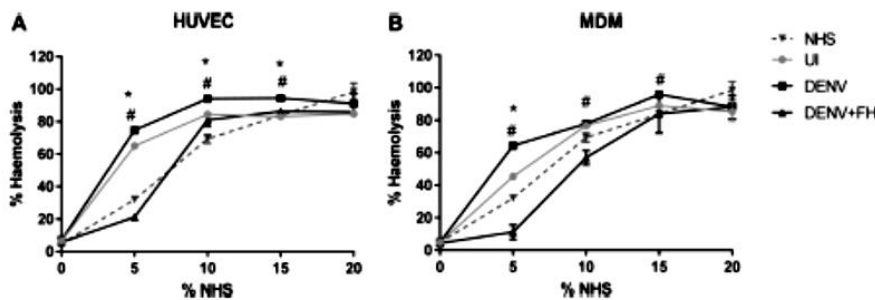


FIG 11 DENV infection releases factors that promote complement AP activity. HUVEC (A) and MDM (B) were isolated and were left uninfected (UI) or DENV infected. At 48 hpi, supernatants were collected, mixed with different concentrations of normal human serum (NHS) and/or purified FH protein, and analyzed for the ability to promote AP activity by quantitation of hemolysis of rabbit erythrocytes under buffer conditions specific for the AP. Results represent the mean \pm standard deviation for duplicate samples and are representative of those from three independent infection experiments. *, $P < 0.05$ for the comparison between uninfected and DENV cell supernatant by one-way ANOVA/Tukey's test; #, $P < 0.05$ for the comparison between DENV and DENV cell supernatant supplemented with purified FH by one-way ANOVA/Tukey's test.

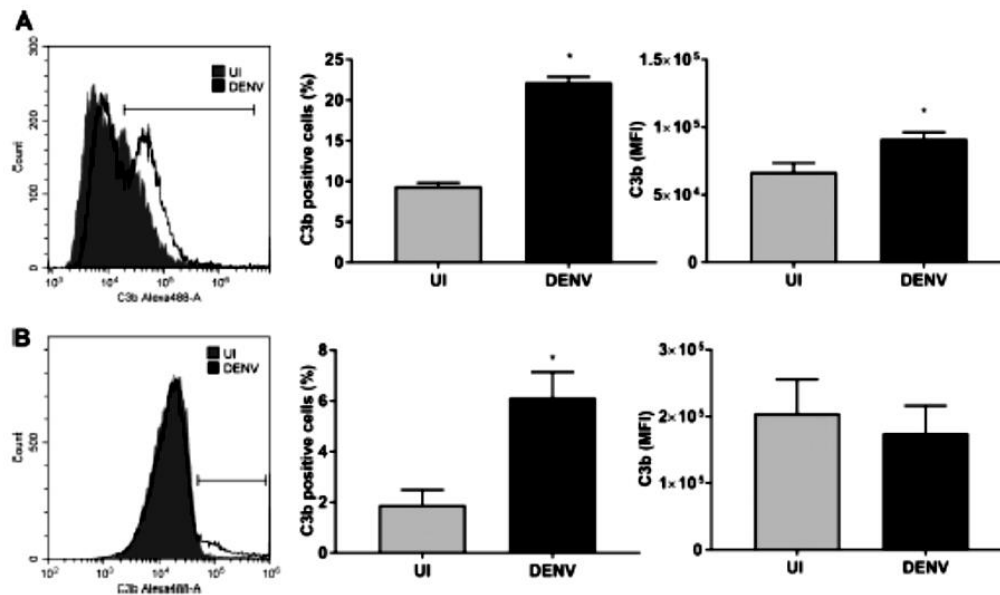


FIG 12 DENV infection results in increased cellular C3b deposition. HUVEC (A) and MDM (B) were isolated and were left uninfected (UI) or DENV infected at MOI of 1 and 3, respectively. At 48 hpi, cells were incubated with NHS for 30 min, detached with 5 mM EDTA, stained for C3b deposition, and analyzed by flow cytometry. Gray and black plots represent C3b staining on uninfected and DENV-infected cells, respectively. The percentage of C3b-positive cells was calculated from the gate indicated on the histogram, and the mean fluorescent intensity (MFI) of the population was determined. Results represent the mean \pm standard deviation for duplicate samples and are representative of those from three independent infection experiments. *, $P < 0.05$, Student's unpaired *t* test.

Although no significant change in intracellular FH protein was detected in MDM, a small but significant increase in intracellular FH protein was detected in DENV-infected HUVEC and a substantial increase in FH was observed following DENV infection of ARPE-19 cells and HREC. For the latter, as with MDM and HUVEC, this was even in the face of a low level of DENV-infected cells in culture. This stronger induction of intracellular levels of FH in HREC than HUVEC correlates with the ability to detect extracellular changes in FH protein levels in HREC. This suggests that DENV infection of only a small number of cells does not of itself preclude detection of increased secreted FH, but the level of intracellular FH protein induction may be restricted in primary MDM and HUVEC compared to that in the cell lines ARPE-19 and HREC. Overall, although significant levels of FH mRNA are induced following DENV infection, there is a poor subsequent increase in FH protein extracellularly. This may, at least in part, be accounted for by increased cell surface binding of FH, as described above, although DENV infection could also influence the production of extracellular FH by blocking intracellular FH translation, inhibiting protein secretion, or inducing FH degradation either inside or outside the cell, and these possible mechanisms remain to be investigated.

One of the primary consequences of poor induction of FH following DENV infection is a reduction in the extracellular negative regulatory capacity for the AP. This is of particular importance in the face of increases in other complement AP components, as described previously for FD (45) and shown here for FB and C3b. The latter finding of increased binding of C3b during DENV infection has also been described previously (60), and the increased C3b binding observed in our study may be related to activation of the AP but could also result from the activity of the classical and lectin pathways. Additionally, the results of our study show for the first time a consistent imbalance in components of the complement AP, with higher relative levels of FB than FH being found in DENV-infected cells from all cell types examined. Notably, this imbalance still

occurs even when extracellular FH protein is significantly induced in the HREC and ARPE-19 cell lines. FB activates the AP by binding C3b to form the AP C3 convertase (C3bBb), which stimulates complement consumption and the production of the anaphylatoxins C3a and C5a (28, 30). Likewise, FH may be recruited to infected cell surfaces to regulate C3b deposition and negatively influence the formation of C3 convertase. Additionally, there may be other cell surface complement regulators, such as conserved repeat 1, monocyte chemoattractant protein (CD46), and decay-accelerating factor (CD55) (50), that may be modulated during DENV infection, and these remain to be investigated. The failure to induce local secretion of FH protein, alongside the increased production of FB, elevated C3b binding to DENV-infected cells, and a greater ability of supernatant from DENV-infected cells to promote AP activity, suggests increased complement AP activity in the local microenvironment of DENV-infected cells. This is consistent with previous reports linking high levels of complement consumption and the hyperactivity of the AP to the severity of DENV-associated vascular leakage (8, 16, 25–27, 45). Recently, it has been shown that the AP ability to lyse rabbit erythrocytes is dependent on the levels of FB and FH, among other factors (61). While the imbalance in the ratio of FH/FB in DENV-infected cells may not be directly or solely responsible for this increased AP activity, our observations of FH and FB changes in ZIKV-infected cells suggest that this ratio may be related to pathogenesis. Similar to DENV infection, ZIKV infection induces FH mRNA but not an increase in FH protein, and in contrast to DENV, ZIKV additionally fails to induce FB protein. Thus, for ZIKV-infected cells, the relative levels of FB and FH are unchanged and C3b deposition and complement activity would be predicted to also be unaffected. In terms of clinical disease, DENV is well described to induce effects on the vascular endothelium, but this is not a characteristic of ZIKV disease. Thus, we propose that the dysregulation and imbalance in the complement AP components FB and FH that we have described here are likely of significance to the pathogenesis of DENV-induced vascular leakage.

It is well described that microorganisms can hijack the complement system by binding to regulatory proteins, such as FH, and utilize their negative regulatory function to downregulate complement AP activity and evade complement function (62–65). West Nile virus NS1 binds to FH, although DENV NS1 does not (64). DENV NS1 does, however, bind C1s and C4 to restrict and evade classical/lectin pathway activation (60) and binds to vitronectin to prevent C9 polymerization and MAC formation (66). Our findings here are in contrast to these previously reported pathogen evasion strategies, with induction of FB but not effective extracellular FH protein production and increased C3b binding to cells providing a mechanism supporting overactivity of complement rather than the DENV-FH interaction providing a complement-pathogen evasion strategy.

As modeled in Fig. 13, in a normal situation, where FB and FH are produced in a balanced ratio, deposition of C3b on cells is tightly controlled by opposing roles of complement AP regulators, leading to controlled production of inactivated C3b (iC3b) and C3 convertase (Fig. 13A). DENV infection of EC and MDM induces FH and FB mRNA and protein inside DENV-infected cells but fails to produce significant amounts of extracellular secreted FH protein in the fluid phase (Fig. 13B). FH can bind back to the surface of both DENV antigen-positive and antigen-negative cells in MDM but mainly DENV antigen-positive cells for HUVEC (Fig. 13B). In DENV-infected cells, this study has defined a reduced FH/FB in the extracellular space, increased AP activity released from cells, and increased C3b binding to cell surfaces (Fig. 13C). The increased ability of secreted components from DENV-infected EC or MDM to activate the AP is reversed by addition of exogenous FH and thus may relate to our described changes in FB and FH or as yet undescribed factors produced from DENV-infected cells that can promote AP activity (Fig. 13C). These overall changes are predicted to result in increased production of C3 convertase (C3bBb) and reduced C3b decay or conversion to iC3b, leading to increased complement activity. For the endothelium, this excessive fluid phase and cell surface complement activity has the potential to affect EC function and promote vascular permeability (Fig. 13C).

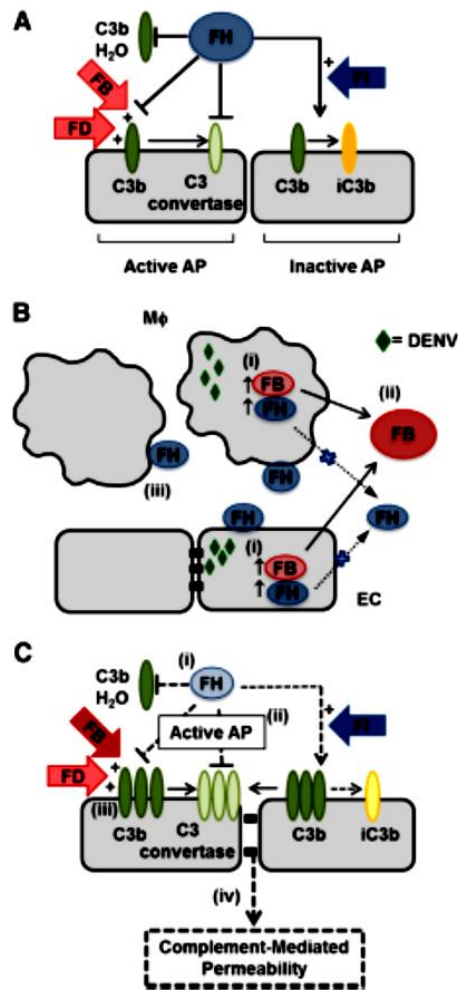


FIG 13 Summary and proposed complement AP interactions during DENV infection. (A) Normally, FB and FH are produced in a balanced ratio and the cleavage of C3, the deposition of C3b, and the formation of either iC3b or C3 convertase on cells are tightly controlled by opposing roles of FB and FH in conjunction with other regulators, such as FD and FI. (B) DENV infection of macrophages (Mφ) and EC (i) induces FB and FH mRNA but intracellular protein only in DENV-antigen positive cells, (ii) induces FB protein but little increase in extracellular FH protein production, and (iii) increases FH binding to cell surfaces of both uninfected DENV antigen-negative and DENV antigen-positive MDM but only in DENV antigen-positive HUVEC. (C) In the local environment of DENV-infected cells, this study shows that there is (i) a reduced amount of FH protein relative to FB, (ii) an increased ability of soluble factors to promote the activity of the AP, and (iii) increased binding of C3b at the cell surface. (iv) In the context of the endothelium, this is predicted to promote vascular permeability.

In conclusion, our study has defined changes in regulators of the complement AP using primary cells relevant to the pathology of DENV infection and disease and the cellular mechanisms by which this pathogenic overactivity of the complement AP may be mediated. It has been hypothesized that during DENV infection, the endothelium coordinates a multitude of signals and factors released by immune cells, like macrophages, which ultimately act on the endothelium to contribute to vascular permeability and hemorrhage (6, 11, 67). This study proposes an additional layer of contributing

signals that affect the EC barrier function during DENV infection: the AP activity in the cellular microenvironment of both macrophages and EC, with DENV induction of FB and deposition of C3b but limited induction of FH, particularly at the protein level at the surface of an infected cell. These results stimulate interest in complement AP regulators, for example, the development of agents to promote FH protein production from MDM and EC, as therapeutics to alleviate complement hyperactivity and potentially reduce DENV-induced vascular permeability and severe forms of DENV disease.

MATERIALS AND METHODS

Cell lines and cell culture. HUVEC were isolated from human umbilical cords collected with approval from the Central Northern Adelaide Health Service Ethics Committee. In brief, HUVEC were isolated by collagenase digestion and cultured on 0.2% (wt/vol) gelatin (Sigma)-coated flasks in M199 medium (HyClone) supplemented with 20% (vol/vol) fetal bovine serum (FBS), 1% penicillin-streptomycin, and 1% glutamine (all from Gibco) plus 0.3% endothelial cell growth supplement (BD Bioscience). HUVEC were utilized in infection studies at passages 1 to 4. Human MDM were isolated from healthy blood donors at the Australian Red Cross Blood Service and collected under ethics approval from the Southern Adelaide Clinical Human Research Ethics Committee (SACHREC). Monocytes were isolated by adherence and cultured for 4 to 5 days in Dulbecco modified Eagle medium (DMEM) supplemented with 10% (vol/vol) FBS, 10% (vol/vol) human heat-inactivated serum, 1% penicillin-streptomycin, and 1% glutamine to differentiate into MDM, as previously described and validated by CD14 and Wright-Giemsa staining (48). Human serum was collected from healthy donors in accordance with SALHN/HREC ethics approval and was determined to be DENV antibody negative by a diagnostic rapid immunochromatographic IgG and IgM assay. Generation and characterization of the HREC line has been described previously (68). The HREC line was cultured in MCDB-131 medium (Sigma-Aldrich) with 5% FBS and endothelial growth factors (EGM-2 SingleQuots supplement, omitting FBS, hydrocortisone, and gentamicin; Clonetics-Lonza, Walkersville, MD). The ARPE-19 cell line (American Type Culture Collection, Manassas, VA) was cultured in DMEM-F-12 medium supplemented with 5% FBS. All cells were grown in a humidified incubator with 5% CO₂ in air and at 37°C.

DENV production and infection. Mon601, a laboratory clone of the DENV serotype 2 New Guinea C strain, was used for infections (69) and is here referred to as DENV. Virus stocks were produced from *in vitro*-transcribed RNA that was transfected into baby hamster kidney clone 21 (BHK-21) cells and amplified in *Aedes albopictus* C6/36 cells. Cell culture supernatants containing virus were harvested, clarified, filtered, and stored at -80°C until use. The titer of infectious virus was determined by plaque assay using African green monkey kidney (Vero) cells and quantitated as the number of PFU per milliliter. HUVEC, ARPE-19 cells, and HREC were either left uninfected or infected with DENV at a multiplicity of infection (MOI) of 1. MDM were infected at an MOI of 3 as previously described (11). After 90 min of infection, the inoculum was removed, the cells were washed with phosphate-buffered saline (PBS; pH 7.4), and fresh medium was added. Supernatants and cells were harvested after 24 and 48 hpi and stored at -80°C until analysis. ZIKV infections utilized the cosmopolitan ZIKV strain PRVABC59, which was amplified in C6/36 cells; stocks were collected, titers were determined, and cells were infected as described above for DENV.

RNA extraction and real-time qRT-PCR. Total RNA was extracted from cells using the TRIzol reagent (Ambion Life Technologies) according to the manufacturer's instructions. The extracted RNA was DNase treated (Zymo Research) and quantitated by spectrophotometry (NanoDrop Elite; Thermo Scientific). RNA (0.5 µg) was reverse transcribed using Moloney murine leukemia virus reverse transcriptase (NEB) and random hexamers (NEB). The cDNA template was subjected to real-time quantitative reverse transcription-PCR (qRT-PCR) using ITaq SYBER green (Bio-Rad) in a Rotor-Gene 600 real-time PCR cycler (Corbett Research) and primers for DENV and cyclophilin as previously described (18). The cyclophilin gene was used as a normalization gene since its expression did not change in DENV-infected cells in our prior studies (18, 48) and, similarly, in the study described herein, where for the same input amount of RNA, threshold cycle (C_t) values for cyclophilin were comparable. For FH PCR, primers were designed to anneal with short consensus repeat 2 (SCR2): forward (F) primer, 5'AGGCCCTGTGGACATC3'; reverse (R) primer, 5'AACTTCACATATAGGAATATC3'. FB PCR primers were as previously reported (70): f primer, 5'ACTGAGCCAAGCAGACAAGC3'; r primer, 5'AGAAGCCAGAAGGACACAC3'. Both FH and FB PCRs were performed under the following conditions: 1 cycle of 95°C for 5 min; 40 cycles of 95°C for 15 s, 59°C for 20 s, and 72°C for 20 s; and 1 cycle of 72°C for 5 min. All PCR mixtures included high- and low-copy-number comparative controls. The results were normalized against those for cyclophilin, and the relative RNA level was determined by the ΔC_t method (71).

Flow cytometry. For FH and DENV staining, HUVEC or MDM were cultured in a 6-well plate and infected as described above. After 48 h, cells were washed twice with PBS and detached by scraping in PBS with 5 mM EDTA. Cells were washed again with PBS and blocked with 1% (wt/vol) bovine serum albumin (BSA) for 30 min at room temperature. Cells were rinsed once with PBS and incubated with a goat anti-human FH (1:25; Calbiochem) for 1 h at room temperature. After three washes with PBS-1% (wt/vol) BSA, cells were incubated for 1 h at room temperature with Alexa Fluor 546-labeled anti-goat immunoglobulin (1:200; Invitrogen). Subsequently, cells were fixed with 2% (wt/vol) paraformaldehyde (Sigma) for 10 min at room temperature. After three washes with PBS-1% (wt/vol) BSA, cells were permeabilized with 0.05% (wt/vol) octylphenoxy poly(ethyleneoxy) ethanol (Igepal CA-630; Sigma) in PBS for 20 min. Cells were washed again with PBS and blocked with 1% (wt/vol) BSA for 30 min at room

temperature. Cells were rinsed once with PBS and incubated overnight at 4°C with a mouse anti-DENV (1:10), D1-4G2-4-15 (ATCC HB-112TM). After three washes with PBS-1% (wt/vol) BSA, cells were incubated for 1 h at room temperature with Alexa Fluor 488-labeled donkey anti-mouse immunoglobulin (1:200; Invitrogen). Following a final set of PBS-BSA washes, cells were analyzed by flow cytometry. Flow cytometry was performed with a CytoFlex S flow cytometer (Beckman Coulter Inc.) and analyzed by CytExpert (version 2.0.0.153) software (Beckman Coulter Inc.).

For detection of C3b deposition, HUVEC or MDM were cultured and infected as described above. At 48 hpi, the culture medium was removed and cells were incubated in M199 medium (HyClone) containing 10% NHS (as the complement source) for 30 min at 37°C in a 5% CO₂ incubator. Cells were also incubated with the corresponding medium containing 10% heat-inactivated serum as a negative control. Cells were washed and detached with PBS-5 mM EDTA. C3b deposition was detected with a mouse anti-human C3b (1:25; BiLegend) and Alexa Fluor 488-labeled donkey anti-mouse immunoglobulin (1:200; Invitrogen). Cells were fixed and analyzed by flow cytometry as described above.

Treatment of TLR ligands. HUVEC or MDM cells were treated with 10 µg/ml poly(I:C) (TLR3) or 1 µg/ml LPS (TLR4) for 24 and 48 h. DENV infection was carried out in parallel and as described above. Supernatants and cells were harvested after 24 and 48 hpi and stored at -80°C until analysis. TLR ligands were purchased from Sigma.

Human complement FH purification. FH was purified from human serum by one-step affinity chromatography using CNBr-activated Sepharose 4B coupled to a sheep anti-human FH polyclonal antibody (pAb) (72). Briefly, total human serum was diluted 1:2 in PBS and loaded onto the column, and the flowthrough was reloaded at least four times. After washing with PBS, FH was eluted with 0.1 M glycine (pH 2.3) and immediately neutralized with 1 M Tris-HCl (pH 8.8). Eluted fractions were analyzed by SDS-PAGE under reducing and nonreducing conditions and Western blotting using the primary goat anti-human FH pAb (1:2,000; Calbiochem) and the secondary anti-goat IgG coupled to horseradish peroxidase (1:30,000; Calbiochem). Bound complexes were detected by chemiluminescence (Clarity Western ECL substrate; Bio-Rad) and visualized with a LAS4000 imaging system (Fuji Imaging Systems). FH-containing fractions were pooled and concentrated using an Amicon Ultra 0.5-ml centrifugal filter (100-molecular-weight cutoff; Millipore), and the purity of FH was reassessed by Western blotting as described above.

Quantitation of FH and FB by ELISA. FH or FB proteins were quantitated in cell culture supernatant by ELISA. For FH detection, 96-well microtiter plates (Greiner) were coated with goat anti-human FH (Calbiochem) at 10 µg/ml diluted in carbonate-bicarbonate buffer, pH 9.6, and incubated overnight at 4°C. Plates were blocked with 2% (wt/vol) BSA (Sigma) diluted in PBS (pH 7.4) for 1 h at 37°C. Purified FH protein, isolated as described above, was used to generate a standard curve. Standards and supernatant samples were diluted in PBS containing 1% (wt/vol) BSA (PBS-BSA) and incubated on the plates for 2 h at 37°C. The plates were washed five times with PBS containing 0.05% (vol/vol) Tween 20 (PBS-T) and incubated with a mouse anti-human FH monoclonal antibody (Abcam) diluted 1:10,000 in PBS-BSA for 1 h at 37°C. The plates were washed again and incubated with an anti-mouse IgG coupled to horseradish peroxidase (Promega) and diluted 1:10,000 in PBS-BSA for 1 h at 37°C. The plates were washed seven times and developed with tetramethylbenzidine peroxidase substrate (KPL), the reactions were stopped with 1 M sulfuric acid, and the absorbance at 450 nm was quantitated in a microplate reader (Beckman Coulter). A standard curve with purified FH was established using a linear regression curve ($R^2 > 0.99$) with eight standard concentrations. The range of detection was from 20 to 1,000 ng/ml. To disrupt possible interactions between FH and viral protein(s), supernatants were treated with 0.05% Triton X-100 (Sigma) for 30 min at room temperature or incubated for 30 min at 56°C and then evaluated by the FH ELISA as described above.

The levels of FB in the cell culture supernatants were measured using a human FB ELISA kit (Abcam) in accordance with the manufacturer's instructions.

AP *in vitro* activity assay. Whole blood was collected under aseptic conditions from a healthy rabbit in accordance with Flinders University Animal Welfare Committee approvals for collection of scavenger material. Blood was collected into a conical flask containing glass beads and gently swirled until a clot formed. The defibrinated blood was decanted and washed three to four times in AP buffer (Veronal-buffered saline containing 0.01 M EGTA and 0.1% gelatin, pH 7.5) until the supernatant was clear. The cells in the cell-containing supernatant were enumerated, and 5×10^7 cells/ml of rabbit erythrocytes were resuspended in AP buffer and used as a master stock for the hemolysis assay.

For the assay, NHS was incubated with AP buffer for 15 min on ice to inactivate the classical and lectin complement pathways. Uninfected and DENV-infected cell supernatants were mixed with treated NHS (to support the AP activity) at from 5 to 20% NHS. To evaluate the possible effect of FH, DENV-infected cell supernatant was supplemented with exogenous purified FH protein at 500 µg/ml and serially diluted with different concentrations of NHS as described above. Fifty microliters of each NHS-supernatant mix was added in duplicate to a flat-bottom 96-well plate (Costar), and 50 µl of the rabbit erythrocyte master stock was overlaid onto the wells. The plate was incubated for 30 min at 37°C with intermittent agitation. Three controls were included in the assay: NHS serially diluted in AP buffer, a 100% hemolysis control consisting of erythrocytes mixed with water 1:1, and an erythrocyte cell blank consisting of erythrocytes mixed with AP buffer 1:1. After incubation, 150 µl ice-cold saline (0.15 M NaCl) was added to all wells except the 100% lysis wells, the plate was centrifuged, and 150 µl of the supernatant was transferred to a new plate. Hemolysis was assessed by measuring the absorbance at 405 nm in a microplate reader (Beckman Coulter), and percent hemolysis was calculated by the following equation: percent lysis = $[(OD_{405} \text{ for the sample} - OD_{405} \text{ for the blank}) / (OD_{405} \text{ for total lysis} - OD_{405} \text{ for the blank})] \times 100$, where OD_{405} is the optical density at 405 nm.

Immunostaining and high-throughput image analysis. HUVEC, MDM, ARPE-19 cells, or HREC (1×10^4) were plated in a 96-well plate (Cell Carrier Ultra; PerkinElmer) and allowed to attach for 24 h. Cells were DENV infected as described above, and at 48 hpi cells were fixed with 2% (wt/vol) paraformaldehyde (Sigma) for 10 min at room temperature. After three washes with PBS, cells were permeabilized with 0.05% (vol/vol) Igepal CA-630 (Sigma) in PBS for 20 min. Cells were washed again with PBS and blocked with 1% (wt/vol) BSA and 2% (vol/vol) normal goat serum diluted in Hanks' balanced salt solution (Gibco) for 30 min at room temperature. The cells were rinsed once with PBS and incubated overnight at 4°C with a mouse anti-DENV (1:10), D1-4G2-4-15 (ATCC HB-112); a goat anti-human FH (1:25; Calbiochem); and a rabbit anti-human FB (1:25; Santa Cruz). After three washes with PBS, the cells were incubated for 1 h at room temperature with the corresponding secondary antibodies: Alexa Fluor 488-labeled donkey anti-mouse immunoglobulin (1:75; Invitrogen), donkey anti-sheep immunoglobulin-Cy3 (1:75; Invitrogen), and Alexa Fluor 647-labeled goat anti-rabbit immunoglobulin (1:75; Invitrogen). Nuclei were stained with Hoechst 33342 (5 $\mu\text{g}/\text{ml}$). Following a final set of PBS washes, cells were imaged with an Operetta high-content imaging system with Harmony software (PerkinElmer) at a $\times 20$ magnification. Forty-nine different images, representing approximately 10,000 cells, were taken for each well. Nuclei and the cytoplasm were discriminated using the Hoechst and Cy3 channels, respectively. The mean Alexa Fluor 488, Cy3, and Alexa Fluor 647 intensity in the cell cytoplasm of each individual cell was calculated. Using visual observation and intensity histograms, an Alexa Fluor 488 intensity threshold was set to define DENV-infected cells. Imaging was performed at the Flinders University Cell Screen South Australia (CeSSA) facility.

Statistical analysis. Results were expressed as the mean \pm standard deviation (SD), and statistical analyses were performed using a two-tailed unpaired Student *t* test or one-way or two-way analysis of variance (ANOVA) in GraphPad Prism (version 7) software (GraphPad Software, La Jolla, CA, USA). Differences were considered statistically significant if *P* was <0.05 .

ACKNOWLEDGMENTS

We thank the following people: Tahlia Hayes for initial establishment of the FH and FB RT-PCR, Yuefang Ma and Andrew J. Stempel for assistance with culture of the retinal cell lines, and Julie Calvert for ongoing technical support.

This research was supported in part by grants from the Flinders Medical Centre Research Foundation and the Australian Research Council (FT130101648 to J. R. Smith). Sheila Cabezas is supported by an Australian international postgraduate research scholarship.

REFERENCES

- Guzman MG, Halstead SB, Artsob H, Buchy P, Farrar J, Gubler DJ, Hunsperger E, Kroeger A, Margolis HS, Martinez E, Nathan MB, Pelegrino JL, Simmons C, Yoksan S, Peeling RW. 2010. Dengue: a continuing global threat. *Nat Rev Microbiol* 8:57–516. <https://doi.org/10.1038/nrmicro2460>.
- Bhatt S, Gething JW, Brady OJ, Messina JP, Farlow AW, Moyes CL, Drake JM, Brownstein JS, Hoen AG, Sankoh O, Myers MF, George DB, Jaenisch T, Wint GR, Simmons CP, Scott TW, Farrar JJ, Hay SI. 2013. The global distribution and burden of dengue. *Nature* 496:504–507. <https://doi.org/10.1038/nature12060>.
- Gubler DJ. 1998. Dengue and dengue hemorrhagic fever. *Clin Microbiol Rev* 11:480–496.
- World Health Organization. 2009. Dengue: guidelines for diagnosis, treatment, prevention and control: new edition. World Health Organization, Geneva, Switzerland.
- Basu A, Chaturvedi UC. 2008. Vascular endothelium: the battlefield of dengue viruses. *FEMS Immunol Med Microbiol* 53:287–299. <https://doi.org/10.1111/j.1574-695X.2008.00420.x>.
- Trung DT, Wills B. 2010. Systemic vascular leakage associated with dengue infections—the clinical perspective. *Curr Top Microbiol Immunol* 338:57–66. https://doi.org/10.1007/978-3-642-02215-9_5.
- Hottz ED, Oliveira MF, Nunes PC, Nogueira RM, Valls-de-Souza R, Da Polan AT, Weyrich AS, Zimmerman GA, Bozza PT, Bozza FA. 2013. Dengue induces platelet activation, mitochondrial dysfunction and cell death through mechanisms that involve DC-SIGN and caspases. *J Thromb Haemost* 11:951–962. <https://doi.org/10.1111/jth.12178>.
- Nascimento EJ, Hottz ED, Garcia-Bates TM, Bozza F, Marques ET, Jr, Barratt-Boyes SM. 2014. Emerging concepts in dengue pathogenesis: interplay between plasmablasts, platelets, and complement in triggering vasculopathy. *Crit Rev Immunol* 34:227–240. <https://doi.org/10.1615/CritRevImmunol.2014010212>.
- Halstead SB. 1989. Antibody, macrophages, dengue virus infection, shock, and hemorrhage: a pathogenetic cascade. *Rev Infect Dis* 11(Suppl 4):S830–S839. https://doi.org/10.1093/clinids/11.Supplement_4.S830.
- Green S, Rothman A. 2006. Immunopathological mechanisms in dengue and dengue hemorrhagic fever. *Curr Opin Infect Dis* 19:429–436. <https://doi.org/10.1097/OI.qco.0000244047.31135.ta>.
- Carr JM, Hocking H, Bunting K, Wright PJ, Davidson A, Gamble J, Burrell CJ, Li P. 2003. Supernatants from dengue virus type-2 infected macrophages induce permeability changes in endothelial cell monolayers. *J Med Virol* 69:521–528. <https://doi.org/10.1002/jmv.10340>.
- Malavige GN, Ogg GS. 2017. Pathogenesis of vascular leak in dengue virus infection. *Immunology* 151:261–269. <https://doi.org/10.1111/imm.12748>.
- Katzelnick LC, Coloma J, Harris E. 2017. Dengue: knowledge gaps, unmet needs, and research priorities. *Lancet Infect Dis* 17:e88–e100. [https://doi.org/10.1016/S1473-3099\(16\)30473-X](https://doi.org/10.1016/S1473-3099(16)30473-X).
- Krishnamurti C, Peat RA, Cutting MA, Rothwell SW. 2002. Platelet adhesion to dengue-2 virus-infected endothelial cells. *Am J Trop Med Hyg* 66:435–441. <https://doi.org/10.4269/ajtmh.2002.66.435>.
- Azizan A, Sweat J, Espino C, Gemmer J, Stark L, Kazanis D. 2006. Differential proinflammatory and angiogenesis-specific cytokine production in human pulmonary endothelial cells, HPMEC-ST16R infected with dengue-2 and dengue-3 virus. *J Virol Methods* 138:211–217. <https://doi.org/10.1016/j.jviro.2006.08.010>.
- Dalrymple NA, Mackow ER. 2012. Endothelial cells elicit immune-enhancing responses to dengue virus infection. *J Virol* 86:6408–6415. <https://doi.org/10.1128/JVI.00213-12>.
- Dalrymple NA, Mackow ER. 2014. Virus interactions with endothelial cell receptors: implications for viral pathogenesis. *Curr Opin Virol* 7:134–140. <https://doi.org/10.1016/j.coviro.2014.06.006>.
- Calvert JK, Helbig KJ, Dimasi D, Cockshell M, Beard MR, Pitson SM, Bonder CS, Carr JM. 2015. Dengue virus infection of primary endothelial cells induces innate immune responses, changes in endothelial cells

- function and is restricted by interferon-stimulated responses. *J Interferon Cytokine Res* 35:654–665. <https://doi.org/10.1089/jir.2014.0195>.
19. Chen YC, Wang SY. 2002. Activation of terminally differentiated human monocytes/macrophages by dengue virus: productive infection, hierarchical production of innate cytokines and chemokines, and the synergistic effect of lipopolysaccharide. *J Virol* 76:9877–9887. <https://doi.org/10.1128/JVI.76.19.9877-9887.2002>.
 20. Assuncao-Miranda I, Amaral FA, Bozza FA, Fagundes CT, Sousa LP, Souza DG, Pacheco P, Barbosa-Lima G, Gomes RN, Bozza PT, Da Polan AT, Teixeira MM, Bozza MT. 2010. Contribution of macrophage migration inhibitory factor to the pathogenesis of dengue virus infection. *FASEB J* 24:218–228. <https://doi.org/10.1096/fj.09-139469>.
 21. Chuang YC, Chen HR, Yeh TM. 2015. Pathogenic roles of macrophage migration inhibitory factor during dengue virus infection. *Mediators Inflamm* 2015:547094. <https://doi.org/10.1155/2015/547094>.
 22. Beaty PR, Puerta-Guardo H, Killingbeck SS, Glasner DR, Hopkins K, Harris E. 2015. Dengue virus NS1 triggers endothelial permeability and vascular leak that is prevented by NS1 vaccination. *Sci Transl Med* 7:304ra141. <https://doi.org/10.1126/scitranslmed.aaa3787>.
 23. Modhiran N, Watterson D, Muller DA, Panetta AK, Sester DP, Liu L, Hume DA, Stacey KJ, Young PR. 2015. Dengue virus NS1 protein activates cells via Toll-like receptor 4 and disrupts endothelial cell monolayer integrity. *Sci Transl Med* 7:304ra142. <https://doi.org/10.1126/scitranslmed.aaa3863>.
 24. Malasit P. 1987. Complement and dengue haemorrhagic fever/shock syndrome. *Southeast Asian J Trop Med Public Health* 18:316–320.
 25. Bokisch VA, Top FH, Jr, Russell PK, Dixon FJ, Muller-Eberhard HJ. 1973. The potential pathogenic role of complement in dengue hemorrhagic shock syndrome. *N Engl J Med* 289:996–1000. <https://doi.org/10.1056/NEJM197311082891902>.
 26. Avirutnan P, Punyadee N, Nolsakran S, Komoltri C, Thiemmecca S, Auethavornanan K, Jaiyungsri A, Kanlaya R, Tangthawomchaikul N, Puttikhant C, Pattanakitsakul SN, Yenchitsornanus PT, Mongkolsapaya J, Kasinrerk W, Sittisombut N, Husmann M, Blettner M, Vasanawathana S, Bhakdi S, Malasit P. 2006. Vascular leakage in severe dengue virus infections: a potential role for the nonstructural viral protein NS1 and complement. *J Infect Dis* 193:1078–1088. <https://doi.org/10.1086/500949>.
 27. Avirutnan P, Malasit P, Sellger B, Bhakdi S, Husmann M. 1998. Dengue virus infection of human endothelial cells leads to chemokine production, complement activation, and apoptosis. *J Immunol* 161:6338–6346.
 28. Merle NS, Noe R, Halbwachs-Mecarelli L, Fremeaux-Bacchi V, Roumenina LT. 2015. Complement system part II: role in immunity. *Front Immunol* 6:257. <https://doi.org/10.3389/fimmu.2015.00257>.
 29. Walport MJ. 2001. Complement. First of two parts. *N Engl J Med* 344:1058–1066. <https://doi.org/10.1056/NEJM200104053441406>.
 30. Merle NS, Church SE, Fremeaux-Bacchi V, Roumenina LT. 2015. Complement system part I—molecular mechanisms of activation and regulation. *Front Immunol* 6:262. <https://doi.org/10.3389/fimmu.2015.00262>.
 31. Meri S. 2016. Self-nonsel discrimination by the complement system. *FEBS Lett* 590:2418–2434. <https://doi.org/10.1002/1873-3468.12284>.
 32. Meri S, Pangburn MK. 1990. Discrimination between activators and nonactivators of the alternative pathway of complement: regulation via a sialic acid/polyanion binding site on factor H. *Proc Natl Acad Sci U S A* 87:3982–3986.
 33. Pangburn MK. 2000. Host recognition and target differentiation by factor H, a regulator of the alternative pathway of complement. *Immunopharmacology* 49:149–157. [https://doi.org/10.1016/S0162-3109\(00\)80300-8](https://doi.org/10.1016/S0162-3109(00)80300-8).
 34. Conrad DH, Carlo JR, Ruddy S. 1978. Interaction of beta1H globulin with cell-bound C3b: quantitative analysis of binding and influence of alternative pathway components on binding. *J Exp Med* 147:1792–1805. <https://doi.org/10.1084/jem.147.6.1792>.
 35. Pangburn MK, Pangburn KL, Kolstinen V, Meri S, Sharma AK. 2000. Molecular mechanisms of target recognition in an innate immune system: Interactions among factor H, C3b, and target in the alternative pathway of human complement. *J Immunol* 164:4742–4751. <https://doi.org/10.4049/jimmunol.164.9.4742>.
 36. Weiler JM, Daha MR, Austen KF, Fearon DT. 1976. Control of the amplification convertase of complement by the plasma protein beta1H. *Proc Natl Acad Sci U S A* 73:3268–3272.
 37. Pangburn MK, Muller-Eberhard HJ. 1984. The alternative pathway of complement. *Springer Semin Immunopathol* 7:163–192. <https://doi.org/10.1007/BF01893019>.
 38. Lambris JD, Lao Z, Oglesby TJ, Atkinson JP, Hack CE, Becherer JD. 1996. Dissection of CR1, factor H, membrane cofactor protein, and factor B binding and functional sites in the third complement component. *J Immunol* 156:4821–4832.
 39. Hellwage J, Jokiranta TS, Friese MA, Woik TU, Kampen E, Zipfel PF, Meri S. 2002. Complement C3b/C3d and cell surface polyanions are recognized by overlapping binding sites on the most carboxyl-terminal domain of complement factor H. *J Immunol* 169:6935–6944. <https://doi.org/10.4049/jimmunol.169.12.6935>.
 40. Clark SJ, Ridge LA, Herbert AP, Hakobyan S, Mulloy B, Lennon R, Wurznner R, Morgan BP, Uhrin D, Bishop PN, Day AJ. 2013. Tissue-specific host recognition by complement factor H is mediated by differential activities of its glycosaminoglycan-binding regions. *J Immunol* 190:2049–2057. <https://doi.org/10.4049/jimmunol.1201751>.
 41. Jokiranta TS, Cheng ZZ, Seeberger H, Jozsi M, Helnen S, Norris M, Remuzzi G, Ormsby R, Gordon DL, Meri S, Hellwage J, Zipfel PF. 2005. Binding of complement factor H to endothelial cells is mediated by the carboxy-terminal glycosaminoglycan binding site. *Am J Pathol* 167:1173–1181. [https://doi.org/10.1016/S0002-9440\(10\)61205-9](https://doi.org/10.1016/S0002-9440(10)61205-9).
 42. Harrison RA. 2018. The properdin pathway: an “alternative activation pathway” or a “critical amplification loop” for C3 and C5 activation? *Semin Immunopathol* 40:15–35. <https://doi.org/10.1007/s00281-017-0661-x>.
 43. Zhang K, Lu Y, Harley KT, Tran MH. 2017. Atypical hemolytic uremic syndrome: a brief review. *Hematol Rep* 9:7053. <https://doi.org/10.4081/hr.2017.7053>.
 44. Jokiranta TS. 2017. HUS and atypical HUS. *Blood* 129:2847–2856. <https://doi.org/10.1182/blood-2016-11-709865>.
 45. Nascimento EJ, Silva AM, Cordeiro MT, Brito CA, Gil LH, Braga-Neto U, Marques ET. 2009. Alternative complement pathway deregulation is correlated with dengue severity. *PLoS One* 4:e6782. <https://doi.org/10.1371/journal.pone.0006782>.
 46. Shrestha S. 2012. Role of complement in dengue virus infection: protection or pathogenesis? *mBio* 3:e00003-12. <https://doi.org/10.1128/mBio.00003-12>.
 47. Wati S, Soo ML, Zilm P, Li P, Paton AW, Burrell CJ, Beard M, Carr JM. 2009. Dengue virus infection induces upregulation of GRP78, which acts to chaperone viral antigen production. *J Virol* 83:12871–12880. <https://doi.org/10.1128/JVI.01419-09>.
 48. Wati S, Li P, Burrell CJ, Carr JM. 2007. Dengue virus (DV) replication in monocyte-derived macrophages is not affected by tumor necrosis factor alpha (TNF-alpha), and DV infection induces altered responsiveness to TNF-alpha stimulation. *J Virol* 81:10161–10171. <https://doi.org/10.1128/JVI.00313-07>.
 49. Carr JM, Ashander LM, Calvert JK, Ma Y, Aiola A, Bracho GG, Chee SP, Appukuttan B, Smith JR. 2017. Molecular responses of human retinal cells to infection with dengue virus. *Mediators Inflamm* 2017:3164375. <https://doi.org/10.1155/2017/3164375>.
 50. Zipfel PF, Skerka C. 2009. Complement regulators and inhibitory proteins. *Nat Rev Immunol* 9:729–740. <https://doi.org/10.1038/nri2620>.
 51. Avirutnan P, Hauhart RE, Marovich MA, Garred P, Atkinson JP, Diamond MS. 2011. Complement-mediated neutralization of dengue virus requires mannose-binding lectin. *mBio* 2:e00276-11. <https://doi.org/10.1128/mBio.00276-11>.
 52. Mehilop E, Ansaiah-Sobrinho C, Johnson S, Engle M, Fremont DH, Pierson TC, Diamond MS. 2007. Complement protein C1q inhibits antibody-dependent enhancement of flavivirus infection in an IgG subclass-specific manner. *Cell Host Microbe* 2:417–426. <https://doi.org/10.1016/j.chom.2007.09.015>.
 53. Yamanaka A, Kosugi S, Konishi E. 2008. Infection-enhancing and -neutralizing activities of mouse monoclonal antibodies against dengue type 2 and 4 viruses are controlled by complement levels. *J Virol* 82:927–937. <https://doi.org/10.1128/JVI.00992-07>.
 54. Ripoché J, Mitchell JA, Erdel A, Madlin C, Moffatt B, Mokoena T, Gordon S, Sim RB. 1988. Interferon gamma induces synthesis of complement alternative pathway proteins by human endothelial cells in culture. *J Exp Med* 168:1917–1922. <https://doi.org/10.1084/jem.168.5.1917>.
 55. Zou L, Feng Y, Li Y, Zhang M, Chen C, Cai J, Gong Y, Wang L, Thurman JM, Wu X, Atkinson JP, Chao W. 2013. Complement factor B is the downstream effector of TLRs and plays an important role in a mouse model of severe sepsis. *J Immunol* 191:5625–5635. <https://doi.org/10.4049/jimmunol.1301903>.
 56. Kaczorowski DJ, Afrizi A, Scott MJ, Kwak JH, Gill R, Edmonds RD, Liu Y, Fan J, Billiar TR. 2010. Pivotal advance: the pattern recognition receptor ligands lipopolysaccharide and polyinosine-polycytidylic acid stimulate factor B synthesis by the macrophage through distinct but overlap-

- ping mechanisms. *J Leukoc Biol* 88:609–618. <https://doi.org/10.1189/jlb.0809588>.
57. Minta JO. 1988. Regulation of complement factor H synthesis in U-937 cells by phorbol myristate acetate, lipopolysaccharide, and IL-1. *J Immunol* 141:1630–1635.
 58. Hajshengallis G, Lambris JD. 2010. Crosstalk pathways between Toll-like receptors and the complement system. *Trends Immunol* 31:154–163. <https://doi.org/10.1016/j.it.2010.01.002>.
 59. Liang Z, Wu S, Li Y, He L, Wu M, Jlang L, Feng L, Zhang P, Huang X. 2011. Activation of Toll-like receptor 3 impairs the dengue virus serotype 2 replication through induction of IFN-beta in cultured hepatoma cells. *PLoS One* 6:e23346. <https://doi.org/10.1371/journal.pone.0023346>.
 60. Avirutnan P, Fuchs A, Hauhart RE, Somnuk P, Youn S, Diamond MS, Atkinson JP. 2010. Antagonism of the complement component C4 by flavivirus nonstructural protein NS1. *J Exp Med* 207:793–806. <https://doi.org/10.1084/jem.20092545>.
 61. Blom AM, Volokhina EB, Fransson V, Stromberg P, Berghard L, Viktorellus M, Molines TE, Lopez-Trascasa M, van den Heuvel LP, Goodship TH, Marchbank KJ, Okroj M. 2014. A novel method for direct measurement of complement convertase activity in human serum. *Clin Exp Immunol* 178:142–153. <https://doi.org/10.1111/cei.12388>.
 62. Parente R, Clark SJ, Inforzato A, Day AJ. 2017. Complement factor H in host defense and immune evasion. *Cell Mol Life Sci* 74:1605–1624. <https://doi.org/10.1007/s00018-016-2418-4>.
 63. Glennie S, Gritzfeld JF, Pennington SH, Garner-Jones M, Coombes N, Hopkins MJ, Vadeslho CF, Miyaji EN, Wang D, Wright AD, Collins AM, Gordon SB, Ferreira DM. 2016. Modulation of nasopharyngeal innate defenses by viral coinfection predisposes individuals to experimental pneumococcal carriage. *Mucosal Immunol* 9:56–67. <https://doi.org/10.1038/mi.2015.35>.
 64. Chung KM, Nybakken GE, Thompson BS, Engle MJ, Marri A, Fremont DH, Diamond MS. 2006. Antibodies against West Nile virus nonstructural protein NS1 prevent lethal infection through Fc gamma receptor-dependent and -independent mechanisms. *J Virol* 80:1340–1351. <https://doi.org/10.1128/JVI.80.3.1340-1351.2006>.
 65. Lee MS, Jones T, Song DY, Jang JH, Jung JU, Gao SJ. 2014. Exploitation of the complement system by oncogenic Kaposi's sarcoma-associated herpesvirus for cell survival and persistent infection. *PLoS Pathog* 10:e1004412. <https://doi.org/10.1371/journal.ppat.1004412>.
 66. Conde JN, da Silva EM, Ailonso D, Coelho DR, Andrade ID, de Medeiros LN, Menezes JL, Barbosa AS, Mohana-Borges R. 2016. Inhibition of the membrane attack complex by dengue virus NS1 through interaction with vitronectin and terminal complement proteins. *J Virol* 90:9570–9581. <https://doi.org/10.1128/JVI.00912-16>.
 67. Spiropoulou CF, Srikiatkachom A. 2013. The role of endothelial activation in dengue hemorrhagic fever and hantavirus pulmonary syndrome. *Virulence* 4:525–536. <https://doi.org/10.4161/viru.25569>.
 68. Bharadwaj AS, Appukuttan B, Wilmarth PA, Pan Y, Stempel AJ, Chipps TJ, Benedetti EE, Zamora DO, Choi D, David LL, Smith JR. 2013. Role of the retinal vascular endothelial cell in ocular disease. *Prog Retin Eye Res* 32:102–180. <https://doi.org/10.1016/j.preteyeres.2012.08.004>.
 69. Gualano RC, Pryor MJ, Cauchi MR, Wright PJ, Davidson AD. 1998. Identification of a major determinant of mouse neurovirulence of dengue virus type 2 using stably cloned genomic-length cDNA. *J Gen Virol* 79(Pt 3):437–446. <https://doi.org/10.1099/0022-1317-79-3-437>.
 70. Timmerman JJ, van der Woude FJ, van Gijlswijk-Janssen DJ, Verweij CL, van Es LA, Daha MR. 1996. Differential expression of complement components in human fetal and adult kidneys. *Kidney Int* 49:730–740. <https://doi.org/10.1038/ki.1996.102>.
 71. Schmittgen TD, Livak KJ. 2008. Analyzing real-time PCR data by the comparative C(T) method. *Nat Protoc* 3:1101–1108. <https://doi.org/10.1038/nprot.2008.73>.
 72. Ormsby RJ, Jokiranta TS, Duthy TG, Griggs KM, Sadlon TA, Glanakis E, Gordon DL. 2006. Localization of the third heparin-binding site in the human complement regulator factor H1. *Mol Immunol* 43:1624–1632. <https://doi.org/10.1016/j.molimm.2005.09.012>.

IV.2 Discussion

A key finding and published above is that DENV induces high levels of FH mRNA but not protein. Furthermore, the results show that some FH protein is still produced by DENV-infected cells but this preferentially re-binds back to the cell surface of DENV-positive EC. This enhanced extracellular binding of FH could explain the lack of induction of secreted cell-free FH upon DENV-stimulation but additionally, DENV could actively block FH translation, inhibiting FH protein secretion or promote FH degradation, or even a combination of these events. This is an area of potential further investigation, for instance through experiments involving quantitation of FH production from DENV-infected cells treated with agents to block proteasomal degradation, such as MG132. Additionally, to investigate this, potential future experiments could study the interaction between viral proteins and FH mRNA using live cell imaging techniques combined with RNA-binding mediated fluorescence resonance energy transfer or trimolecular fluorescent complementation (Shyu and Hu, 2008, Lorenz, 2009), approaches that have been used for the study of interactions between RNA and viral proteins from HIV and influenza virus (Vercruysse et al., 2011, Yin et al., 2013). Interestingly, during these PhD studies other cell lines, such as MEF and Huh7 liver cells, were observed to also have a discord between the expression of FH mRNA without corresponding protein production. Thus, there may be specific cellular control points that determine if FH mRNA is translated into protein, and it may be that DENV infection acts via these existing regulatory mechanisms resulting in mRNA induction without FH protein expression. Future studies are still needed to determine the mechanisms by which FH protein production is apparently prevented in DENV-infected cells.

The experiments published here have also begun to investigate different components of the AP in MDM and EC and links have been made to potential pathogenic effects on the endothelium. Future experiments involving measurement of C3b deposition, actions of anaphylotoxins C3a and C5a and AP activity levels could be performed on DENV-infected EC cultured with supernatants from DENV-infected macrophages, to assess the direct influence of complement factors coming from infected macrophages on the endothelium. Such studies could be performed using *in vitro* EC permeability models, as used previously in our laboratory (Carr et al., 2003, Calvert et al., 2015).

Overall this study has provided new evidence of the interplay between complement AP regulatory components (FH and FB) and DENV infection in *in vitro* scenarios; however, the

factors that regulate the expression and induction of FB and FH in the context of DENV infection remain to be investigated. Thus, the next chapter aims to decipher putative transcription factors responsible for mediating FB and FH transcriptional regulation and to investigate the role of IFN- β , a cytokine with a central anti-viral role against DENV infection (Dalrymple and Mackow, 2012b, Dalrymple and Mackow, 2012a, Calvert et al., 2015), in the induction of both FB and FH mRNA and proteins in DENV infection models.

CHAPTER V THE ROLE OF INTERFERON IN DRIVING CHANGES IN FH AND FB EXPRESSION DURING DENV INFECTION

V.1 Introduction

While the studies described in chapter IV have demonstrated the potential for interesting changes in FH at the protein level, results also demonstrate induction and changes in mRNA levels for FB and FH during DENV infection. It was hypothesised that these changes are induced at the transcriptional level by biological stimuli and transcription factors (TF) such as IFN, TNF- α and their respective STAT and NF κ B TF may control this induction. While the biological functions of FB and FH are well characterised, less is known about the expression and regulation of these factors and there is no data on regulation during DENV infection. There are only a few studies that have sought to identify the transcriptional regulatory regions of either FB or FH in order to predict the basal and expected gene expression characteristics in hepatic and non-hepatic cell lines (Wu et al., 1987, Munoz-Canoves et al., 1990, Ward et al., 1997, Kain et al., 1998, Kindermann et al., 2005). There are precedents in the literature demonstrating that FB and FH, along with other complement proteins, are 'acute phase reactants' (Markiewski and Lambris, 2007, Pionnier et al., 2014), that can be induced by common innate stimuli such as stimulation of PRR (Sahly et al., 2009, Kaczorowski et al., 2010) and production of IFN (Friese et al., 2000, Thomas et al., 2000, Schlaf et al., 2001). Additionally, prior work from our laboratory has shown that IFN- β has a central role in limiting DENV infection in EC by inducing antiviral ISGs (Dalrymple and Mackow, 2012b, Dalrymple and Mackow, 2012a, Calvert et al., 2015), and thus, type I IFN regulation of FB and FH in EC during DENV infection, may be of particular interest.

Promoter analysis and the identification of TF are essential to identify what may control the transcription initiation of a particular gene. Thus, TF are important to determine whether or not a gene is likely to be expressed and how much mRNA and consequently protein is likely to be produced following a particular biological stimulus. The Genomatix MatInspector software is a powerful tool for *in silico* prediction of potential TF binding sites (Quandt et al., 1995, Cartharius et al., 2005). The benefit of the MatInspector program to identify putative TFs, is the in-built library that comprises 634 matrices of TF binding sites representing the largest library available for public searches (Cartharius et al., 2005). The

vertebrate matrices contain around 366 000 human, mouse and rat promoter sequences with an average length of 1184 bp (Quandt et al., 1995, Cartharius et al., 2005).

The current study has utilised the Genomatix MatInspector software for the *in silico* prediction of potential TF in the human FB and FH promoters that may be of relevance to induction of transcription of these mRNA's during a DENV infection. Additionally, to complement the *in silico* predictions by MatInspector, the role of IFN- β released from DENV-infected cells in driving the induction of FB and FH mRNA during DENV infection was experimentally assessed.

V.2 Results

V.2.1 MatInspector computational prediction of transcription factor binding sites in the human FB and FH promoters

Using the MatInspector software program an analysis of FH and FB promoters was performed with a number of stringent criteria. Firstly, the analysis used only sequence data for the human FB and FH promoter associated with at least one verified coding transcript. The core sequence of a matrix (or binding site) is defined as the four usually highest conserved position of the matrix. The maximum core similarity of 1.0 reflects when the highest conserved bases of a matrix match exactly in the sequence, while a matrix similarity score reaches 1.0 when the test sequence corresponds to the most conserved nucleotide at each position of the matrix (Quandt et al., 1995, Cartharius et al., 2005). Secondly, here a core similarity value was fixed to 0.75 and an optimised matrix similarity threshold was set at 0.8, to minimise the number of false-positive matches for each individual matrix. These are relatively stringent selection criterion aimed at identifying TF families with highly conserved core sequence TF binding determinants.

The analysis of the human FB and FH promoters by MatInspector revealed a total of 389 and 457 potential TF binding sites, respectively. To filter and refine these matches down to the most probable TF binding sites, different output parameters were considered. Those TFs with a matrix similarity higher than 0.85, with at least one line of supporting evidence (i.e. experimental and/or literature citation) were considered as promising functional TF. This narrowed the predicted TF to only seven for both human FB and FH promoters (Table V-1, Table V-2, Figure V-1 A and Figure V-2 A).

Table V-1. Putative transcription binding sites in the human FB promoter region

Matrix Family ^a	Detailed Family Information	Number of Elements	Line of Evidence
V\$CREB	cAMP-responsive element binding proteins	7	Overlaps with constrained elements
V\$EGRF	EGR/nerve growth factor induced protein C & related factors	8	Correlates with ChIPSeq peak of V\$EGRF (TF: EGR1)
V\$SRFF	Serum response element binding factor	2	Correlates with ChIPSeq peak of V\$SRFF (TF: SRF)
V\$MTF1	Metal induced transcription factor	2	FB is regulated by V\$MTF1 (TF: MTF1) FB is co-cited with V\$MTF1 (TF: MTF1)
V\$NFKB	Nuclear factor kappa beta	2	FB is co-cited with V\$NF κ B (TF: NFKB1)
V\$IRFF	Interferon regulatory factors	3	FB co-cited with V\$IRFF (TF: STAT1)
V\$STAT	Signal transducer and activator of transcription	3	FB is co-cited with V\$STAT (TF: STAT1, STAT3) Correlates with ChIPSeq peak of V\$STAT (TF: STAT1, STAT2)

^a Matrix Family: as defined by MatInspector a matrix family group individual matrices that have similar binding properties.

Table V-2. Putative transcription binding sites in the human FH promoter region

Matrix Family ^a	Detailed Family Information	Number of Elements	Line of Evidence
V\$CAAT	CCAAT binding factors	4	Correlates with ChIPSeq peak of V\$CAAT (TF: Nuclear factor YA and YB)
V\$CREB	cAMP-responsive element binding proteins	5	FH is co-cited with V\$CREB (TF: CREB1, JUN)
V\$ETSF	Human and murine ETS1 factors	5	Correlates with ChIPSeq peak of V\$ETSF (TF: ETV1)
V\$FKHD	Fork head domain factors	17	FH is co-cited with V\$FKHD (TF: FOXO3)
V\$NFKB	Nuclear factor kappa beta	1	FH is co-cited with V\$NF κ B (TF: NFKB1)
V\$IRFF	Interferon regulatory factors	5	Correlates with ChIPSeq peak of V\$IRFF (TF: IRF1, STAT1). FH is co-cited with V\$IRFF (TF: IRF1, IRF8, STAT1)
V\$STAT	Signal transducer and activator of transcription	9	Overlaps with constrained element. Correlates with ChIPSeq peak of V\$STAT (TF: STAT1, STAT3) CFH is co-cited with V\$STAT (TF: STAT1)

^a Matrix Family: as defined by MatInspector a matrix family group individual matrices that have similar binding properties.

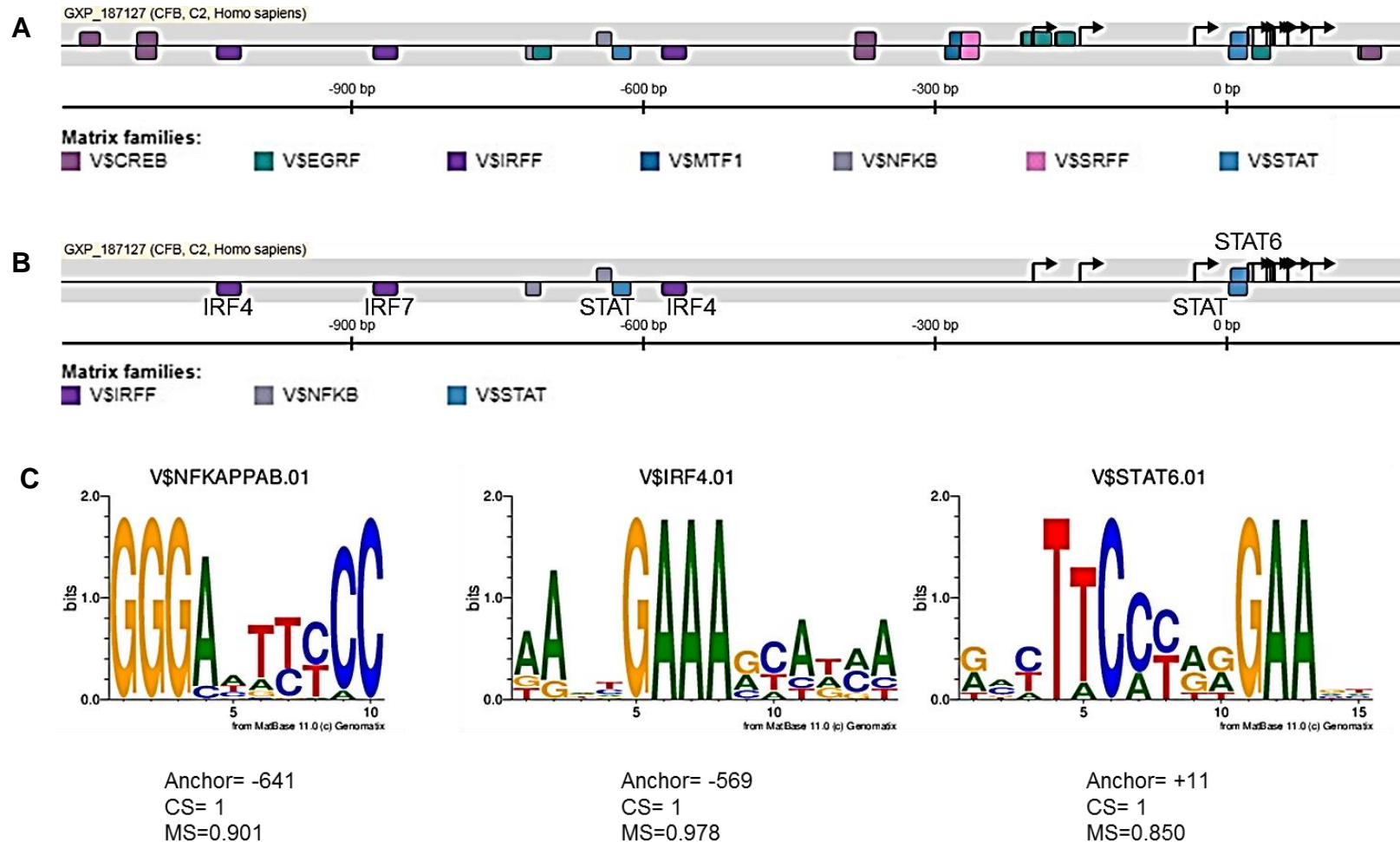


Figure V-1. Identification of putative transcription factor binding sites in the human FB promoter region using MatInspector software

(A) Schematic localisation of TF in the promoter sequence (1200 bp upstream from the transcription start site). (B) Identification of specific members of NF κ B, IRFF and STAT families. (C) A graphical representation of the sequence logo of the NF κ B, IRF4 and STAT6 matrices consensus generated by MatInspector. Each logo consists of stacks of symbols, one stack for each position in the sequence. The overall height of the stack indicates the sequence conservation at that position; while the height of symbols within the stack indicates the relative frequency of each amino or nucleic acid at that position. Nucleotides in big capital letters denote the core sequence defined by MatInspector. CS: core similarity, MS: matrix similarity.

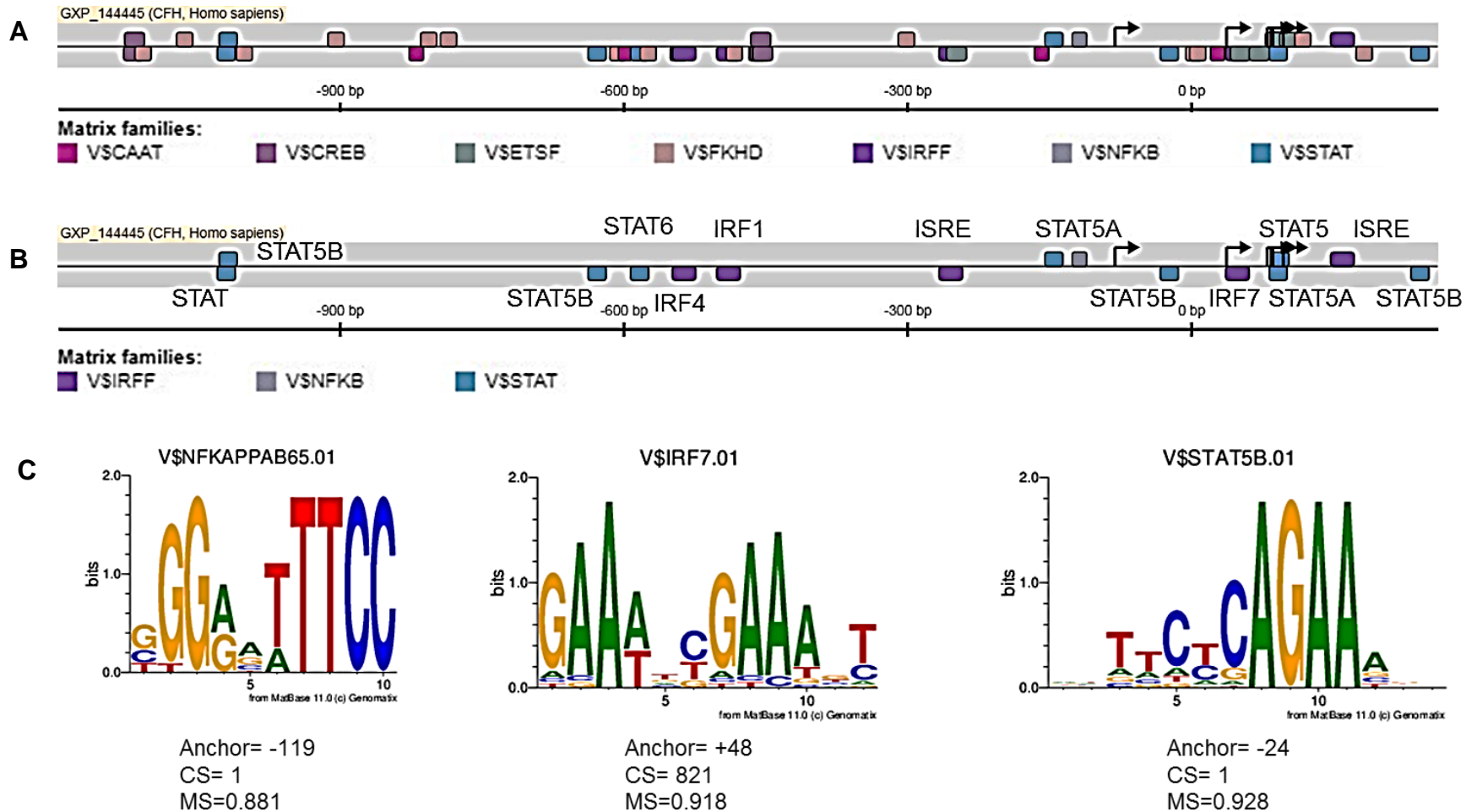


Figure V-2. Identification of putative transcription factor binding sites in the human FH promoter region using MatInspector software

(A) Schematic localisation of TF in the promoter sequence (1200 bp upstream of the transcription start site). (B) Identification of specific members of NFκβ, IRFF and STAT families. (C) A graphical representation of a sequence logo of the NFκβ, IRF7 and STAT5B matrices consensus generated by MatInspector. Each logo consists of stacks of symbols, one stack for each position in the sequence. The overall height of the stack indicates the sequence conservation at that position; while the height of symbols within the stack indicates the relative frequency of each amino or nucleic acid at that position. Nucleotides in big capital letters denote the core sequence defined by MatInspector. CS: core similarity, MS: matrix similarity.

The FB promoter (GXP_187127) associated with 13 identified coding transcripts, revealed the presence of seven cAMP responsive elements (CREB) distributed across the promoter region. Also, eight EGR/nerve growth factor induced protein C & related factors (EGRF), two serum response element binding factors (SRFF) and two metal induced transcription factors (MTF1) were identified and all located mainly close to the transcription start site (Table V-1, Figure V-1 A). CREB binding sites overlapped with constrained elements (Table V-1), which means that this TF overlaps with a region of the human genome that is annotated as evolutionary highly conserved. EGRF and SRFF were found to overlap with ChIP-Seq peaks suggesting a region of the promoter likely to be protein bound (Table V-1), and a real interaction between these TF and the human FB promoter sequence. Both these forms of evidence (overlapping with constrained elements and ChIP-Seq regions) constitute strong experimental data to support a legitimate TF binding site (Cartharius et al., 2005). MTF1, on the other hand, has been identified experimentally to induce FB gene expression in doxycycline-inducible human adenocarcinoma HT-29 cell line overexpressing MTF-1 (Kindermann et al., 2005), consistent with the promoter containing a MTF1 binding site. Additionally, the FB promoter contains two $\text{NF}\kappa\beta$, three STAT and three interferon regulatory factors (IRFF) predicted TF binding elements (Table V-1, Figure V-1 A). All these families of TFs: $\text{NF}\kappa\beta$, STAT and IRFF, have been co-cited with FB in the literature, representing circumstantial evidence supporting an association. Since $\text{NF}\kappa\beta$, STAT and IRFF matrix families, are possible factors implicated during DENV infection, the analysis was extended to specifically identify which members of the family were present (Figure V-1 B and Table V-3). STAT6 and another STAT binding site (not specified by MatInspector) are found very close to the transcription start site while the third STAT binding site is located in the middle of the promoter region (at -623) (Figure V-1 B). One IRF4 binding site is next to the STAT located at -623. The other IRF4 and one IRF7 TFs are positioned distally in the FB promoter sequence, between -800 and -1000 bp (Figure V-1 B). The two $\text{NF}\kappa\beta$ binding sites are also located around the middle of the promoter region, specifically between STAT and IRF7 binding sites (Figure V-1 B). All the seven TFs identified for FB promoter showed a matrix similarity higher than 0.85. As an example of this, a graphical representation of the $\text{NF}\kappa\beta$, IRF4 and STAT6 matrices consensus generated by MatInspector is shown in Figure V-1 C.

A number of different TFs were identified in the FH promoter. The FH promoter (GXP_144445) associated with six coding transcripts, revealed the presence of common

and highly conserved promoter elements such as the CAAT box (which bound to consensus sequence CCAAT) and ETSF (human E26 transformation-specific family factors) elements (Table V-2, Figure V-2 A). In addition, five CREB and 17 fork head domain factors (FKHD) were found. While CAAT, CREB and FKHD are dispersed across the FH promoter, the five ETSF are concentrated at the transcription start site (Figure V-2 A). Several lines of evidence, experimental and theoretical, were found that support an association of these TFs with the FH promoter (Table V-2). CAAT and ETSF were found to be overlapping with ChIP-Seq regions of a member of the CAAT and ETSF families, respectively, whereas CREB and FKHD TFs have been co-cited in the literature with FH (Table V-2). MatInspector analysis also revealed the presence of one NF κ B (located close to the transcription start site), five IRFF and nine STAT binding sites (Table V-2, Figure V-2 A). These three matches appeared to have both theoretical and experimental evidence suggesting a legitimate association of the corresponding TF binding site (Table V-2). Several members of the IRFF and STAT families were identified to be probably associated with FH promoter (Figure V-2 B, Table V-3). In the case of the IRFF family, IRF1, IRF4, IRF7 and two ISRE were found. Interestingly, IRF7 and one ISRE are located close to the transcription start site while the other ISRE, IRF1 and IRF4 are situated close to the middle of the FH promoter (Figure V-2 B). Of note, five members of the STAT family, including STAT5 and the two related proteins STAT5A and 5B are positioned very close to the transcription start site, whereas STAT6 and three other STAT binding sites (two STAT5B) are found in the middle (~ 600bp) and distal (~ 1100bp) to the transcription start site, respectively (Figure V-2 B). Similarly, as described for FB promoter, the seven TFs identified for FH promoter showed a matrix similarity higher than 0.85. A graphical representation of this evidence is shown in Figure V-2 C for NF κ B, STAT5b and IRF7.

Table V-3. Summary of key predicted TF elements in the human FB and FH promoter regions

	V\NF\kappa$B	V\$IRFF				V\$STAT		
	NFκB	IRF1	IRF4	IFR7	ISRE	STAT	STAT5	STAT6
FB	2	-	2	1	-	2	-	1
FH	1	1	1	1	2	1	7	1

V.2.2 IFN- β regulates FB and FH expression in HUVEC but not in MDM

The computational analysis above, suggests that members of the IRFF and STAT matrix family could be involved in regulation of the FB and FH promoters. IRF and STAT TF's are well recognised for their roles in innate and adaptive immunity (Borden et al., 2007) and in particular the role in induction of IFN and ISGs. Prior work in our laboratory has demonstrated a role for IFN- β in inducing ISG expression in DENV-infected EC and thus, the role of endogenously produced IFN- β from DENV-infected cells in the induction of FB and FH mRNA and protein production was investigated.

HUVEC and MDM were infected and incubated with a neutralising antibody against IFN- β , at a concentration previously shown to block the induction of ISGs (Calvert et al., 2015). In agreement with previous results (Calvert et al., 2015), infectious virus release was only modestly affected (Figure V-3 A); however, a significant increase in DENV RNA level was observed at 48h pi in HUVEC incubated with the IFN- β blocking antibody (Figure V-3 B). As expected, treatment of cells with the IFN- β blocking antibody reduced the levels of mRNA for ISGs, viperin, IFIT-1, and OAS-1 but not IFN- β itself (Figure V-4) (Calvert et al., 2015). Similar to these ISG responses, treatment of HUVEC with the IFN- β blocking antibody inhibited DENV induction of FB and FH mRNA at 48h pi (Figure V-5 A). Accordingly, FB protein levels were also reduced in the supernatant of DENV-infected cells (Figure V-5 B) but, consistent with results in chapter IV, there was no DENV induction of FH protein and subsequently no effect of IFN- β antibody treatment (Figure V-5 B).

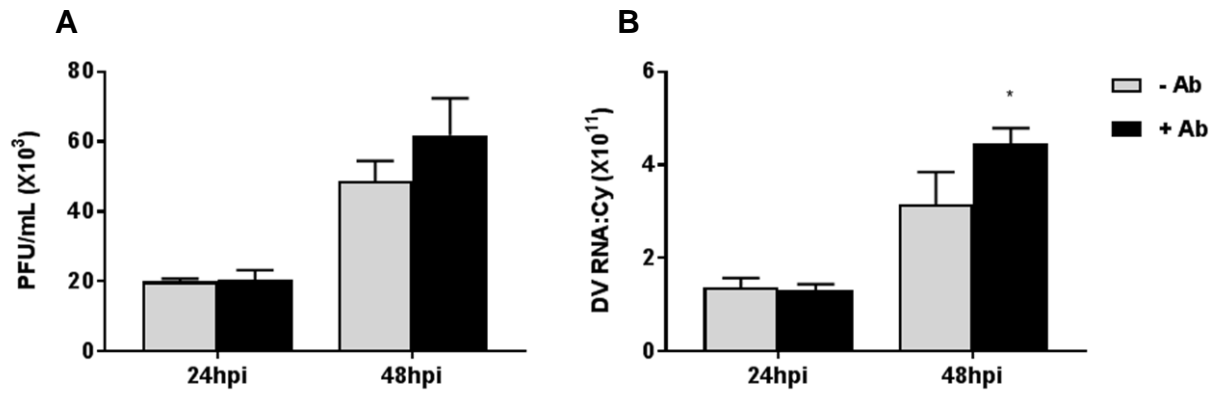


Figure V-3. Blocking of IFN- β actions increases DENV mRNA in HUVEC

HUVEC were left uninfected or DENV infected and incubated with control antibody (-Ab) or 1000 U/ml of a neutralizing antibody against IFN- β (+Ab). At 24 and 48hpi supernatants were collected, cells were lysed and total RNA extracted and analysed for infectious virus release by plaque assay (**A**) and DENV RNA by RT-PCR (**B**). PCR results for DENV RNA were normalized against cyclophilin. Results represent mean \pm standard deviation from duplicate samples and are representative of at least three experiments. * $p < 0.05$ relative to uninfected, comparison +/- Ab treatment, Student's unpaired t -test.

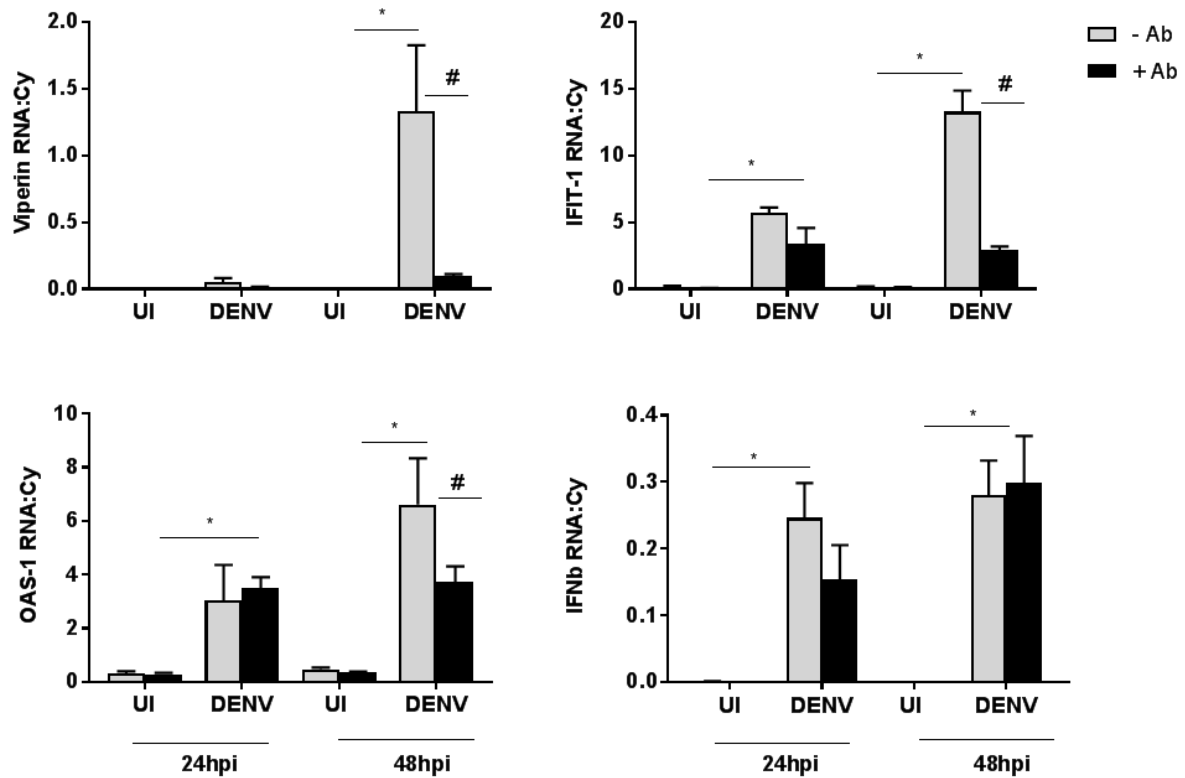


Figure V-4. Blocking of IFN- β actions reduces mRNA for DENV-induced ISGs in HUVEC

HUVEC were left uninfected or DENV infected and incubated with control antibody (-Ab) or 1000 U/ml of a neutralizing antibody against IFN- β (+Ab). At 24 and 48hpi supernatants were collected, cells were lysed and total RNA extracted and analysed for: Viperin, IFIT-1, OAS-1 and IFN- β mRNA by RT-PCR. PCR results were normalized against cyclophilin. Results represent mean \pm standard deviation from duplicate samples and are representative of at least three experiments. * $p < 0.05$ relative to uninfected, # $p < 0.05$ comparison +/- Ab treatment, two-way ANOVA/ Dunnett's test.

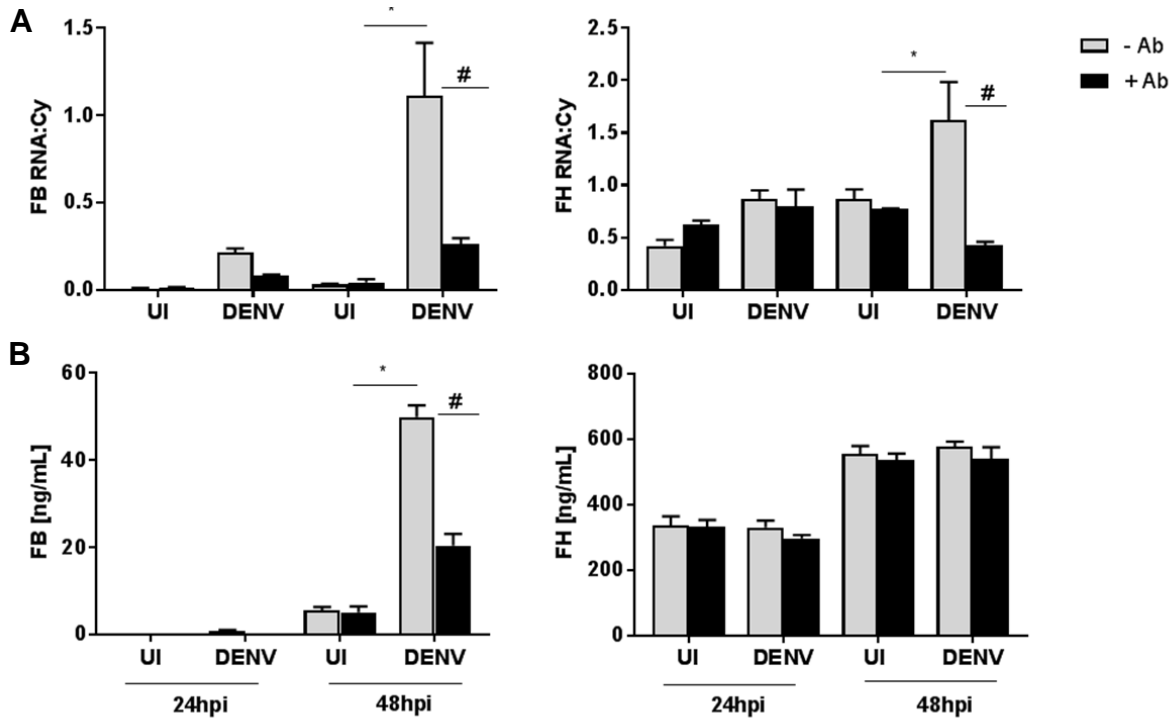


Figure V-5. Blocking of IFN- β actions reduces mRNA for DENV-induced FH and FB mRNA and protein in HUVEC

HUVEC were left uninfected or DENV infected and incubated with control antibody (-Ab) or 1000 U/ml of a neutralizing antibody against IFN- β (+Ab). At 24 and 48hpi supernatants were collected, cells were lysed and total RNA extracted and analysed for (A) FB and FH mRNA by RT-PCR. PCR results were normalized against cyclophilin. (B) FB and FH proteins analysed by ELISA. Results represent mean \pm standard deviation from duplicate samples and are representative of at least three experiments. * $p < 0.05$ relative to uninfected, # $p < 0.05$ comparison +/- Ab treatment, two-way ANOVA/ Dunnett's test.

The same experimental approach was applied to DENV-infected MDM. As with HUVEC, DENV-infected MDM incubated with IFN- β blocking antibody showed no effect on the production of infectious virus (Figure V-6 A), although a significant increase in DENV replication, as measured by production of DENV RNA, was detected at 48h pi (Figure V-6 B). Even though ISG mRNA levels were induced in DENV-infected MDM, in contrast to the IFN- β dependency of ISG induction in HUVEC, the levels of viperin, IFIT-1, OAS-1 and IFN- β mRNAs were not affected when IFN- β activity was blocked in MDM (Figure V-7). Similarly, FB and FH mRNA were induced in DENV-infected MDM but there was no significant change in FB and FH mRNA or FB protein levels following IFN- β antibody treatment of MDM (Figure V-8 A and B). Again, consistent with previous findings, FH protein was not induced by DENV and not affected by IFN- β antibody blockade (Figure V-8 B). These results indicate that DENV-induction of FB and FH is regulated in a manner that parallels ISGs such as viperin, IFIT-1 and OAS-1 and that this is driven by IFN- β in HUVEC, but not in macrophages.

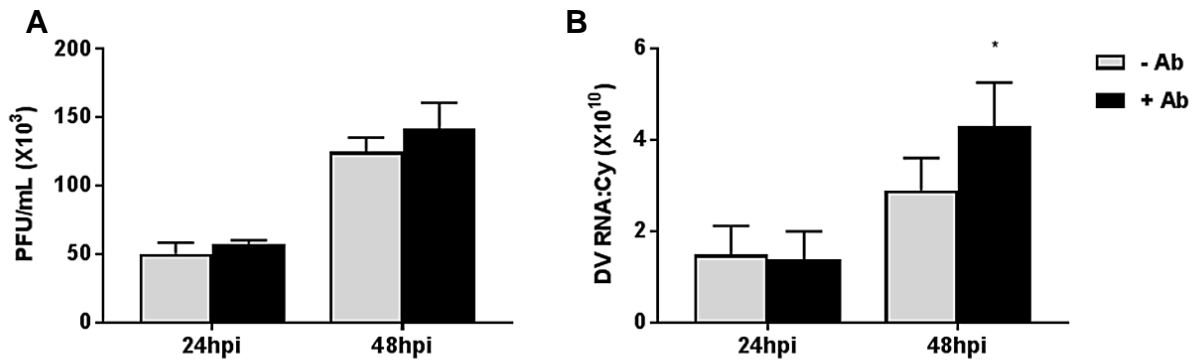


Figure V-6. Blocking of IFN- β actions induces DENV mRNA in MDM

MDM were left uninfected or DENV infected and incubated with control antibody (-Ab) or 1000 U/ml of a neutralizing antibody against IFN- β (+Ab). At 24 and 48hpi supernatants were collected, cells were lysed and total RNA extracted and analysed for infectious virus release by plaque assay (**A**) and DENV RNA by RT-PCR (**B**). PCR results for DENV RNA were normalized against cyclophilin. Results represent mean \pm standard deviation from duplicate samples and are representative of at least three experiments. * $p < 0.05$ relative to uninfected, comparison +/- Ab treatment, Student's unpaired *t*-test.

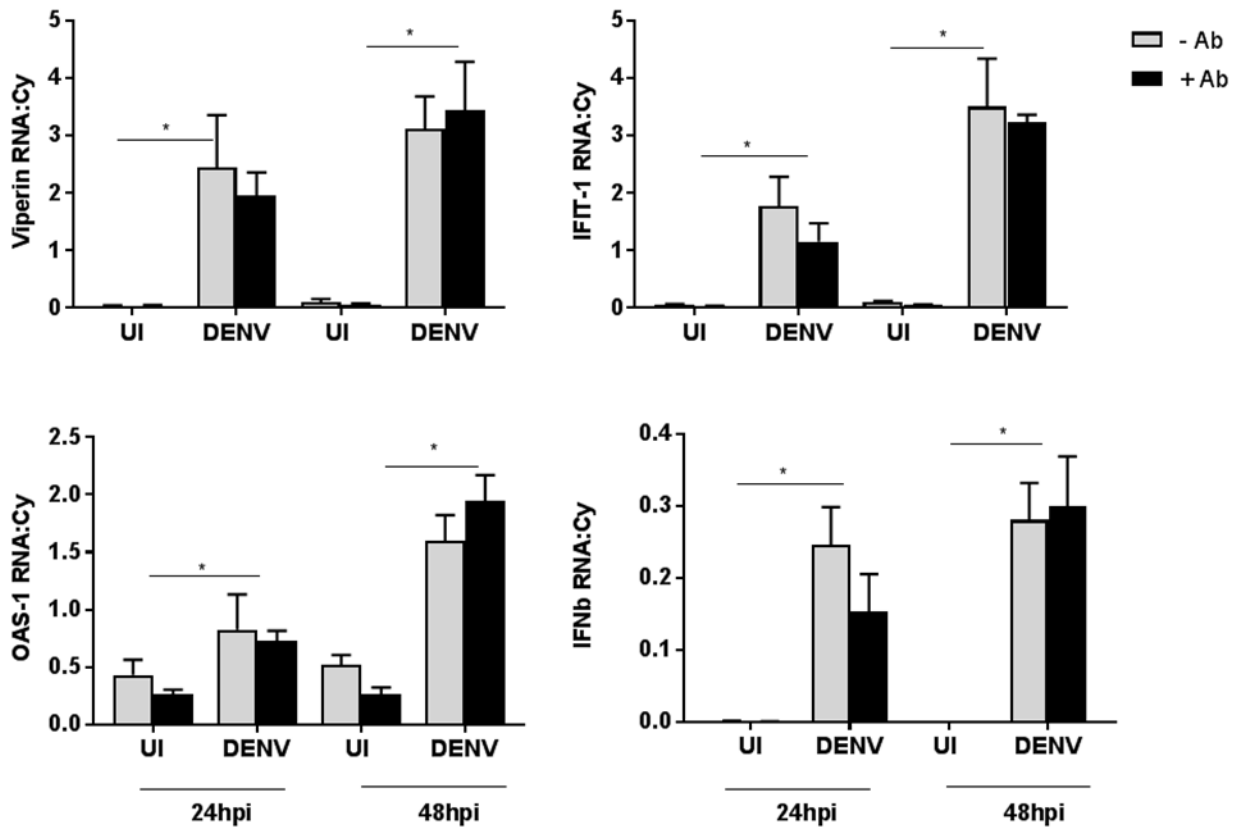


Figure V-7. Blocking of IFN- β actions has no effect on mRNA for DENV-induced ISGs in MDM

MDM were left uninfected or DENV infected and incubated with control antibody (-Ab) or 1000 U/ml of a neutralizing antibody against IFN- β (+Ab). At 24 and 48hpi supernatants were collected, cells were lysed and total RNA extracted and analysed for: Viperin, IFIT-1, OAS-1 and IFN- β mRNA by RT-PCR. PCR results were normalized against cyclophilin. Results represent mean \pm standard deviation from duplicate samples and are representative of at least three experiments. * $p < 0.05$ relative to uninfected, # $p < 0.05$ comparison +/- Ab treatment, two-way ANOVA/ Dunnett's test.

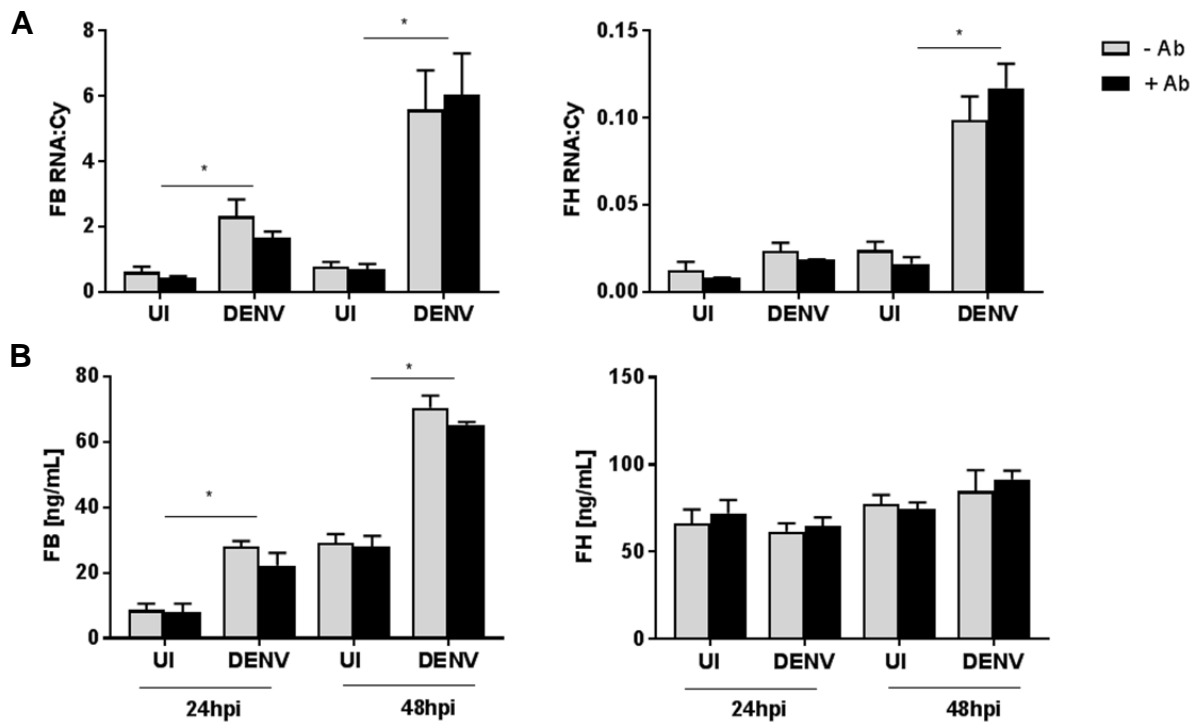


Figure V-8. Blocking of IFN- β actions has no effect DENV-induced FH and FB in MDM

MDM were left uninfected or DENV infected and incubated with control antibody (-Ab) or 1000 U/ml of a neutralizing antibody against IFN- β (+Ab). At 24 and 48hpi supernatants were collected, cells were lysed and total RNA extracted and analysed for (A) FB and FH mRNA by RT-PCR. PCR results were normalized against cyclophilin. (B) FB and FH proteins analysed by ELISA. Results represent mean \pm standard deviation from duplicate samples and are representative of at least three experiments. * $p < 0.05$ relative to uninfected, two-way ANOVA/ Dunnett's test.

V.3 Discussion

This study has performed an *in silico* approach to identified potential TF binding sites in the human FB and FH promoters that may be responsible for directing FB and FH gene transcription. Outcomes identified a number of potential TF binding sites, including IFN-responsive elements and the role of these in driving FB and FH mRNA was demonstrated with *in vitro* laboratory evidence.

To select the most likely TF binding sites from the data using the MatInspector software, the approach combined analysis of experimentally verified promoters that were linked to coding transcripts, with stringent matrix scores higher than 0.85 and both experimental evidence and co-citation of TF and FH or FB in the literature. For both FB and FH sequences, a relevant and common TF was identified: CREB. CREB induces transcription of genes in response to stimulation of the cAMP pathway and specifically, CREB has been proven to regulate the IFN- γ promoter (Samten et al., 2005, Samten et al., 2008). While it is well known that the proximal promoter of IFN- γ , -73 to -48 bp upstream of the transcription start site, is essential and sufficient for IFN- γ expression (Penix et al., 1993), another study has demonstrated that TF of the family CREB/ATF/AP-1 (CREB/activating transcription factor/activator protein 1) bind to the proximal promoter of IFN- γ to up-regulate IFN- γ transcription (Samten et al., 2008). This was specifically demonstrated in T-cells in response to antigens from *Mycobacterium tuberculosis* using competitive electrophoretic mobility shift assay and promoter pull-down assay (Samten et al., 2008). Further, IFN- γ is considered as the primary inducer of both FB and FH promoters in human and mouse species (Thomas et al., 2000, Schlaf et al., 2001, Wu et al., 2016). In fact, IFN- γ has been demonstrated to induce FB and FH expression not only in hepatic cells (Huh7 and HepG2 cells) but also in fibroblasts, EC, epithelial cells, neurons and monocytes (Lappin and Whaley, 1990, Lappin et al., 1992, Friese et al., 2000, Thomas et al., 2000, Friese et al., 2003, Wu et al., 2007). The presence of CREB binding sites close to the transcription start site in the FB promoter and in the middle of FH promoter region but next to IRFF elements, support the idea that IFN- γ and FB and FH genes are co-regulated by CREB family elements, with the potential for CREB-induced IFN- γ to further activate FB and FH genes, via elements, as below.

Likewise, other common TF were present in both FB and FH promoters, including the important regulatory motifs, NF κ B, IRFF and STAT. In the FB promoter, two NF κ B binding

sites are located between STAT and IRF7 TFs in the middle of the promoter region while a unique NF κ B element is present in the FH promoter, and proximal to the transcription start site. Notably, the ChIP-seq analysis of 37 different promoters has shown that a single and a strong NF κ B motif is usually sufficient to support strong binding to a promoter (Tong et al., 2016) and thus this single NF κ B TF binding site is likely to be functional. It is well known that NF κ B plays a major and complex role in the transcriptional regulation of an extensive number of genes which are related to the control of the inflammatory response (Hoesel and Schmid, 2013, Tong et al., 2016) and thus a role of NF κ B in FB and FH gene expression is not unexpected. Additionally, DENV has a number of mechanisms for inducing NF κ B. Specifically, DENV NS1 and NS2B3 have been shown to induce NF κ B activation in HepG2 cells, EC and murine mononuclear phagocytes (RAW264.7 cells) using luciferase reporter assays (Silva et al., 2011, Lin et al., 2014, Cheng et al., 2015). The activation of NF κ B is also well known to occur upon recognition of TLR3 or TLR7 with double-strand or single-strand RNA, respectively; both pathways known to occur following DENV infection (reviewed in (Sprokholt et al., 2017)). In addition, TNF α , a factor known to be induced during DENV infection and that contributes to the pathogenesis of DENV disease, is a well-known activator of the NF κ B pathway. Thus, in the context of DENV infection, NF κ B is likely to be induced or activated and FB and FH promoters have the capacity to respond to this.

At the same time, NF κ B does not function alone and is part of a network of factors driving responses to pathogens, and IRFF and STAT also play an important role (Hoesel and Schmid, 2013). IRF4 is present in FB and FH promoters (two elements in FB and one in FH, Table V-3); however the expression of IRF4 is restricted to T and B-cell lineages, is not induced by IFN but rather T-cell receptor stimulation (Nakaya et al., 2001, Sato et al., 2001, Zhang et al., 2017b). Thus, IRF4 is unlikely to be important in responses of infected cells to DENV infection but could influence FH and FB production from activated T and B-cells. These cell types however, have not previously been reported to be major sites for FH and FB production. The IRFF element most relevant to DENV infection and identified in the FB promoter is IRF7, although this motif is located distal to the transcription start site. IRF7 is also present in the human FH promoter, along with IRF1 and two ISRE elements (Table V-3). In this case, IRF7 and one ISRE element are proximal to the transcription start site. IRF7, along with IRF3, are considered the master regulators of type I IFN (IFN- α/β) responses. The expression of the IRF-7 gene is totally dependent on IFN- α/β

signalling, (Marie et al., 1998, Sato et al., 1998) and promotes induction of IFN- β , as well as other ISGs after binding to CREB binding protein 1 (Miyamoto et al., 1988). Both CREB and IRF7 TF binding sites are predicted in human FB and FH promoters, and these elements in particular point to a role for type I IFN in driving FB and FH gene transcription. This was further analysed experimentally, as discussed below. Likewise, ISRE elements (located in FH promoter region) are present in the promoters of ISGs; and IRF7 along with IRF3 can bind to ISRE elements and activate the transcription of these genes (Schmid et al., 2010).

Furthermore, the antiviral role of IRF1 (present in FH promoter) and IRF7 (present in both FB and FH promoters) is well established, and has been demonstrated in *in vitro* and *in vivo* studies for encephalomyocarditis virus, vesicular stomatitis virus, herpes simplex virus, lymphocytic choriomeningitis virus and DENV, among others (Zhang and Pagano, 1997, Yoneyama et al., 1998, Carlin et al., 2017). Thus, the presence of IRFF and ISRE elements in the FH and FB promoters strongly suggests regulation of these genes by type I IFN.

In general, the induction of IRFF typically results in the activation of STAT elements (Nan et al., 2018). The strong dependence on STAT elements was evident in both FB and FH promoters. Of note, two STAT binding elements are located proximal to the transcription start site of FB promoter, one STAT6 and another STAT binding site not specified by MatInspector. Likewise, five STAT binding sites are present close to the transcription start site in the FH promoter, although in this case all are members of the STAT5 family (STAT5a and 5b). The role of STAT6 is still largely unknown but it has been shown to participate in regulating acquired immunity involving IL-4 and IL-13 secretion by activated T and B lymphocytes and mast cells (reviewed in (Nan et al., 2018)), both cytokines known to be induced upon DENV infection (Maneehan et al., 2013). Similarly, STAT5 is activated in the presence of an inflammatory response, specifically in response to various cytokines including members of the IL-2 (IL-2, IL-7, IL-15, IL-21) and IL-3 (IL-3, IL-5) families (Kisseleva et al., 2002). Notably, IL-2, IL-21 and IL-5 are induced in DF and DHF patients (Maneehan et al., 2013). Therefore, it is possible that both human FB and FH promoters could be activated upon DENV infection in response to the inflammatory response induced and the presence of the above cytokines through STAT6 and 5, respectively. On the other hand, a recent study has experimentally verified that STAT1 regulates human FB promoter expression in renal epithelial cells (Wu et al., 2016). Using a luciferase reporter assay the

authors showed that STAT1 transfection led to a sixfold increase in FB promoter activity, while the luciferase signal was unchanged in cells transfected with STAT1 responsive elements mutated in the FB promoter (Wu et al., 2016). Likewise, STAT1 has been proven to induce the expression of FH in RPE cells and this expression is triggered in the presence of IL-27 (Amadi-Obi et al., 2012). Using RT-PCR and Western blot techniques, the authors found increased FH mRNA and protein in retinas isolated from wild-type mice cultured in medium containing IL-27 compared to retinas harvested from C57BL/6, STAT1-deficient mice (Amadi-Obi et al., 2012). STAT1 activates gene transcription via homo- and heterodimer formation with IRF9 to form the complex ISGF3 that moves to the nucleus and binds to promoter ISRE. As described above, ISRE are found in the FH promoter and likely mediate similar actions of STAT1 in regulating FH gene expression during DENV infection.

On the other hand, the expression of FH has been demonstrated to be affected in settings of oxidative stress, such as in RPE cells exposed to H₂O₂ (Wu et al., 2007). Using a dual-luciferase reporter assay the authors showed that the IFN- γ -induced stimulation of FH promoter activity was significantly reduced by H₂O₂-induced oxidative stress. Further, the same study revealed that RPE cells submitted to oxidative stress induced acetylation of forkhead box O3 (FOXO3) which enhanced FOXO3 binding to the FH promoter and inhibited STAT1 induction of the FH promoter (Wu et al., 2007). Previous observations suggested that FOXO proteins, that constitute a large family of TF with pivotal roles during both ontogenesis and adult life (Birkenkamp and Coffey, 2003), may function as either transcriptional activators or repressors (Birkenkamp and Coffey, 2003). Strikingly, our MatInspector analysis revealed the presence of 17 FKHD including several members of the FOXO protein family that according to this evidence (Wu et al., 2007) could be putative inhibitors of FH promoter via interference with STAT1/ISRE. Since oxidative stress is well known to occur during flavivirus infections, such as DENV (Valero et al., 2013) it would be predicted that this will induce FOXO3 binding to the FH promoter and downregulate FH gene expression. This is not what we observed experimentally *in vitro* (Chapter IV), but there may be an important balance between oxidative stress-induced FOXO3 inhibition of FH and IFN-driven activation of FH gene expression via STAT1/ISGF3/ISRE, with the final outcome dependent on the local environment of the infected cell.

Considering that IRF1, IRF7 and STAT1 are potential TF of FB and FH promoters along with the fact that these elements are important inducers of IFN- β (Platanias, 2005), this study further investigated, experimentally, the influence of IFN- β in FB and FH gene expression and protein production. Here we show that FH and FB are regulated in MDM and EC in a manner that correlates with induction of other ISGs in each cell type. IFN- β is a known stimulus for ISGs in EC (Dalrymple and Mackow, 2012a, Calvert et al., 2015) and in agreement with previous findings (Calvert et al., 2015), results confirmed the induction of the ISGs viperin, IFIT-1 and OAS-1 in DENV-infected HUVEC and further we report the induction of these ISGs in DENV-infected MDM. Again, consistent with our previous study, the induction of these ISGs was blocked by a neutralising IFN- β antibody in HUVEC (Calvert et al., 2015) but, surprisingly, not in MDM. Likewise, while blocking IFN- β stimulation blocks the DENV-induction of both FB and FH mRNA in HUVEC, blocking IFN- β did not have any effect on FH and FB in MDM. These results show for the first time, that endogenously produced IFN- β is one of the drivers of induction of FH and FB mRNA and FB protein in DENV-infected HUVEC but not MDM, consistent with the IFN- β dependency of induction of ISGs in HUVEC but again, not MDM. Since IFN- β stimulation is known to act via STAT1, IRF1 and IRF7 elements, as our MatInspector analysis predicts are present in the FB and FH promoters, this suggests that these elements may be functional in driving FB and FH gene expression during DENV infection in EC. Direct evidence for this, such as via promoter-reporter assays, using the STAT1 inhibitor nifuroxazide, or using constructs with the predicted promoter elements deleted, remain to conclusively demonstrate the roles of these elements in DENV-induced IFN- β driven responses. The lack of endogenously produced IFN- β in driving ISGs, including FH and FB transcription in MDM, is unlikely to be due to a lack of IFN- β production by MDM which is known to occur following DENV infection of this cell type (Duran et al., 2016). Additionally, blocking IFN- β in DENV-infected MDM did still enhance DENV RNA levels, and thus a functional effect on blocking endogenously produced IFN- β has been elicited. The rationale for the lack of IFN- β regulation of ISGs, FB and FH in DENV-infected MDM remains to be determined.

Consistent with our lack of effect of IFN- β on FH and FB in primary MDM, a recent study has demonstrated that neither IFN- α nor IFN- β has any effect on FH production in human monocyte-derived dendritic cells, a professional antigen presenting cell type related to macrophages (Dixon et al., 2017). Our results reinforce the idea that factors other than

type I IFN, such as IFN- γ , the well-known regulator of FB and FH in several cell lines (Lappin et al., 1992, Friese et al., 2000, Friese et al., 2003, Wu et al., 2007), may be driving the expression of FH and FB in monocyte/macrophage cell types. Interestingly, this suggests cell type dependency in the local factors that may be important in driving ISGs, FH and FB production and this is a potential area of future investigation.

While the experimental data above and similarities in many of the predicted promoter elements for FH and FB suggest co-ordinated expression of these factors, there are additional differences in promoter elements, such as IRF1, ISRE and STAT5 binding elements, that predict distinct gene regulation. The factors and situations that stimulate disparate FH and FB gene expression are of future interest as a mechanism for specifically promoting (via FB) or negatively regulating (via FH) the complement AP activity.

In conclusion this chapter has demonstrated that the induction of both human FB and FH promoters are likely triggered by similar pathways that involve the activation of NF κ B, IRF1 and 7 and STAT binding elements and are driven by IFN- β in some cell types. Our results have uncovered new potential areas of study of the regulation of FH and FB in cell types important for pathogenesis of DENV and demonstrate the utility of computational predictions in directing and interpreting laboratory experimentation.

Considering these results, it was decided to further investigate production and roles of FB and FH in a mouse model of DENV infection that is deficient in type I and type II IFN receptors (AG129), to evaluate the role of other pathways such as NF κ B and IFN-independent STAT binding sites in FB and FH regulation in the absence of IFN stimulated responses.

CHAPTER VI EVALUATION OF FB AND FH DURING DENGUE VIRUS INFECTION IN *IN VIVO* MODELS

VI.1 Introduction

Previous chapters of this study have demonstrated that the disproportionate production of FB, an activator of the AP, and FH, a major negative regulator, during DENV infection could be associated with disease severity. *In vitro* studies in macrophages and EC, two major targets for DENV replication and pathogenesis *in vivo*, respectively, have shown that while FB protein is increased upon DENV infection, FH protein is unchanged. The imbalance between these two factors along with the increased C3b deposition on DENV-infected cells and the ability of DENV-infected supernatants to promote AP-mediated lytic activity is predicted to result in higher complement activity and increased vascular permeability, a hallmark of dengue disease.

Considering the above results, this study was extended to *in vivo* scenarios, human and mouse, in order to investigate possible alterations of the AP in a natural host and in a published *in vivo* model of DENV-induced haemorrhagic disease, respectively. Given that humans are natural hosts of DENV, this model is ideal to study disease pathogenesis; however, the human model is limited due to ethical considerations and to observational non-invasive studies. To date, there are only a few studies in humans that have investigated the complement AP and have suggested that excessive complement activation of the AP could be associated with severe forms of DENV disease i.e. DHF and DSS (Bokisch et al., 1973, Nascimento et al., 2009, Nascimento et al., 2014).

On the other hand, more information can be gained from animal models, but the lack of a suitable animal model is a key drawback that has restricted our understanding of DENV pathogenesis (Plummer and Shresta, 2014a, Plummer and Shresta, 2014b). The development of a useful mouse model has been hampered since immunocompetent mice are naturally resistant to DENV infection. While in humans DENV inhibits IFN signalling pathways to establish infection, in immunocompetent mouse cells the virus is unable to do so due to the inability of non-structural viral proteins to counteract mouse STAT2 and STING (Ashour et al., 2010, Aguirre et al., 2012). As a consequence, a variety of immunocompromised mouse models defective in innate responses and the IFN system have been successfully developed as an alternative platform for DENV infection (Ashour et al., 2010, Tan et al., 2010, Ng et al., 2014). Among them, the AG129 mouse model,

deficient in IFN α/β and γ receptors, has been shown to allow effective replication of DENV, resulting in circulating viremia and haemorrhagic disease (Tan et al., 2010, Tan et al., 2011, Ng et al., 2014, Lee et al., 2016, Martinez Gomez et al., 2016). The infection of these animals with a non-mouse-adapted DENV-2 strain (D2Y98P) recapitulates key biological and clinical features observed in humans such as cytokine storm, liver damage, and vascular leakage, hallmarks of DENV disease, and thus is considered a suitable animal model to study DENV disease pathogenesis (Tan et al., 2010, Ng et al., 2014). The AG129-D2Y98P DENV infection model has been further extended to also reflect the increased severity of disease that is associated with secondary infection and to reproduce ADE of infection. In this model, DENV-2 infection of young mice born to DENV-1-immune mothers leads to reduced survival, earlier onset of disease and correlated with higher viremia and increased vascular leakage compared to DENV-2-infected mice born to dengue naïve mothers (Ng et al., 2014, Lee et al., 2016).

In this study, changes in FB and FH in DENV-seropositive patients were evaluated and compared with the levels in DENV-seronegative patients. Secondly, the levels of FB and FH were measured over the course of infection in AG129 mice infected with DENV and in a model of infection of mouse pups with pre-existing maternal heterotypic antibody, reflecting models of 'severe dengue' and 'more severe secondary dengue'. Finally, a promoter analysis was performed to assist our interpretation of results and assess the potential effects of lack of IFN receptors in the AG129 mouse model on responses of FB and FH genes expression during DENV infection.

VI.2 Results

VI.2.1 FH is unchanged but FB is reduced in dengue seropositive compared with seronegative patient samples

Analysis of FH and FB protein was performed on serum samples from a cohort sent for diagnostic DENV serology (NS1, IgM and IgG) and composed of 8 DENV-seronegative and 29 DENV-seropositive patients. FB protein levels were significantly lower in DENV-seropositive patients (533.8 ± 17.33) than in DENV-seronegative individuals (647.9 ± 59.95) (Figure VI-1 A), although protein levels in some patients from both groups were above the reference range for normal FB (200-500 $\mu\text{g/ml}$) (Forristal et al., 1977, Silva et al., 2012) The levels of FH in the DENV-seropositive patients were not significantly different to those in the DENV-seronegative subjects (570.8 ± 6.095 ; 531 ± 34.24 , respectively), and comparable to that reported as the average concentration of FH in human serum ($\sim 500 \mu\text{g/ml}$) (Adinolfi and Zenthon, 1982, Silva et al., 2012, van Beek et al., 2018) (Figure VI-1 B). Thus, there were no changes for FH but a reduction for FB protein levels in the circulation during DENV infection, suggestive of complement consumption.

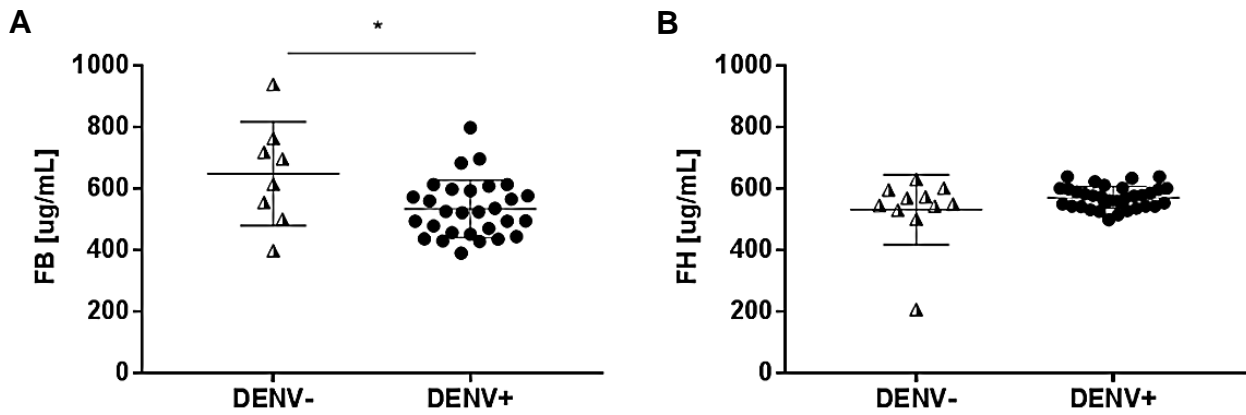


Figure VI-1. FH is unchanged but FB is reduced during primary dengue infection in humans

FB (A) and FH (B) levels were quantitated by ELISA in a cohort of fever cases in the returned traveller to SA, with suspected DENV infection and who subsequently returned negative (DENV-, n=8) or positive (DENV+, n=29) by DENV serology. Results represent the mean \pm standard deviation. * $p < 0.05$, Student's unpaired t -test.

VI.2.2 Protein levels of FB are unchanged but FH is decreased during severe disease in DENV-infected AG129 mice, although mRNA for both proteins is induced in the liver

The AG129 mouse model is a published and established model to study DENV disease pathogenesis and thus, changes in FB and FH were quantitated in DENV-infected AG129 mice. The circulating levels of both proteins were quantitated over the course of an acute infection and the period of viremia in the serum of animals infected with DENV, at 10^4 PFU (Figure VI-2). While FB protein did not change during the acute infection (Figure VI-2 A), FH protein was significantly decreased at 4dpi (Figure VI-2 B), a time point that corresponds to the peak of viremia in these animals (Appendix 3). Since our prior data (Chapter IV), showed that the ratio of FB:FH was altered during DENV infection *in vitro*, the association between FH and FB was assessed at each time point by correlation analysis. No significant association was observed between FB and FH in UI, 2 or 4dpi following DENV infection. Although not significant, there is a trend towards a negative correlation between FH and FB at 4dpi (Figure VI-2 C).

Since the liver is considered a major source for circulating FH and FB, and these factors can also be produced by the kidney, FB and FH mRNA levels were quantitated in the liver and kidney. Results demonstrate a significant induction of both FH and FB mRNA at 4dpi in the liver (Figure VI-3 A). In contrast, the levels of both factors were unchanged in the kidney of these animals (Figure VI-3 B). Of note, these results contrast to the circulation where FB is unchanged and FH protein decreases at 4dpi. Thus, these results indicate that induction of FH and FB mRNA in the liver does not translate into an increase in circulating protein during DENV infection.

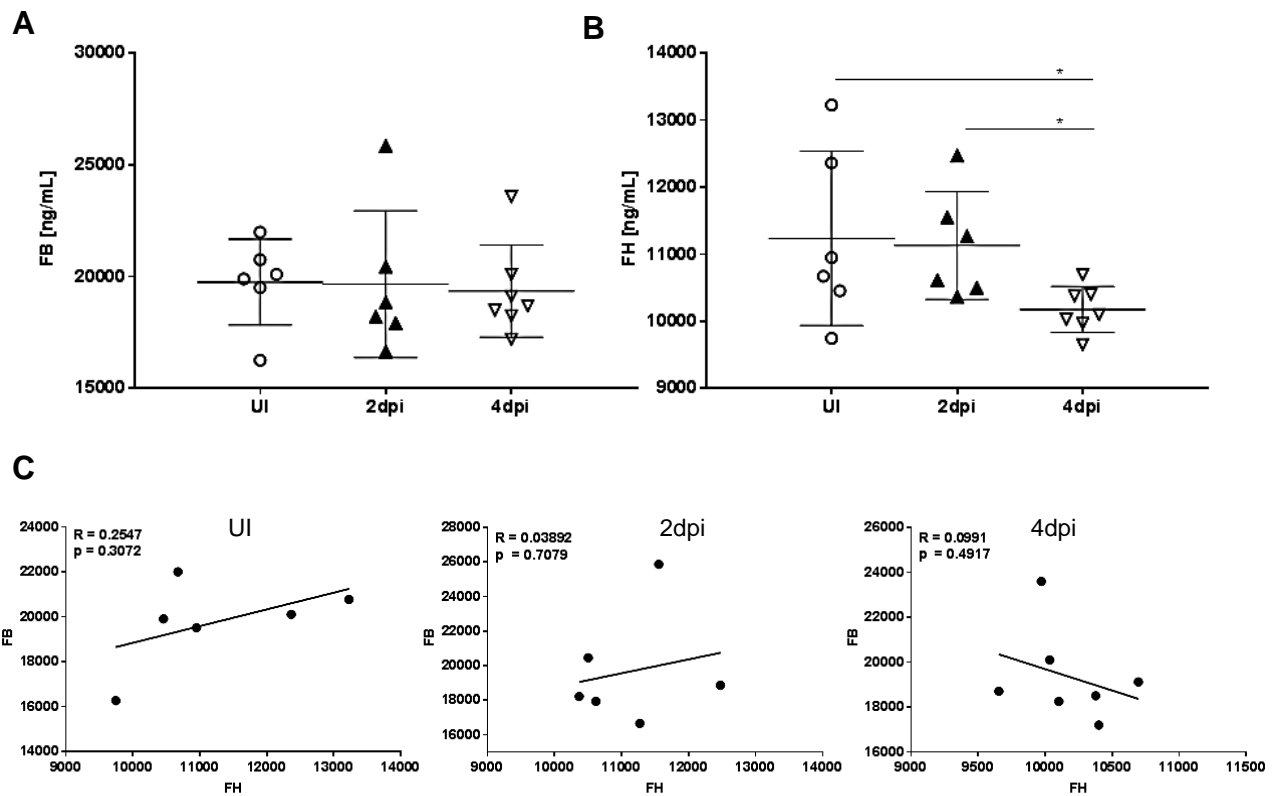


Figure VI-2. Circulating FH is decreased but FB is unchanged during acute primary dengue infection in AG129 mice

Five- to six- weeks old AG129 mice were left uninfected (n=6) or subcutaneously infected (n=6 2dpi; n=7 4dpi) with 10^4 PFU/mouse of DENV-2 strain D2Y98P. At the indicated time points mice were euthanized, blood harvested and serum subjected to ELISA for quantitation of (A) FB and (B) FH protein levels. Results represent the mean \pm standard deviation from each mouse group. * $p < 0.05$, one-way ANOVA/ Tukey's test. (C) Correlation analysis between FB and FH protein values in individual animals (Spearman correlation).

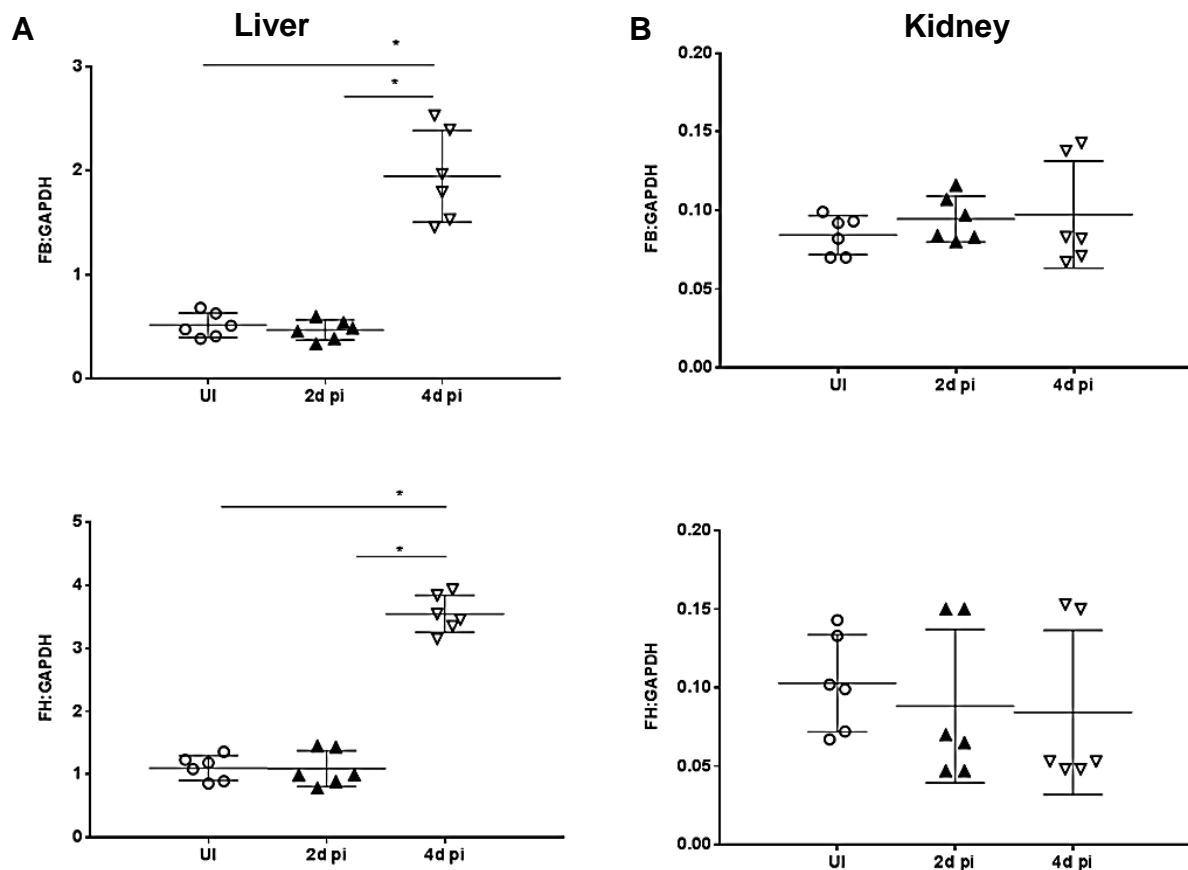


Figure VI-3. Circulating changes of FB and FH are not reflected by mRNA in the liver or kidney of DENV-infected AG129 mice

Five- to six- weeks old AG129 mice were left uninfected (n=6) or subcutaneously infected (n=6 2dpi; n=7 4dpi) with 10^4 PFU/mouse of DENV-2 strain D2Y98P. At the indicated time points mice were euthanized, livers (**A**) and kidneys (**B**) harvested, total RNA extracted and subjected to RT-PCR for FB and FH. Results were normalized against GAPDH and relative mRNA levels quantitated by Δ Ct method. Results represent the mean \pm standard deviation from each mouse group. * $p < 0.05$, one-way ANOVA/ Tukey's test.

VI.2.3 Protein levels of FH are decreased but FB are increased during acute, more severe secondary dengue infection in AG129 mice

There is an increased incidence of severe DENV disease associated with a secondary infection or pre-existing antibody (Guzman and Kouri, 2008), theoretically due to ADE of infection (Halstead and O'Rourke, 1977b, Halstead and O'Rourke, 1977a). A model to reflect this has been established and published by Prof Sylvie Alonso (Ng et al., 2014). This model reflects primary DENV-2 (10^3 PFU) infection of AG129 mice borne to dengue naïve mothers (DENV-N) and ADE of infection with AG129 mice borne to DENV-1 immune mothers (DENV-I). Changes in circulating FB and FH were defined in this mouse model of severe (DENV-N) and more severe secondary DENV disease (DENV-I). Again, and in agreement with Figure VI-2 A, FB was unchanged in the early stages of AG129 DENV-N animals. In contrast, FB was significantly increased in the serum of AG129 DENV-I mice at 3dpi (Figure VI-4 A). FH protein tended to decline but was not significantly different at 3dpi in AG129 DENV-N mice but significantly decreased in the serum of AG129 DENV-I mice at 3dpi (Figure VI-4 B). Although a reciprocal relationship approached significance in UI mice, correlation analysis again showed no significant association between FB and FH (Figure VI-4 C).

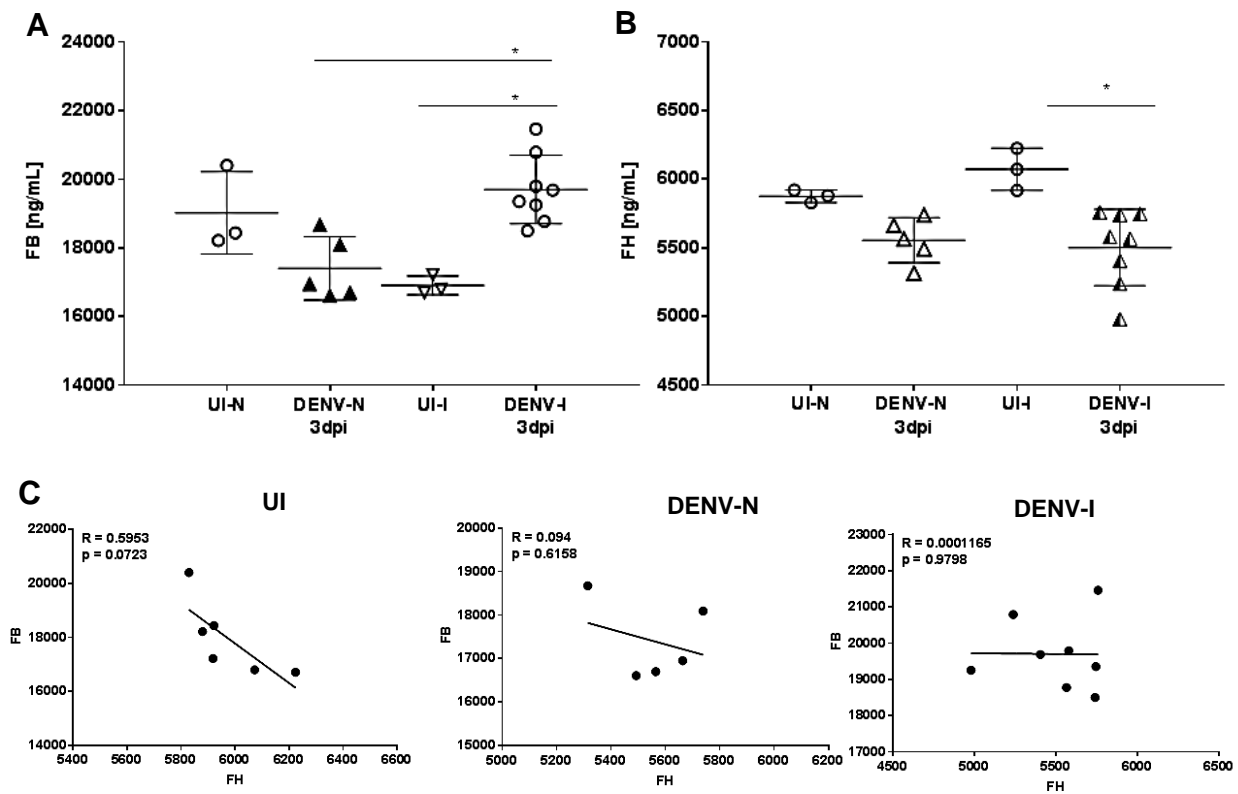


Figure VI-4. Circulating FH is decreased and FB increased during acute, severe secondary dengue infection in AG129 mice

Five- to six- weeks old AG129 mice born to either DENV-1 immune (DENV-I) or dengue naïve (DENV-N) mothers were left uninfected (UI-N, UI-I, n=3 each group) or subcutaneously infected with 10^3 PFU of DENV-2 strain D2Y98P (DENV-N, n=5; DENV-I, n=8). At 3dpi mice were euthanized and blood harvested and serum collected for ELISA quantitation of (A) FB and (B) FH protein levels. Results represent the mean \pm standard deviation from each mouse group. * $p < 0.05$, one-way ANOVA/ Tukey's test. (C) Correlation analysis between FB and FH protein values in individual animals (Spearman correlation).

VI.2.4 FB and FH are unchanged at moribund stage during DENV infection but deranged in the model of severe secondary DENV infection in AG129 mice

In both the DENV-AG129 models used above, the mice reach a point of ethical termination of the experiment and become moribund with vascular leakage. The timing that this occurs however, differs with the DENV infection of naïve animals at day 11-21 pi and in DENV-immune animals and severe secondary DENV-disease at 6 dpi (Ng et al., 2014). In the DENV-AG129 mouse model infected with 10^4 PFU, neither FB nor FH protein was significantly altered in the circulation at moribund stage (Figure VI-5 A and B). In this model, mice became moribund and samples were harvested at very late times pi (20-22 days). Similarly, no significant changes were observed in liver FB mRNA (Figure VI-5 C), although, surprisingly, a significant decrease was detected in kidney FB mRNA in DENV-infected animals (Figure VI-5 D). Consistent with FH mRNA changes in the liver during early infection, FH mRNA in the liver was significantly increased at the moribund stage in DENV-AG129 mice (Figure VI-5 C), while kidney FH mRNA was unchanged upon infection in these animals (Figure VI-5 D). In the model of severe secondary DENV infection, moribund stage was onset at 6dpi in the DENV-I group but 12-18 dpi in the DENV-N group (Ng et al., 2014). In DENV-N mice infected with DENV (10^3 PFU), circulating FB protein decreased at 6dpi (Figure VI-6 A). Likewise, in DENV-I mice, reflecting ADE of infection and more severe disease, FB protein significantly decreased and the levels were significantly lower than in DENV-N mice (Figure VI-6 A). FH protein, increased in both DENV-N and DENV-I mice at 6dpi, and further this effect was significantly higher in DENV-I compared to DENV-N mice (Figure VI-6 B). Unfortunately, we did not collect day 6pi for the 10^4 PFU challenge in Figure VI-2 or Figure VI-5 which would have been the comparator for DENV-N at 6dpi in Figure VI-6. As in all previous situations there was no significant association between FB and FH proteins in the circulation by correlation analysis (Figure VI-6 C). Neither mRNA for FH or FB were altered in the liver or kidney of DENV-N or DENV-I mice at 6dpi (Figure VI-7 A and B). Thus again, the changes in FB and FH proteins in the circulation, do not correspond with a change in liver or kidney FB and FH mRNA (Figure VI-7 A and B). These results of DENV-I at day 6pi (representing moribund stage) contrasts to the 10^4 PFU DENV infection model at moribund stage (day 20-22pi) (Figure VI-5 C and D) where FB was decreased in kidney and FH mRNA increased in the liver.

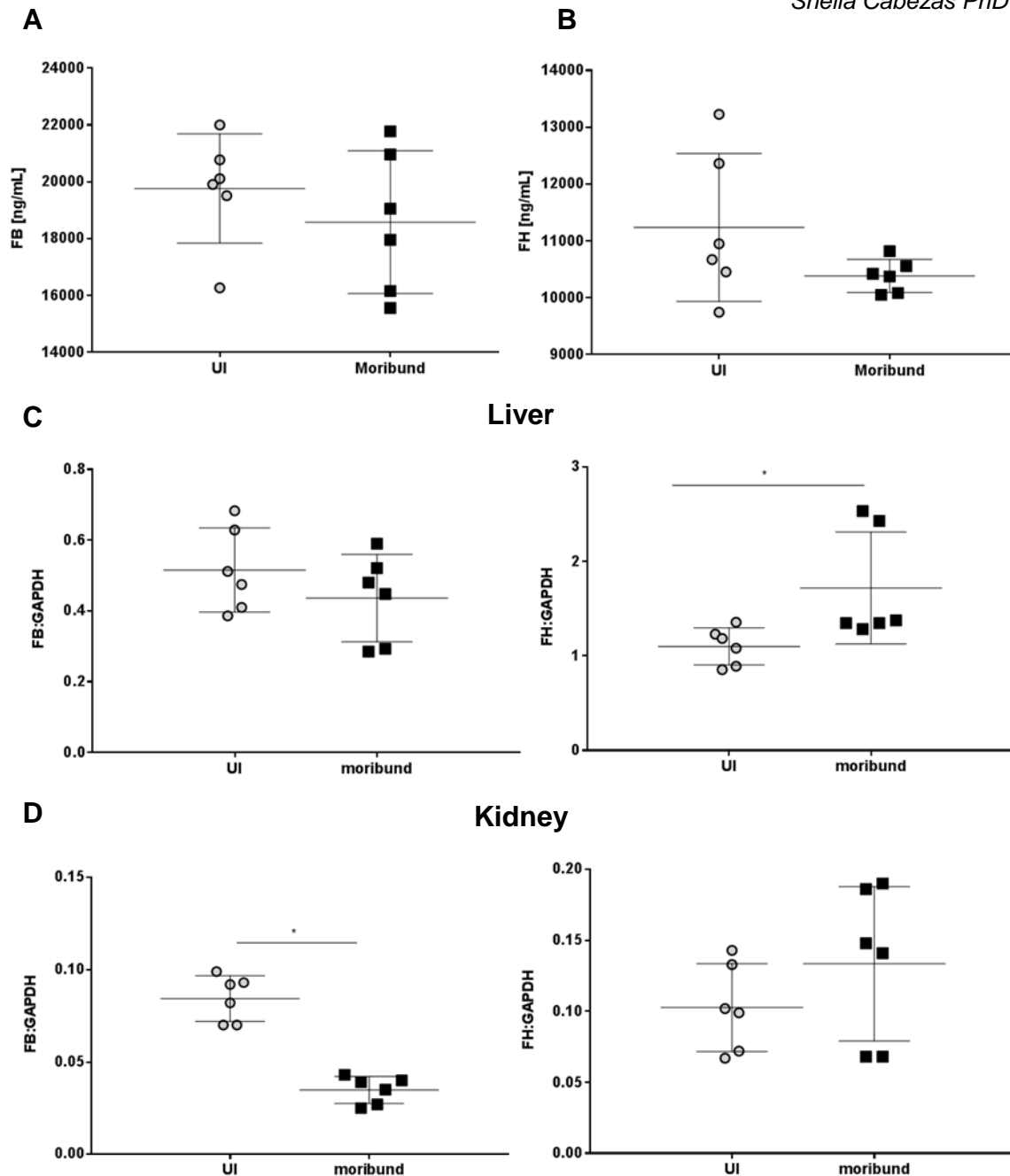


Figure VI-5. At moribund stage, complement is unchanged during DENV infection of AG129 mice

Five- to six- weeks old AG129 mice were left uninfected (n=6) or subcutaneously infected (n=6) with 10^4 PFU/mouse of DENV-2 strain D2Y98P. At moribund stage (20dpi) mice were humanely euthanized. Blood was harvested and serum collected for ELISA quantitation of (A) FB and (B) FH protein levels. Livers (C) and kidneys (D) were harvested, total RNA extracted and subjected to RT-PCR for FB and FH. Results were normalized against GAPDH and relative mRNA levels quantitated by Δ Ct method. Results represent the mean \pm standard deviation from each mouse group. * $p < 0.05$, Student's unpaired *t*-test.

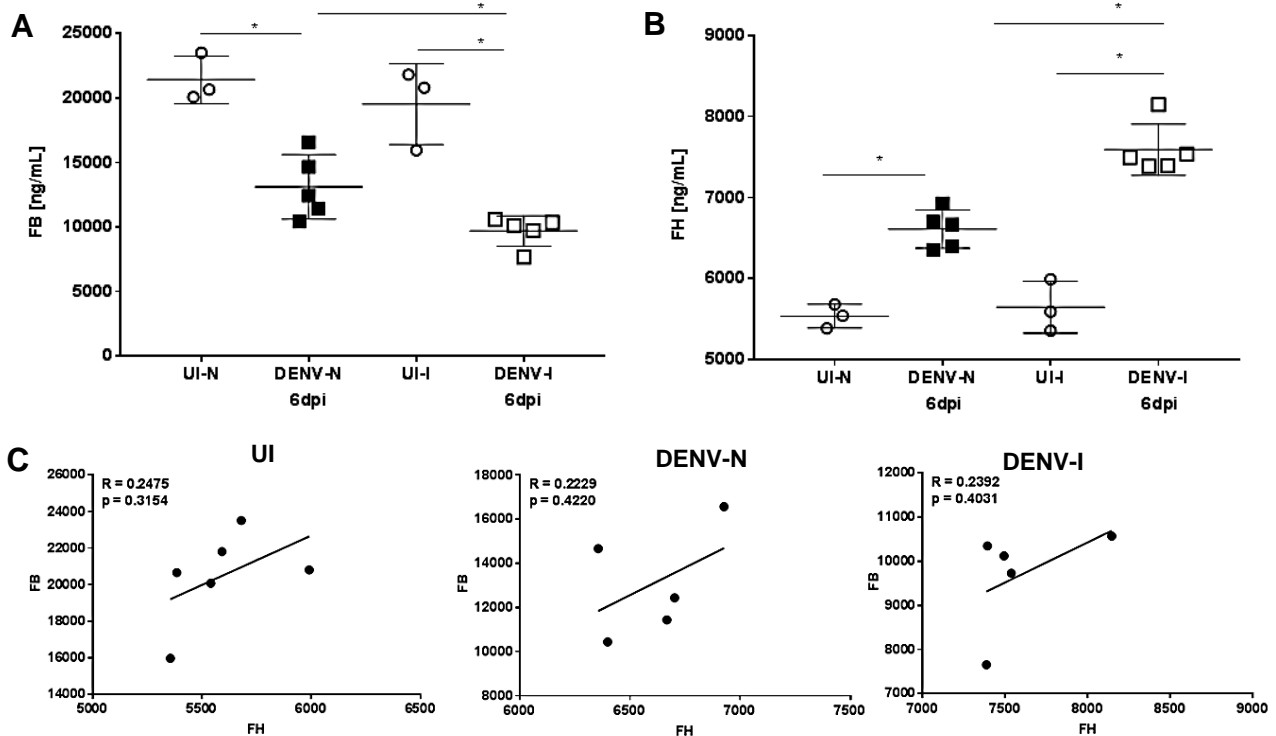


Figure VI-6. Complement is deranged during late stages of severe secondary DENV infection in AG129 mice

Five- to six- weeks old AG129 mice born to either DENV-1 immune (DENV-I) or dengue naïve (DENV-N) mothers were left uninfected (UI-N, UI-I, n=3 each group) or subcutaneously infected with 10^3 PFU of DENV-2 strain D2Y98P (n=5 each group). At 6dpi mice were euthanized and blood harvested and serum collected for ELISA quantitation of (A) FB and (B) FH protein levels. Results represent the mean \pm standard deviation from each mouse group. * $p < 0.05$, one-way ANOVA/ Tukey's test. (C) Correlation analysis between FB and FH protein values in individual animals (Spearman correlation).

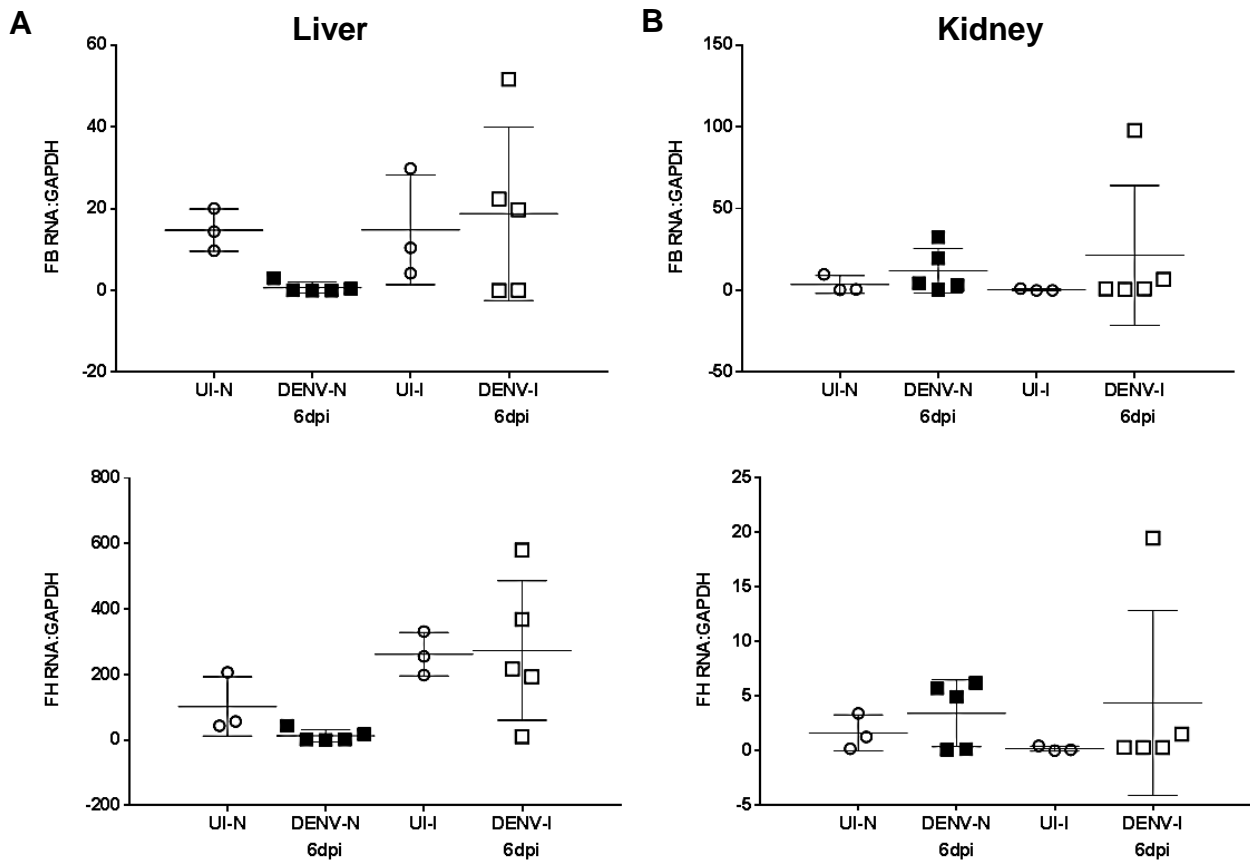


Figure VI-7. FB and FH mRNA levels are unchanged in the liver or kidney during severe secondary DENV infection in AG129 mice

Five- to six- weeks old AG129 mice born to either DENV-1 immune (DENV-I) or dengue naïve (DENV-N) mothers were left uninfected (UI-N, UI-I, $n=3$ each group) or subcutaneously infected with 10^3 PFU of DENV-2 strain D2Y98P ($n=5$ each group). At 6 dpi mice were euthanized, livers (A) and kidneys (B) harvested, total RNA extracted and subjected to RT-PCR for FB and FH. Results were normalized against GAPDH and relative mRNA levels quantitated by ΔC_t method. Results represent the mean \pm standard deviation from each mouse group. * $p < 0.05$, one-way ANOVA/ Tukey's test.

VI.2.5 FH and FB promoters contain potentially important IFN-driven elements

A major difference in the human and mouse models above is the lack of IFN signalling responses in the AG129 mouse. Our data from chapter V demonstrate that the human FH and FB promoters contain numerous IFN-responsive elements and that IFN- β contributes to the induction of FH and FB from EC during DENV infection *in vitro*. To investigate if similar elements could contribute to FH and FB regulation in the mouse, an *in silico* promoter analysis of mouse FH and FB was performed, again using MatInspector software as in chapter V.

Using stringency for identification of a promoter by evidence of an associated transcript and a matrix similarity for TF binding site > 0.85 , as utilised in chapter V, MatInspector analysis defined the presence of seven NF κ B, five IRFF and 11 STAT binding sites in the mouse FB promoter (Figure VI-8). The comparison between mouse and human FB promoters show strong dependence on proximal STAT elements (Figure VI-8). Also, the mouse promoter contains five proximal IRF elements whereas there are only three that are found distally in the human promoter. The mouse FB promoter contains four predicted NF κ B sites around the -300 region and a further three >-600 while the human FB promoter contains only two NF κ B binding sites at around -600 relative to the transcription start site (Figure VI-8). A number of IRFF family binding sites are present in the human and mouse promoters, with some similarities evident (Table VI-1). In particular, IRF4 and 7 are predicted to regulate both mouse and human FB promoters, while additionally, IRF1 and IRF3 TF binding sites are present in the mouse but not human FB promoter (Table VI-1). Of note, six STAT3 binding sites were predicted in the mouse FB promoter, while this TF was not present in the human promoter region (Table VI-1).

MatInspector analysis of mouse FH promoter predicted the presence of four IRFF and nine STAT binding sites (Figure VI-9). This predicted dependency on IRFF and STAT regulation is also seen with the human FH promoter, although surprisingly, and in contrast to human FH promoter, no NF κ B or ISRE binding sites were found in the mouse FH promoter sequence (Figure VI-9). Again as shown for the FB promoter, several common members of the IRFF and STAT families were identified in both the human and mouse FH promoters (Table VI-1), with IRF4 and 7, STAT 5 and 6 predicted in promoters from both species (Table VI-1) and IRF1 found in the human and IRF2 and IRF3 found in the mouse promoter only.

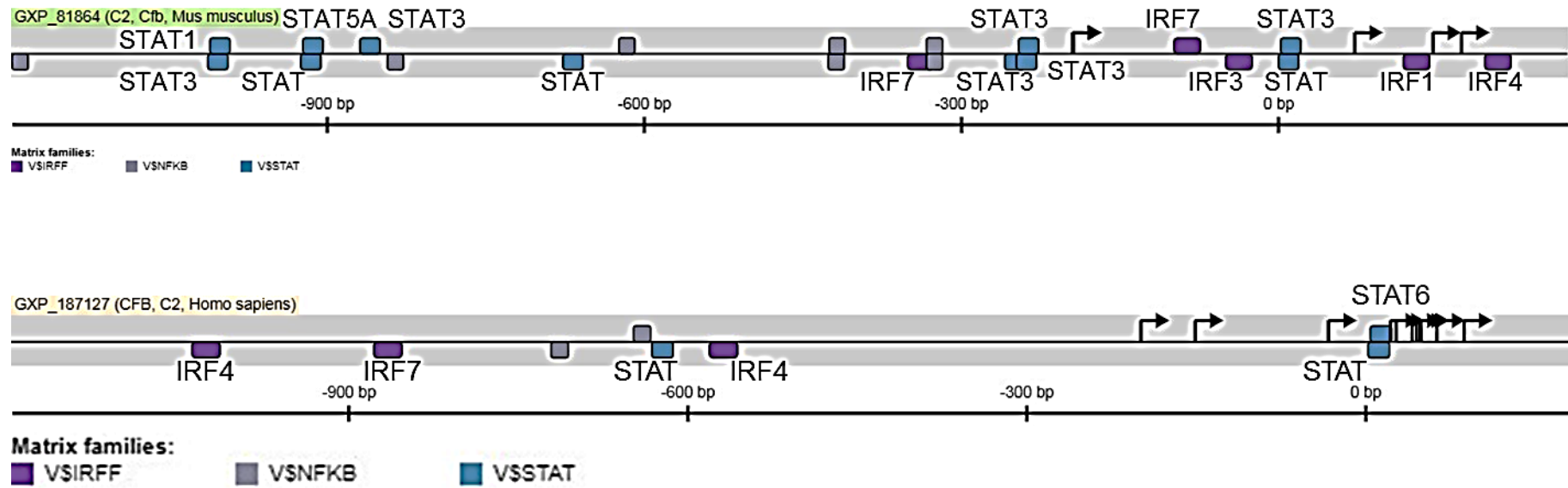


Figure VI-8. Comparison between mouse and human FB promoters

Schematic localisation of the NF κ B, IRFF and STAT TF binding sites in the mouse and human FB promoter sequences (1200 bp upstream the transcription start site). TF were identified using MatInspector software.

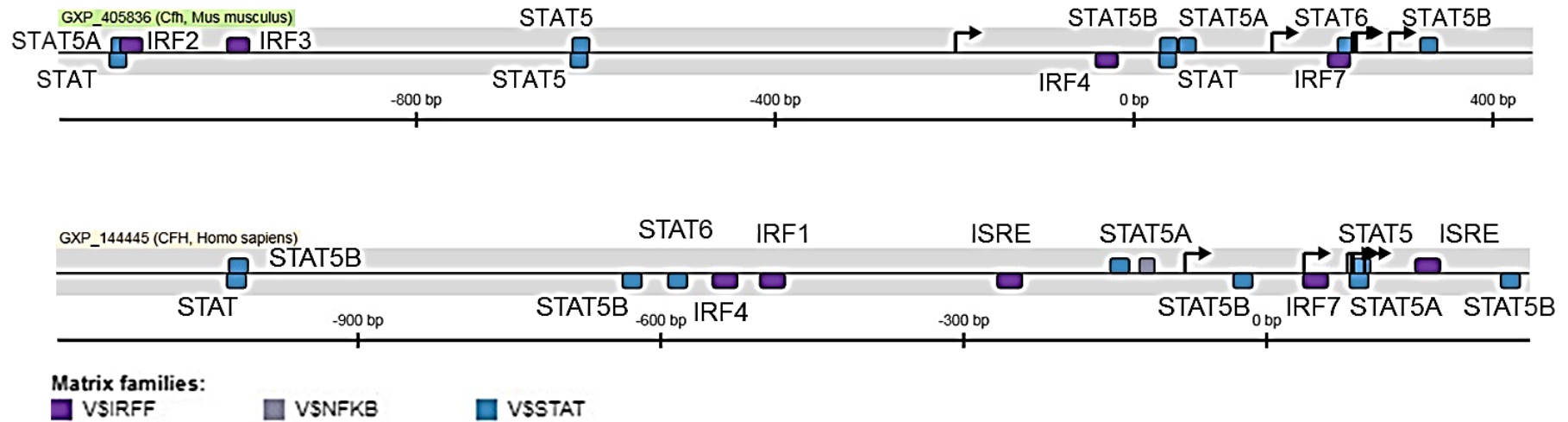


Figure VI-9. Comparison between mouse and human FH promoters

Schematic localisation of the NFκβ, IRFF and STAT TF binding sites in the mouse and human FH promoter sequences (1200 bp upstream the transcription start site). TF were identified using MatInspector software.

Table VI-1. Comparison between human and mouse FB and FH promoters

		V\$NF κ B	V\$IRFF						V\$STAT				
		NFkb	IRF1	IRF2	IRF3	IRF4	IRF7	ISRE	STAT	STAT1	STAT3	STAT5	STAT6
FB	Human	2	-	-	-	2	1	-	2	-	-	-	1
	Mouse	7	1	-	1	1	2	-	3	1	6	1	-
FH	Human	1	1	-	-	1	1	2	1	-	-	7	1
	Mouse	-	-	2	1	1	7	-	2	-	-	6	1

VI.2.6 FB mRNA but not FH is increased in the brain of immunocompetent mouse model at end-stage disease

The above promoter analysis re-inforces the importance of IFN responses in regulating FH and FB and thus, to investigate the induction of FB and FH during DENV infection *in vivo* in a scenario with a fully competent IFN response an intracranial mouse DENV infection model was utilised. C57BL/6 mice were infected by intracranial injection with DENV-2 and brain tissues were collected at 1, 3 and 6 dpi by Dr Wisam Al Shujairi. The latest time point (6dpi) represents high-level DENV-replication in the brain without signs of DENV disease; characterised by on-set of weight loss (6-7dpi) and neurological signs (8-9dpi) (Al-Shujairi et al., 2017). Our data show a rapid and significant induction of FB mRNA as early as 3dpi, with FB mRNA levels increasing with time (Figure VI-10 A) and correlating with a prior defined increase in DENV RNA, IFN- β and ISGs such as viperin (Al-Shujairi et al., 2017). In contrast, FH mRNA levels remained unchanged throughout the entire time course of infection (Figure VI-10 B). Thus, only FB mRNA is induced while FH mRNA does not change following DENV infection in the brain of immunocompetent mice.

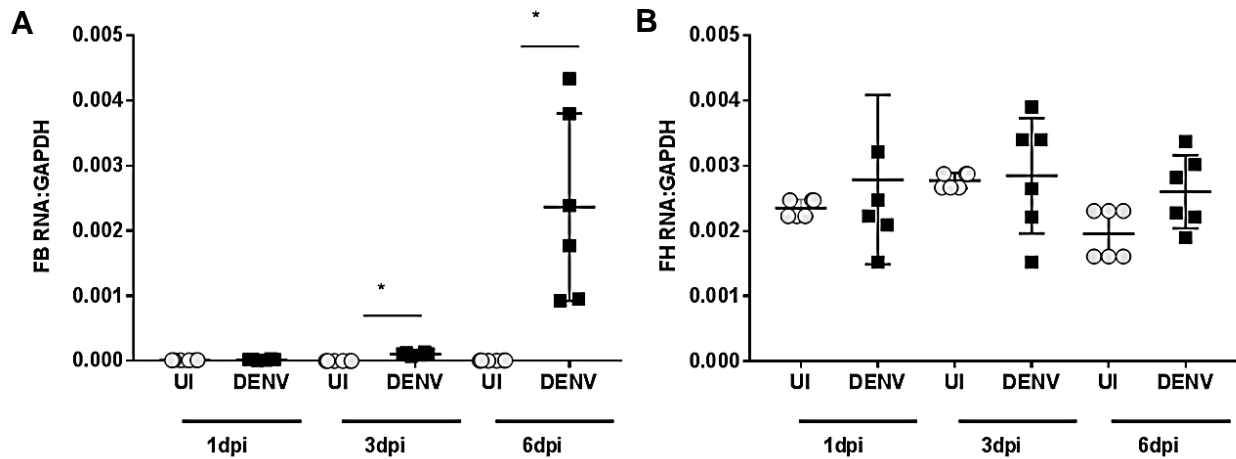


Figure VI-10. FB mRNA but not FH is increased in brain following intracranial DENV infection

Three- to four-week-old C57BL/6 mice were infected by intracranial injection with DENV-2 MON601 or mock infected (n=6 each group). At the indicated time points mice were euthanized, brains harvested and total RNA extracted and subjected to RT-PCR for (A) FB and (B) FH. Results were normalized against GAPDH and relative mRNA levels quantitated by ΔC_t method. Results represent the mean \pm standard deviation from each mouse group. * $p < 0.05$, one-way ANOVA/Tukey's test.

VI.3 Discussion

The present study has investigated changes in FB and FH following DENV infection in two *in vivo* models, human and mouse, to evaluate possible alterations of the AP pathway and compare two scenarios that differ in terms of IFN signalling. First, FB and FH proteins were evaluated and compared within a human cohort of returned travellers to South Australia with febrile syndrome and presenting for DENV diagnostic testing. This cohort was stratified into DENV-seronegative and seropositive patients. Both DENV-seronegative and seropositive groups were comparable in terms of age and gender and the characteristics of this cohort have been published (Quinn et al., 2018). Of the eight DENV-seronegative subjects three reflected fever of unknown origin while five were diagnosed with gastrointestinal or parasitic infections (data not shown). The levels of FB were significantly lower in the DENV-seropositive group compared to the DENV-seronegative group. Both groups, however, showed a distribution of a large number of data points above the reference range for normal FB of 200-500ug/ml, suggesting potential activation of the AP. For DENV this appears to be more limited than other non-DENV infectious diseases and is consistent with the relatively low CRP values also described in the DENV-seropositive patients from this cohort (Quinn et al., 2018) and in other studies (Nascimento et al., 2009, Tavakolipoor et al., 2016). Both CRP and complement proteins, such as FB are considered acute phase reactants (Markiewski and Lambris, 2007, Pionnier et al., 2014) and in particular complement components are increased during viral infections. For example C4 during acute HIV infection (Huson et al., 2015), C3 during acute hepatitis B virus infection (Lei et al., 2013), C3d in chronic HCV infection (Weiner et al., 2004) and CRP and C3 in patients with severe influenza (Gao et al., 2017). The relationship of circulating FB to AP activity is complex, with increased FB indicative of stimulation of AP activity but conversely low FB also indicative of high AP activity, due to cleavage of FB and thus complement consumption of FB. Lower levels of FB have previously been reported in patients with severe DENV disease, specifically during the shock period, reportedly due to complement 'consumption' and degradation of FB protein (Bokisch et al., 1973, Churdboonchart et al., 1983). The DENV cohort used in our study represents primary DENV infection in returned travellers, with only 14% of the patients in the DENV-seropositive cohort presenting with DENV warning signs and none of these patients developing severe dengue (Quinn et al., 2018). It remains to be determined if the lower level of FB in our DENV-seropositive compared to seronegative patients in this cohort reflects a poorer induction of FB or greater complement consumption, relative to other

infectious diseases.

The analysis of circulating FH protein levels shown that there was no change in DENV-seropositive patients compared to the levels in DENV-seronegative individuals. Again, this is consistent with previous findings that have reported no variation in FH during the acute phase in DF patients (Nascimento et al., 2009). Notably, the same study revealed that plasma levels of FH were lower during the acute phase in DHF patients compare to those in DF patients and healthy individuals (Nascimento et al., 2009). The authors suggested that DHF individuals have a limited capacity to sustain normal FH levels during the acute viral infection due to genetic factors (Nascimento et al., 2009). Regardless of the cause of FH alterations, it seems that circulating FH is not induced during acute DENV infection in DF patients and circulating FH decreases in DHF. Again unfortunately, our cohort does not include severe DENV (DHF) patients and while our results confirm the prior finding of no change in circulating FH in DF patients our study cannot confirm that a reduction in circulating FH occurs during severe DENV.

Thus, our human cohort has some limitations: the absence of a healthy control group and the lack of DENV-infected patients with severe disease. One advantage however of using the DENV-seronegative group as a comparator, is that the samples have been through the same diagnostic sample handling process to account for any potential sample degradation. The lack of severe DENV can be addressed using a patient cohort from a DENV endemic country, where both dengue and severe dengue patients will be represented and this should be investigated in future work.

Alternatively, to address the lack of data representing severe DENV disease, this study was extended to two different immunocompromised mouse models. Both of these models utilised AG129 mice, deficient in IFN signalling, and induced severe disease that mimics some features of DHF in humans (Ng et al., 2014). A low-dose 10^4 PFU DENV infection in AG129 mice induces acute viremia, peaking at 4dpi, with vascular leakage and moribund stage days-weeks after the viremia has cleared (Ng et al., 2014). The AG129 model infected with DENV (10^3 PFU), involved infection of young mice born to DENV naïve mothers (DENV-N) or from mothers challenged and recovered from a DENV-1 infection prior to mating (DENV-I) (Ng et al., 2014). The DENV-N animals are reported to develop severe acute DENV disease where viremia increases rapidly from 3dpi, accompanied by ruffled fur, hunched back and severe diarrhoea, a warning sign of severe dengue in humans (Ng et al., 2014). The DENV-I mice in this model with pre-existing maternal

antibody progressed into lethargy very quick and reached the moribund stage and ethical termination of experiments at 6dpi (Ng et al., 2014). Additionally, DENV-I animals at moribund stage (6dpi) are characterised by increased vascular permeability in multiple organs (liver, kidney, intestine and spleen) compared to moribund DENV-N animals, which represents an enhanced disease severity in DENV-I mice. What is more, the difference in the numbers of samples evaluated at 3 (eight samples) and 6 (five samples) dpi is due to the fact that three DENV-I mice reached the ethical end-point of experiment at 5 dpi and were euthanised, which highlights the severity of the disease in the model with prior maternal DENV immunity. In the primary DENV 10^4 PFU model, levels of circulating FB protein were unchanged during the entire course of infection (2-4dpi or moribund 20-22 dpi). Similarly, in the comparable AG129 DENV-N 10^3 PFU model, FB did not change during the acute phase of infection (day 3), but decreased later (day 6) during infection. In AG129 DENV-I infected with DENV (10^3 PFU), FB increases early at 3dpi but then again decreased at 6dpi, when the mice became moribund and was significantly lower than DENV-N mice at 6dpi. The observation of increased FB during severe secondary acute infection and the following decreased at moribund stage of DENV-I mice is consistent with activation of FB as an acute phase reactant, then subsequent decrease in FB due to complement consumption and excessive activity. Once again, these results are in agreement with the decline in FB observed in DHF patients during the shock phase (Bokisch et al., 1973). Together, circulating FB protein levels in the AG129 mouse model of DENV infection at 6dpi, but not earlier, reflect the late decline in FB reported in DHF (severe DENV) in humans (Bokisch et al., 1973, Churdboonchart et al., 1983) and our results further suggest that acute increase in FB and degree of this late decline in FB is associated with the severity of disease.

In the primary DENV 10^4 PFU model, FH protein underwent a transient significant decrease at 4dpi, with levels of circulating FH protein restored at moribund stage (20-22dpi). Similarly, FH protein in AG129 mice infected with 10^3 PFU DENV showed an initial decrease at 3dpi, although this was only significant in DENV-I mice, followed by an increase at 6dpi for both DENV-N and DENV-I mice. In DENV-N mice the increase in FH at 6dpi, is significantly less than DENV-I, where at this time point the mice are not moribund and have less severe DENV disease. This early decreases in FH levels are again consistent with prior reports in DHF cases (Nascimento et al., 2009) while the increase at late stages of severe disease has not been previously reported. An increase in FH at this time point, when FB is declining and there is presumptive complement

consumption, may reflect homeostatic mechanisms to bring the excessive complement activity under control.

Together, these results suggest that the pathology of DENV disease in mice may be reflective of DENV in humans during the early viremic phase and during severe haemorrhagic disease, with changes in complement FB and FH similar in both models of infection. Results support the notion that DENV infection induces dysregulation of the AP, not only at the local environment in macrophages and EC as was demonstrated in chapter IV, but also in the circulation.

In general, circulating changes of FB and FH proteins were not reflected by mRNA changes in the liver or kidney of the AG129 mice. Irrespective of the levels of FB and FH proteins in the serum, at 4dpi, liver FB and FH mRNAs increased during DENV infection. FH mRNA was still increased at moribund stage in the primary 10^4 PFU DENV infection model but neither FB nor FH mRNA was altered at 6dpi of the DENV-N and DENV-I models, despite a significant increase in FH and decline in FB protein in the circulation of these DENV-infected mice. Animals infected with 10^4 PFU DENV display normal or mild organ damage which could explain the ability of the liver to produce FB and FH mRNA during the peak of viremia, and even at moribund stage. Likewise, no major damages have been observed in the liver of DENV-N or DENV-I mice (Ng et al., 2014), although no significant FB or FH mRNA response was observed in this case. Regardless, the implication here is that in the setting of either acute or haemorrhagic DENV disease, the liver is not the main source of circulating FH and FB proteins.

Considering the similarity between the circulating changes in FB and FH during DENV infection in humans and the AG129 mouse model, with the latter deficient in IFN signalling pathways, a MatInspector analysis was performed *in silico* with a particular focus on putative TF associated with the IFN or inflammatory response that could regulate the FB and FH promoters in both mouse and human. Results of chapter V have already identified IRFF, STAT and NF κ B elements as potential regulators of the human FB and FH promoters (see Figure V-1 and Figure V-2). Similarly, several members of the families of IRFF and STAT were also present in the mouse FB and FH promoters. Further, the putative identification of IRFF elements suggests that the mouse FB and FH genes should be influenced by IFN. In chapter V, results have shown that FH and FB are induced by IFN- β , at least in EC. Additionally IFN- γ , is a major regulator of human FB and FH promoters, as discussed in chapter V, and is also a major regulator of murine FB and FH

mRNAs (Nonaka et al., 1989a, Nonaka et al., 1989b, Vik, 1996, Huang et al., 2002). Both type I (IFN- β) and type II (IFN- γ) signalling responses are lacking in our AG129 mouse model, due to the genetic lack of IFNAR α/β and γ -receptors, suggesting the induction of FB and FH reported here in the DENV-infected AG129 mouse must be mediated by factors other than IFN.

TNF α is a factor known to be induced during DENV infection in humans and mice, and has been associated with increased disease severity (Tan et al., 2010, Ng et al., 2014). TNF- α can exert transcriptional changes in a cell via NF κ B response elements. NF κ B responsive elements are shared by the human and mouse FB promoter, but in contrast to the human FH promoter, no NF κ B binding site was predicted in the mouse FH promoter. This observation is supported by the literature, where a mouse FB promoter-luciferase reporter construct with the NF κ B binding sites located at -433 and -423 mutated has reduced promoter activity in macrophages stimulated with TNF α (Huang et al., 2002). In the same study, LPS (a TLR4 ligand) was also shown to induce FB promoter activity by a mechanism, requiring the -433 and -423 NF κ B binding sites (Huang et al., 2002). Since DENV NS1 protein has been recently shown to stimulate TLR4 (Modhiran et al., 2015), the induction of FB in DENV-infected AG129 mice lacking IFN signalling pathway, may be mediated through NF κ B and TLR pathways. Furthermore, IL-6, a cytokine significantly elevated in DENV-infected AG129 mice (Tan et al., 2010, Ng et al., 2014), has been identified as an activator of STAT3 promoting acute phase gene expression such as IL-11, IL-21, IL-27 as well as granulocyte colony stimulating factor. The mouse FB promoter contains at least six predicted STAT3 responsive elements, suggesting additional cytokine-mediated pathways that may act via the STAT3 TF to induce the mouse FB promoter.

Since the mouse FH promoter lacks predicted NF κ B responsive elements, mouse FH may not be influenced by TNF α in the same manner as human FH would during a DENV infection. The mouse FH promoter however, shows a strong influence of STAT elements, mainly STAT5. STAT5 can be activated by inflammatory cytokines including members of the IL-2 (IL-2, IL-7, IL-15, IL-21) and IL-3 families (IL-3, IL-5) (reviewed in (Kisseleva et al., 2002), thus it is possible that the mouse FH promoter could be activated during DENV infection through actions of these cytokines. IL-2, IL-21 and IL-5 are reported to be increased during DENV infection in humans (Maneekean et al., 2013), but changes in these cytokines have not yet been reported in the DENV-AG129 mouse, and may be an area of

future study. Additionally, the conventional notion that IFN-activated TF only consist of phosphorylated STATs (the canonical STAT pathway) is being challenged with growing evidence of un-phosphorylated STATs playing a role in gene regulation (non-canonical pathway) (Au-Yeung et al., 2013). For instance, ISGs such as OAS-1 and IFI-27 have been shown to be expressed in STAT1-deficient cells that had been reconstituted with un-phosphorylated Y701F STAT1 mutant (Cheon and Stark, 2009). On the other hand, it has been described that some viruses such as Epstein-Barr virus, Kaposi's sarcoma-associated herpesvirus, HIV-1 and porcine reproductive and respiratory syndrome virus (PRRSV), are able to induce serine monophosphorylation of STATs in the absence of IFN signalling pathways, which imply novel functions of STATs during virus infection and pathogenesis (McLaren et al., 2007, King, 2013, Nan et al., 2018). Epstein-Barr virus is capable of specifically promoting the expression of several ISGs (ISG15K, ISG54K, and ISG56K) in an IFN-independent manner by inducing STAT1 phosphorylation (Ruvolo et al., 2003, McLaren et al., 2007). Studies on Kaposi's sarcoma-associated herpesvirus have demonstrated serine monophosphorylation of STAT3 leading to elevation of STAT3-dependent genes, including IL-6, and transforming growth factor- β (King, 2013). PRRSV and HIV-1 on the other hand, also promote IFN-independent serine monophosphorylation of STAT1 and STAT1 and 3, respectively, resulting in higher levels of pro-inflammatory cytokine gene expression *in vitro* (Chaudhuri et al., 2008, Yu et al., 2013). Therefore, it appears that expression of particular genes can be promoted by un-phosphorylated STAT or IFN-independent monophosphorylation of STATs which may constitute an alternative explanation for the induction of FH mRNA in DENV-infected AG129 mice lacking IFN responses. Prior evidence from DENV infection of primary EC in our laboratory have demonstrated DENV induction of un-phosphorylated STAT1 (Calvert et al., 2015), and the ability of DENV to drive IFN-independent STAT1-mediated gene transcription could be further investigated.

Altogether these results support the idea that for human and mouse FH and FB, the circulating complement responses during a natural infection in humans compared with an experimental infection in the AG129-IFN deficient mouse are similar, and associated with disease severity, suggesting this is a valid model to study the role of FB and FH in the pathogenesis of severe DENV disease. The predicted differences in important IFN-driven and NF κ B-responsive elements in the FH and FB promoters, however suggest DENV-induced responses in the human and AG129 mouse model may be triggered through different mechanisms. This suggests that while the AG129 DENV-mouse model may not

be reflective of the complete natural response of the AP to DENV infection, the model may be useful in delineating the contribution of IFN-dependent and $\text{NF}\kappa\beta$ -driven responses of FB and FH during DENV infection. In particular, since IRFF TFs and specifically, $\text{IFN-}\gamma$ drives FB and FH induction in human and mouse, an alternative mouse model such as $\text{IFNAR}^{-/}$, deficient only in $\text{IFN}\alpha/\beta$ receptor (Prestwood et al., 2012b), could be a feasible platform to study the regulation of FB and FH by DENV-induced $\text{IFN-}\gamma$ in more depth.

Given that both FB and FH human and mouse promoters showed a strong dependence of IFN-regulatory elements, the regulation of FH and FB by DENV was investigated in an intracranial model of DENV infection in immunocompetent mice with a fully competent IFN response. The brain is an important site of immune privilege, where DENV can successfully replicate, and prior studies from our laboratory have demonstrated increasing DENV RNA with time, increase in brain CD8^+ T-cells and induction of ISGs (Al-Shujairi et al., 2017). Surprisingly, however, the induction of ISGs such as viperin appeared prior to the induction of $\text{IFN-}\beta$, suggesting that DENV-induction of ISGs in this brain model of infection may occur in an $\text{IFN-}\beta$ independent manner (Al-Shujairi et al., 2017). FB mRNA was rapidly induced from 3dpi and by 6dpi FB mRNA was even higher, corresponding with the increasing levels of viral RNA and viperin mRNA levels in the brain (Al-Shujairi et al., 2017). Surprisingly, FH mRNA did not change during the entire course of infection even in the context of a fully immune competent system. These results contrast to our prior data in MDM and EC (Chapter IV), where both FB and FH appear co-ordinately induced by DENV in a manner that parallels other ISGs, such as viperin. Here, in contrast, FH is not induced in the same manner as FB and other ISGs in this tissue. Excluding differences in IRFF and ISRE since IFN signalling is absent in this system, comparison of the FH and FB promoters in the mouse suggests that these different responses in the brain may be mediated by $\text{NF}\kappa\beta$ responsive elements, present in mouse FB but not FH, or STAT1/STAT3 elements acting in an IFN-independent manner, as described above. Additionally, considering that $\text{IFN-}\gamma$ is a major regulator of FH expression (Schlaf et al., 2002, Kim et al., 2009, Amadi-Obi et al., 2012), and the brain is an important source of this cytokine (Wei et al., 2000) it is surprising that elevated levels of FH mRNA were not observed following DENV infection. DENV induction of $\text{IFN-}\gamma$, however, has not been validated to occur in the DENV-infected mouse brain, and this remains to be defined. The implication of the divergent responses of FB and FH during DENV infection in the brain is, assuming other components of the AP pathway such as C3 are present, a predicted increase in the activity of the AP. The role of the complement AP in controlling, clearing or

driving pathology during viral infection in the brain has never been investigated and is an exciting area of future study.

In summary, in this study similar responses of complement FB and FH were found during DENV infection in humans and immunocompromised mice lacking IFN signalling pathways, and support the use of this mouse model to further investigate mechanisms that control the activity of the complement AP and the pathogenesis of DENV infection.

CHAPTER VII GENERAL DISCUSSION AND FUTURE DIRECTIONS

Infection caused by DENV is considered the most important mosquito-borne viral disease of humans in the world (Guzman et al., 2010, Bhatt et al., 2013). Recent reports from the WHO indicate that more than 40% of the world's population is at risk of DENV infection, with an estimated 390 million infections worldwide each year in more than 100 countries (WHO, 2009, Bhatt et al., 2013). Dengvaxia[®], the unique vaccine available against DENV, exhibits low protective capacity against the serotypes 1 and 2 and is only safe to use in individuals living in endemic areas (Guy and Jackson, 2016, Wichmann et al., 2017). In addition, there are no antiviral therapies for DENV infection, only supportive treatments for DENV-infected patients. Thus, there is a real need not only to prevent the infection but also to treat the disease. To develop ways to treat the disease, more knowledge of the mediators of DENV pathogenesis are needed.

Multiple factors are already known to contribute to the pathogenesis of DENV disease including increased viral load, cross-reactive T-cell responses, the presence of heterotypic non-neutralising antibodies during a secondary infection, and the 'cytokine storm' (Halstead, 1989, Halstead, 2003, Green and Rothman, 2006, Rothman, 2011). The role of the complement system in DENV pathogenesis has been controversial. While a number of studies have reported a beneficial role of the complement system, particularly the LP in protecting against DENV (Avirutnan et al., 2011), evidence has also suggested a role for complement in the pathogenesis of DENV disease. Specifically, dysregulation of the AP of the complement system is associated with severe forms of the disease, DHF and DSS (Nascimento et al., 2009). This evidence prompted us to investigate the changes in two main regulatory factors of the AP with opposing roles in the complement cascade: FB a positive mediator, and FH a negative regulator, in the context of DENV infection. The current thesis describes a sequence of experiments in *in vitro* and *in vivo* models of DENV infection directed to study the way the complement AP responds to DENV infection with a view to understanding how this may influence DENV disease.

In chapter III, essential assays were established that were then applied to human and mouse models of DENV infection. Further improvements could be the generation of specific assays to discriminate FH and FHL-1 proteins, and investigate the cleavage of FB. In chapter IV induction of FH and FB mRNA and proteins in DENV-infected EC and macrophages, important primary cell types relevant to DENV infection *in vivo*, was defined.

Results show a significant increase in FB and FH mRNA in DENV-infected cells but surprisingly this corresponded to an increase only in FB and not FH protein. These changes were accompanied by other measures reflecting increased hyperactivity of the AP during DENV infection; the ratio between FB and FH proteins showed an increase in FB (the activator) relative to FH (the negative regulator) in DENV-infected compared with uninfected cells, increased deposition of C3b on DENV-infected cells along with enhanced ability of DENV-infected supernatants to promote AP lytic activity *in vitro*. This could result in augmented C3 convertase activity, increased formation of complement activation products such as the anaphylotoxins C3a and C5a, and the MAC (C5b-9) that could directly act on EC and adversely affect their function. One important aspect not addressed in our studies is the effects of these changes in AP activity on the DENV-infected macrophage, a key site for DENV replication and a potential target for complement-mediated clearance. Future studies may, for instance, address the ability of the AP to lyse or effect the inflammatory cytokine/chemokine expression profile of DENV-infected macrophages *in vitro*. Our studies predicted that these overall changes in complement AP activity, locally at the endothelium could result in increased DENV-induced vascular leakage, a hallmark of DENV disease. As a first step towards testing the relationship between changes in FB and FH and DENV-induced pathology, studies were undertaken using *in vivo* models of DENV infection, as discussed further below.

Results of this thesis have also made progress into defining factors that may control the induction of FH and FB mRNA during DENV infection and suggest a role for type I IFN (IFN- β) and other factors with well-defined roles in innate immune responses in control of FH and FB gene expression (Chapter V). Using the MatInspector software tool to identify TF binding sites, several IFN-responsive elements along with NF κ B and STAT binding elements were identified within the human FB and FH promoter regions. This suggests that both FH and FB are triggered by similar stimuli and intracellular signalling pathways. By blocking the action of endogenously produced IFN- β , it was experimentally demonstrated that this cytokine with a central role in regulating innate anti-viral immune responses against DENV, also regulates induction of both FB and FH mRNA in DENV-infected cells. Interestingly, IFN- β regulation of FB and FH was observed in EC but not in MDM. Previous studies have demonstrated that IFN- γ is a major inducer of FH and FB in several cell types including hepatocytes, fibroblasts, macrophages, epithelial and endothelial cells (Lappin et al., 1992, Friese et al., 2000, Friese et al., 2003, Wu et al., 2007) and a potential area of future investigation is defining the role of IFN- γ in driving the

expression of these factors in DENV-infected monocyte/macrophages. Additionally, ongoing work of an honours student in our laboratory extends from this study and will define the FH promoter elements responsive to DENV infection through analysis of the activity of a FH-Luciferase reporter construct in DENV-infected cells, and effects of treatment with STAT inhibitors or with selected elements deleted from the FH promoter.

The findings from chapter IV were also extended to investigate the changes in FB and FH in AG129 mice, a mouse model of DENV infection deficient in type I and type II IFN receptors (Chapter VI). Data shows an early decrease in FH protein while FB significantly increases in the serum of DENV-infected animals experiencing the most severe forms of DENV disease. Further, a late decrease in FB and increase in FH protein was detected in mice with severe DENV suggesting excessive complement consumption and activity late in disease. Surprisingly, changes in circulating FB and FH proteins were not reflected by changes in liver mRNA, suggesting that in contrast to the literature, either this tissue is not the major source of these circulating proteins or that circulating responses during DENV infection are driven by translational rather than transcriptional regulation. Importantly, these alterations in the level of both proteins in the circulation of DENV-infected AG129 mice are indicative of hyper-activation of the AP and are consistent with the responses described in DHF and DSS patients (Bokisch et al., 1973, Nascimento et al., 2009). Further, since AG129 mice lack IFN receptors, the changes observed in FH and FB during DENV infection of AG129 mice are reflective of IFN-signalling independent regulation.

Thus, the mouse FB and FH promoters were assessed for potential TF binding sites, again using the MatInspector software. The results show the presence of IFN regulatory elements, but also STAT and/or NF κ B-responsive elements in both mouse FB and FH promoters (Chapter VI). This data combined with the existing literature (Huang et al., 2002) suggest that the mouse FB promoter may be regulated by inflammatory mediators such as TNF α and IL-6, factors known respectively to stimulate NF κ B and STAT pathways, and that are also known to be induced in DENV-infected AG129 mice (Tan et al., 2010, Ng et al., 2014). In contrast, the mouse FH promoter lacks NF κ B binding elements, but may be induced by STAT TF. The *in vivo* regulation of FH and FB during DENV infection could be further defined through infection of mice lacking genes to drive these potential TF, such as the IFNAR^{-/-} mouse model, deficient only in IFN- α/β receptor (Prestwood et al., 2012b) to investigate the role of IFN- γ stimulation, or STAT-deficient mice such as STAT1^{-/-} or STAT2^{-/-} (Chen et al., 2008, Perry et al., 2011) to define the role

of the ISRE, or TNF- $\alpha^{-/-}$ mice (Glasner et al., 2017) to investigate the potential role of the NF κ B element. Similarly, macrophages and EC could be isolated from AG129 mice and DENV-infected *in vitro* to investigate the role of IFN signalling in the induction of FH and FB.

Dysregulation of the AP has been extensively studied in atypical haemolytic-uremic syndrome (a-HUS), a human disease that is also characterised by damage to the endothelium and increased vascular leakage (Zhang et al., 2017a). The best treatment for this rare disease is based on the administration of Eculizumab, a humanised murine monoclonal antibody against C5, which prevents C5 cleavage and thus inhibits C5a release and the assembly of the terminal pathway of the complement system (Cofieill et al., 2015). This drug is considered the most expensive drug in the world and therefore, other protocols including plasma exchange/infusion have been used as an alternative treatment in this setting (Kerr and Richards, 2012). This however, is a drastic measure and although plasma exchange has significantly improved morbidity and mortality in a-HUS patients (Waters and Licht, 2011) it is unlikely to be applicable to treatment of severe DENV, particularly given the large number of DENV cases, often in resource poor settings. Interestingly, the dysregulation of the AP described in a-HUS is not due to the lack of FH induction; rather in the majority of cases is caused by mutations in FH and other negative regulators of the AP such as FI and CD46 (Zhang et al., 2017a). Based on this lack of negative regulation of the AP in a-HUS, other possible therapeutic strategies include the development of a plasma-derived FH concentrate (Fakhouri et al., 2010), the production of recombinant FH protein (Schmidt et al., 2011) or TT30, a FH fusion protein that binds to CR2 and blocks C3-derived fragments accumulation on activated surfaces, MAC formation and haemolysis of red blood cells (Fridkis-Hareli et al., 2011). Recently, a nanobody that prevents proconvertase assembly by inhibiting FB binding to C3b has been proposed as a powerful tool to decay AP activity (Jensen et al., 2018). Thus, there are a growing number of agents with the potential to promote FH actions and regulate the AP. Our study may be the starting point for the future development of novel potential agents such as these to promote FH levels and downregulate the AP activity during DENV infection. Additionally, our study has identified that although FH mRNA is induced by DENV, the protein levels are unchanged, and thus approaches to specifically promote FH protein production from DENV-infected macrophages and EC might be a feasible strategy to counteract the imbalance in FH:FB levels during DENV infection. Lastly, while this study has clearly demonstrated deficits in FH and FB that could link to AP hyperactivity during DENV, it

would also be interesting to investigate the role of other complement AP negative regulators such as FI and CD46, to define the breadth of dysregulation of this system during DENV infection.

VII.1 Conclusions

This study has contributed to the knowledge and understanding of the regulation of the AP during DENV infection, in particular through changes in FH and FB. Outcomes suggest potential new roles of the AP complement cascade in DENV disease and propose new layers in the cellular mechanisms that may alter EC barrier function and could contribute to vascular permeability and haemorrhage during DENV infection. The dysregulation of the AP that has been demonstrated here occurs within the local environment of EC and MDM, and also in the circulation of DENV-infected mice, providing fundamental knowledge in both primary *in vitro* and small animal *in vivo* model systems for future laboratory investigations. Importantly, DENV-induced changes in complement FB and FH are similar in both human and mouse models of DENV infection demonstrating the utility of the AG129 mouse model for the study of the role of complement AP in DENV pathogenesis. Altogether this study provides encouragement for the identification of new therapeutic agents to control DENV-induced dysregulation of the AP as a potential avenue for preventing the increased vascular permeability and treating the severe forms of DENV disease.

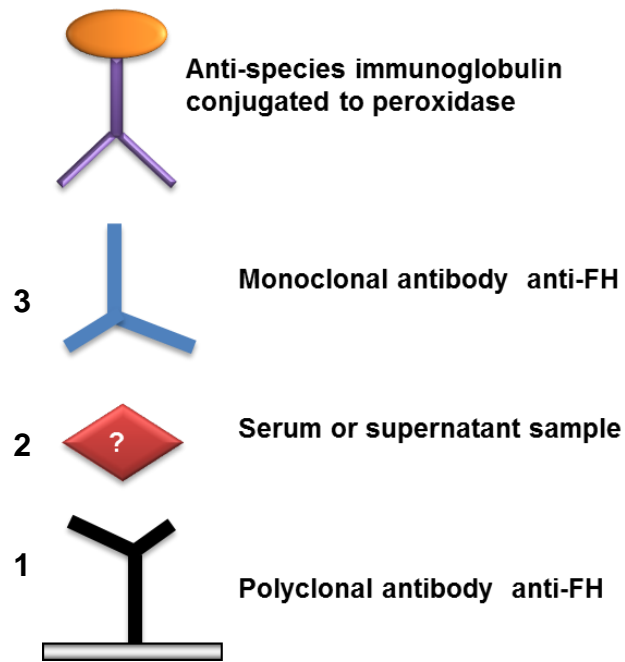
APPENDICES

Appendix 1. Analysis sequence of building blocks used in the high-throughput imaging system (Operetta)

Cells were fixed, permeabilised and subsequently immunostained as described in chapter II, section II.2.17. Images from 49 fields of view were taken and quantitated using Harmony software (PerkinElmer) with the following analysis sequence. Building blocks were created and defined with [] as below.

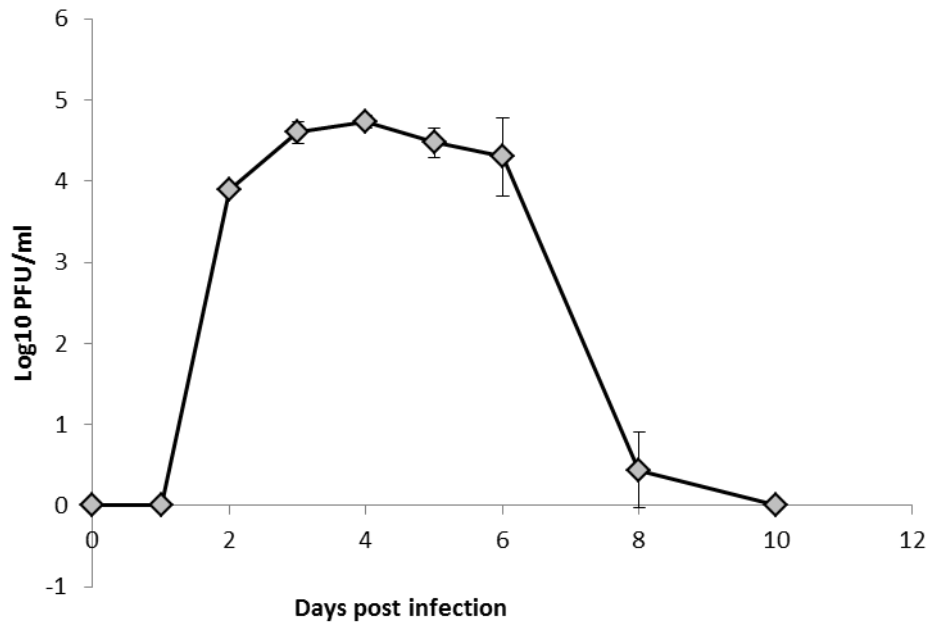
Analysis Sequence

1. [Input Image]- Stack processing Individual Planes
2. [Find Nuclei]- Channel Hoechst; Method: B; Output Population: Nuclei
3. [Find Cytoplasm]- Channel Cy3, Nuclei: all cells, Method: B; Output Population: all cells
4. [Calculate Intensity Properties]- Channel Alexa 488, Population: all cells, Region: Cytoplasm, Output Properties : A488 intensity cell
5. [Select Population]- Population: all cells, Method: Filter by Property A488 intensity cell Mean : > 800, Output Population: DENV-positive
6. [Select Population (2)]- Population: all cells, Method: Filter by Property A488 intensity cell Mean : < 800, Output Population : DENV-negative
7. [Calculate Intensity Properties (2)]- Channel: Cy3, Population: DENV-positive, Region: Cell, Output Properties : Cy3 intensity DENV-positive
8. [Calculate Intensity Properties (3)]- Channel: Cy3, Population: DENV-negative, Region: Cell, Output Properties: Cy3 intensity DENV-negative
9. [Calculate Intensity Properties (4)]- Channel: Cy3, Population: all cells, Region: Cell, Output Properties: Cy3 intensity all cells
- 10.[Calculate Intensity Properties (5)]- Channel: Alexa647, Population: DENV- positive, Region: Cell, Output Properties: Alexa647 intensity DENV-positive mean
- 11.[Calculate Intensity Properties (6)]- Channel: Alexa647, Population: DENV-negative, Region: Cell, Output Properties: Alexa647 intensity DENV-negative mean
- 12.[Calculate Intensity Properties (7)]- Channel: Alexa647, Population: all cells, Region: Cell, Output Properties: Alexa647 intensity all cells mean



Appendix 2. Schematic representation of the sandwich ELISA developed to detect human and mouse FH proteins

A broadly cross-reactive anti-FH polyclonal antibody is immobilized (1) to increase the possibility of capturing any available FH protein in serum sample or cell supernatant (2) while a monoclonal antibody is used as a detecting molecule to increase the specificity of the assay (3).



Appendix 3. Course of viremia in AG129 mice infected with 10⁴ PFU of D2Y98P strain.

Five- to six- weeks old AG129 mice were infected with 10⁴ PFU/mouse of DENV-2 strain D2Y98P. At the indicated time points mice were euthanized, blood harvested and serum subjected to plaque assay for viremia quantitation. This figure was kindly provided by Dr. Penny Rudd, Griffith University, Queensland, Australia.

BIBLIOGRAPHY

- AASA-CHAPMAN, M. M., HOLUIGUE, S., AUBIN, K., WONG, M., JONES, N. A., CORNFORTH, D., PELLEGRINO, P., NEWTON, P., WILLIAMS, I., BORROW, P. & MCKNIGHT, A. 2005. Detection of antibody-dependent complement-mediated inactivation of both autologous and heterologous virus in primary human immunodeficiency virus type 1 infection. *J Virol*, 79, 2823-30.
- ACOSTA, E. G., CASTILLA, V. & DAMONTE, E. B. 2008. Functional entry of dengue virus into *Aedes albopictus* mosquito cells is dependent on clathrin-mediated endocytosis. *J Gen Virol*, 89, 474-84.
- ACOSTA, E. G., CASTILLA, V. & DAMONTE, E. B. 2009. Alternative infectious entry pathways for dengue virus serotypes into mammalian cells. *Cell Microbiol*, 11, 1533-49.
- ACOSTA, E. G., CASTILLA, V. & DAMONTE, E. B. 2012. Differential requirements in endocytic trafficking for penetration of dengue virus. *PLoS One*, 7, e44835.
- ACOSTA, E. G., KUMAR, A. & BARTENSCHLAGER, R. 2014a. Revisiting dengue virus-host cell interaction: new insights into molecular and cellular virology. *Adv Virus Res*, 88, 1-109.
- ACOSTA, E. G., PICCINI, L. E., TALARICO, L. B., CASTILLA, V. & DAMONTE, E. B. 2014b. Changes in antiviral susceptibility to entry inhibitors and endocytic uptake of dengue-2 virus serially passaged in Vero or C6/36 cells. *Virus Res*, 184, 39-43.
- ADINOLFI, M., DOBSON, N. C. & BRADWELL, A. R. 1981. Synthesis of two components of human complement, beta 1H and C3bINA, during fetal life. *Acta Paediatr Scand*, 70, 705-10.
- ADINOLFI, M. & ZENTHON, J. 1982. Complement and disease: a review. *J R Soc Med*, 75, 121-3.
- AGUIRRE, S., MAESTRE, A. M., PAGNI, S., PATEL, J. R., SAVAGE, T., GUTMAN, D., MARINGER, K., BERNAL-RUBIO, D., SHABMAN, R. S., SIMON, V., RODRIGUEZ-MADOZ, J. R., MULDER, L. C., BARBER, G. N. & FERNANDEZ-SESMA, A. 2012. DENV inhibits type I IFN production in infected cells by cleaving human STING. *PLoS Pathog*, 8, e1002934.
- AL-SHUJAIRI, W. H., CLARKE, J. N., DAVIES, L. T., ALSHARIFI, M., PITSON, S. M. & CARR, J. M. 2017. Intracranial Injection of Dengue Virus Induces Interferon Stimulated Genes and CD8+ T Cell Infiltration by Sphingosine Kinase 1 Independent Pathways. *PLoS One*, 12, e0169814.
- ALCON, S., TALARMIN, A., DEBRUYNE, M., FALCONAR, A., DEUBEL, V. & FLAMAND, M. 2002. Enzyme-linked immunosorbent assay specific to Dengue virus type 1 nonstructural protein NS1 reveals circulation of the antigen in the blood during the acute phase of disease in patients experiencing primary or secondary infections. *J Clin Microbiol*, 40, 376-81.
- ALHOOT, M. A., WANG, S. M. & SEKARAN, S. D. 2012. RNA interference mediated inhibition of dengue virus multiplication and entry in HepG2 cells. *PLoS One*, 7, e34060.
- ALPER, C. A., GOODKOFISKY, I. & LEPOW, I. H. 1973. The relationship of glycine-rich glycoprotein to factor B in the properdin system and to the cobra factor-binding protein of human serum. *J Exp Med*, 137, 424-37.
- AMADI-OBI, A., YU, C. R., DAMBUZA, I., KIM, S. H., MARRERO, B. & EGWUAGU, C. E. 2012. Interleukin 27 induces the expression of complement factor H (CFH) in the retina. *PLoS One*, 7, e45801.
- AMURA, C. R., RENNER, B., LYUBCHENKO, T., FAUBEL, S., SIMONIAN, P. L. & THURMAN, J. M. 2012. Complement activation and toll-like receptor-2 signaling

- contribute to cytokine production after renal ischemia/reperfusion. *Mol Immunol*, 52, 249-57.
- AN, J., KIMURA-KURODA, J., HIRABAYASHI, Y. & YASUI, K. 1999. Development of a novel mouse model for dengue virus infection. *Virology*, 263, 70-7.
- ANDERS, K. L., NGUYET, N. M., CHAU, N. V., HUNG, N. T., THUY, T. T., LIEN LE, B., FARRAR, J., WILLS, B., HIEN, T. T. & SIMMONS, C. P. 2011. Epidemiological factors associated with dengue shock syndrome and mortality in hospitalized dengue patients in Ho Chi Minh City, Vietnam. *Am J Trop Med Hyg*, 84, 127-34.
- ANDERSON, R., WANG, S., OSIOWY, C. & ISSEKUTZ, A. C. 1997. Activation of endothelial cells via antibody-enhanced dengue virus infection of peripheral blood monocytes. *J Virol*, 71, 4226-32.
- AOKI, C., HIDARI, K. I., ITONORI, S., YAMADA, A., TAKAHASHI, N., KASAMA, T., HASEBE, F., ISLAM, M. A., HATANO, K., MATSUOKA, K., TAKI, T., GUO, C. T., TAKAHASHI, T., SAKANO, Y., SUZUKI, T., MIYAMOTO, D., SUGITA, M., TERUNUMA, D., MORITA, K. & SUZUKI, Y. 2006. Identification and characterization of carbohydrate molecules in mammalian cells recognized by dengue virus type 2. *J Biochem*, 139, 607-14.
- APPANNA, R., HUAT, T. L., SEE, L. L., TAN, P. L., VADIVELU, J. & DEVI, S. 2007. Cross-reactive T-cell responses to the nonstructural regions of dengue viruses among dengue fever and dengue hemorrhagic fever patients in Malaysia. *Clin Vaccine Immunol*, 14, 969-77.
- APPANNA, R., PONNAMPALAVANAR, S., LUM CHAI SEE, L. & SEKARAN, S. D. 2010. Susceptible and protective HLA class 1 alleles against dengue fever and dengue hemorrhagic fever patients in a Malaysian population. *PLoS One*, 5.
- APPANNA, R., WANG, S. M., PONNAMPALAVANAR, S. A., LUM, L. C. & SEKARAN, S. D. 2012. Cytokine factors present in dengue patient sera induces alterations of junctional proteins in human endothelial cells. *Am J Trop Med Hyg*, 87, 936-42.
- ASHOUR, J., LAURENT-ROLLE, M., SHI, P. Y. & GARCIA-SASTRE, A. 2009. NS5 of dengue virus mediates STAT2 binding and degradation. *J Virol*, 83, 5408-18.
- ASHOUR, J., MORRISON, J., LAURENT-ROLLE, M., BELICHA-VILLANUEVA, A., PLUMLEE, C. R., BERNAL-RUBIO, D., WILLIAMS, K. L., HARRIS, E., FERNANDEZ-SESMA, A., SCHINDLER, C. & GARCIA-SASTRE, A. 2010. Mouse STAT2 restricts early dengue virus replication. *Cell Host Microbe*, 8, 410-21.
- ATKINSON, J. P. & GOODSHIP, T. H. 2007. Complement factor H and the hemolytic uremic syndrome. *J Exp Med*, 204, 1245-8.
- AU-YEUNG, N., MANDHANA, R. & HORVATH, C. M. 2013. Transcriptional regulation by STAT1 and STAT2 in the interferon JAK-STAT pathway. *JAKSTAT*, 2, e23931.
- AVIRUTNAN, P., FUCHS, A., HAUHART, R. E., SOMNUKE, P., YOUN, S., DIAMOND, M. S. & ATKINSON, J. P. 2010. Antagonism of the complement component C4 by flavivirus nonstructural protein NS1. *J Exp Med*, 207, 793-806.
- AVIRUTNAN, P., HAUHART, R. E., MAROVICH, M. A., GARRED, P., ATKINSON, J. P. & DIAMOND, M. S. 2011. Complement-mediated neutralization of dengue virus requires mannose-binding lectin. *MBio*, 2.
- AVIRUTNAN, P., PUNYADEE, N., NOISAKRAN, S., KOMOLTRI, C., THIEMMECA, S., AUETHAVORNANAN, K., JAIRUNGSRI, A., KANLAYA, R., TANGTHAWORNCHAIKUL, N., PUTTIKHUNT, C., PATTANAKITSAKUL, S. N., YENCHITSOMANUS, P. T., MONGKOLSAPAYA, J., KASINRERK, W., SITTISOMBUT, N., HUSMANN, M., BLETTNER, M., VASANAWATHANA, S., BHAKDI, S. & MALASIT, P. 2006. Vascular leakage in severe dengue virus infections: a potential role for the nonstructural viral protein NS1 and complement. *J Infect Dis*, 193, 1078-88.
- BASU, A., JAIN, P., GANGODKAR, S. V., SHETTY, S. & GHOSH, K. 2008. Dengue 2

- virus inhibits in vitro megakaryocytic colony formation and induces apoptosis in thrombopoietin-inducible megakaryocytic differentiation from cord blood CD34+ cells. *FEMS Immunol Med Microbiol*, 53, 46-51.
- BEATTY, P. R., PUERTA-GUARDO, H., KILLINGBECK, S. S., GLASNER, D. R., HOPKINS, K. & HARRIS, E. 2015. Dengue virus NS1 triggers endothelial permeability and vascular leak that is prevented by NS1 vaccination. *Sci Transl Med*, 7, 304ra141.
- BEEBE, D. P. & COOPER, N. R. 1981. Neutralization of vesicular stomatitis virus (VSV) by human complement requires a natural IgM antibody present in human serum. *J Immunol*, 126, 1562-8.
- BELMUSTO-WORN, V. E., SANCHEZ, J. L., MCCARTHY, K., NICHOLS, R., BAUTISTA, C. T., MAGILL, A. J., PASTOR-CAUNA, G., ECHEVARRIA, C., LAGUNA-TORRES, V. A., SAMAME, B. K., BALDEON, M. E., BURANS, J. P., OLSON, J. G., BEDFORD, P., KITCHENER, S. & MONATH, T. P. 2005. Randomized, double-blind, phase III, pivotal field trial of the comparative immunogenicity, safety, and tolerability of two yellow fever 17D vaccines (Arlvax and YF-VAX) in healthy infants and children in Peru. *Am J Trop Med Hyg*, 72, 189-97.
- BENTE, D. A., MELKUS, M. W., GARCIA, J. V. & RICO-HESSE, R. 2005. Dengue fever in humanized NOD/SCID mice. *J Virol*, 79, 13797-9.
- BERNET, J., MULLICK, J., SINGH, A. K. & SAHU, A. 2003. Viral mimicry of the complement system. *J Biosci*, 28, 249-64.
- BETTONI, S., BRESIN, E., REMUZZI, G., NORIS, M. & DONADELLI, R. 2016. Insights into the Effects of Complement Factor H on the Assembly and Decay of the Alternative Pathway C3 Proconvertase and C3 Convertase. *J Biol Chem*, 291, 8214-30.
- BHATT, S., GETHING, P. W., BRADY, O. J., MESSINA, J. P., FARLOW, A. W., MOYES, C. L., DRAKE, J. M., BROWNSTEIN, J. S., HOEN, A. G., SANKOH, O., MYERS, M. F., GEORGE, D. B., JAENISCH, T., WINT, G. R., SIMMONS, C. P., SCOTT, T. W., FARRAR, J. J. & HAY, S. I. 2013. The global distribution and burden of dengue. *Nature*, 496, 504-7.
- BHATTACHARJEE, A., LEHTINEN, M. J., KAJANDER, T., GOLDMAN, A. & JOKIRANTA, T. S. 2010. Both domain 19 and domain 20 of factor H are involved in binding to complement C3b and C3d. *Mol Immunol*, 47, 1686-91.
- BIRKENKAMP, K. U. & COFFER, P. J. 2003. Regulation of cell survival and proliferation by the FOXO (Forkhead box, class O) subfamily of Forkhead transcription factors. *Biochem Soc Trans*, 31, 292-7.
- BLACKMORE, T. K., HELLWAGE, J., SADLON, T. A., HIGGS, N., ZIPFEL, P. F., WARD, H. M. & GORDON, D. L. 1998. Identification of the second heparin-binding domain in human complement factor H. *J Immunol*, 160, 3342-8.
- BLACKMORE, T. K., SADLON, T. A., WARD, H. M., LUBLIN, D. M. & GORDON, D. L. 1996. Identification of a heparin binding domain in the seventh short consensus repeat of complement factor H. *J Immunol*, 157, 5422-7.
- BLANEY, J. E., JR., HANSON, C. T., FIRESTONE, C. Y., HANLEY, K. A., MURPHY, B. R. & WHITEHEAD, S. S. 2004. Genetically modified, live attenuated dengue virus type 3 vaccine candidates. *Am J Trop Med Hyg*, 71, 811-21.
- BLAUM, B. S., HANNAN, J. P., HERBERT, A. P., KAVANAGH, D., UHRIN, D. & STEHLE, T. 2015. Structural basis for sialic acid-mediated self-recognition by complement factor H. *Nat Chem Biol*, 11, 77-82.
- BLOK, J. 1985. Genetic relationships of the dengue virus serotypes. *J Gen Virol*, 66 (Pt 6), 1323-5.
- BOKISCH, V. A., TOP, F. H., JR., RUSSELL, P. K., DIXON, F. J. & MULLER-EBERHARD, H. J. 1973. The potential pathogenic role of complement in dengue hemorrhagic

- shock syndrome. *N Engl J Med*, 289, 996-1000.
- BONAPARTE, R. S., HAIR, P. S., BANTHIA, D., MARSHALL, D. M., CUNNION, K. M. & KRISHNA, N. K. 2008. Human astrovirus coat protein inhibits serum complement activation via C1, the first component of the classical pathway. *J Virol*, 82, 817-27.
- BORDEN, E. C., SEN, G. C., UZE, G., SILVERMAN, R. H., RANSOHOFF, R. M., FOSTER, G. R. & STARK, G. R. 2007. Interferons at age 50: past, current and future impact on biomedicine. *Nat Rev Drug Discov*, 6, 975-90.
- BOUSSEMARY, T., BABE, P., SIBILLE, G., NEYRET, C. & BERCHEL, C. 2001. Prenatal transmission of dengue: two new cases. *J Perinatol*, 21, 255-7.
- BRAY, M., ZHAO, B. T., MARKOFF, L., ECKELS, K. H., CHANOCK, R. M. & LAI, C. J. 1989. Mice immunized with recombinant vaccinia virus expressing dengue 4 virus structural proteins with or without nonstructural protein NS1 are protected against fatal dengue virus encephalitis. *J Virol*, 63, 2853-6.
- BROOIMANS, R. A., VAN DER ARK, A. A., BUURMAN, W. A., VAN ES, L. A. & DAHA, M. R. 1990. Differential regulation of complement factor H and C3 production in human umbilical vein endothelial cells by IFN-gamma and IL-1. *J Immunol*, 144, 3835-40.
- BUTTHEP, P., CHUNHAKAN, S., YOKSAN, S., TANGNARARATCHAKIT, K. & CHUANSUMRIT, A. 2012. Alteration of cytokines and chemokines during febrile episodes associated with endothelial cell damage and plasma leakage in dengue hemorrhagic fever. *Pediatr Infect Dis J*, 31, e232-8.
- CALVERT, J. K., HELBIG, K. J., DIMASI, D., COCKSHELL, M., BEARD, M. R., PITSON, S. M., BONDER, C. S. & CARR, J. M. 2015. Dengue Virus Infection of Primary Endothelial Cells Induces Innate Immune Responses, Changes in Endothelial Cells Function and Is Restricted by Interferon-Stimulated Responses. *J Interferon Cytokine Res*, 35, 654-65.
- CARLIN, A. F., PLUMMER, E. M., VIZCARRA, E. A., SHEETS, N., JOO, Y., TANG, W., DAY, J., GREENBAUM, J., GLASS, C. K., DIAMOND, M. S. & SHRESTA, S. 2017. An IRF-3-, IRF-5-, and IRF-7-Independent Pathway of Dengue Viral Resistance Utilizes IRF-1 to Stimulate Type I and II Interferon Responses. *Cell Rep*, 21, 1600-1612.
- CAROD-ARTAL, F. J., WICHMANN, O., FARRAR, J. & GASCON, J. 2013. Neurological complications of dengue virus infection. *Lancet Neurol*, 12, 906-19.
- CARR, J. M., HOCKING, H., BUNTING, K., WRIGHT, P. J., DAVIDSON, A., GAMBLE, J., BURRELL, C. J. & LI, P. 2003. Supernatants from dengue virus type-2 infected macrophages induce permeability changes in endothelial cell monolayers. *J Med Virol*, 69, 521-8.
- CARTHARIUS, K., FRECH, K., GROTE, K., KLOCKE, B., HALTMEIER, M., KLINGENHOFF, A., FRISCH, M., BAYERLEIN, M. & WERNER, T. 2005. MatInspector and beyond: promoter analysis based on transcription factor binding sites. *Bioinformatics*, 21, 2933-42.
- CHAKRAVARTI, A. & KUMARIA, R. 2006. Circulating levels of tumour necrosis factor-alpha & interferon-gamma in patients with dengue & dengue haemorrhagic fever during an outbreak. *Indian J Med Res*, 123, 25-30.
- CHAN, K. W., WATANABE, S., KAVISHNA, R., ALONSO, S. & VASUDEVAN, S. G. 2015. Animal models for studying dengue pathogenesis and therapy. *Antiviral Res*, 123, 5-14.
- CHAU, T. N., QUYEN, N. T., THUY, T. T., TUAN, N. M., HOANG, D. M., DUNG, N. T., LIEN LE, B., QUY, N. T., HIEU, N. T., HIEU, L. T., HIEN, T. T., HUNG, N. T., FARRAR, J. & SIMMONS, C. P. 2008. Dengue in Vietnamese infants--results of infection-enhancement assays correlate with age-related disease epidemiology, and cellular immune responses correlate with disease severity. *J Infect Dis*, 198, 516-24.

- CHAUDHURI, A., YANG, B., GENDELMAN, H. E., PERSIDSKY, Y. & KANMOGNE, G. D. 2008. STAT1 signaling modulates HIV-1-induced inflammatory responses and leukocyte transmigration across the blood-brain barrier. *Blood*, 111, 2062-72.
- CHEN, H. C., HOFMAN, F. M., KUNG, J. T., LIN, Y. D. & WU-HSIEH, B. A. 2007a. Both virus and tumor necrosis factor alpha are critical for endothelium damage in a mouse model of dengue virus-induced hemorrhage. *J Virol*, 81, 5518-26.
- CHEN, H. C., LAI, S. Y., SUNG, J. M., LEE, S. H., LIN, Y. C., WANG, W. K., CHEN, Y. C., KAO, C. L., KING, C. C. & WU-HSIEH, B. A. 2004. Lymphocyte activation and hepatic cellular infiltration in immunocompetent mice infected by dengue virus. *J Med Virol*, 73, 419-31.
- CHEN, J. P., LU, H. L., LAI, S. L., CAMPANELLA, G. S., SUNG, J. M., LU, M. Y., WU-HSIEH, B. A., LIN, Y. L., LANE, T. E., LUSTER, A. D. & LIAO, F. 2006. Dengue virus induces expression of CXC chemokine ligand 10/IFN-gamma-inducible protein 10, which competitively inhibits viral binding to cell surface heparan sulfate. *J Immunol*, 177, 3185-92.
- CHEN, M., FORRESTER, J. V. & XU, H. 2007b. Synthesis of complement factor H by retinal pigment epithelial cells is down-regulated by oxidized photoreceptor outer segments. *Exp Eye Res*, 84, 635-45.
- CHEN, S. T., LIN, Y. L., HUANG, M. T., WU, M. F., CHENG, S. C., LEI, H. Y., LEE, C. K., CHIOU, T. W., WONG, C. H. & HSIEH, S. L. 2008. CLEC5A is critical for dengue-virus-induced lethal disease. *Nature*, 453, 672-6.
- CHEN, Y., MAGUIRE, T., HILEMAN, R. E., FROMM, J. R., ESKO, J. D., LINHARDT, R. J. & MARKS, R. M. 1997. Dengue virus infectivity depends on envelope protein binding to target cell heparan sulfate. *Nat Med*, 3, 866-71.
- CHEN, Y. C., WANG, S. Y. & KING, C. C. 1999. Bacterial lipopolysaccharide inhibits dengue virus infection of primary human monocytes/macrophages by blockade of virus entry via a CD14-dependent mechanism. *J Virol*, 73, 2650-7.
- CHENG, Y. L., LIN, Y. S., CHEN, C. L., WAN, S. W., OU, Y. D., YU, C. Y., TSAI, T. T., TSENG, P. C. & LIN, C. F. 2015. Dengue Virus Infection Causes the Activation of Distinct NF-kappaB Pathways for Inducible Nitric Oxide Synthase and TNF-alpha Expression in RAW264.7 Cells. *Mediators Inflamm*, 2015, 274025.
- CHEON, H. & STARK, G. R. 2009. Unphosphorylated STAT1 prolongs the expression of interferon-induced immune regulatory genes. *Proc Natl Acad Sci U S A*, 106, 9373-8.
- CHUANSUMRIT, A. & CHAIYARATANA, W. 2014. Hemostatic derangement in dengue hemorrhagic fever. *Thromb Res*, 133, 10-6.
- CHUANSUMRIT, A., PHIMOLTHARES, V., TARDTONG, P., TAPANeya-OLARN, C., TAPANeya-OLARN, W., KOWSATHIT, P. & CHANTAROJSIRI, T. 2000. Transfusion requirements in patients with dengue hemorrhagic fever. *Southeast Asian J Trop Med Public Health*, 31, 10-4.
- CHUNG, K. M., LISZEWSKI, M. K., NYBAKKEN, G., DAVIS, A. E., TOWNSEND, R. R., FREMONT, D. H., ATKINSON, J. P. & DIAMOND, M. S. 2006. West Nile virus nonstructural protein NS1 inhibits complement activation by binding the regulatory protein factor H. *Proc Natl Acad Sci U S A*, 103, 19111-6.
- CHURDBOONCHART, V., BHAMARAPRAVATI, N. & FUTRAKUL, P. 1983. Crossed immunoelectrophoresis for the detection of split products of the third complement in dengue hemorrhagic fever. I. Observations in patients' plasma. *Am J Trop Med Hyg*, 32, 569-76.
- CHURDBOONCHART, V., BHAMARAPRAVATI, N., PEAMPRAPRECHA, S. & SIRINAVIN, S. 1991. Antibodies against dengue viral proteins in primary and secondary dengue hemorrhagic fever. *Am J Trop Med Hyg*, 44, 481-93.
- CHYE, J. K., LIM, C. T., NG, K. B., LIM, J. M., GEORGE, R. & LAM, S. K. 1997. Vertical

- transmission of dengue. *Clin Infect Dis*, 25, 1374-7.
- CLARK, S. J., RIDGE, L. A., HERBERT, A. P., HAKOBYAN, S., MULLOY, B., LENNON, R., WURZNER, R., MORGAN, B. P., UHRIN, D., BISHOP, P. N. & DAY, A. J. 2013. Tissue-specific host recognition by complement factor H is mediated by differential activities of its glycosaminoglycan-binding regions. *J Immunol*, 190, 2049-57.
- CLAS, F., SCHMIDT, G. & LOOS, M. 1985. The role of the classical pathway for the bactericidal effect of normal sera against gram-negative bacteria. *Curr Top Microbiol Immunol*, 121, 19-72.
- COFIELL, R., KUKREJA, A., BEDARD, K., YAN, Y., MICKLE, A. P., OGAWA, M., BEDROSIAN, C. L. & FAAS, S. J. 2015. Eculizumab reduces complement activation, inflammation, endothelial damage, thrombosis, and renal injury markers in aHUS. *Blood*, 125, 3253-62.
- CONDE, J. N., DA SILVA, E. M., ALLONSO, D., COELHO, D. R., ANDRADE, I. D., DE MEDEIROS, L. N., MENEZES, J. L., BARBOSA, A. S. & MOHANA-BORGES, R. 2016. Inhibition of the Membrane Attack Complex by Dengue Virus NS1 through Interaction with Vitronectin and Terminal Complement Proteins. *J Virol*, 90, 9570-9581.
- CONRAD, D. H., CARLO, J. R. & RUDDY, S. 1978. Interaction of beta1H globulin with cell-bound C3b: quantitative analysis of binding and influence of alternative pathway components on binding. *J Exp Med*, 147, 1792-1805.
- COSTA, V. V., FAGUNDES, C. T., VALADAO, D. F., CISALPINO, D., DIAS, A. C., SILVEIRA, K. D., KANGUSSU, L. M., AVILA, T. V., BONFIM, M. R., BONAVENTURA, D., SILVA, T. A., SOUSA, L. P., RACHID, M. A., VIEIRA, L. Q., MENEZES, G. B., DE PAULA, A. M., ATRASHEUSKAYA, A., IGNATYEV, G., TEIXEIRA, M. M. & SOUZA, D. G. 2012. A model of DENV-3 infection that recapitulates severe disease and highlights the importance of IFN-gamma in host resistance to infection. *PLoS Negl Trop Dis*, 6, e1663.
- COULTHARD, L. G. & WOODRUFF, T. M. 2015. Is the complement activation product C3a a proinflammatory molecule? Re-evaluating the evidence and the myth. *J Immunol*, 194, 3542-8.
- CRILL, W. D. & CHANG, G. J. 2004. Localization and characterization of flavivirus envelope glycoprotein cross-reactive epitopes. *J Virol*, 78, 13975-86.
- CRILL, W. D., HUGHES, H. R., DELOREY, M. J. & CHANG, G. J. 2009. Humoral immune responses of dengue fever patients using epitope-specific serotype-2 virus-like particle antigens. *PLoS One*, 4, e4991.
- CRILL, W. D. & ROEHRIG, J. T. 2001. Monoclonal antibodies that bind to domain III of dengue virus E glycoprotein are the most efficient blockers of virus adsorption to Vero cells. *J Virol*, 75, 7769-73.
- CROWTHER, J. 2009. The ELISA guidebook (2nd edition) Methods in Molecular Biology. *Humana Press Inc.*, 149, 1-566.
- CRUZ-OLIVEIRA, C., FREIRE, J. M., CONCEICAO, T. M., HIGA, L. M., CASTANHO, M. A. & DA POIAN, A. T. 2015. Receptors and routes of dengue virus entry into the host cells. *FEMS Microbiol Rev*, 39, 155-70.
- CUMMINGS, K. L., WAGGONER, S. N., TACKE, R. & HAHN, Y. S. 2007. Role of complement in immune regulation and its exploitation by virus. *Viral Immunol*, 20, 505-24.
- DA COSTA, X. J., BROCKMAN, M. A., ALICOT, E., MA, M., FISCHER, M. B., ZHOU, X., KNIPE, D. M. & CARROLL, M. C. 1999. Humoral response to herpes simplex virus is complement-dependent. *Proc Natl Acad Sci U S A*, 96, 12708-12.
- DALRYMPLE, N. A. & MACKOW, E. R. 2012a. Endothelial cells elicit immune-enhancing responses to dengue virus infection. *J Virol*, 86, 6408-15.
- DALRYMPLE, N. A. & MACKOW, E. R. 2012b. Roles for endothelial cells in dengue virus

- infection. *Adv Virol*, 2012, 840654.
- DALRYMPLE, N. A. & MACKOW, E. R. 2014. Virus interactions with endothelial cell receptors: implications for viral pathogenesis. *Curr Opin Virol*, 7, 134-40.
- DAUCHEL, H., JULEN, N., LEMERCIER, C., DAVEAU, M., OZANNE, D., FONTAINE, M. & RIPOCHE, J. 1990. Expression of complement alternative pathway proteins by endothelial cells. Differential regulation by interleukin 1 and glucocorticoids. *Eur J Immunol*, 20, 1669-75.
- DAVIS, A. E., 3RD, HARRISON, R. A. & LACHMANN, P. J. 1984. Physiologic inactivation of fluid phase C3b: isolation and structural analysis of C3c, C3d,g (alpha 2D), and C3g. *J Immunol*, 132, 1960-6.
- DIXON, K. O., O'FLYNN, J., KLAR-MOHAMAD, N., DAHA, M. R. & VAN KOOTEN, C. 2017. Properdin and factor H production by human dendritic cells modulates their T-cell stimulatory capacity and is regulated by IFN-gamma. *Eur J Immunol*, 47, 470-480.
- DONG, T., MORAN, E., VINH CHAU, N., SIMMONS, C., LUHN, K., PENG, Y., WILLS, B., PHUONG DUNG, N., THI THU THAO, L., HIEN, T. T., MCMICHAEL, A., FARRAR, J. & ROWLAND-JONES, S. 2007. High pro-inflammatory cytokine secretion and loss of high avidity cross-reactive cytotoxic T-cells during the course of secondary dengue virus infection. *PLoS One*, 2, e1192.
- DOURADINHA, B., MCBURNEY, S. P., SOARES DE MELO, K. M., SMITH, A. P., KRISHNA, N. K., BARRATT-BOYES, S. M., EVANS, J. D., NASCIMENTO, E. J. & MARQUES, E. T., JR. 2014. C1q binding to dengue virus decreases levels of infection and inflammatory molecules transcription in THP-1 cells. *Virus Res*, 179, 231-4.
- DUAN, Z. L., LI, Q., WANG, Z. B., XIA, K. D., GUO, J. L., LIU, W. Q. & WEN, J. S. 2012. HLA-A*0201-restricted CD8+ T-cell epitopes identified in dengue viruses. *Virology*, 9, 259.
- DUANGCHINDA, T., DEJNIRATTISAI, W., VASANAWATHANA, S., LIMPITIKUL, W., TANGTHAWORNCHAIKUL, N., MALASIT, P., MONGKOLSAPAYA, J. & SCREATION, G. 2010. Immunodominant T-cell responses to dengue virus NS3 are associated with DHF. *Proc Natl Acad Sci U S A*, 107, 16922-7.
- DURAN, A., VALERO, N., MOSQUERA, J., DELGADO, L., ALVAREZ-MON, M. & TORRES, M. 2016. Role of the myeloid differentiation primary response (MYD88) and TIR-domain-containing adapter-inducing interferon-beta (TRIF) pathways in dengue. *Life Sci*, 162, 33-40.
- DURBIN, A. P., MCARTHUR, J., MARRON, J. A., BLANEY, J. E., JR., THUMAR, B., WANIONEK, K., MURPHY, B. R. & WHITEHEAD, S. S. 2006. The live attenuated dengue serotype 1 vaccine rDEN1Delta30 is safe and highly immunogenic in healthy adult volunteers. *Hum Vaccin*, 2, 167-73.
- ENDO, Y., MATSUSHITA, M. & FUJITA, T. 2015. New insights into the role of ficolins in the lectin pathway of innate immunity. *Int Rev Cell Mol Biol*, 316, 49-110.
- ENDO, Y., NAKAZAWA, N., IWAKI, D., TAKAHASHI, M., MATSUSHITA, M. & FUJITA, T. 2010. Interactions of ficolin and mannose-binding lectin with fibrinogen/fibrin augment the lectin complement pathway. *J Innate Immun*, 2, 33-42.
- ENDY, T. P. 2014. Dengue human infection model performance parameters. *J Infect Dis*, 209 Suppl 2, S56-60.
- ESTALLER, C., KOISTINEN, V., SCHWAEBLE, W., DIERICH, M. P. & WEISS, E. H. 1991. Cloning of the 1.4-kb mRNA species of human complement factor H reveals a novel member of the short consensus repeat family related to the carboxy terminal of the classical 150-kDa molecule. *J Immunol*, 146, 3190-6.
- EZEKOWITZ, R. A., KUHLMAN, M., GROOPMAN, J. E. & BYRN, R. A. 1989. A human serum mannose-binding protein inhibits in vitro infection by the human

- immunodeficiency virus. *J Exp Med*, 169, 185-96.
- FAGUNDES, C. T., COSTA, V. V., CISALPINO, D., AMARAL, F. A., SOUZA, P. R., SOUZA, R. S., RYFFEL, B., VIEIRA, L. Q., SILVA, T. A., ATRASHEUSKAYA, A., IGNATYEV, G., SOUSA, L. P., SOUZA, D. G. & TEIXEIRA, M. M. 2011. IFN-gamma production depends on IL-12 and IL-18 combined action and mediates host resistance to dengue virus infection in a nitric oxide-dependent manner. *PLoS Negl Trop Dis*, 5, e1449.
- FAKHOURI, F., DE JORGE, E. G., BRUNE, F., AZAM, P., COOK, H. T. & PICKERING, M. C. 2010. Treatment with human complement factor H rapidly reverses renal complement deposition in factor H-deficient mice. *Kidney Int*, 78, 279-86.
- FALGOUT, B., BRAY, M., SCHLESINGER, J. J. & LAI, C. J. 1990. Immunization of mice with recombinant vaccinia virus expressing authentic dengue virus nonstructural protein NS1 protects against lethal dengue virus encephalitis. *J Virol*, 64, 4356-63.
- FEARON, D. T. 1979. Activation of the alternative complement pathway. *CRC Crit Rev Immunol*, 1, 1-32.
- FEARON, D. T. & AUSTEN, K. F. 1975. Properdin: binding to C3b and stabilization of the C3b-dependent C3 convertase. *J Exp Med*, 142, 856-63.
- FERNANDEZ-MESTRE, M. T., GENDZEKHADZE, K., RIVAS-VETENCOURT, P. & LAYRISSE, Z. 2004. TNF-alpha-308A allele, a possible severity risk factor of hemorrhagic manifestation in dengue fever patients. *Tissue Antigens*, 64, 469-72.
- FERREIRA, V. P., PANGBURN, M. K. & CORTES, C. 2010. Complement control protein factor H: the good, the bad, and the inadequate. *Mol Immunol*, 47, 2187-97.
- FORRISTAL, J., IITAKA, K., VALLOTA, E. H. & WEST, C. D. 1977. Correlations between serum factor B and C3b inactivator levels in normal subjects and in patients with infections, nephrosis and hypocomplementaemic glomerulonephritis. *Clin Exp Immunol*, 28, 61-71.
- FRIAS-STAHOLI, N., DORNER, M., MARUKIAN, S., BILLERBECK, E., LABITT, R. N., RICE, C. M. & PLOSS, A. 2014. Utility of humanized BLT mice for analysis of dengue virus infection and antiviral drug testing. *J Virol*, 88, 2205-18.
- FRIDKIS-HARELI, M., STOREK, M., MAZSAROFF, I., RISITANO, A. M., LUNDBERG, A. S., HORVATH, C. J. & HOLERS, V. M. 2011. Design and development of TT30, a novel C3d-targeted C3/C5 convertase inhibitor for treatment of human complement alternative pathway-mediated diseases. *Blood*, 118, 4705-13.
- FRIED, J. R., GIBBONS, R. V., KALAYANAROOJ, S., THOMAS, S. J., SRIKIATKHACHORN, A., YOON, I. K., JARMAN, R. G., GREEN, S., ROTHMAN, A. L. & CUMMINGS, D. A. 2010. Serotype-specific differences in the risk of dengue hemorrhagic fever: an analysis of data collected in Bangkok, Thailand from 1994 to 2006. *PLoS Negl Trop Dis*, 4, e617.
- FRIEDMAN, H. M., COHEN, G. H., EISENBERG, R. J., SEIDEL, C. A. & CINES, D. B. 1984. Glycoprotein C of herpes simplex virus 1 acts as a receptor for the C3b complement component on infected cells. *Nature*, 309, 633-5.
- FRIES, L. F., FRIEDMAN, H. M., COHEN, G. H., EISENBERG, R. J., HAMMER, C. H. & FRANK, M. M. 1986. Glycoprotein C of herpes simplex virus 1 is an inhibitor of the complement cascade. *J Immunol*, 137, 1636-41.
- FRIESE, M. A., HELLWAGE, J., JOKIRANTA, T. S., MERI, S., MULLER-QUERNHEIM, H. J., PETER, H. H., EIBEL, H. & ZIPFEL, P. F. 2000. Different regulation of factor H and FHL-1/reconectin by inflammatory mediators and expression of the two proteins in rheumatoid arthritis (RA). *Clin Exp Immunol*, 121, 406-15.
- FRIESE, M. A., MANUELIAN, T., JUNNIKALA, S., HELLWAGE, J., MERI, S., PETER, H. H., GORDON, D. L., EIBEL, H. & ZIPFEL, P. F. 2003. Release of endogenous anti-inflammatory complement regulators FHL-1 and factor H protects synovial fibroblasts during rheumatoid arthritis. *Clin Exp Immunol*, 132, 485-95.

- FUCHS, A., LIN, T. Y., BEASLEY, D. W., STOVER, C. M., SCHWAEBLE, W. J., PIERSON, T. C. & DIAMOND, M. S. 2010. Direct complement restriction of flavivirus infection requires glycan recognition by mannose-binding lectin. *Cell Host Microbe*, 8, 186-95.
- FUNAHARA, Y., OGAWA, K., FUJITA, N. & OKUNO, Y. 1987. Three possible triggers to induce thrombocytopenia in dengue virus infection. *Southeast Asian J Trop Med Public Health*, 18, 351-5.
- FUREDOR, W., AGIS, H., WILLHEIM, M., BANKL, H. C., MAIER, U., KISHI, K., MULLER, M. R., CZERWENKA, K., RADASZKIEWICZ, T., BUTTERFIELD, J. H., KLAPPACHER, G. W., SPERR, W. R., OPPERMANN, M., LECHNER, K. & VALENT, P. 1995. Differential expression of complement receptors on human basophils and mast cells. Evidence for mast cell heterogeneity and CD88/C5aR expression on skin mast cells. *J Immunol*, 155, 3152-60.
- GAMBLE, J., BETHELL, D., DAY, N. P., LOC, P. P., PHU, N. H., GARTSIDE, I. B., FARRAR, J. F. & WHITE, N. J. 2000. Age-related changes in microvascular permeability: a significant factor in the susceptibility of children to shock? *Clin Sci (Lond)*, 98, 211-6.
- GAO, R., WANG, L., BAI, T., ZHANG, Y., BO, H. & SHU, Y. 2017. C-Reactive Protein Mediating Immunopathological Lesions: A Potential Treatment Option for Severe Influenza A Diseases. *EBioMedicine*, 22, 133-142.
- GARRED, P., HONORE, C., MA, Y. J., MUNTHE-FOG, L. & HUMMELSHOJ, T. 2009. MBL2, FCN1, FCN2 and FCN3-The genes behind the initiation of the lectin pathway of complement. *Mol Immunol*, 46, 2737-44.
- GIANNAKIS, E., JOKIRANTA, T. S., MALE, D. A., RANGANATHAN, S., ORMSBY, R. J., FISCHETTI, V. A., MOLD, C. & GORDON, D. L. 2003. A common site within factor H SCR 7 responsible for binding heparin, C-reactive protein and streptococcal M protein. *Eur J Immunol*, 33, 962-9.
- GIBBONS, R. V., KALANAROOJ, S., JARMAN, R. G., NISALAK, A., VAUGHN, D. W., ENDY, T. P., MAMMEN, M. P., JR. & SRIKIATKHACHORN, A. 2007. Analysis of repeat hospital admissions for dengue to estimate the frequency of third or fourth dengue infections resulting in admissions and dengue hemorrhagic fever, and serotype sequences. *Am J Trop Med Hyg*, 77, 910-3.
- GIL, L., COBAS, K., LAZO, L., MARCOS, E., HERNANDEZ, L., SUZARTE, E., IZQUIERDO, A., VALDES, I., BLANCO, A., PUENTES, P., ROMERO, Y., PEREZ, Y., GUZMAN, M. G., GUILLEN, G. & HERMIDA, L. 2016. A Tetravalent Formulation Based on Recombinant Nucleocapsid-like Particles from Dengue Viruses Induces a Functional Immune Response in Mice and Monkeys. *J Immunol*, 197, 3597-3606.
- GIL, L., LAZO, L., VALDES, I., SUZARTE, E., YEN, P., RAMIREZ, R., ALVAREZ, M., DUNG, L. T., COBAS, K., MARCOS, E., PEREZ, Y., GUZMAN, M. G., N, D. H., GUILLEN, G. & HERMIDA, L. 2017. The tetravalent formulation of domain III-capsid proteins recalls memory B- and T-cell responses induced in monkeys by an experimental dengue virus infection. *Clin Transl Immunology*, 6, e148.
- GIL, L., LOPEZ, C., BLANCO, A., LAZO, L., MARTIN, J., VALDES, I., ROMERO, Y., FIGUEROA, Y., GUILLEN, G. & HERMIDA, L. 2009. The cellular immune response plays an important role in protecting against dengue virus in the mouse encephalitis model. *Viral Immunol*, 22, 23-30.
- GIL, L., MARCOS, E., IZQUIERDO, A., LAZO, L., VALDES, I., AMBALA, P., OCHOLA, L., HITLER, R., SUZARTE, E., ALVAREZ, M., KIMITI, P., NDUNG'U, J., KARIUKI, T., GUZMAN, M. G., GUILLEN, G. & HERMIDA, L. 2015. The protein DIIC-2, aggregated with a specific oligodeoxynucleotide and adjuvanted in alum, protects mice and monkeys against DENV-2. *Immunol Cell Biol*, 93, 57-66.
- GLASNER, D. R., PUERTA-GUARDO, H., BEATTY, P. R. & HARRIS, E. 2018. The Good,

- the Bad, and the Shocking: The Multiple Roles of Dengue Virus Nonstructural Protein 1 in Protection and Pathogenesis. *Annu Rev Virol*.
- GLASNER, D. R., RATNASIRI, K., PUERTA-GUARDO, H., ESPINOSA, D. A., BEATTY, P. R. & HARRIS, E. 2017. Dengue virus NS1 cytokine-independent vascular leak is dependent on endothelial glycocalyx components. *PLoS Pathog*, 13, e1006673.
- GOLDBERGER, G., ARNAOUT, M. A., ADEN, D., KAY, R., RITS, M. & COLTEN, H. R. 1984. Biosynthesis and postsynthetic processing of human C3b/C4b inactivator (factor I) in three hepatoma cell lines. *J Biol Chem*, 259, 6492-7.
- GORDON, D. L., KAUFMAN, R. M., BLACKMORE, T. K., KWONG, J. & LUBLIN, D. M. 1995. Identification of complement regulatory domains in human factor H. *J Immunol*, 155, 348-56.
- GREEN, A. M., BEATTY, P. R., HADJILAOU, A. & HARRIS, E. 2014. Innate immunity to dengue virus infection and subversion of antiviral responses. *J Mol Biol*, 426, 1148-60.
- GREEN, S. & ROTHMAN, A. 2006. Immunopathological mechanisms in dengue and dengue hemorrhagic fever. *Curr Opin Infect Dis*, 19, 429-36.
- GROMOWSKI, G. D. & BARRETT, A. D. 2007. Characterization of an antigenic site that contains a dominant, type-specific neutralization determinant on the envelope protein domain III (ED3) of dengue 2 virus. *Virology*, 366, 349-60.
- GUALANO, R. C., PRYOR, M. J., CAUCHI, M. R., WRIGHT, P. J. & DAVIDSON, A. D. 1998. Identification of a major determinant of mouse neurovirulence of dengue virus type 2 using stably cloned genomic-length cDNA. *J Gen Virol*, 79 (Pt 3), 437-46.
- GUBLER, D. J. 1998. Dengue and dengue hemorrhagic fever. *Clin Microbiol Rev*, 11, 480-96.
- GUNN, B. M., MORRISON, T. E., WHITMORE, A. C., BLEVINS, L. K., HUESTON, L., FRASER, R. J., HERRERO, L. J., RAMIREZ, R., SMITH, P. N., MAHALINGAM, S. & HEISE, M. T. 2012. Mannose binding lectin is required for alphavirus-induced arthritis/myositis. *PLoS Pathog*, 8, e1002586.
- GUNTHER, V. J., PUTNAK, R., ECKELS, K. H., MAMMEN, M. P., SCHERER, J. M., LYONS, A., SZTEIN, M. B. & SUN, W. 2011. A human challenge model for dengue infection reveals a possible protective role for sustained interferon gamma levels during the acute phase of illness. *Vaccine*, 29, 3895-904.
- GUY, B., BARBAN, V., MANTEL, N., AGUIRRE, M., GULIA, S., PONTVIANNE, J., JOURDIER, T. M., RAMIREZ, L., GREGOIRE, V., CHARNAY, C., BURDIN, N., DUMAS, R. & LANG, J. 2009. Evaluation of interferences between dengue vaccine serotypes in a monkey model. *Am J Trop Med Hyg*, 80, 302-11.
- GUY, B. & JACKSON, N. 2016. Dengue vaccine: hypotheses to understand CYD-TDV-induced protection. *Nat Rev Microbiol*, 14, 45-54.
- GUY, B., SAVILLE, M. & LANG, J. 2010. Development of Sanofi Pasteur tetravalent dengue vaccine. *Hum Vaccin*, 6.
- GUZMAN, M. G., DEUBEL, V., PELEGRINO, J. L., ROSARIO, D., MARRERO, M., SARIOL, C. & KOURI, G. 1995. Partial nucleotide and amino acid sequences of the envelope and the envelope/nonstructural protein-1 gene junction of four dengue-2 virus strains isolated during the 1981 Cuban epidemic. *Am J Trop Med Hyg*, 52, 241-6.
- GUZMAN, M. G., HALSTEAD, S. B., ARTSOB, H., BUCHY, P., FARRAR, J., GUBLER, D. J., HUNSPERGER, E., KROEGER, A., MARGOLIS, H. S., MARTINEZ, E., NATHAN, M. B., PELEGRINO, J. L., SIMMONS, C., YOKSAN, S. & PEELING, R. W. 2010. Dengue: a continuing global threat. *Nat Rev Microbiol*, 8, S7-16.
- GUZMAN, M. G. & KOURI, G. 2008. Dengue haemorrhagic fever integral hypothesis: confirming observations, 1987-2007. *Trans R Soc Trop Med Hyg*, 102, 522-3.
- GUZMAN, M. G., KOURI, G., VALDES, L., BRAVO, J., VAZQUEZ, S. & HALSTEAD, S. B.

2002. Enhanced severity of secondary dengue-2 infections: death rates in 1981 and 1997 Cuban outbreaks. *Rev Panam Salud Publica*, 11, 223-7.
- HAIR, P. S., GRONEMUS, J. Q., CRAWFORD, K. B., SALVI, V. P., CUNNION, K. M., THIELENS, N. M., ARLAUD, G. J., RAWAL, N. & KRISHNA, N. K. 2010. Human astrovirus coat protein binds C1q and MBL and inhibits the classical and lectin pathways of complement activation. *Mol Immunol*, 47, 792-8.
- HALSTEAD, S. B. 1989. Antibody, macrophages, dengue virus infection, shock, and hemorrhage: a pathogenetic cascade. *Rev Infect Dis*, 11 Suppl 4, S830-9.
- HALSTEAD, S. B. 2002. Dengue. *Curr Opin Infect Dis*, 15, 471-6.
- HALSTEAD, S. B. 2003. Neutralization and antibody-dependent enhancement of dengue viruses. *Adv Virus Res*, 60, 421-67.
- HALSTEAD, S. B. 2007. Dengue. *Lancet*, 370, 1644-52.
- HALSTEAD, S. B. 2014. Dengue Antibody-Dependent Enhancement: Knowns and Unknowns. *Microbiol Spectr*, 2.
- HALSTEAD, S. B. & O'ROURKE, E. J. 1977a. Antibody-enhanced dengue virus infection in primate leukocytes. *Nature*, 265, 739-41.
- HALSTEAD, S. B. & O'ROURKE, E. J. 1977b. Dengue viruses and mononuclear phagocytes. I. Infection enhancement by non-neutralizing antibody. *J Exp Med*, 146, 201-17.
- HALSTEAD, S. B., SHOTWELL, H. & CASALS, J. 1973a. Studies on the pathogenesis of dengue infection in monkeys. I. Clinical laboratory responses to primary infection. *J Infect Dis*, 128, 7-14.
- HALSTEAD, S. B., SHOTWELL, H. & CASALS, J. 1973b. Studies on the pathogenesis of dengue infection in monkeys. II. Clinical laboratory responses to heterologous infection. *J Infect Dis*, 128, 15-22.
- HANNAN, J. P., LASKOWSKI, J., THURMAN, J. M., HAGEMAN, G. S. & HOLERS, V. M. 2016. Mapping the Complement Factor H-Related Protein 1 (CFHR1):C3b/C3d Interactions. *PLoS One*, 11, e0166200.
- HARRIS, S. L., FRANK, I., YEE, A., COHEN, G. H., EISENBERG, R. J. & FRIEDMAN, H. M. 1990. Glycoprotein C of herpes simplex virus type 1 prevents complement-mediated cell lysis and virus neutralization. *J Infect Dis*, 162, 331-7.
- HARRISON, R. A. 2018. The properdin pathway: an "alternative activation pathway" or a "critical amplification loop" for C3 and C5 activation? *Semin Immunopathol*, 40, 15-35.
- HELLWAGE, J., JOKIRANTA, T. S., FRIESE, M. A., WOLK, T. U., KAMPEN, E., ZIPFEL, P. F. & MERI, S. 2002. Complement C3b/C3d and cell surface polyanions are recognized by overlapping binding sites on the most carboxyl-terminal domain of complement factor H. *J Immunol*, 169, 6935-44.
- HENCHAL, E. A. & PUTNAK, J. R. 1990. The dengue viruses. *Clin Microbiol Rev*, 3, 376-96.
- HENEIN, S., SWANSTROM, J., BYERS, A. M., MOSER, J. M., SHAIK, S. F., BONAPARTE, M., JACKSON, N., GUY, B., BARIC, R. & DE SILVA, A. M. 2017. Dissecting Antibodies Induced by a Chimeric Yellow Fever-Dengue, Live-Attenuated, Tetravalent Dengue Vaccine (CYD-TDV) in Naive and Dengue-Exposed Individuals. *J Infect Dis*, 215, 351-358.
- HILLEBRANDT, S., WASMUTH, H. E., WEISKIRCHEN, R., HELLERBRAND, C., KEPPELER, H., WERTH, A., SCHIRIN-SOKHAN, R., WILKENS, G., GEIER, A., LORENZEN, J., KOHL, J., GRESSNER, A. M., MATERN, S. & LAMMERT, F. 2005. Complement factor 5 is a quantitative trait gene that modifies liver fibrogenesis in mice and humans. *Nat Genet*, 37, 835-43.
- HOESEL, B. & SCHMID, J. A. 2013. The complexity of NF-kappaB signaling in inflammation and cancer. *Mol Cancer*, 12, 86.

- HOMBACH, J., BARRETT, A. D., CARDOSA, M. J., DEUBEL, V., GUZMAN, M., KURANE, I., ROEHRIG, J. T., SABCHAREON, A. & KIENY, M. P. 2005. Review on flavivirus vaccine development. Proceedings of a meeting jointly organised by the World Health Organization and the Thai Ministry of Public Health, 26-27 April 2004, Bangkok, Thailand. *Vaccine*, 23, 2689-95.
- HORSTMANN, R. D., PANGBURN, M. K. & MULLER-EBERHARD, H. J. 1985. Species specificity of recognition by the alternative pathway of complement. *J Immunol*, 134, 1101-4.
- HOURCADE, D. E. 2006. The role of properdin in the assembly of the alternative pathway C3 convertases of complement. *J Biol Chem*, 281, 2128-32.
- HOVIS, K. M., JONES, J. P., SADLON, T., RAVAL, G., GORDON, D. L. & MARCONI, R. T. 2006. Molecular analyses of the interaction of *Borrelia hermsii* FhbA with the complement regulatory proteins factor H and factor H-like protein 1. *Infect Immun*, 74, 2007-14.
- HSIEH, M. F., LAI, S. L., CHEN, J. P., SUNG, J. M., LIN, Y. L., WU-HSIEH, B. A., GERARD, C., LUSTER, A. & LIAO, F. 2006. Both CXCR3 and CXCL10/IFN-inducible protein 10 are required for resistance to primary infection by dengue virus. *J Immunol*, 177, 1855-63.
- HUANG, K. J., LI, S. Y., CHEN, S. C., LIU, H. S., LIN, Y. S., YEH, T. M., LIU, C. C. & LEI, H. Y. 2000. Manifestation of thrombocytopenia in dengue-2-virus-infected mice. *J Gen Virol*, 81, 2177-82.
- HUANG, Y., KREIN, P. M., MURUVE, D. A. & WINSTON, B. W. 2002. Complement factor B gene regulation: synergistic effects of TNF-alpha and IFN-gamma in macrophages. *J Immunol*, 169, 2627-35.
- HUANG, Y. H., CHANG, B. I., LEI, H. Y., LIU, H. S., LIU, C. C., WU, H. L. & YEH, T. M. 1997. Antibodies against dengue virus E protein peptide bind to human plasminogen and inhibit plasmin activity. *Clin Exp Immunol*, 110, 35-40.
- HUANG, Y. H., LIU, C. C., WANG, S. T., LEI, H. Y., LIU, H. L., LIN, Y. S., WU, H. L. & YEH, T. M. 2001. Activation of coagulation and fibrinolysis during dengue virus infection. *J Med Virol*, 63, 247-51.
- HUNG, J. J., HSIEH, M. T., YOUNG, M. J., KAO, C. L., KING, C. C. & CHANG, W. 2004. An external loop region of domain III of dengue virus type 2 envelope protein is involved in serotype-specific binding to mosquito but not mammalian cells. *J Virol*, 78, 378-88.
- HUSON, M. A., WOUTERS, D., VAN MIERLO, G., GROBUSCH, M. P., ZEERLEDER, S. S. & VAN DER POLL, T. 2015. HIV Coinfection Enhances Complement Activation During Sepsis. *J Infect Dis*, 212, 474-83.
- HYAMS, C., TRZCINSKI, K., CAMBERLEIN, E., WEINBERGER, D. M., CHIMALAPATI, S., NOURSADEGHI, M., LIPSITCH, M. & BROWN, J. S. 2013. Streptococcus pneumoniae capsular serotype invasiveness correlates with the degree of factor H binding and opsonization with C3b/iC3b. *Infect Immun*, 81, 354-63.
- IMRIE, A., MEEKS, J., GURARY, A., SUKHBATAAR, M., KITSUTANI, P., EFFLER, P. & ZHAO, Z. 2007. Differential functional avidity of dengue virus-specific T-cell clones for variant peptides representing heterologous and previously encountered serotypes. *J Virol*, 81, 10081-91.
- ISAAC, L., AIVAZIAN, D., TANIGUCHI-SIDLE, A., EBANKS, R. O., FARAH, C. S., FLORIDO, M. P., PANGBURN, M. K. & ISENMAN, D. E. 1998. Native conformations of human complement components C3 and C4 show different dependencies on thioester formation. *Biochem J*, 329 (Pt 3), 705-12.
- JARVA, H., JOKIRANTA, T. S., HELLWAGE, J., ZIPFEL, P. F. & MERI, S. 1999. Regulation of complement activation by C-reactive protein: targeting the complement inhibitory activity of factor H by an interaction with short consensus

- repeat domains 7 and 8-11. *J Immunol*, 163, 3957-62.
- JAYASEKERA, J. P., MOSEMAN, E. A. & CARROLL, M. C. 2007. Natural antibody and complement mediate neutralization of influenza virus in the absence of prior immunity. *J Virol*, 81, 3487-94.
- JEEWANDARA, C., ADIKARI, T. N., GOMES, L., FERNANDO, S., FERNANDO, R. H., PERERA, M. K., ARIYARATNE, D., KAMALADASA, A., SALIMI, M., PRATHAPAN, S., OGG, G. S. & MALAVIGE, G. N. 2015. Functionality of dengue virus specific memory T cell responses in individuals who were hospitalized or who had mild or subclinical dengue infection. *PLoS Negl Trop Dis*, 9, e0003673.
- JENSEN, R. K., PIHL, R., GADEBERG, T. A. F., JENSEN, J. K., ANDERSEN, K. R., THIEL, S., LAURSEN, N. S. & ANDERSEN, G. R. 2018. A potent complement factor C3-specific nanobody inhibiting multiple functions in the alternative pathway of human and murine complement. *J Biol Chem*, 293, 6269-6281.
- JI, X., OLINGER, G. G., ARIS, S., CHEN, Y., GEWURZ, H. & SPEAR, G. T. 2005. Mannose-binding lectin binds to Ebola and Marburg envelope glycoproteins, resulting in blocking of virus interaction with DC-SIGN and complement-mediated virus neutralization. *J Gen Virol*, 86, 2535-42.
- JINDADAMRONGWECH, S., THEPPARIT, C. & SMITH, D. R. 2004. Identification of GRP 78 (BiP) as a liver cell expressed receptor element for dengue virus serotype 2. *Arch Virol*, 149, 915-27.
- JOHNSON, A. J. & ROEHRIG, J. T. 1999. New mouse model for dengue virus vaccine testing. *J Virol*, 73, 783-6.
- JOHNSON, J. B., GRANT, K. & PARKS, G. D. 2009. The paramyxoviruses simian virus 5 and mumps virus recruit host cell CD46 to evade complement-mediated neutralization. *J Virol*, 83, 7602-11.
- JOKIRANTA, T. S., HELLWAGE, J., KOISTINEN, V., ZIPFEL, P. F. & MERI, S. 2000. Each of the three binding sites on complement factor H interacts with a distinct site on C3b. *J Biol Chem*, 275, 27657-62.
- KACZOROWSKI, D. J., AFRAZI, A., SCOTT, M. J., KWAK, J. H., GILL, R., EDMONDS, R. D., LIU, Y., FAN, J. & BILLIAR, T. R. 2010. Pivotal advance: The pattern recognition receptor ligands lipopolysaccharide and polyinosine-polycytidylic acid stimulate factor B synthesis by the macrophage through distinct but overlapping mechanisms. *J Leukoc Biol*, 88, 609-18.
- KAIN, S. J., MALDONADO, M. J. & VIK, D. P. 1998. Analysis of the promoter region of the murine complement factor H gene. *Biochim Biophys Acta*, 1397, 241-6.
- KEMPER, C., PANGBURN, M. K. & FISHELSON, Z. 2014. Complement nomenclature 2014. *Mol Immunol*, 61, 56-8.
- KERR, H. & RICHARDS, A. 2012. Complement-mediated injury and protection of endothelium: lessons from atypical haemolytic uraemic syndrome. *Immunobiology*, 217, 195-203.
- KIM, Y. H., HE, S., KASE, S., KITAMURA, M., RYAN, S. J. & HINTON, D. R. 2009. Regulated secretion of complement factor H by RPE and its role in RPE migration. *Graefes Arch Clin Exp Ophthalmol*, 247, 651-9.
- KINDERMANN, B., DORING, F., BUDCZIES, J. & DANIEL, H. 2005. Zinc-sensitive genes as potential new target genes of the metal transcription factor-1 (MTF-1). *Biochem Cell Biol*, 83, 221-9.
- KING, C. A. 2013. Kaposi's sarcoma-associated herpesvirus kaposin B induces unique monophosphorylation of STAT3 at serine 727 and MK2-mediated inactivation of the STAT3 transcriptional repressor TRIM28. *J Virol*, 87, 8779-91.
- KISSELEVA, T., BHATTACHARYA, S., BRAUNSTEIN, J. & SCHINDLER, C. W. 2002. Signaling through the JAK/STAT pathway, recent advances and future challenges. *Gene*, 285, 1-24.

- KITTESEN, D. J., CHIANESE-BULLOCK, K. A., YAO, Z. Q., BRACIALE, T. J. & HAHN, Y. S. 2000. Interaction between complement receptor gC1qR and hepatitis C virus core protein inhibits T-lymphocyte proliferation. *J Clin Invest*, 106, 1239-49.
- KNOPE, K. E., DOGGETT, S. L., KURUCZ, N., JOHANSEN, C. A., NICHOLSON, J., FELDMAN, R., SLY, A., HOBBY, M., EL SAADI, D., MULLER, M., JANSEN, C. C., MUZARI, O. M., NATIONAL, A. & MALARIA ADVISORY, C. 2014. Arboviral diseases and malaria in Australia, 2011-12: annual report of the National Arbovirus and Malaria Advisory Committee. *Commun Dis Intell Q Rep*, 38, E122-42.
- KOISTINEN, V. 1991. Effect of complement-protein-C3b density on the binding of complement factor H to surface-bound C3b. *Biochem J*, 280 (Pt 1), 255-9.
- KOMA, T., VELJKOVIC, V., ANDERSON, D. E., WANG, L. F., ROSSI, S. L., SHAN, C., SHI, P. Y., BEASLEY, D. W., BUKREYEVA, N., SMITH, J. N., HALLAM, S., HUANG, C., VON MESSLING, V. & PAESSLER, S. 2018. Zika virus infection elicits auto-antibodies to C1q. *Sci Rep*, 8, 1882.
- KOPF, M., ABEL, B., GALLIMORE, A., CARROLL, M. & BACHMANN, M. F. 2002. Complement component C3 promotes T-cell priming and lung migration to control acute influenza virus infection. *Nat Med*, 8, 373-8.
- KORAKA, P., SUHARTI, C., SETIATI, T. E., MAIRUHU, A. T., VAN GORP, E., HACK, C. E., JUFFRIE, M., SUTARYO, J., VAN DER MEER, G. M., GROEN, J. & OSTERHAUS, A. D. 2001. Kinetics of dengue virus-specific serum immunoglobulin classes and subclasses correlate with clinical outcome of infection. *J Clin Microbiol*, 39, 4332-8.
- KOSTAVASILI, I., SAHU, A., FRIEDMAN, H. M., EISENBERG, R. J., COHEN, G. H. & LAMBRIS, J. D. 1997. Mechanism of complement inactivation by glycoprotein C of herpes simplex virus. *J Immunol*, 158, 1763-71.
- KOURI, G. P., GUZMAN, M. G. & BRAVO, J. R. 1987. Why dengue haemorrhagic fever in Cuba? 2. An integral analysis. *Trans R Soc Trop Med Hyg*, 81, 821-3.
- KRISHNAN, M. N., SUKUMARAN, B., PAL, U., AGAISSE, H., MURRAY, J. L., HODGE, T. W. & FIKRIG, E. 2007. Rab 5 is required for the cellular entry of dengue and West Nile viruses. *J Virol*, 81, 4881-5.
- KRISTENSEN, T. & TACK, B. F. 1986. Murine protein H is comprised of 20 repeating units, 61 amino acids in length. *Proc Natl Acad Sci U S A*, 83, 3963-7.
- KRISTENSEN, T., WETSEL, R. A. & TACK, B. F. 1986. Structural analysis of human complement protein H: homology with C4b binding protein, beta 2-glycoprotein I, and the Ba fragment of B2. *J Immunol*, 136, 3407-11.
- KUADKITKAN, A., WIKAN, N., FONGSARAN, C. & SMITH, D. R. 2010. Identification and characterization of prohibitin as a receptor protein mediating DENV-2 entry into insect cells. *Virology*, 406, 149-61.
- KUHN, R. J., ZHANG, W., ROSSMANN, M. G., PLETNEV, S. V., CORVER, J., LENCHES, E., JONES, C. T., MUKHOPADHYAY, S., CHIPMAN, P. R., STRAUSS, E. G., BAKER, T. S. & STRAUSS, J. H. 2002. Structure of dengue virus: implications for flavivirus organization, maturation, and fusion. *Cell*, 108, 717-25.
- KUHN, S., SKERKA, C. & ZIPFEL, P. F. 1995. Mapping of the complement regulatory domains in the human factor H-like protein 1 and in factor H1. *J Immunol*, 155, 5663-70.
- KUHN, S. & ZIPFEL, P. F. 1996. Mapping of the domains required for decay acceleration activity of the human factor H-like protein 1 and factor H. *Eur J Immunol*, 26, 2383-7.
- KURUVILLA, J. G., TROYER, R. M., DEVI, S. & AKKINA, R. 2007. Dengue virus infection and immune response in humanized RAG2(-/-)gamma(c)(-/-) (RAG-hu) mice. *Virology*, 369, 143-52.
- LANGGARTNER, J., AUDEBERT, F., SCHOLMERICH, J. & GLUCK, T. 2002. Dengue

- virus infection transmitted by needle stick injury. *J Infect*, 44, 269-70.
- LANTERI, M. C. & BUSCH, M. P. 2012. Dengue in the context of "safe blood" and global epidemiology: to screen or not to screen? *Transfusion*, 52, 1634-9.
- LAPPIN, D. F., GUC, D., HILL, A., MCSHANE, T. & WHALEY, K. 1992. Effect of interferon-gamma on complement gene expression in different cell types. *Biochem J*, 281 (Pt 2), 437-42.
- LAPPIN, D. F. & WHALEY, K. 1990. Interferon-induced transcriptional and post-transcriptional modulation of factor H and C4 binding-protein synthesis in human monocytes. *Biochem J*, 271, 767-72.
- LARSEN, C. P., WHITEHEAD, S. S. & DURBIN, A. P. 2015. Dengue Human Infection Models to Advance Dengue Vaccine Development. *Vaccine*.
- LEE, K. G., XU, S., KANG, Z. H., HUO, J., HUANG, M., LIU, D., TAKEUCHI, O., AKIRA, S. & LAM, K. P. 2012. Bruton's tyrosine kinase phosphorylates Toll-like receptor 3 to initiate antiviral response. *Proc Natl Acad Sci U S A*, 109, 5791-6.
- LEE, P. X., ONG, L. C., LIBAU, E. A. & ALONSO, S. 2016. Relative Contribution of Dengue IgG Antibodies Acquired during Gestation or Breastfeeding in Mediating Dengue Disease Enhancement and Protection in Type I Interferon Receptor-Deficient Mice. *PLoS Negl Trop Dis*, 10, e0004805.
- LEI, X., GAO, X., YANG, J., SUN, Y., SAI, Y., YOU, W. & YUAN, H. 2013. The genotype C could play a key role in hepatitis B virus associated nephritis among the northwest Chinese children. *Eur J Intern Med*, 24, 835-8.
- LERNER, A. M., SHIPPEY, M. J. & CRANE, L. R. 1974. Serologic responses to herpes simplex virus in rabbits: complement-requiring neutralizing, conventional neutralizing, and passive hemagglutinating antibodies. *J Infect Dis*, 129, 623-36.
- LI, Q., LI, Y. X., STAHL, G. L., THURMAN, J. M., HE, Y. & TONG, H. H. 2011. Essential role of factor B of the alternative complement pathway in complement activation and opsonophagocytosis during acute pneumococcal otitis media in mice. *Infect Immun*, 79, 2578-85.
- LIBRATY, D. H., ENDY, T. P., KALAYANAROOJ, S., CHANSIRIWONGS, W., NISALAK, A., GREEN, S., ENNIS, F. A. & ROTHMAN, A. L. 2002a. Assessment of body fluid compartment volumes by multifrequency bioelectrical impedance spectroscopy in children with dengue. *Trans R Soc Trop Med Hyg*, 96, 295-9.
- LIBRATY, D. H., YOUNG, P. R., PICKERING, D., ENDY, T. P., KALAYANAROOJ, S., GREEN, S., VAUGHN, D. W., NISALAK, A., ENNIS, F. A. & ROTHMAN, A. L. 2002b. High circulating levels of the dengue virus nonstructural protein NS1 early in dengue illness correlate with the development of dengue hemorrhagic fever. *J Infect Dis*, 186, 1165-8.
- LICHT, C. & FREMEAUX-BACCHI, V. 2009. Hereditary and acquired complement dysregulation in membranoproliferative glomerulonephritis. *Thromb Haemost*, 101, 271-8.
- LICHT, C., PLUTHERO, F. G., LI, L., CHRISTENSEN, H., HABBIG, S., HOPPE, B., GEARY, D. F., ZIPFEL, P. F. & KAHR, W. H. 2009. Platelet-associated complement factor H in healthy persons and patients with atypical HUS. *Blood*, 114, 4538-45.
- LIN, J. C., LIN, S. C., CHEN, W. Y., YEN, Y. T., LAI, C. W., TAO, M. H., LIN, Y. L., MIAW, S. C. & WU-HSIEH, B. A. 2014. Dengue viral protease interaction with NF-kappaB inhibitor alpha/beta results in endothelial cell apoptosis and hemorrhage development. *J Immunol*, 193, 1258-67.
- LIN, Y. L., LIAO, C. L., CHEN, L. K., YEH, C. T., LIU, C. I., MA, S. H., HUANG, Y. Y., HUANG, Y. L., KAO, C. L. & KING, C. C. 1998. Study of Dengue virus infection in SCID mice engrafted with human K562 cells. *J Virol*, 72, 9729-37.
- LINDENBACH, B. D. & RICE, C. M. 1999. Genetic interaction of flavivirus nonstructural proteins NS1 and NS4A as a determinant of replicase function. *J Virol*, 73, 4611-21.

- LINDENBACH, B. D., THIEL, H.J. AND RICE, C.M. 2011. Flaviviridae: The Viruses and Their Replication. *In: Knipe, D.M. and Howley, O.M., Eds., Fields Virology, 5th Edition, Lippincot William & Wilkins, Philadelphia.* , 1101-1151.
- LISZEWSKI, M. K. & ATKINSON, J. P. 1996. Membrane cofactor protein (MCP; CD46). Isoforms differ in protection against the classical pathway of complement. *J Immunol*, 156, 4415-21.
- LISZEWSKI, M. K., FARRIES, T. C., LUBLIN, D. M., ROONEY, I. A. & ATKINSON, J. P. 1996. Control of the complement system. *Adv Immunol*, 61, 201-83.
- LISZEWSKI, M. K., LEUNG, M. K., HAUHART, R., BULLER, R. M., BERTRAM, P., WANG, X., ROSENGARD, A. M., KOTWAL, G. J. & ATKINSON, J. P. 2006. Structure and regulatory profile of the monkeypox inhibitor of complement: comparison to homologs in vaccinia and variola and evidence for dimer formation. *J Immunol*, 176, 3725-34.
- LIU, S., CHEN, J., CAI, X., WU, J., CHEN, X., WU, Y. T., SUN, L. & CHEN, Z. J. 2013. MAVS recruits multiple ubiquitin E3 ligases to activate antiviral signaling cascades. *Elife*, 2, e00785.
- LOEVEN, M. A., ROPS, A. L., LEHTINEN, M. J., VAN KUPPEVELT, T. H., DAHA, M. R., SMITH, R. J., BAKKER, M., BERDEN, J. H., RABELINK, T. J., JOKIRANTA, T. S. & VAN DER VLAG, J. 2016. Mutations in complement factor H impair alternative pathway regulation on mouse glomerular endothelial cells in vitro. *J Biol Chem*.
- LOKE, H., BETHELL, D. B., PHUONG, C. X., DUNG, M., SCHNEIDER, J., WHITE, N. J., DAY, N. P., FARRAR, J. & HILL, A. V. 2001. Strong HLA class I--restricted T cell responses in dengue hemorrhagic fever: a double-edged sword? *J Infect Dis*, 184, 1369-73.
- LORENZ, M. 2009. Visualizing protein-RNA interactions inside cells by fluorescence resonance energy transfer. *RNA*, 15, 97-103.
- LUHN, K., SIMMONS, C. P., MORAN, E., DUNG, N. T., CHAU, T. N., QUYEN, N. T., THAO LE, T. T., VAN NGOC, T., DUNG, N. M., WILLS, B., FARRAR, J., MCMICHAEL, A. J., DONG, T. & ROWLAND-JONES, S. 2007. Increased frequencies of CD4+ CD25(high) regulatory T cells in acute dengue infection. *J Exp Med*, 204, 979-85.
- LUPLERTLOP, N., MISSE, D., BRAY, D., DELEUZE, V., GONZALEZ, J. P., LEARDKAMOLKARN, V., YSSEL, H. & VEAS, F. 2006. Dengue-virus-infected dendritic cells trigger vascular leakage through metalloproteinase overproduction. *EMBO Rep*, 7, 1176-81.
- MACKENZIE, J. M., JONES, M. K. & YOUNG, P. R. 1996. Immunolocalization of the dengue virus nonstructural glycoprotein NS1 suggests a role in viral RNA replication. *Virology*, 220, 232-40.
- MACKENZIE, J. M., KHROMYKH, A. A., JONES, M. K. & WESTAWAY, E. G. 1998. Subcellular localization and some biochemical properties of the flavivirus Kunjin nonstructural proteins NS2A and NS4A. *Virology*, 245, 203-15.
- MALAVIGE, G. N. & OGG, G. S. 2017. Pathogenesis of vascular leak in dengue virus infection. *Immunology*, 151, 261-269.
- MALLIK, B., KATRAGADDA, M., SPRUCE, L. A., CARAFIDES, C., TSOKOS, C. G., MORIKIS, D. & LAMBRIS, J. D. 2005. Design and NMR characterization of active analogues of compstatin containing non-natural amino acids. *J Med Chem*, 48, 274-86.
- MAMMEN, M. P., LYONS, A., INNIS, B. L., SUN, W., MCKINNEY, D., CHUNG, R. C., ECKELS, K. H., PUTNAK, R., KANESA-THASAN, N., SCHERER, J. M., STATLER, J., ASHER, L. V., THOMAS, S. J. & VAUGHN, D. W. 2014. Evaluation of dengue virus strains for human challenge studies. *Vaccine*, 32, 1488-94.
- MANEEKAN, P., LEAUNGWUTIWONG, P., MISSE, D. & LUPLERTLOP, N. 2013. T

- helper (Th) 1 and Th2 cytokine expression profile in dengue and malaria infection using magnetic bead-based bio-plex assay. *Southeast Asian J Trop Med Public Health*, 44, 31-6.
- MANGADA, M. M. & ROTHMAN, A. L. 2005. Altered cytokine responses of dengue-specific CD4+ T cells to heterologous serotypes. *J Immunol*, 175, 2676-83.
- MARCHETTE, N. J., HALSTEAD, S. B., FALKLER, W. A., JR., STENHOUSE, A. & NASH, D. 1973. Studies on the pathogenesis of dengue infection in monkeys. 3. Sequential distribution of virus in primary and heterologous infections. *J Infect Dis*, 128, 23-30.
- MARCOS, E., LAZO, L., GIL, L., IZQUIERDO, A., SUZARTE, E., VALDES, I., BLANCO, A., ANCIZAR, J., ALBA, J. S., PEREZ YDE, L., COBAS, K., ROMERO, Y., GUILLEN, G., GUZMAN, M. G. & HERMIDA, L. 2016. Dengue encephalitis-associated immunopathology in the mouse model: Implications for vaccine developers and antigens inducer of cellular immune response. *Immunol Lett*, 176, 51-6.
- MARIE, I., DURBIN, J. E. & LEVY, D. E. 1998. Differential viral induction of distinct interferon-alpha genes by positive feedback through interferon regulatory factor-7. *EMBO J*, 17, 6660-9.
- MARKIEWSKI, M. M. & LAMBRIS, J. D. 2007. The role of complement in inflammatory diseases from behind the scenes into the spotlight. *Am J Pathol*, 171, 715-27.
- MAROVICH, M., GROUARD-VOGEL, G., LOUDER, M., ELLER, M., SUN, W., WU, S. J., PUTVATANA, R., MURPHY, G., TASSANEETRITHEP, B., BURGESS, T., BIRX, D., HAYES, C., SCHLESINGER-FRANKEL, S. & MASCOLA, J. 2001. Human dendritic cells as targets of dengue virus infection. *J Investig Dermatol Symp Proc*, 6, 219-24.
- MARTIN, H. L., ADAMS, M., HIGGINS, J., BOND, J., MORRISON, E. E., BELL, S. M., WARRINER, S., NELSON, A. & TOMLINSON, D. C. 2014. High-content, high-throughput screening for the identification of cytotoxic compounds based on cell morphology and cell proliferation markers. *PLoS One*, 9, e88338.
- MARTINA, B. E., KORAKA, P. & OSTERHAUS, A. D. 2009. Dengue virus pathogenesis: an integrated view. *Clin Microbiol Rev*, 22, 564-81.
- MARTINEZ GOMEZ, J. M., ONG, L. C., LAM, J. H., BINTE AMAN, S. A., LIBAU, E. A., LEE, P. X., ST JOHN, A. L. & ALONSO, S. 2016. Maternal Antibody-Mediated Disease Enhancement in Type I Interferon-Deficient Mice Leads to Lethal Disease Associated with Liver Damage. *PLoS Negl Trop Dis*, 10, e0004536.
- MASSEY, A. J. 2015. Multiparametric Cell Cycle Analysis Using the Operetta High-Content Imager and Harmony Software with PhenoLOGIC. *PLoS One*, 10, e0134306.
- MASTELLOS, D. C., REIS, E. S., YANCOPOULOU, D., HAJISHENGALLIS, G., RICKLIN, D. & LAMBRIS, J. D. 2016. From orphan drugs to adopted therapies: Advancing C3-targeted intervention to the clinical stage. *Immunobiology*, 221, 1046-57.
- MATHEW, A., KURANE, I., GREEN, S., STEPHENS, H. A., VAUGHN, D. W., KALAYANAROOJ, S., SUNTAYAKORN, S., CHANDANAYINGYONG, D., ENNIS, F. A. & ROTHMAN, A. L. 1998. Predominance of HLA-restricted cytotoxic T-lymphocyte responses to serotype-cross-reactive epitopes on nonstructural proteins following natural secondary dengue virus infection. *J Virol*, 72, 3999-4004.
- MATHEW, A. & ROTHMAN, A. L. 2008. Understanding the contribution of cellular immunity to dengue disease pathogenesis. *Immunol Rev*, 225, 300-13.
- MCCURRY, K. R., KOOYMAN, D. L., DIAMOND, L. E., BYRNE, G. W., LOGAN, J. S. & PLATT, J. L. 1995. Transgenic expression of human complement regulatory proteins in mice results in diminished complement deposition during organ xenoperfusion. *Transplantation*, 59, 1177-82.
- MCHARG, S., CLARK, S. J., DAY, A. J. & BISHOP, P. N. 2015. Age-related macular

- degeneration and the role of the complement system. *Mol Immunol*, 67, 43-50.
- MCLAREN, J., ROWE, M. & BRENNAN, P. 2007. Epstein-Barr virus induces a distinct form of DNA-bound STAT1 compared with that found in interferon-stimulated B lymphocytes. *J Gen Virol*, 88, 1876-86.
- MEDICUS, R. G., GOTZE, O. & MULLER-EBERHARD, H. J. 1976. Alternative pathway of complement: recruitment of precursor properdin by the labile C3/C5 convertase and the potentiation of the pathway. *J Exp Med*, 144, 1076-93.
- MEERTENS, L., CARNEC, X., LECOIN, M. P., RAMDASI, R., GUIVEL-BENHASSINE, F., LEW, E., LEMKE, G., SCHWARTZ, O. & AMARA, A. 2012. The TIM and TAM families of phosphatidylserine receptors mediate dengue virus entry. *Cell Host Microbe*, 12, 544-57.
- MEHLHOP, E., ANSARAH-SOBRINHO, C., JOHNSON, S., ENGLE, M., FREMONT, D. H., PIERSON, T. C. & DIAMOND, M. S. 2007. Complement protein C1q inhibits antibody-dependent enhancement of flavivirus infection in an IgG subclass-specific manner. *Cell Host Microbe*, 2, 417-26.
- MEHLHOP, E. & DIAMOND, M. S. 2006. Protective immune responses against West Nile virus are primed by distinct complement activation pathways. *J Exp Med*, 203, 1371-81.
- MEHLHOP, E., WHITBY, K., OLIPHANT, T., MARRI, A., ENGLE, M. & DIAMOND, M. S. 2005. Complement activation is required for induction of a protective antibody response against West Nile virus infection. *J Virol*, 79, 7466-77.
- MERI, S. 2016. Self-nonsel self discrimination by the complement system. *FEBS Lett*, 590, 2418-34.
- MERI, S., MORGAN, B. P., DAVIES, A., DANIELS, R. H., OLAVESSEN, M. G., WALDMANN, H. & LACHMANN, P. J. 1990. Human protectin (CD59), an 18,000-20,000 MW complement lysis restricting factor, inhibits C5b-8 catalysed insertion of C9 into lipid bilayers. *Immunology*, 71, 1-9.
- MERI, S. & PANGBURN, M. K. 1990. A mechanism of activation of the alternative complement pathway by the classical pathway: protection of C3b from inactivation by covalent attachment to C4b. *Eur J Immunol*, 20, 2555-61.
- MERI, S. & PANGBURN, M. K. 1994. Regulation of alternative pathway complement activation by glycosaminoglycans: specificity of the polyanion binding site on factor H. *Biochem Biophys Res Commun*, 198, 52-9.
- MERLE, N. S., CHURCH, S. E., FREMEAUX-BACCHI, V. & ROUMENINA, L. T. 2015a. Complement System Part I - Molecular Mechanisms of Activation and Regulation. *Front Immunol*, 6, 262.
- MERLE, N. S., NOE, R., HALBWACHS-MECARELLI, L., FREMEAUX-BACCHI, V. & ROUMENINA, L. T. 2015b. Complement System Part II: Role in Immunity. *Front Immunol*, 6, 257.
- MILDER, F. J., GOMES, L., SCHOUTEN, A., JANSSEN, B. J., HUIZINGA, E. G., ROMIJN, R. A., HEMRIKA, W., ROOS, A., DAHA, M. R. & GROS, P. 2007. Factor B structure provides insights into activation of the central protease of the complement system. *Nat Struct Mol Biol*, 14, 224-8.
- MILLER, J. L., DE WET, B. J., MARTINEZ-POMARES, L., RADCLIFFE, C. M., DWEK, R. A., RUDD, P. M. & GORDON, S. 2008. The mannose receptor mediates dengue virus infection of macrophages. *PLoS Pathog*, 4, e17.
- MILLIGAN, G. N., SARATHY, V. V., INFANTE, E., LI, L., CAMPBELL, G. A., BEATTY, P. R., HARRIS, E., BARRETT, A. D. & BOURNE, N. 2015. A Dengue Virus Type 4 Model of Disseminated Lethal Infection in AG129 Mice. *PLoS One*, 10, e0125476.
- MIYAMOTO, M., FUJITA, T., KIMURA, Y., MARUYAMA, M., HARADA, H., SUDO, Y., MIYATA, T. & TANIGUCHI, T. 1988. Regulated expression of a gene encoding a nuclear factor, IRF-1, that specifically binds to IFN-beta gene regulatory elements.

Cell, 54, 903-13.

- MODHIRAN, N., WATTERSON, D., MULLER, D. A., PANETTA, A. K., SESTER, D. P., LIU, L., HUME, D. A., STACEY, K. J. & YOUNG, P. R. 2015. Dengue virus NS1 protein activates cells via Toll-like receptor 4 and disrupts endothelial cell monolayer integrity. *Sci Transl Med*, 7, 304ra142.
- MOI, M. L., TAKASAKI, T., OMATSU, T., NAKAMURA, S., KATAKAI, Y., AMI, Y., SUZAKI, Y., SAIJO, M., AKARI, H. & KURANE, I. 2014. Demonstration of marmosets (*Callithrix jacchus*) as a non-human primate model for secondary dengue virus infection: high levels of viraemia and serotype cross-reactive antibody responses consistent with secondary infection of humans. *J Gen Virol*, 95, 591-600.
- MOI, M. L., TAKASAKI, T., SAIJO, M. & KURANE, I. 2013. Dengue virus infection-enhancing activity of undiluted sera obtained from patients with secondary dengue virus infection. *Trans R Soc Trop Med Hyg*, 107, 51-8.
- MOLD, C., GEWURZ, H. & DU CLOS, T. W. 1999. Regulation of complement activation by C-reactive protein. *Immunopharmacology*, 42, 23-30.
- MOLINS, B., FUENTES-PRIOR, P., ADAN, A., ANTON, R., AROSTEGUI, J. I., YAGUE, J. & DICK, A. D. 2016. Complement factor H binding of monomeric C-reactive protein downregulates proinflammatory activity and is impaired with at risk polymorphic CFH variants. *Sci Rep*, 6, 22889.
- MONATH, T. P., MCCARTHY, K., BEDFORD, P., JOHNSON, C. T., NICHOLS, R., YOKSAN, S., MARCHESANI, R., KNAUBER, M., WELLS, K. H., ARROYO, J. & GUIRAKHOO, F. 2002. Clinical proof of principle for ChimeriVax: recombinant live, attenuated vaccines against flavivirus infections. *Vaccine*, 20, 1004-18.
- MONGKOLSAPAYA, J., DEJNIRATTISAI, W., XU, X. N., VASANAWATHANA, S., TANGTHAWORNCHAIKUL, N., CHAIRUNSRI, A., SAWASDIVORN, S., DUANGCHINDA, T., DONG, T., ROWLAND-JONES, S., YENCHITSOMANUS, P. T., MCMICHAEL, A., MALASIT, P. & SREATON, G. 2003. Original antigenic sin and apoptosis in the pathogenesis of dengue hemorrhagic fever. *Nat Med*, 9, 921-7.
- MONGKOLSAPAYA, J., DUANGCHINDA, T., DEJNIRATTISAI, W., VASANAWATHANA, S., AVIRUTNAN, P., JAIRUNGSRI, A., KHEMNU, N., TANGTHAWORNCHAIKUL, N., CHOTIYARNWONG, P., SAE-JANG, K., KOCH, M., JONES, Y., MCMICHAEL, A., XU, X., MALASIT, P. & SREATON, G. 2006. T cell responses in dengue hemorrhagic fever: are cross-reactive T cells suboptimal? *J Immunol*, 176, 3821-9.
- MORGAN, B. P. & HARRIS, C. L. 2015. Complement, a target for therapy in inflammatory and degenerative diseases. *Nat Rev Drug Discov*, 14, 857-77.
- MORGAN, H. P., MERTENS, H. D., GUARIENTO, M., SCHMIDT, C. Q., SOARES, D. C., SVERGUN, D. I., HERBERT, A. P., BARLOW, P. N. & HANNAN, J. P. 2012. Structural analysis of the C-terminal region (modules 18-20) of complement regulator factor H (FH). *PLoS One*, 7, e32187.
- MORRIS, K. M., ADEN, D. P., KNOWLES, B. B. & COLTEN, H. R. 1982. Complement biosynthesis by the human hepatoma-derived cell line HepG2. *J Clin Invest*, 70, 906-13.
- MORRISON, T. E., FRASER, R. J., SMITH, P. N., MAHALINGAM, S. & HEISE, M. T. 2007. Complement contributes to inflammatory tissue destruction in a mouse model of Ross River virus-induced disease. *J Virol*, 81, 5132-43.
- MORRISON, T. E., SIMMONS, J. D. & HEISE, M. T. 2008. Complement receptor 3 promotes severe ross river virus-induced disease. *J Virol*, 82, 11263-72.
- MOSSO, C., GALVAN-MENDOZA, I. J., LUDERT, J. E. & DEL ANGEL, R. M. 2008. Endocytic pathway followed by dengue virus to infect the mosquito cell line C6/36 HT. *Virology*, 378, 193-9.
- MOTA, J. & RICO-HESE, R. 2009. Humanized mice show clinical signs of dengue fever according to infecting virus genotype. *J Virol*, 83, 8638-45.

- MOTA, J. & RICO-HESE, R. 2011. Dengue virus tropism in humanized mice recapitulates human dengue fever. *PLoS One*, 6, e20762.
- MUKHOPADHYAY, S., KUHN, R. J. & ROSSMANN, M. G. 2005. A structural perspective of the flavivirus life cycle. *Nat Rev Microbiol*, 3, 13-22.
- MULLER-EBERHARD, H. J. & GOTZE, O. 1972. C3 proactivator convertase and its mode of action. *J Exp Med*, 135, 1003-8.
- MULLER, D. A., DEPELSENAIRE, A. C. & YOUNG, P. R. 2017. Clinical and Laboratory Diagnosis of Dengue Virus Infection. *J Infect Dis*, 215, S89-S95.
- MULLER, D. A. & YOUNG, P. R. 2013. The flavivirus NS1 protein: molecular and structural biology, immunology, role in pathogenesis and application as a diagnostic biomarker. *Antiviral Res*, 98, 192-208.
- MUNOZ-CANOVES, P., VIK, D. P. & TACK, B. F. 1990. Mapping of a retinoic acid-responsive element in the promoter region of the complement factor H gene. *J Biol Chem*, 265, 20065-8.
- NAKAYA, T., SATO, M., HATA, N., ASAGIRI, M., SUEMORI, H., NOGUCHI, S., TANAKA, N. & TANIGUCHI, T. 2001. Gene induction pathways mediated by distinct IRFs during viral infection. *Biochem Biophys Res Commun*, 283, 1150-6.
- NAN, Y., WU, C. & ZHANG, Y. J. 2018. Interferon Independent Non-Canonical STAT Activation and Virus Induced Inflammation. *Viruses*, 10.
- NASCIMENTO, E. J., HOTTZ, E. D., GARCIA-BATES, T. M., BOZZA, F., MARQUES, E. T., JR. & BARRATT-BOYES, S. M. 2014. Emerging concepts in dengue pathogenesis: interplay between plasmablasts, platelets, and complement in triggering vasculopathy. *Crit Rev Immunol*, 34, 227-40.
- NASCIMENTO, E. J., SILVA, A. M., CORDEIRO, M. T., BRITO, C. A., GIL, L. H., BRAGANETO, U. & MARQUES, E. T. 2009. Alternative complement pathway deregulation is correlated with dengue severity. *PLoS One*, 4, e6782.
- NASIRUDEEN, A. M., WONG, H. H., THIEN, P., XU, S., LAM, K. P. & LIU, D. X. 2011. RIG-I, MDA5 and TLR3 synergistically play an important role in restriction of dengue virus infection. *PLoS Negl Trop Dis*, 5, e926.
- NAVARRO-SANCHEZ, E., ALTMAYER, R., AMARA, A., SCHWARTZ, O., FIESCHI, F., VIRELIZIER, J. L., ARENZANA-SEISDEDOS, F. & DESPRES, P. 2003. Dendritic-cell-specific ICAM3-grabbing non-integrin is essential for the productive infection of human dendritic cells by mosquito-cell-derived dengue viruses. *EMBO Rep*, 4, 723-8.
- NG, J. K., ZHANG, S. L., TAN, H. C., YAN, B., MARTINEZ, J. M., TAN, W. Y., LAM, J. H., TAN, G. K., OOI, E. E. & ALONSO, S. 2014. First experimental in vivo model of enhanced dengue disease severity through maternally acquired heterotypic dengue antibodies. *PLoS Pathog*, 10, e1004031.
- NGUYEN, T. H., NGUYEN, T. L., LEI, H. Y., LIN, Y. S., LE, B. L., HUANG, K. J., LIN, C. F., DO, Q. H., VU, T. Q., LAM, T. M., YEH, T. M., HUANG, J. H., LIU, C. C. & HALSTEAD, S. B. 2005. Association between sex, nutritional status, severity of dengue hemorrhagic fever, and immune status in infants with dengue hemorrhagic fever. *Am J Trop Med Hyg*, 72, 370-4.
- NICHOLS, E. M., BARBOUR, T. D., PAPPWORTH, I. Y., WONG, E. K., PALMER, J. M., SHEERIN, N. S., PICKERING, M. C. & MARCHBANK, K. J. 2015. An extended mini-complement factor H molecule ameliorates experimental C3 glomerulopathy. *Kidney Int*, 88, 1314-1322.
- NILSSON, B. & NILSSON EKDAHL, K. 2012. The tick-over theory revisited: is C3 a contact-activated protein? *Immunobiology*, 217, 1106-10.
- NIMMANNITYA, S., HALSTEAD, S. B., COHEN, S. N. & MARGIOTTA, M. R. 1969. Dengue and chikungunya virus infection in man in Thailand, 1962-1964. I. Observations on hospitalized patients with hemorrhagic fever. *Am J Trop Med Hyg*,

- 18, 954-71.
- NONAKA, M., GITLIN, J. D. & COLTEN, H. R. 1989a. Regulation of human and murine complement: comparison of 5' structural and functional elements regulating human and murine complement factor B gene expression. *Mol Cell Biochem*, 89, 1-14.
- NONAKA, M., ISHIKAWA, N., PASSWELL, J., NATSUUME-SAKAI, S. & COLTEN, H. R. 1989b. Tissue-specific initiation of murine complement factor B mRNA transcription. *J Immunol*, 142, 1377-82.
- OKAMOTO, K., KINOSHITA, H., PARQUET MDEL, C., RAEKIANSYAH, M., KIMURA, D., YUI, K., ISLAM, M. A., HASEBE, F. & MORITA, K. 2012. Dengue virus strain DEN2 16681 utilizes a specific glycochain of syndecan-2 proteoglycan as a receptor. *J Gen Virol*, 93, 761-70.
- OKEMEFUNA, A. I., NAN, R., MILLER, A., GOR, J. & PERKINS, S. J. 2010. Complement factor H binds at two independent sites to C-reactive protein in acute phase concentrations. *J Biol Chem*, 285, 1053-65.
- OMATSU, T., MOI, M. L., HIRAYAMA, T., TAKASAKI, T., NAKAMURA, S., TAJIMA, S., ITO, M., YOSHIDA, T., SAITO, A., KATAKAI, Y., AKARI, H. & KURANE, I. 2011. Common marmoset (*Callithrix jacchus*) as a primate model of dengue virus infection: development of high levels of viraemia and demonstration of protective immunity. *J Gen Virol*, 92, 2272-80.
- OMATSU, T., MOI, M. L., TAKASAKI, T., NAKAMURA, S., KATAKAI, Y., TAJIMA, S., ITO, M., YOSHIDA, T., SAITO, A., AKARI, H. & KURANE, I. 2012. Changes in hematological and serum biochemical parameters in common marmosets (*Callithrix jacchus*) after inoculation with dengue virus. *J Med Primatol*, 41, 289-96.
- ONLAMOON, N., NOISAKRAN, S., HSIAO, H. M., DUNCAN, A., VILLINGER, F., ANSARI, A. A. & PERNG, G. C. 2010. Dengue virus-induced hemorrhage in a nonhuman primate model. *Blood*, 115, 1823-34.
- ORMSBY, R. J., JOKIRANTA, T. S., DUTHY, T. G., GRIGGS, K. M., SADLON, T. A., GIANNAKIS, E. & GORDON, D. L. 2006. Localization of the third heparin-binding site in the human complement regulator factor H1. *Mol Immunol*, 43, 1624-32.
- PAES, M. V., PINHAO, A. T., BARRETO, D. F., COSTA, S. M., OLIVEIRA, M. P., NOGUEIRA, A. C., TAKIYA, C. M., FARIAS-FILHO, J. C., SCHATZMAYR, H. G., ALVES, A. M. & BARTH, O. M. 2005. Liver injury and viremia in mice infected with dengue-2 virus. *Virology*, 338, 236-46.
- PANG, J., HSU, J. P., YEO, T. W., LEO, Y. S. & LYE, D. C. 2017. Diabetes, cardiac disorders and asthma as risk factors for severe organ involvement among adult dengue patients: A matched case-control study. *Sci Rep*, 7, 39872.
- PANG, T., CARDOSA, M. J. & GUZMAN, M. G. 2007. Of cascades and perfect storms: the immunopathogenesis of dengue haemorrhagic fever-dengue shock syndrome (DHF/DSS). *Immunol Cell Biol*, 85, 43-5.
- PANGBURN, M. K. & MULLER-EBERHARD, H. J. 1984. The alternative pathway of complement. *Springer Semin Immunopathol*, 7, 163-92.
- PANGBURN, M. K. & MULLER-EBERHARD, H. J. 1986. The C3 convertase of the alternative pathway of human complement. Enzymic properties of the bimolecular proteinase. *Biochem J*, 235, 723-30.
- PANGBURN, M. K., PANGBURN, K. L., KOISTINEN, V., MERI, S. & SHARMA, A. K. 2000. Molecular mechanisms of target recognition in an innate immune system: interactions among factor H, C3b, and target in the alternative pathway of human complement. *J Immunol*, 164, 4742-51.
- PANGBURN, M. K., SCHREIBER, R. D. & MULLER-EBERHARD, H. J. 1981. Formation of the initial C3 convertase of the alternative complement pathway. Acquisition of C3b-like activities by spontaneous hydrolysis of the putative thioester in native C3. *J Exp Med*, 154, 856-67.

- PARENTE, R., CLARK, S. J., INFORZATO, A. & DAY, A. J. 2017. Complement factor H in host defense and immune evasion. *Cell Mol Life Sci*, 74, 1605-1624.
- PAUPY, C., DELATTE, H., BAGNY, L., CORBEL, V. & FONTENILLE, D. 2009. Aedes albopictus, an arbovirus vector: from the darkness to the light. *Microbes Infect*, 11, 1177-85.
- PENIX, L., WEAVER, W. M., PANG, Y., YOUNG, H. A. & WILSON, C. B. 1993. Two essential regulatory elements in the human interferon gamma promoter confer activation specific expression in T cells. *J Exp Med*, 178, 1483-96.
- PERERA, R. & KUHN, R. J. 2008. Structural proteomics of dengue virus. *Curr Opin Microbiol*, 11, 369-77.
- PEREZ, A. B., GARCIA, G., SIERRA, B., ALVAREZ, M., VAZQUEZ, S., CABRERA, M. V., RODRIGUEZ, R., ROSARIO, D., MARTINEZ, E., DENNY, T. & GUZMAN, M. G. 2004. IL-10 levels in Dengue patients: some findings from the exceptional epidemiological conditions in Cuba. *J Med Virol*, 73, 230-4.
- PERLMUTTER, D. H., COLTEN, H. R., ADAMS, S. P., MAY, L. T., SEHGAL, P. B. & FALLON, R. J. 1989. A cytokine-selective defect in interleukin-1 beta-mediated acute phase gene expression in a subclone of the human hepatoma cell line (HEPG2). *J Biol Chem*, 264, 7669-74.
- PERRY, S. T., BUCK, M. D., LADA, S. M., SCHINDLER, C. & SHRESTA, S. 2011. STAT2 mediates innate immunity to Dengue virus in the absence of STAT1 via the type I interferon receptor. *PLoS Pathog*, 7, e1001297.
- PIERSON, T. C. 2010. Modeling antibody-enhanced dengue virus infection and disease in mice: protection or pathogenesis? *Cell Host Microbe*, 7, 85-6.
- PIERSON, T. C. & DIAMOND, M. S. 2008. Molecular mechanisms of antibody-mediated neutralisation of flavivirus infection. *Expert Rev Mol Med*, 10, e12.
- PIONNIER, N., ADAMEK, M., MIEST, J. J., HARRIS, S. J., MATRAS, M., RAKUS, K. L., IRNAZAROW, I. & HOOLE, D. 2014. C-reactive protein and complement as acute phase reactants in common carp *Cyprinus carpio* during CyHV-3 infection. *Dis Aquat Organ*, 109, 187-99.
- PLATANIAS, L. C. 2005. Mechanisms of type-I- and type-II-interferon-mediated signalling. *Nat Rev Immunol*, 5, 375-86.
- PLUMMER, E. & SHRESTA, S. 2014a. Animal models in dengue. *Methods Mol Biol*, 1138, 377-90.
- PLUMMER, E. M. & SHRESTA, S. 2014b. Mouse models for dengue vaccines and antivirals. *J Immunol Methods*, 410, 34-8.
- PRESTWOOD, T. R., MAY, M. M., PLUMMER, E. M., MORAR, M. M., YAUCH, L. E. & SHRESTA, S. 2012a. Trafficking and replication patterns reveal splenic macrophages as major targets of dengue virus in mice. *J Virol*, 86, 12138-47.
- PRESTWOOD, T. R., MORAR, M. M., ZELLWEGER, R. M., MILLER, R., MAY, M. M., YAUCH, L. E., LADA, S. M. & SHRESTA, S. 2012b. Gamma interferon (IFN-gamma) receptor restricts systemic dengue virus replication and prevents paralysis in IFN-alpha/beta receptor-deficient mice. *J Virol*, 86, 12561-70.
- PRIYADARSHINI, D., GADIA, R. R., TRIPATHY, A., GURUKUMAR, K. R., BHAGAT, A., PATWARDHAN, S., MOKASHI, N., VAIDYA, D., SHAH, P. S. & CECILIA, D. 2010. Clinical findings and pro-inflammatory cytokines in dengue patients in Western India: a facility-based study. *PLoS One*, 5, e8709.
- PRYOR, M. J., CARR, J. M., HOCKING, H., DAVIDSON, A. D., LI, P. & WRIGHT, P. J. 2001. Replication of dengue virus type 2 in human monocyte-derived macrophages: comparisons of isolates and recombinant viruses with substitutions at amino acid 390 in the envelope glycoprotein. *Am J Trop Med Hyg*, 65, 427-34.
- PUERTA-GUARDO, H., GLASNER, D. R. & HARRIS, E. 2016. Dengue Virus NS1 Disrupts the Endothelial Glycocalyx, Leading to Hyperpermeability. *PLoS Pathog*,

12, e1005738.

- PUERTA-GUARDO, H., RAYA-SANDINO, A., GONZALEZ-MARISCAL, L., ROSALES, V. H., AYALA-DAVILA, J., CHAVEZ-MUNGIA, B., MARTINEZ-FONG, D., MEDINA, F., LUDERT, J. E. & DEL ANGEL, R. M. 2013. The cytokine response of U937-derived macrophages infected through antibody-dependent enhancement of dengue virus disrupts cell apical-junction complexes and increases vascular permeability. *J Virol*, 87, 7486-501.
- QUANDT, K., FRECH, K., KARAS, H., WINGENDER, E. & WERNER, T. 1995. MatInd and MatInspector: new fast and versatile tools for detection of consensus matches in nucleotide sequence data. *Nucleic Acids Res*, 23, 4878-84.
- QUINN, E. J., CHEONG, A. H., CALVERT, J. K., HIGGINS, G., HAHESEY, T., GORDON, D. L. & CARR, J. M. 2018. Clinical Features and Laboratory Findings of Travelers Returning to South Australia with Dengue Virus Infection. *Trop. Med. Infect. Dis.*, 3, 1-14.
- QUINTOS FN, L. L., JULIANO L, REYES A, LACSON P 1954. Hemorrhagic fever observed among children in the Philippines. *Philipp J Pediatr* 3, 1–19.
- RABAA, M. A., GIRERD-CHAMBAZ, Y., DUONG THI HUE, K., VU TUAN, T., WILLS, B., BONAPARTE, M., VAN DER VLIET, D., LANGEVIN, E., CORTES, M., ZAMBRANO, B., DUNOD, C., WARTEL-TRAM, A., JACKSON, N. & SIMMONS, C. P. 2017. Genetic epidemiology of dengue viruses in phase III trials of the CYD tetravalent dengue vaccine and implications for efficacy. *Elife*, 6.
- RAMAKRISHNAN, L., PILLAI, M. R. & NAIR, R. R. 2015. Dengue vaccine development: strategies and challenges. *Viral Immunol*, 28, 76-84.
- RANKINE-MULLINGS, A., REID, M. E., MOO SANG, M., RICHARDS-DAWSON, M. A. & KNIGHT-MADDEN, J. M. 2015. A Retrospective Analysis of the Significance of Haemoglobin SS and SC in Disease Outcome in Patients With Sickle Cell Disease and Dengue Fever. *EBioMedicine*, 2, 937-41.
- RAUT, C. G., DEOLANKAR, R. P., KOLHAPURE, R. M. & GOVERDHAN, M. K. 1996. Susceptibility of laboratory-bred rodents to the experimental infection with dengue virus type 2. *Acta Virol*, 40, 143-6.
- REY, F. A. 2003. Dengue virus envelope glycoprotein structure: new insight into its interactions during viral entry. *Proc Natl Acad Sci U S A*, 100, 6899-901.
- REYES-DEL VALLE, J., CHAVEZ-SALINAS, S., MEDINA, F. & DEL ANGEL, R. M. 2005. Heat shock protein 90 and heat shock protein 70 are components of dengue virus receptor complex in human cells. *J Virol*, 79, 4557-67.
- REYES-DEL VALLE, J. & DEL ANGEL, R. M. 2004. Isolation of putative dengue virus receptor molecules by affinity chromatography using a recombinant E protein ligand. *J Virol Methods*, 116, 95-102.
- RICHARDS, R. L., GEWURZ, H., OSMAND, A. P. & ALVING, C. R. 1977. Interactions of C-reactive protein and complement with liposomes. *Proc Natl Acad Sci U S A*, 74, 5672-6.
- RICKLIN, D., HAJISHENGALLIS, G., YANG, K. & LAMBRIS, J. D. 2010. Complement: a key system for immune surveillance and homeostasis. *Nat Immunol*, 11, 785-97.
- RICKLIN, D., REIS, E. S., MASTELLOS, D. C., GROS, P. & LAMBRIS, J. D. 2016. Complement component C3 - The "Swiss Army Knife" of innate immunity and host defense. *Immunol Rev*, 274, 33-58.
- RICO-HESSE, R. 2010. Dengue virus virulence and transmission determinants. *Curr Top Microbiol Immunol*, 338, 45-55.
- RICO-HESSE, R., HARRISON, L. M., SALAS, R. A., TOVAR, D., NISALAK, A., RAMOS, C., BOSHELL, J., DE MESA, M. T., NOGUEIRA, R. M. & DA ROSA, A. T. 1997. Origins of dengue type 2 viruses associated with increased pathogenicity in the Americas. *Virology*, 230, 244-51.

- RIPOCHE, J., DAY, A. J., HARRIS, T. J. & SIM, R. B. 1988a. The complete amino acid sequence of human complement factor H. *Biochem J*, 249, 593-602.
- RIPOCHE, J., MITCHELL, J. A., ERDEI, A., MADIN, C., MOFFATT, B., MOKOENA, T., GORDON, S. & SIM, R. B. 1988b. Interferon gamma induces synthesis of complement alternative pathway proteins by human endothelial cells in culture. *J Exp Med*, 168, 1917-22.
- RODRIGO, W. W., BLOCK, O. K., LANE, C., SUKUPOLVI-PETTY, S., GONCALVEZ, A. P., JOHNSON, S., DIAMOND, M. S., LAI, C. J., ROSE, R. C., JIN, X. & SCHLESINGER, J. J. 2009. Dengue virus neutralization is modulated by IgG antibody subclass and Fc gamma receptor subtype. *Virology*, 394, 175-82.
- ROLLINS, S. A. & SIMS, P. J. 1990. The complement-inhibitory activity of CD59 resides in its capacity to block incorporation of C9 into membrane C5b-9. *J Immunol*, 144, 3478-83.
- ROSENGARD, A. M., LIU, Y., NIE, Z. & JIMENEZ, R. 2002. Variola virus immune evasion design: expression of a highly efficient inhibitor of human complement. *Proc Natl Acad Sci U S A*, 99, 8808-13.
- ROSSEN, R. D., MICHAEL, L. H., KAGIYAMA, A., SAVAGE, H. E., HANSON, G., REISBERG, M. A., MOAKE, J. N., KIM, S. H., SELF, D. & WEAKLEY, S. 1988. Mechanism of complement activation after coronary artery occlusion: evidence that myocardial ischemia in dogs causes release of constituents of myocardial subcellular origin that complex with human C1q in vivo. *Circ Res*, 62, 572-84.
- ROTHMAN, A. L. 2010. Cellular immunology of sequential dengue virus infection and its role in disease pathogenesis. *Curr Top Microbiol Immunol*, 338, 83-98.
- ROTHMAN, A. L. 2011. Immunity to dengue virus: a tale of original antigenic sin and tropical cytokine storms. *Nat Rev Immunol*, 11, 532-43.
- RUSSELL, R. C., CURRIE, B. J., LINDSAY, M. D., MACKENZIE, J. S., RITCHIE, S. A. & WHELAN, P. I. 2009. Dengue and climate change in Australia: predictions for the future should incorporate knowledge from the past. *Med J Aust*, 190, 265-8.
- RUVOLO, V., NAVARRO, L., SAMPLE, C. E., DAVID, M., SUNG, S. & SWAMINATHAN, S. 2003. The Epstein-Barr virus SM protein induces STAT1 and interferon-stimulated gene expression. *J Virol*, 77, 3690-701.
- SABIN, A. B. 1950. The dengue group of viruses and its family relationships. *Bacteriol Rev*, 14, 225-32.
- SABIN, A. B. 1952. Research on dengue during World War II. *Am J Trop Med Hyg*, 1, 30-50.
- SADLON, T. A., PARKER, S. J. & GORDON, D. L. 1994. Regulation of C3 deposition on gp120 coated CD4 positive cells by decay accelerating factor and factor H. *Immunol Cell Biol*, 72, 461-70.
- SAEEDI, B. J. & GEISS, B. J. 2013. Regulation of flavivirus RNA synthesis and capping. *Wiley Interdiscip Rev RNA*, 4, 723-35.
- SAHLY, H., KEISARI, Y. & OFEK, I. 2009. Manno(rhamno)biose-containing capsular polysaccharides of *Klebsiella pneumoniae* enhance opsono-stimulation of human polymorphonuclear leukocytes. *J Innate Immun*, 1, 136-44.
- SAIFUDDIN, M., PARKER, C. J., PEEPLES, M. E., GORNY, M. K., ZOLLA-PAZNER, S., GHASSEMI, M., ROONEY, I. A., ATKINSON, J. P. & SPEAR, G. T. 1995. Role of virion-associated glycosylphosphatidylinositol-linked proteins CD55 and CD59 in complement resistance of cell line-derived and primary isolates of HIV-1. *J Exp Med*, 182, 501-9.
- SAIRENJI, T., SULLIVAN, J. L. & HUMPHREYS, R. E. 1984. Complement-dependent, Epstein-Barr virus-neutralizing antibody appearing early in the sera of patients with infectious mononucleosis. *J Infect Dis*, 149, 763-8.
- SAKAUE, T., TAKEUCHI, K., MAEDA, T., YAMAMOTO, Y., NISHI, K. & OHKUBO, I.

2010. Factor H in porcine seminal plasma protects sperm against complement attack in genital tracts. *J Biol Chem*, 285, 2184-92.
- SALAS-BENITO, J. S. & DEL ANGEL, R. M. 1997. Identification of two surface proteins from C6/36 cells that bind dengue type 4 virus. *J Virol*, 71, 7246-52.
- SAMTEN, B., HOWARD, S. T., WEIS, S. E., WU, S., SHAMS, H., TOWNSEND, J. C., SAFI, H. & BARNES, P. F. 2005. Cyclic AMP response element-binding protein positively regulates production of IFN-gamma by T cells in response to a microbial pathogen. *J Immunol*, 174, 6357-63.
- SAMTEN, B., TOWNSEND, J. C., WEIS, S. E., BHOUMIK, A., KLUCAR, P., SHAMS, H. & BARNES, P. F. 2008. CREB, ATF, and AP-1 transcription factors regulate IFN-gamma secretion by human T cells in response to mycobacterial antigen. *J Immunol*, 181, 2056-64.
- SARATHY, V. V., WHITE, M., LI, L., GORDER, S. R., PYLES, R. B., CAMPBELL, G. A., MILLIGAN, G. N., BOURNE, N. & BARRETT, A. D. 2015. A lethal murine infection model for dengue virus 3 in AG129 mice deficient in type I and II interferon receptors leads to systemic disease. *J Virol*, 89, 1254-66.
- SARIOL, C. A., MARTINEZ, M. I., RIVERA, F., RODRIGUEZ, I. V., PANTOJA, P., ABEL, K., ARANA, T., GIAVEDONI, L., HODARA, V., WHITE, L. J., ANGLERO, Y. I., MONTANER, L. J. & KRAISELBURD, E. N. 2011. Decreased dengue replication and an increased anti-viral humoral response with the use of combined Toll-like receptor 3 and 7/8 agonists in macaques. *PLoS One*, 6, e19323.
- SATO, M., HATA, N., ASAGIRI, M., NAKAYA, T., TANIGUCHI, T. & TANAKA, N. 1998. Positive feedback regulation of type I IFN genes by the IFN-inducible transcription factor IRF-7. *FEBS Lett*, 441, 106-10.
- SATO, M., TANIGUCHI, T. & TANAKA, N. 2001. The interferon system and interferon regulatory factor transcription factors -- studies from gene knockout mice. *Cytokine Growth Factor Rev*, 12, 133-42.
- SCHERER, W. F., RUSSELL, P. K., ROSEN, L., CASALS, J. & DICKERMAN, R. W. 1978. Experimental infection of chimpanzees with dengue viruses. *Am J Trop Med Hyg*, 27, 590-9.
- SCHLAF, G., BEISEL, N., POLLOK-KOPP, B., SCHIEFERDECKER, H., DEMBERG, T. & GOTZE, O. 2002. Constitutive expression and regulation of rat complement factor H in primary cultures of hepatocytes, Kupffer cells, and two hepatoma cell lines. *Lab Invest*, 82, 183-92.
- SCHLAF, G., DEMBERG, T., BEISEL, N., SCHIEFERDECKER, H. L. & GOTZE, O. 2001. Expression and regulation of complement factors H and I in rat and human cells: some critical notes. *Mol Immunol*, 38, 231-9.
- SCHLESINGER, J. J., FOLTZER, M. & CHAPMAN, S. 1993. The Fc portion of antibody to yellow fever virus NS1 is a determinant of protection against YF encephalitis in mice. *Virology*, 192, 132-41.
- SCHMID, S., MORDSTEIN, M., KOCHS, G., GARCIA-SASTRE, A. & TENOEVER, B. R. 2010. Transcription factor redundancy ensures induction of the antiviral state. *J Biol Chem*, 285, 42013-22.
- SCHMIDT, C. Q., HERBERT, A. P., HOCKING, H. G., UHRIN, D. & BARLOW, P. N. 2008a. Translational mini-review series on complement factor H: structural and functional correlations for factor H. *Clin Exp Immunol*, 151, 14-24.
- SCHMIDT, C. Q., HERBERT, A. P., KAVANAGH, D., GANDY, C., FENTON, C. J., BLAUM, B. S., LYON, M., UHRIN, D. & BARLOW, P. N. 2008b. A new map of glycosaminoglycan and C3b binding sites on factor H. *J Immunol*, 181, 2610-9.
- SCHMIDT, C. Q., SLINGSBY, F. C., RICHARDS, A. & BARLOW, P. N. 2011. Production of biologically active complement factor H in therapeutically useful quantities. *Protein Expr Purif*, 76, 254-63.

- SCHMIDT, N. J. & LENNETTE, E. H. 1975. Neutralizing antibody responses to varicella-zoster virus. *Infect Immun*, 12, 606-13.
- SCHMITTGEN, T. D. & LIVAK, K. J. 2008. Analyzing real-time PCR data by the comparative C(T) method. *Nat Protoc*, 3, 1101-8.
- SCHWAEBLE, W., SCHWAIGER, H., BROOIMANS, R. A., BARBIERI, A., MOST, J., HIRSCH-KAUFFMANN, M., TIEFENTHALER, M., LAPPIN, D. F., DAHA, M. R., WHALEY, K. & ET AL. 1991. Human complement factor H. Tissue specificity in the expression of three different mRNA species. *Eur J Biochem*, 198, 399-404.
- SCHWAEBLE, W., ZWIRNER, J., SCHULZ, T. F., LINKE, R. P., DIERICH, M. P. & WEISS, E. H. 1987. Human complement factor H: expression of an additional truncated gene product of 43 kDa in human liver. *Eur J Immunol*, 17, 1485-9.
- SCHWAEBLE, W. J. & REID, K. B. 1999. Does properdin crosslink the cellular and the humoral immune response? *Immunol Today*, 20, 17-21.
- SCREATON, G. & MONGKOLSAPAYA, J. 2006. T cell responses and dengue haemorrhagic fever. *Novartis Found Symp*, 277, 164-71; discussion 171-6, 251-3.
- SESSIONS, O. M., KHAN, K., HOU, Y., MELTZER, E., QUAM, M., SCHWARTZ, E., GUBLER, D. J. & WILDER-SMITH, A. 2013. Exploring the origin and potential for spread of the 2013 dengue outbreak in Luanda, Angola. *Glob Health Action*, 6, 21822.
- SEYA, T., OKADA, M., MATSUMOTO, M., HONG, K. S., KINOSHITA, T. & ATKINSON, J. P. 1991. Preferential inactivation of the C5 convertase of the alternative complement pathway by factor I and membrane cofactor protein (MCP). *Mol Immunol*, 28, 1137-47.
- SHINKAI, Y., RATHBUN, G., LAM, K. P., OLTZ, E. M., STEWART, V., MENDELSON, M., CHARRON, J., DATTA, M., YOUNG, F., STALL, A. M. & ET AL. 1992. RAG-2-deficient mice lack mature lymphocytes owing to inability to initiate V(D)J rearrangement. *Cell*, 68, 855-67.
- SHRESTA, S. 2012. Role of complement in dengue virus infection: protection or pathogenesis? *MBio*, 3.
- SHRESTA, S., KYLE, J. L., SNIDER, H. M., BASAVAPATNA, M., BEATTY, P. R. & HARRIS, E. 2004. Interferon-dependent immunity is essential for resistance to primary dengue virus infection in mice, whereas T- and B-cell-dependent immunity are less critical. *J Virol*, 78, 2701-10.
- SHRESTA, S., SHARAR, K. L., PRIGOZHIN, D. M., BEATTY, P. R. & HARRIS, E. 2006. Murine model for dengue virus-induced lethal disease with increased vascular permeability. *J Virol*, 80, 10208-17.
- SHRESTA, S., SHARAR, K. L., PRIGOZHIN, D. M., SNIDER, H. M., BEATTY, P. R. & HARRIS, E. 2005. Critical roles for both STAT1-dependent and STAT1-independent pathways in the control of primary dengue virus infection in mice. *J Immunol*, 175, 3946-54.
- SHYU, Y. J. & HU, C. D. 2008. Fluorescence complementation: an emerging tool for biological research. *Trends Biotechnol*, 26, 622-30.
- SIERRA, B., ALEGRE, R., PEREZ, A. B., GARCIA, G., STURN-RAMIREZ, K., OBASANJO, O., AGUIRRE, E., ALVAREZ, M., RODRIGUEZ-ROCHE, R., VALDES, L., KANKI, P. & GUZMAN, M. G. 2007. HLA-A, -B, -C, and -DRB1 allele frequencies in Cuban individuals with antecedents of dengue 2 disease: advantages of the Cuban population for HLA studies of dengue virus infection. *Hum Immunol*, 68, 531-40.
- SILVA, A. S., TEIXEIRA, A. G., BAVIA, L., LIN, F., VELLETRI, R., BELFORT, R., JR. & ISAAC, L. 2012. Plasma levels of complement proteins from the alternative pathway in patients with age-related macular degeneration are independent of Complement Factor H Tyr(4)(0)(2)His polymorphism. *Mol Vis*, 18, 2288-99.

- SILVA, B. M., SOUSA, L. P., GOMES-RUIZ, A. C., LEITE, F. G., TEIXEIRA, M. M., DA FONSECA, F. G., PIMENTA, P. F., FERREIRA, P. C., KROON, E. G. & BONJARDIM, C. A. 2011. The dengue virus nonstructural protein 1 (NS1) increases NF-kappaB transcriptional activity in HepG2 cells. *Arch Virol*, 156, 1275-9.
- SIM, E., WOOD, A. B., HSIUNG, L. M. & SIM, R. B. 1981. Pattern of degradation of human complement fragment, C3b. *FEBS Lett*, 132, 55-60.
- SIMMONS, C. P., DONG, T., CHAU, N. V., DUNG, N. T., CHAU, T. N., THAO LE, T. T., DUNG, N. T., HIEN, T. T., ROWLAND-JONES, S. & FARRAR, J. 2005. Early T-cell responses to dengue virus epitopes in Vietnamese adults with secondary dengue virus infections. *J Virol*, 79, 5665-75.
- SJOBERG, A. P., TROUW, L. A., CLARK, S. J., SJOLANDER, J., HEINEGARD, D., SIM, R. B., DAY, A. J. & BLOM, A. M. 2007. The factor H variant associated with age-related macular degeneration (His-384) and the non-disease-associated form bind differentially to C-reactive protein, fibromodulin, DNA, and necrotic cells. *J Biol Chem*, 282, 10894-900.
- SKERKA, C., LAUER, N., WEINBERGER, A. A., KEILHAUER, C. N., SUHNEL, J., SMITH, R., SCHLOTZER-SCHREHARDT, U., FRITSCH, L., HEINEN, S., HARTMANN, A., WEBER, B. H. & ZIPFEL, P. F. 2007. Defective complement control of factor H (Y402H) and FHL-1 in age-related macular degeneration. *Mol Immunol*, 44, 3398-406.
- SMITH, C. A., PANGBURN, M. K., VOGEL, C. W. & MULLER-EBERHARD, H. J. 1984. Molecular architecture of human properdin, a positive regulator of the alternative pathway of complement. *J Biol Chem*, 259, 4582-8.
- SPEAR, G. T., LURAIN, N. S., PARKER, C. J., GHASSEMI, M., PAYNE, G. H. & SAIFUDDIN, M. 1995. Host cell-derived complement control proteins CD55 and CD59 are incorporated into the virions of two unrelated enveloped viruses. Human T cell leukemia/lymphoma virus type I (HTLV-I) and human cytomegalovirus (HCMV). *J Immunol*, 155, 4376-81.
- SPROKHOLT, J., HELGERS, L. C. & GEIJTENBEEK, T. B. 2017. Innate immune receptors drive dengue virus immune activation and disease. *Future Virol*, 13, 287-305.
- SRIDHARAN, A., CHEN, Q., TANG, K. F., OOI, E. E., HIBBERD, M. L. & CHEN, J. 2013. Inhibition of megakaryocyte development in the bone marrow underlies dengue virus-induced thrombocytopenia in humanized mice. *J Virol*, 87, 11648-58.
- STEPHENS, H. A., KLAYTHONG, R., SIRIKONG, M., VAUGHN, D. W., GREEN, S., KALAYANAROOJ, S., ENDY, T. P., LIBRATY, D. H., NISALAK, A., INNIS, B. L., ROTHMAN, A. L., ENNIS, F. A. & CHANDANAYINGYONG, D. 2002. HLA-A and -B allele associations with secondary dengue virus infections correlate with disease severity and the infecting viral serotype in ethnic Thais. *Tissue Antigens*, 60, 309-18.
- STOERMER, K. A. & MORRISON, T. E. 2011. Complement and viral pathogenesis. *Virology*, 411, 362-73.
- STOHLMAN, S. A., WISSEMAN, C. L., JR., EYLAR, O. R. & SILVERMAN, D. J. 1975. Dengue virus-induced modifications of host cell membranes. *J Virol*, 16, 1017-26.
- SURESH, M., MOLINA, H., SALVATO, M. S., MASTELLOS, D., LAMBRIS, J. D. & SANDOR, M. 2003. Complement component 3 is required for optimal expansion of CD8 T cells during a systemic viral infection. *J Immunol*, 170, 788-94.
- TAN, F. L., LOH, D. L., PRABHAKARAN, K., TAMBYAH, P. A. & YAP, H. K. 2005. Dengue haemorrhagic fever after living donor renal transplantation. *Nephrol Dial Transplant*, 20, 447-8.
- TAN, G. K., NG, J. K., LIM, A. H., YEO, K. P., ANGELI, V. & ALONSO, S. 2011. Subcutaneous infection with non-mouse adapted Dengue virus D2Y98P strain

- induces systemic vascular leakage in AG129 mice. *Ann Acad Med Singapore*, 40, 523-32.
- TAN, G. K., NG, J. K., TRASTI, S. L., SCHUL, W., YIP, G. & ALONSO, S. 2010. A non mouse-adapted dengue virus strain as a new model of severe dengue infection in AG129 mice. *PLoS Negl Trop Dis*, 4, e672.
- TASSANEETRITHEP, B., BURGESS, T. H., GRANELLI-PIPERNO, A., TRUMPFHELLER, C., FINKE, J., SUN, W., ELLER, M. A., PATTANAPANYASAT, K., SARASOMBATH, S., BIRX, D. L., STEINMAN, R. M., SCHLESINGER, S. & MAROVICH, M. A. 2003. DC-SIGN (CD209) mediates dengue virus infection of human dendritic cells. *J Exp Med*, 197, 823-9.
- TAVAKOLIPOOR, P., SCHMIDT-CHANASIT, J., BURCHARD, G. D. & JORDAN, S. 2016. Clinical features and laboratory findings of dengue fever in German travellers: A single-centre, retrospective analysis. *Travel Med Infect Dis*, 14, 39-44.
- THOMAS, A., GASQUE, P., VAUDRY, D., GONZALEZ, B. & FONTAINE, M. 2000. Expression of a complete and functional complement system by human neuronal cells in vitro. *Int Immunol*, 12, 1015-23.
- THOMAS, S., REDFERN, J. B., LIDBURY, B. A. & MAHALINGAM, S. 2006. Antibody-dependent enhancement and vaccine development. *Expert Rev Vaccines*, 5, 409-12.
- TIMMERMAN, J. J., VAN DER WOUDE, F. J., VAN GIJLSWIJK-JANSSEN, D. J., VERWEIJ, C. L., VAN ES, L. A. & DAHA, M. R. 1996. Differential expression of complement components in human fetal and adult kidneys. *Kidney Int*, 49, 730-40.
- TOMASELLO, D. & SCHLAGENHAUF, P. 2013. Chikungunya and dengue autochthonous cases in Europe, 2007-2012. *Travel Med Infect Dis*, 11, 274-84.
- TONG, A. J., LIU, X., THOMAS, B. J., LISSNER, M. M., BAKER, M. R., SENAGOLAGE, M. D., ALLRED, A. L., BARISH, G. D. & SMALE, S. T. 2016. A Stringent Systems Approach Uncovers Gene-Specific Mechanisms Regulating Inflammation. *Cell*, 165, 165-179.
- TSAI, Y. T., CHANG, S. Y., LEE, C. N. & KAO, C. L. 2009. Human TLR3 recognizes dengue virus and modulates viral replication in vitro. *Cell Microbiol*, 11, 604-15.
- TSIFTSOGLU, S. A., WILLIS, A. C., LI, P., CHEN, X., MITCHELL, D. A., RAO, Z. & SIM, R. B. 2005. The catalytically active serine protease domain of human complement factor I. *Biochemistry*, 44, 6239-49.
- TU, Z., LI, Q., BU, H. & LIN, F. 2010. Mesenchymal stem cells inhibit complement activation by secreting factor H. *Stem Cells Dev*, 19, 1803-9.
- TU, Z., LI, Q., CHOU, H. S., HSIEH, C. C., MEYERSON, H., PETERS, M. G., BU, H., FUNG, J. J., QIAN, S., LU, L. & LIN, F. 2011. Complement mediated hepatocytes injury in a model of autoantibody induced hepatitis. *Immunobiology*, 216, 528-34.
- UMAREDDY, I., CHAO, A., SAMPATH, A., GU, F. & VASUDEVAN, S. G. 2006. Dengue virus NS4B interacts with NS3 and dissociates it from single-stranded RNA. *J Gen Virol*, 87, 2605-14.
- UPANAN, S., KUADKITKAN, A. & SMITH, D. R. 2008. Identification of dengue virus binding proteins using affinity chromatography. *J Virol Methods*, 151, 325-8.
- VALDES, K., ALVAREZ, M., PUPO, M., VAZQUEZ, S., RODRIGUEZ, R. & GUZMAN, M. G. 2000. Human Dengue antibodies against structural and nonstructural proteins. *Clin Diagn Lab Immunol*, 7, 856-7.
- VALERO, N., MOSQUERA, J., ANEZ, G., LEVY, A., MARCUCCI, R. & DE MON, M. A. 2013. Differential oxidative stress induced by dengue virus in monocytes from human neonates, adult and elderly individuals. *PLoS One*, 8, e73221.
- VAN BEEK, A. E., KAMP, A., KRUIHOF, S., NIEUWENHUY, E. J., WOUTERS, D., JONGERIUS, I., RISPENS, T., KUIJPERS, T. W. & GELDERMAN, K. A. 2018. Reference Intervals of Factor H and Factor H-Related Proteins in Healthy Children.

Front Immunol, 9, 1727.

- VAN DER MATEN, E., DE BONT, C. M., DE GROOT, R., DE JONGE, M. I., LANGEREIS, J. D. & VAN DER FLIER, M. 2016. Alternative pathway regulation by factor H modulates *Streptococcus pneumoniae* induced proinflammatory cytokine responses by decreasing C5a receptor crosstalk. *Cytokine*, 88, 281-286.
- VAN DER MOST, R. G., MURALI-KRISHNA, K., AHMED, R. & STRAUSS, J. H. 2000. Chimeric yellow fever/dengue virus as a candidate dengue vaccine: quantitation of the dengue virus-specific CD8 T-cell response. *J Virol*, 74, 8094-101.
- VAN DER SCHAAR, H. M., RUST, M. J., WAARTS, B. L., VAN DER ENDE-METSELAAR, H., KUHN, R. J., WILSCHUT, J., ZHUANG, X. & SMIT, J. M. 2007. Characterization of the early events in dengue virus cell entry by biochemical assays and single-virus tracking. *J Virol*, 81, 12019-28.
- VAUGHN, D. W., GREEN, S., KALAYANAROOJ, S., INNIS, B. L., NIMMANNITYA, S., SUNTAYAKORN, S., ENDY, T. P., RAENGSAKULRACH, B., ROTHMAN, A. L., ENNIS, F. A. & NISALAK, A. 2000. Dengue viremia titer, antibody response pattern, and virus serotype correlate with disease severity. *J Infect Dis*, 181, 2-9.
- VAUGHN, D. W., GREEN, S., KALAYANAROOJ, S., INNIS, B. L., NIMMANNITYA, S., SUNTAYAKORN, S., ROTHMAN, A. L., ENNIS, F. A. & NISALAK, A. 1997. Dengue in the early febrile phase: viremia and antibody responses. *J Infect Dis*, 176, 322-30.
- VELAZQUEZ, L., FELLOUS, M., STARK, G. R. & PELLEGRINI, S. 1992. A protein tyrosine kinase in the interferon alpha/beta signaling pathway. *Cell*, 70, 313-22.
- VERCRUYSSSE, T., PAWAR, S., DE BORGGRAEVE, W., PARDON, E., PAVLAKIS, G. N., PANNECOUQUE, C., STEYAERT, J., BALZARINI, J. & DAELEMANS, D. 2011. Measuring cooperative Rev protein-protein interactions on Rev responsive RNA by fluorescence resonance energy transfer. *RNA Biol*, 8, 316-24.
- VERITY, E. E., WILLIAMS, L. A., HADDAD, D. N., CHOY, V., O'LOUGHLIN, C., CHATFIELD, C., SAKSENA, N. K., CUNNINGHAM, A., GELDER, F. & MCPHEE, D. A. 2006. Broad neutralization and complement-mediated lysis of HIV-1 by PEHRG214, a novel caprine anti-HIV-1 polyclonal antibody. *AIDS*, 20, 505-15.
- VIK, D. P. 1996. Regulation of expression of the complement factor H gene in a murine liver cell line by interferon-gamma. *Scand J Immunol*, 44, 215-22.
- VIK, D. P., MUNOZ-CANOVES, P., CHAPLIN, D. D. & TACK, B. F. 1990. Factor H. *Curr Top Microbiol Immunol*, 153, 147-62.
- VOLANAKIS, J. E., BARNUM, S. R., GIDDENS, M. & GALLA, J. H. 1985. Renal filtration and catabolism of complement protein D. *N Engl J Med*, 312, 395-9.
- WAHALA, W. M., KRAUS, A. A., HAYMORE, L. B., ACCAVITTI-LOPER, M. A. & DE SILVA, A. M. 2009. Dengue virus neutralization by human immune sera: role of envelope protein domain III-reactive antibody. *Virology*, 392, 103-13.
- WALPORT, M. J. 2001. Complement. First of two parts. *N Engl J Med*, 344, 1058-66.
- WAN, S. W., LIN, C. F., LU, Y. T., LEI, H. Y., ANDERSON, R. & LIN, Y. S. 2012. Endothelial cell surface expression of protein disulfide isomerase activates beta1 and beta3 integrins and facilitates dengue virus infection. *J Cell Biochem*, 113, 1681-91.
- WAN, S. W., LIN, C. F., YEH, T. M., LIU, C. C., LIU, H. S., WANG, S., LING, P., ANDERSON, R., LEI, H. Y. & LIN, Y. S. 2013. Autoimmunity in dengue pathogenesis. *J Formos Med Assoc*, 112, 3-11.
- WARD, H. M., HIGGS, N. H., BLACKMORE, T. K., SADLON, T. A. & GORDON, D. L. 1997. Cloning and analysis of the human complement factor H gene promoter. *Immunol Cell Biol*, 75, 508-10.
- WATERS, A. M. & LICHT, C. 2011. aHUS caused by complement dysregulation: new therapies on the horizon. *Pediatr Nephrol*, 26, 41-57.

- WATI, S., LI, P., BURRELL, C. J. & CARR, J. M. 2007. Dengue virus (DV) replication in monocyte-derived macrophages is not affected by tumor necrosis factor alpha (TNF-alpha), and DV infection induces altered responsiveness to TNF-alpha stimulation. *J Virol*, 81, 10161-71.
- WEGE, A. K., MELKUS, M. W., DENTON, P. W., ESTES, J. D. & GARCIA, J. V. 2008. Functional and phenotypic characterization of the humanized BLT mouse model. *Curr Top Microbiol Immunol*, 324, 149-65.
- WEI, Y. P., KITA, M., SHINMURA, K., YAN, X. Q., FUKUYAMA, R., FUSHIKI, S. & IMANISHI, J. 2000. Expression of IFN-gamma in cerebrovascular endothelial cells from aged mice. *J Interferon Cytokine Res*, 20, 403-9.
- WEILER, J. M., DAHA, M. R., AUSTEN, K. F. & FEARON, D. T. 1976. Control of the amplification convertase of complement by the plasma protein beta1H. *Proc Natl Acad Sci U S A*, 73, 3268-72.
- WEINER, S. M., THIEL, J., BERG, T., WEBER, S., KRUMME, B., PETER, H. H., RUMP, L. C. & GROTZ, W. H. 2004. Impact of in vivo complement activation and cryoglobulins on graft outcome of HCV-infected renal allograft recipients. *Clin Transplant*, 18, 7-13.
- WEISKOPF, D., ANGELO, M. A., DE AZEREDO, E. L., SIDNEY, J., GREENBAUM, J. A., FERNANDO, A. N., BROADWATER, A., KOLLA, R. V., DE SILVA, A. D., DE SILVA, A. M., MATTIA, K. A., DORANZ, B. J., GREY, H. M., SHRESTA, S., PETERS, B. & SETTE, A. 2013. Comprehensive analysis of dengue virus-specific responses supports an HLA-linked protective role for CD8+ T cells. *Proc Natl Acad Sci U S A*, 110, E2046-53.
- WHALEY, K. & RUDDY, S. 1976. Modulation of the alternative complement pathways by beta 1 H globulin. *J Exp Med*, 144, 1147-63.
- WHITEHORN, J., VAN, V. C. & SIMMONS, C. P. 2014. Dengue human infection models supporting drug development. *J Infect Dis*, 209 Suppl 2, S66-70.
- WHO 2009. *Dengue: Guidelines for Diagnosis, Treatment, Prevention and Control: New Edition*. Geneva.
- WICHIT, S., JITMITTRAPHAP, A., HIDARI, K. I., THAISOMBOONSUK, B., PETMITR, S., UBOL, S., AOKI, C., ITONORI, S., MORITA, K., SUZUKI, T., SUZUKI, Y. & JAMPANGERN, W. 2011. Dengue virus type 2 recognizes the carbohydrate moiety of neutral glycosphingolipids in mammalian and mosquito cells. *Microbiol Immunol*, 55, 135-40.
- WICHMANN, O., VANNICE, K., ASTURIAS, E. J., DE ALBUQUERQUE LUNA, E. J., LONGINI, I., LOPEZ, A. L., SMITH, P. G., TISSERA, H., YOON, I. K. & HOMBACH, J. 2017. Live-attenuated tetravalent dengue vaccines: The needs and challenges of post-licensure evaluation of vaccine safety and effectiveness. *Vaccine*, 35, 5535-5542.
- WILLIAMS, C. R., MINCHAM, G., RITCHIE, S. A., VIENNET, E. & HARLEY, D. 2014. Bionomic response of *Aedes aegypti* to two future climate change scenarios in far north Queensland, Australia: implications for dengue outbreaks. *Parasit Vectors*, 7, 447.
- WU, L. C., MORLEY, B. J. & CAMPBELL, R. D. 1987. Cell-specific expression of the human complement protein factor B gene: evidence for the role of two distinct 5'-flanking elements. *Cell*, 48, 331-42.
- WU, M., CHEN, M., JING, Y., GU, J., MEI, S., YAO, Q., ZHOU, J., YANG, M., SUN, L., WANG, W., HU, H., WUTHRICH, R. P. & MEI, C. 2016. The C-terminal tail of polycystin-1 regulates complement factor B expression by signal transducer and activator of transcription 1. *Am J Physiol Renal Physiol*, 310, F1284-94.
- WU, S. J., GROUARD-VOGEL, G., SUN, W., MASCOLA, J. R., BRACHTTEL, E., PUTVATANA, R., LOUDER, M. K., FILGUEIRA, L., MAROVICH, M. A., WONG, H.

- K., BLAUVELT, A., MURPHY, G. S., ROBB, M. L., INNES, B. L., BIRX, D. L., HAYES, C. G. & FRANKEL, S. S. 2000. Human skin Langerhans cells are targets of dengue virus infection. *Nat Med*, 6, 816-20.
- WU, Z., LAUER, T. W., SICK, A., HACKETT, S. F. & CAMPOCHIARO, P. A. 2007. Oxidative stress modulates complement factor H expression in retinal pigmented epithelial cells by acetylation of FOXO3. *J Biol Chem*, 282, 22414-25.
- YAMANAKA, A., KOSUGI, S. & KONISHI, E. 2008. Infection-enhancing and -neutralizing activities of mouse monoclonal antibodies against dengue type 2 and 4 viruses are controlled by complement levels. *J Virol*, 82, 927-37.
- YAUCH, L. E., PRESTWOOD, T. R., MAY, M. M., MORAR, M. M., ZELLWEGER, R. M., PETERS, B., SETTE, A. & SHRESTA, S. 2010. CD4+ T cells are not required for the induction of dengue virus-specific CD8+ T cell or antibody responses but contribute to protection after vaccination. *J Immunol*, 185, 5405-16.
- YAUCH, L. E., ZELLWEGER, R. M., KOTTURI, M. F., QUTUBUDDIN, A., SIDNEY, J., PETERS, B., PRESTWOOD, T. R., SETTE, A. & SHRESTA, S. 2009. A protective role for dengue virus-specific CD8+ T cells. *J Immunol*, 182, 4865-73.
- YAZI MENDOZA, M., SALAS-BENITO, J. S., LANZ-MENDOZA, H., HERNANDEZ-MARTINEZ, S. & DEL ANGEL, R. M. 2002. A putative receptor for dengue virus in mosquito tissues: localization of a 45-kDa glycoprotein. *Am J Trop Med Hyg*, 67, 76-84.
- YIN, J., ZHU, D., ZHANG, Z., WANG, W., FAN, J., MEN, D., DENG, J., WEI, H., ZHANG, X. E. & CUI, Z. 2013. Imaging of mRNA-protein interactions in live cells using novel mCherry trimolecular fluorescence complementation systems. *PLoS One*, 8, e80851.
- YODER, S. M., ZHU, Y., IKIZLER, M. R. & WRIGHT, P. F. 2004. Role of complement in neutralization of respiratory syncytial virus. *J Med Virol*, 72, 688-94.
- YONEYAMA, M., SUHARA, W., FUKUHARA, Y., FUKUDA, M., NISHIDA, E. & FUJITA, T. 1998. Direct triggering of the type I interferon system by virus infection: activation of a transcription factor complex containing IRF-3 and CBP/p300. *EMBO J*, 17, 1087-95.
- YU, Y., WANG, R., NAN, Y., ZHANG, L. & ZHANG, Y. 2013. Induction of STAT1 phosphorylation at serine 727 and expression of proinflammatory cytokines by porcine reproductive and respiratory syndrome virus. *PLoS One*, 8, e61967.
- ZELLWEGER, R. M. & SHRESTA, S. 2014. Mouse models to study dengue virus immunology and pathogenesis. *Front Immunol*, 5, 151.
- ZHANG, H., ZHOU, G., ZHI, L., YANG, H., ZHAI, Y., DONG, X., ZHANG, X., GAO, X., ZHU, Y. & HE, F. 2005. Association between mannose-binding lectin gene polymorphisms and susceptibility to severe acute respiratory syndrome coronavirus infection. *J Infect Dis*, 192, 1355-61.
- ZHANG, J., HU, M. M., WANG, Y. Y. & SHU, H. B. 2012. TRIM32 protein modulates type I interferon induction and cellular antiviral response by targeting MITA/STING protein for K63-linked ubiquitination. *J Biol Chem*, 287, 28646-55.
- ZHANG, J., LI, G., LIU, X., WANG, Z., LIU, W. & YE, X. 2009. Influenza A virus M1 blocks the classical complement pathway through interacting with C1qA. *J Gen Virol*, 90, 2751-8.
- ZHANG, K., LU, Y., HARLEY, K. T. & TRAN, M. H. 2017a. Atypical Hemolytic Uremic Syndrome: A Brief Review. *Hematol Rep*, 9, 7053.
- ZHANG, L. & PAGANO, J. S. 1997. IRF-7, a new interferon regulatory factor associated with Epstein-Barr virus latency. *Mol Cell Biol*, 17, 5748-57.
- ZHANG, X., ZHANG, Z., HE, S., FU, Y., CHEN, Y., YI, N., JIANG, Y., GENG, W. & SHANG, H. 2017b. FOXO3, IRF4, and XIAP Are Correlated with Immune Activation in HIV-1-Infected Men Who Have Sex with Men During Early HIV Infection. *AIDS*

Res Hum Retroviruses, 33, 172-180.

- ZHOU, W. 2012. The new face of anaphylatoxins in immune regulation. *Immunobiology*, 217, 225-34.
- ZINZULA, L. & TRAMONTANO, E. 2013. Strategies of highly pathogenic RNA viruses to block dsRNA detection by RIG-I-like receptors: hide, mask, hit. *Antiviral Res*, 100, 615-35.
- ZIPFEL, P. F. & SKERKA, C. 2009. Complement regulators and inhibitory proteins. *Nat Rev Immunol*, 9, 729-40.
- ZOU, J., XIE, X., WANG, Q. Y., DONG, H., LEE, M. Y., KANG, C., YUAN, Z. & SHI, P. Y. 2015. Characterization of dengue virus NS4A and NS4B protein interaction. *J Virol*, 89, 3455-70.